DESIGN OF REGIONAL PILLARS FOR THE KHUSELEKA ORE REPLACEMENT PROJECT (KORP) – UG2

Clarence Mutsvanga

A research report submitted to the Faculty of Engineering and Built Environment, University of the Witwatersrand, Johannesburg, in partial fulfilment of the requirements for the degree of Master of Science in Engineering

Johannesburg 2017

DECLARATION

I declare that this research report is my own unaided work. It is being submitted for the Degree of Master of Science in Engineering to the University of Witwatersrand, Johannesburg. It has not been submitted before for any degree or examination to any other University.

………………………………………..

(Signature of candidate)

……5th……. day of ……JULY……………………..year……2017…………………

at………WITS, JOHANNESBURG…………………..

ABSTRACT

Depletion of mineral resources is a reality of mining. It is critical that as resources get depleted, new reserves are subsequently opened up continuously if a mine is to continue operating. Failure to open up new reserves will result in a mining operation running out of reserves and ultimately ceasing operations. Besides the economic considerations of an ore reserve such as the grade and tonnage, stability of the mining operation is of equal importance. A mine should remain stable for the entire period that it remains operational.

Pillars play a critical role in ensuring the stability of an excavation; actually, regional pillars ensure the overall stability of a mine. It therefore goes without saying, pillar design is an integral component of any successful mine design.

This project was undertaken with the objective of ensuring that the new reserves being opened up in the Khuseleka Ore Replacement Project (KORP) section are not only profitable, but also stable. This was done through

a) maximisation of extraction ratio, thereby maximising the mines' profitability.

b) designing the regional pillar layout for the KORP section using current empirical and numerical pillar design methods and comparing the results to come up with the most optimal design.

c) ensuring the stability of the on and off reef mine infrastructure by determining the Rockwall Condition Factor (RCF) values on the footwall infrastructure due to pillars left above and thus prevent damage to these excavations through stress induced failures. Consideration was given to the standard Khuseleka footwall infrastructure layouts for the design based on the planning department's layout of haulages and crosscuts for the KORP section. The layout of the footwall excavations indicated that the pillars would be differently sized thereby having an influence on the APS, pillar strength and factors of safety of the regional pillars.

d) numerical modelling analysis of the effects of leaving stabilizing pillars on the 27 raise line where the haulages intersect the reef horizon.

The methodology employed for this undertaking involved a critical literature review of existing pillar design methods, applying and comparing them, and coming up with an economic and safe design.

To be able to design a pillar layout that met the objectives listed above, engineering design principles had to be applied. It involved gathering the relevant geological and geotechnical

information required as input parameters for the different empirical and numerical analyses methods.

What came out from this project was that each method employed yielded its own set of results. This highlighted the need to understand the context under which a design is carried out and the shortcomings of each method employed. It showed how important it is to have all the relevant information of not only the characteristics of the rock mass in which an excavation will be made, but also on the strengths and limitations of the tools available to design a structure. It highlighted the fact that to minimize uncertainty and have a more robust design, it was necessary to spend time and effort in gathering as much relevant data as possible. In the end engineering judgment was used to decide on the best method or system to employ in the design of the pillars.

In memory of my father and mentor, Clever Mutsvanga a man of principle and wisdom.

ACKNOWLEDGEMENTS

First and foremost I would like to express my appreciation and gratitude to my supervisor Tawanda Zvarivadza, for the time, knowledge and effort in making sure that this project came to fruition. Your guidance and advice is greatly appreciated.

Sincere appreciation goes to Anglo Platinum and Khuseleka management for the financial and professional assistance in making it possible for me to complete this course. The Khuseleka rock engineering department staff is also acknowledged for some of the input data used for the project, with special mention going to Craig Slement who gave up his free time to teach me MAP3D.

Sincere gratitude to lecturers and staff at University of the Witwatersrand for the knowledge gained during courses and lectures which made it possible for me to do this project.

Special thanks to my wife and sons for accepting and understanding that I could not be with them all the time as I had to attend courses, study and do this project. Thank you for your patience and understanding.

Last, but definitely not the least, thank you, to the Almighty for the gift of life and blessings bestowed upon me. As the bible says in Zechariah 4 verse 6 ‘Not by might nor by power, but by My Spirit, says the Lord of hosts’.

TABLE OF CONTENTS

CONTENTS **PAGE**

DECLARATION ..... **i**

ABSTRACT ..... **ii**

ACKNOWLEDGEMENTS ..... **v**

TABLE OF CONTENTS ..... **vi**

LIST OF FIGURES ..... **xi**

LIST OF TABLES ..... **xiii**

LIST OF SYMBOLS ..... **xv**

NOMENCLATURE ..... **xvi**

CHAPTER 1: INTRODUCTION **1**

1.1 Use of the Design Principles in Rock Engineering for Pillar Design **1**

1.1.1 Principle 1: Clarity of design objective and functional requirements 1

1.1.2 Principle 2: Minimum uncertainty of geological conditions 2

1.1.3 Principle 3: Simplicity of design components 2

1.1.4 Principle 4: State of the art practice 2

1.1.5 Principle 5: Optimisation 2

1.1.6 Principle 6: Constructability 3

1.2 Mine Setting **4**

1.3 Geology **6**

1.3.1 Bushveld Complex 6

1.3.2 Stratigraphy 8

1.4 Pillar Design **12**

1.4.1 Pillar Strength 12

1.4.2 Pillar Load 12

1.4.3 Foundation Strength 12

1.4.4 Pillar Spacing 12

1.4.5 Placement of Footwall Excavations 13

1.5 Research Background/Context **13**

1.6 Definition of the Research Problem **13**

1.7 Project Justification **14**

1.8 Project Objectives **14**

1.9 Contents of the Research Report **14**

CHAPTER 2: LITERATURE REVIEW ON PILLAR DESIGN **16**

2.1 Introduction **16**

2.2 Khuseleka Shaft's Current Mining and Stability Strategy **17**

2.2.1 Mining Method ...17
2.2.2 Regional Pillar Design Strategy ...18
2.2.3 Placement of Regional Pillars ...19
2.3 Pillar Loads ...20
2.3.1 Tributary Area Theory ...20
2.3.2 Coates Method ...21
2.3.3 Numerical Modelling ...22
2.4 Pillar Strength ...24
2.4.1 Salamon and Munro (1967) Formula ...24
2.4.2 Hedley and Grant (1972) Formula ...25
2.4.3 Watson, et al (2008) Merensky Pillar Strength Formula ...25
2.4.4 Potvin, Hudyma and Miller (1989) Pillar Strength Formula ...26
2.4.5 Vonn Kimmelmann, Hyde and Madwick (1984) Pillar Strength Formula ...26
2.4.6 Krauland and Soder (1987) Pillar Strength Formula ...27
2.4.7 Sjoberg (1992) Pillar Strength Formula ...27
2.4.8 Lunder and Pakalnis (1997) Pillar Strength Formula ...27
2.4.9 Stacey and Page (1986) Pillar Strength Formula ...28
2.4.10 Summary of Empirical Pillar Strength Equations ...28
2.5 Width: Height Ratio ...30
2.6 Factor of Safety ...31
2.7 Rock mass Strength ...31
2.7.1 Mohr-Coulomb Criterion ...31
2.7.2 Hoek-Brown Failure Criterion ...33
2.7.3 Barton's Q criterion ...33
2.7.4 Design Rock Mass Strength (DRMS) ...34
2.8 Foundation Strength ...34
2.8.1 Terzaghi's Formula ...35
2.8.2 Hansen's Formula ...36
2.9 Pillar Spacing ...37
2.10 Placement of Footwall Excavations ...37
2.10.1 Rockwall Condition Factor Criterion ...38
2.10.2 Overstoping ...38
2.10.3 Numerical Modelling ...39
2.11 In-situ Stress Determination ...39
2.12 Conclusions ...41
CHAPTER 3: METHODOLOGY ...43

3.1 Introduction **43**
3.2 Review of the mine's current pillar design strategy **43**
3.3 Use of empirical methods for pillar design **43**
3.4 Analysis of seismic events associated with pillar failure **43**
3.5 Physical analysis of any failed pillars in the back areas **44**
3.6 Conduct numerical modelling to analyse pillar stresses and RCF values on footwall excavations **44**
3.7 Rock strength tests on drilled core from UG2 KORP section underground will be undertaken. **44**
3.8 Use of laboratory rock test data from other operations **44**
3.9 In-situ stresses and k-ratio for project **45**
3.10 Rock mass classification and rock mass strength determination **45**
3.11 Conclusions **45**
CHAPTER 4: DETERMINATION OF ROCK PROPERTIES AND PARAMETERS TO USE FOR PILLAR DESIGN IN THE KORP SECTION **46**
4.1 Introduction **46**
4.2 Mining Depths in KORP Section **46**
4.3 Reef Elevation-Footwall Excavation Middling **47**
4.4 Core **48**
4.5 Determination of Elastic Properties of Rock **49**
4.5.1 Apparatus 50
4.5.2 Sample Preparation and Test Results 50
4.5.3 Test Notes 53
4.6 Rock Property Test Performed on other Operations **54**
4.7 Rock Stresses Measurements and Determination **57**
4.8 Pillar Height **60**
4.9 K value (Rock Mass Strength) Determination **61**
4.9.1 Rock mass Classification at Khuseleka Shaft 61
4.9.2 Hoek – Brown 65
4.9.3 Mohr – Coulomb 66
4.9.4 Strength Value Using Q system 68
4.9.5 Design Rock Mass Strength (DRMS) 69
4.9.6 RocLab Software 69
4.10 Choosing the rock mass strength to use in pillar design **71**
4.11 Foundation Strength **72**
4.11.1 2.5 x rock strength of foundation rock 72
4.11.2 Terzaghi's Formula 72

4.11.3 Hansen's Formula 72
4.12 Conclusions 73
CHAPTER 5: PILLAR DESIGN 75
5.1 Introduction 75
5.2 Khuseleka Pillar Design Strategy 75
5.2.1 Pillar Strength 76
5.2.2 Average Pillar Stress 77
5.2.3 Factor of Safety 79
5.2.4 Foundation Strength 79
5.2.5 Pillar Spacing 79
5.2.6 Back Analysis of Cut Pillars 79
5.3 Pillar Design 82
5.3.1 Hedley and Grant Pillar Strength Equation 83
5.3.2 Watson et al Pillar Strength Equation 83
5.3.3 Potvin, et al Pillar Strength Equation 84
5.3.4 Von Kimmelmann et al Pillar Strength Equation 84
5.3.5 Krauland and Soder Pillar Strength Equation 85
5.3.6 Sjoberg Pillar Strength Equation 85
5.3.7 Lunder and Pakalnis Pillar Strength Equation 86
5.3.8 Stacey and Page Pillar Strength Equation 86
5.4 Pillar Loads 88
5.5 Factor of Safety 88
5.6 Width: Height Ratio 88
5.7 Comparison of the Results Using Different Pillar Strengths Equations 88
5.8 Foundation Strength 90
5.9 Pillar Spacing 90
5.10 Placement of Footwall Excavations 91
5.10.1 Overstoping 91
5.10.2 Rockwall Condition Factor 92
5.11 Pillar Layout Design 93
5.12 Conclusions 94
CHAPTER 6: NUMERICAL MODELLING 96
6.1 Introduction 96
6.2 Examine2D 96
6.2.1 Failure Criterion and Material Properties 97
6.2.2 Pillar Design 97

6.2.3 Comparison of Pillar Loads Obtained Using Stacey and Page Pillar Strength Equation Vs Using Examine2D ... 99

6.3 Lamodel ... 100

6.3.1 Comparison of Pillar Loads Obtained Using Stacey and Page Pillar Strength Equation Vs Using Lamodel ... 101

6.4 Map3D ... 102

6.4.1 Methodology of Analysis ... 102

6.4.2 Numerical Modelling Results ... 105

6.4.3 Comparison of Pillar Loads Obtained Using Stacey and Page Pillar Strength Equation Vs Using Map3D ... 107

6.4.4 Comparison of Pillar Loads Using the Different Methods Discussed ... 107

6.5 Redesign of Pillars Using Examine2D and Map3D ... 108

6.5.1 Redesign of Pillars Using Examine2D ... 108

6.5.2 Redesign of Pillars Using Map3D ... 109

6.5.3 Conclusions ... 111

6.6 Determination of RCF values Using Map3D Program ... 112

6.6.1 Introduction ... 112

6.6.2 16 Level RCF ... 112

6.6.3 19 - 28 Level RCF ... 114

6.6.4 Conclusions ... 115

6.7 Effect of Leaving Stability Pillars on Haulage-Reef Intersection Using Map3D Program ... 116

6.7.1 Introduction ... 116

6.7.2 Design Criteria ... 117

6.7.3 Conclusions ... 120

CHAPTER 7: CONCLUSIONS AND RECOMMENDATIONS ... 121

REFERENCES ... 124

Appendix A: Raiseline Middling Distances in KORP Section ... 128

Appendix B: Elastic Property Graphs for KORP Rock Samples ... 133

Appendix C: KORP Stoping Widths from Survey ... 140

Appendix D: Rock Mass Classification Input Data for KORP Section ... 146

Appendix E: KORP Geoassay Log Boreholes ... 151

LIST OF FIGURES

Figure 1.1: Illustration of the Eastern, Western and Northern Limb of the Bushveld Complex: Khuseleka shaft area circled in red (Langwieder, 2007). 4
Figure 1.2: Locality map (Langwieder, 2007). 5
Figure 1.3: Thembelani Mine (Khuseleka and Thembelani Shafts) UG2 Reef Mineral Rights Plan (Langwieder, 2007). 5
Figure 1.4: Thembelani Mine (Khuseleka and Thembelani Shafts) MR Mineral Rights Plan (Langwieder, 2007). 6
Figure 1.5: General geology map of the western part of the Rustenburg Platinum Mines lease area (underground workings in dark blue for MR and green for UG2), the crosscutting linear features represent dykes (blue and green) and for the project important faults (purple) as well as the suboutcrops of the UG2 (apple green), MR (red) and the LG6 (orange) (Langwieder, 2007). 7
Figure 1.6: Stratigraphic Column for the MR in Rustenburg (Langwieder, 2007). 8
Figure 1.7: Stratigraphic Column for the UG2 Reef at Khuseleka (Langwieder, 2007) 9
Figure 2.1: Pillar design flowchart (York, et al., 1998). 16
Figure 2.2: Plan view of a typical breast configured stope on the MR (Ozbay & Roberts, 1988). 18
Figure 2.3: Schematic of Khuseleka Pillar Design Layout (Priest, 2013) 19
Figure 2.4: Plan showing tributary area theory layout (Brady & Brown, 2005) 20
Figure 2.5: Comparison of the empirical pillar strength formulae (Martin & Maybee, 2000)...29
Figure 2.6: Graphical representation of different pillar types with their associated stress-strain curves (Y = yield, C= crush) (Ryder & Jager, 2002)..30
Figure 2.7: (a) Mohr's f(σ) hypothesis (b) Mohr-Coulomb in τ-σ space (c) Mohr-Coulomb in σ1 – σ3 space (Goodman, 1989)……...32
Figure 2.8: Foundation strength for pillar stability (Stacey & Page, 1986)..............................36
Figure 2.9: Diagram showing concept of overstoping (COMRO, 1988) 38
Figure 2.10: Influence of field static stresses on the development of blast fractures (Brady & Brown, 2005) 40
Figure 2.11: Stresses working on the blast fractures (Middindi, 2013)....................................40
Figure 4.1: Drilling layout for diamond drill hole where testing samples were obtained (Mutsvanga, 2016) 48
Figure 4.2: Borehole CTM03 soon after being brought to surface..49
Figure 4.3: Amsler Testing machine with the specimen loaded..50
Figure 4.4: Specimen at failure after UCM test..53
Figure 4.5: A blast socket taken in a panel mining towards south-east...................................58
Figure 4.6: Plan of the panel were the socket was observed and measured 59
Figure 4.7: UG2 reef in a stoping panel..61
Figure 4.8: Mohr-Coulomb in σ_1- σ_3 space for chromitite (UG2 reef).....................................66
Figure 4.9: Mohr-Coulomb in σ1- σ3 space for pyroxenite (HW) 67
Figure 4.10: Mohr-Coulomb in σ1- σ3 space for peg-pyroxenite (FW)..................................68
Figure 4.11: Comparison of the different foundation strengths calculated using the different criteria. 73
Figure 5.1: Plan showing a typical mining layout in the UG2 reef horizon at Khuseleka prior to the design of regional pillars..75
Figure 5.2: APS values for the business plan pillars – Khuseleka UG2, east levels 16 to 23 (Clark, 2016). 77

Figure 5.3: APS values for the business plan pillars – Khuseleka UG2, west levels 16 to 23 (Clark, 2016). 78
Figure 5.4: APS values for the business plan pillars – Khuseleka UG2, east levels 23 to 27 (Clark, 2016) 78
Figure 5.5: Plan showing the regional pillar cut between 27 and 26 cross cuts 80
Figure 5.6: A photo of the pillar cut in 15-27 5E panel 81
Figure 5.7: A photo of the pillar cut in 15-27 6E panel 81
Figure 5.8: MicroStation CAD program pillar layout of the KORP section based on the design criteria 94
Figure 6.1: A typical layout to calculate APS using Examine2D at different depths 98
Figure 6.2: Graphical representation of the Comparison of APS calculated using Stacey and Page equation and Examine2D at different depths below surface 100
Figure 6.3: Graphical representation of comparison of APS calculated using Stacey and Page formula and those using Lamodel at different depths below surface 102
Figure 6.4: The five rows of pillars from 19 to 28 levels fenced in MicroStation for modelling 103
Figure 6.5: The model constructed for the pillars. Note the middle pillars where meshing was reduced for more refined analysis. 104
Figure 6.6: Control parameters, these were left as default as per program manual suggestion. 104
Figure 6.7: Material properties of the UG2 reef rock (chromitite), based on lab values and Rocklab values in Tables 4.4 and 4.16 respectively 105
Figure 6.8: Pre-mining stress state based on stress measurement values in Section 4.7 of this report. 105
Figure 6.9: Map3D plot of the pillars that were analysed, showing the stress state in the pillars. A single pillar is zoomed in for a clearer plot. 106
Figure 6.10: Graphical representation of comparison of APS calculated using Stacey and Page formula and those using Map3D at different depths below surface 107
Figure 6.11: Graphical representation of comparison of APS calculated using Stacey and Page formula and the 3 numerical modelling programs 108
Figure 6.12: A Map3D model of the RAW and haulage at 16 level running above 19 level (note the high RCF values on the pillar position) 113
Figure 6.13: Graphical representation of the RCF values modelled along the haulage and RAW on 16 level mined above 19 level stoping 113
Figure 6.14: A Map3D model of the 19 to 27 level haulages running below their respective levels (No noticeable spike in RCF values) 114
Figure 6.15: Graphical representation of the RCF values modelled along the haulages from 19 to 28 level 115
Figure 6.16: Plan showing areas where the reef intersects 16 and 19 haulage 117
Figure 6.17: Map3D plot showing model of pillar to be left over 19 level haulage (Black portion are the pillars and coloured portion are areas to be mined out) 118
Figure 6.18: Map3D plot showing Sigma 1 along the 19 level haulages. 118
Figure 6.19: Map3D plot showing RCF values along the 19 level haulages. 119
Figure 6.20: RCF values along the 19 level east and west haulages. Current values before mining are also illustrated as well as the position of the pillars 119

LIST OF TABLES

Table 1.1: The 10 step methodology for rock engineering design in relation to design principles (Bieniawski, 1993). 3
Table 1.2: Information regarding the reefs currently mined at Khuseleka 11
Table 2.1: Summary of empirical pillar strength equations for hard rock pillars 29
Table 2.2: Summary of rock mass strength criteria 34
Table 2.3: Design criteria for KORP regional pillars 42
Table 4.1: Mining Depths for KORP Section 47
Table 4.2: Reef elevation-footwall excavation middlings 47
Table 4.3: Logged information of borehole (CTM03) from Sables program 49
Table 4.4: IDs and properties of samples tested 52
Table 4.5: Bathopele's UCS tests results 55
Table 4.6: Bathopele's TCS tests results 55
Table 4.7: Bathopele's Brazilian Tensile strength tests results 56
Table 4.8: Bathopele's Direct Shear tests results 56
Table 4.9: Details of the virgin stress tensors (van der Heever & Piper, 2013) 57
Table 4.10: Summary of norite rock properties at the measurement site 59
Table 4.11: Measured vs Calculated virgin stresses for Siphumelele Mine 60
Table 4.12: Qualitative Classification of rock mass based on Q (Barton, et al., 1974) 63
Table 4.13: Qualitative Classification of rock mass based on RMR (Bieniawski, 1989) 64
Table 4.14: Average Q and RMR values for KORP trial section 64
Table 4.15: Calculated Hoek-Brown values using the Hoek-Brown Criterion 65
Table 4.16: Calculated Parameters from RocLab Software 70
Table 4.17: Summary of rock mass strengths derived from different strength criteria 71
Table 5.1: The pillar widths at different levels 76
Table 5.2: Design of Pillars using Hedley and Grant Equation 83
Table 5.3: Design of Pillars using Watson et al Equation 84
Table 5.4: Design of Pillars using Potvin, et al Equation 84
Table 5.5: Design of Pillars using Von Kimmelmann et al Equation 85
Table 5.6: Design of Pillars using Kraulan and Soder Equation 85
Table 5.7: Design of Pillars using Sjoberg Equation 86
Table 5.8: Design of Pillars using Lunder and Pakalnis Equation 86
Table 5.9: Design of Pillars using Stacey and Page Equation 87
Table 5.10: Comparison of Pillar Widths Based on Different Pillar Strength Equations 89
Table 5.11: Comparison of Pillar Strengths Based on Different Pillar Strength Equations 89
Table 5.12: Comparison of APS Based on Different Pillar Strength Equations 89
Table 5.13: Comparison of FOS Based on Different Pillar Strength Equations 90
Table 5.14: Comparison of W: H Ratio Based on Different Pillar Strength Equations 90
Table 5.15: Comparison of Extraction Ratio Based on Different Pillar Strength Equations 90
Table 5.16: RCF calculations at different depths below surface in the KORP section 92
Table 5.17: An empirical relationship between the RCF value and the support requirements (Jager & Ryder, 1999) 93
Table 6.1: Material properties to be used in the analysis 97
Table 6.2: APS results from Examine2D analysis 99
Table 6.3: Material properties to be used in the analysis 100
Table 6.4: APS results from Lamodel analysis 101
Table 6.5: APS results from Map3D analysis 106

Table 6.6: Comparison of Previous and Final results with Examine2D Analysis....................109
Table 6.7: APS results using Map3D on Redesigned Pillars..110
Table 6.8: Comparison of Examine2D and Map3D values based on final analysis.................110

LIST OF SYMBOLS

σ_c	Rock's Uniaxial Compressive Strength (MPa)
g	Gravitational acceleration (m/s^2)
ρ, γ	Material Density (kg/m^3)
σ_1	Major Principal Stress (MPa)
σ_2	Intermediate Principal Stress (MPa)
σ_3	Minor Principal Stress (MPa)
E	Modulus of Elasticity (GPa)
ν	Poisson's ratio
K	Pillar rock mass strength value (MPa)
F	RCF factor representing σ_c downgrade
o	Degrees
φ	Angle of internal friction
c	Cohesion (MPa)

NOMENCLATURE

RPM – Rustenburg Platinum Mines

KORP – Khuseleka Ore Replacement Project

TORP – Townlands Ore Replacement Project (Pre2010 name for KORP)

UG2 – Upper Group 2, PGE bearing reef type

MR –Merensky Reef, PGE bearing reef type

RCF – Rockwall Condition Factor

TAT – Tributary Area Theory

MPa – Mega Pascals

APS – Average Pillar Stress

UCS – Uniaxial Compress Strength

MRMR – Mining Rock Mass Rating

RCF – Rockwall Condition Factor

Townlands Shaft – (Pre2010 name for Khuseleka Shaft)

ISRM – International Society for Rock Mechanics

IMS – Institute of Mine Seismology

w/h – Width to Height Ratio

FOS – Factor of Safety

DBS – Depth Below Surface

2D – Two Dimensional numerical modelling

3D – Three Dimensional numerical modelling

CHAPTER 1: INTRODUCTION

How can a mine be profitable while maintaining the stability of its workings? This question has vexed generations of miners since the ancient Egyptian and Roman empires started economically extracting minerals from the ground. As mineral extraction has moved from surface rock picking to mining at several thousand meters below surface in the gold mines of South Africa, this question has become even more pertinent.

Pillars, which are pieces of unmined ground surrounded by mined voids, have proven to be amongst the most effective means of maintaining mine stability. What is also clear from experience is that sometimes leaving pillars haphazardly without a planned layout can, in cases, worsen the instability of an excavation as this may lead to seismic risk. There are also economic consequences associated with pillars: pillars that are too big will unnecessarily leave valuable ore underground and pillars that are too small will not adequately support the ground and be potentially unstable thereby increasing artificial support costs. It is therefore critical that pillars are properly designed if they are to perform the function for which they are intended for and a mine to operate profitably.

The purpose of this project was to use current methods to design a pillar layout for an extension of the mine of which a brief summary of the pillar design methods is given in this introductory chapter. A summary of the geology and setting of the mine is also given here. Also addressed in this chapter are the research background and context under which this project was carried out, definition of the research problem, justification and the objectives of the research project. Contents of the research report are also presented.

1.1 Use of the Design Principles in Rock Engineering for Pillar Design

Stacey, (2003) discussed the design principles of Bieniawski, (1992), dealing specifically with engineering design in the rock mechanics field. He defined a series of design principles specific to rock engineering. In the context of this project these principles are very relevant as the whole process of designing the pillars for the KORP section incorporates these principles. These principles are summarised below.

1.1.1 Principle 1: Clarity of design objective and functional requirements

A statement of the “problem” and a statement of the design objectives, taking account of any constraints that are present, to satisfy this problem, is essential to any design process. This principle highlights the need to fully understand the problem so as to avoid finding a solution not relevant to the problem as this could mean a loss both financially and time wise. The problems to be solved through this project were very clear; resources are being depleted and the area of the mine where this ore will be replaced has to be designed in a way that allows it to be profitable and safe for the duration of the mine operation.

1.1.2 Principle 2: Minimum uncertainty of geological conditions

The rock mass in which mining takes place is very variable. Rock engineering design therefore takes place in an environment of considerable uncertainty. This project required data to be collected in the field, stress measurements and laboratory tests of similar rock from other mines to be collected and laboratory rock elastic properties tests conducted so as to bring some certainty and confidence to the design.

1.1.3 Principle 3: Simplicity of design components

This principle states that a design should be broken down into a series of simpler components. This means that in the broader context - simpler designs, design methods and design analyses are easier to understand and therefore are likely to be more robust. Where there is a simpler way, it is preferred to a complex or sophisticated way, provided it addresses the design requirements.

Simple empirical methods were employed in the design of pillars and the results compared with more robust and sophisticated numerical modelling tools.

1.1.4 Principle 4: State of the art practice

Up to date concepts, analyses and methods must be used whenever appropriate. The chapter on literature review shows that this principle was applied in this project.

1.1.5 Principle 5: Optimisation

Risk involves numerous factors including safety, cost, productivity, seismicity, water, manpower, etc. Therefore to minimise risk, designs must be optimised. In addition, since conditions in which mining takes place (economic, political, mineral price, depth, seismicity, geology, etc.) change over time, it is likely that designs will need to be optimised again when conditions change. An optimised design will result from the evaluation of the output from alternative designs. Monitoring will provide data that may facilitate design optimisation. During mining, monitoring will be carried out in order to validate some of the assumptions made during the design stage.

1.1.6 Principle 6: Constructability

If the design cannot be implemented safely and efficiently it does not satisfy this principle and therefore it is also not optimised. It was necessary to review the design and repeat, either partially or completely, the design methodology. This principle as the one above will require monitoring during implementation of the designed pillars.

In designing the pillars for the KORP section all the principles were applied. The last two will only be implemented when mining commences and monitoring systems are put in place to ensure that the design is the most optimal.

Bieniawski, (1993), also showed how these principles are linked to a ten step design methodology. The link is given between the step in the methodology and the corresponding principle. This link is illustrated in Table 1.1.

Table 1.1: The 10 step methodology for rock engineering design in relation to design principles (Bieniawski, 1993).

STEP	DESCRIPTION	DESIGN PRINCIPLE
1	**Statement of the problem** (performance objective)	1
2	**Function requirements and constraints** (design variable and design issues)	1
3	**Collection of information** (site characterisation, rock properties, groundwater, in-situ stresses)	2
4	**Concept formulation** (geotechnical model)	3
5	**Analysis of solution components** (analytical, numerical, empirical, observational methods)	3,4
6	**Synthesis and specifications for alternative solutions** (shapes, sizes, locations, orientations of excavations)	3,4
7	**Evaluation** (performance assessment)	5
8	**Optimisation** (performance assessment)	5
9	**Recommendation**	6
10	**Implementation** (efficient excavation, and monitoring)	6

1.2 Mine Setting

Khuseleka shaft is part of Thembelani mine. It is located within the Bushveld Complex where platinum bearing reefs are mined. The shaft is approximately 5.5km from the centre of the city of Rustenburg, North West Province, South Africa.

The shaft is at the far west extremity of Anglo Platinum's Rustenburg Section, abutting Thembelani Mine (AngloAmerican Platinum) on the East, Impala Mine (Implats) on the west and Kwezi shaft (Aquarius Platinum) on the south. Figure 1.1 below shows entire bushveld complex, Figure 1.2, the location of Khuseleka Upper Group 2 (UG2) section relative to other Anglo shafts and other mines within Rustenburg, Figures 1.3 and 1.4 are the UG2 and Merensky Reef (MR) mineral rights plans respectively (Snyman, 2015).

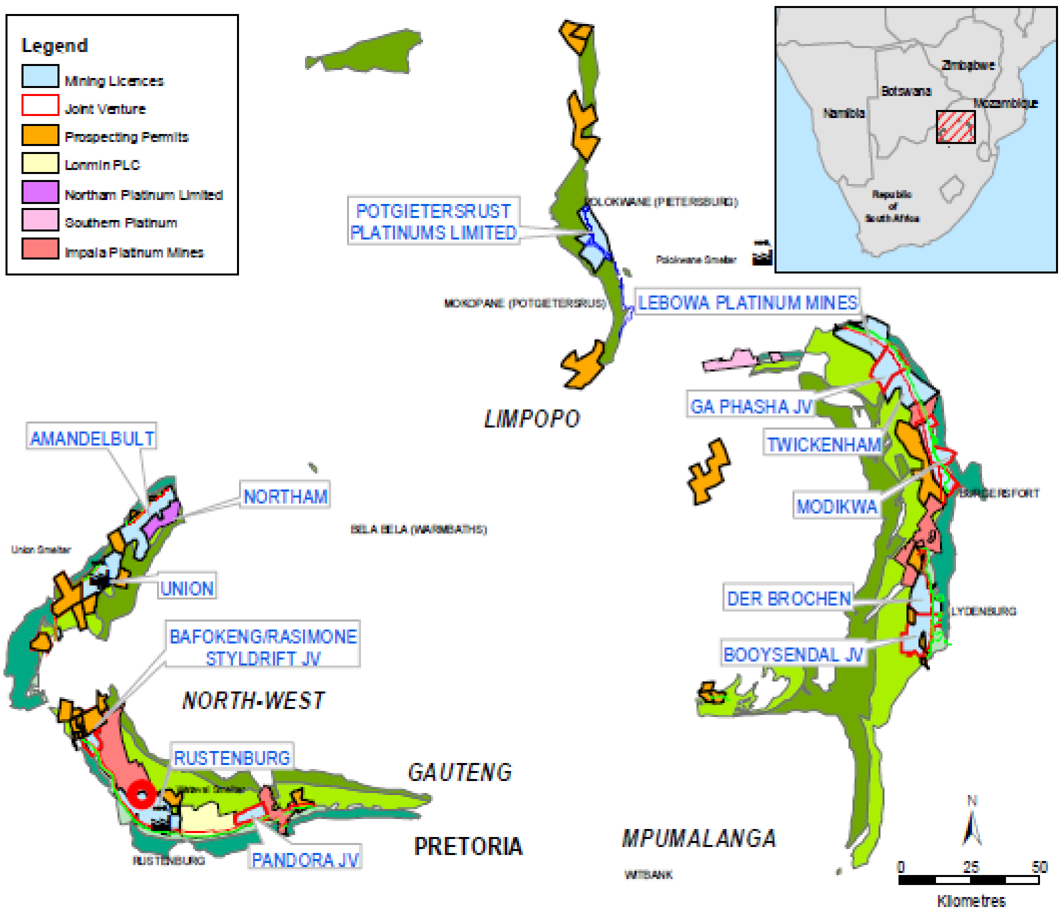

Figure 1.1: Illustration of the Eastern, Western and Northern Limb of the Bushveld Complex: Khuseleka shaft area circled in red (Langwieder, 2007).

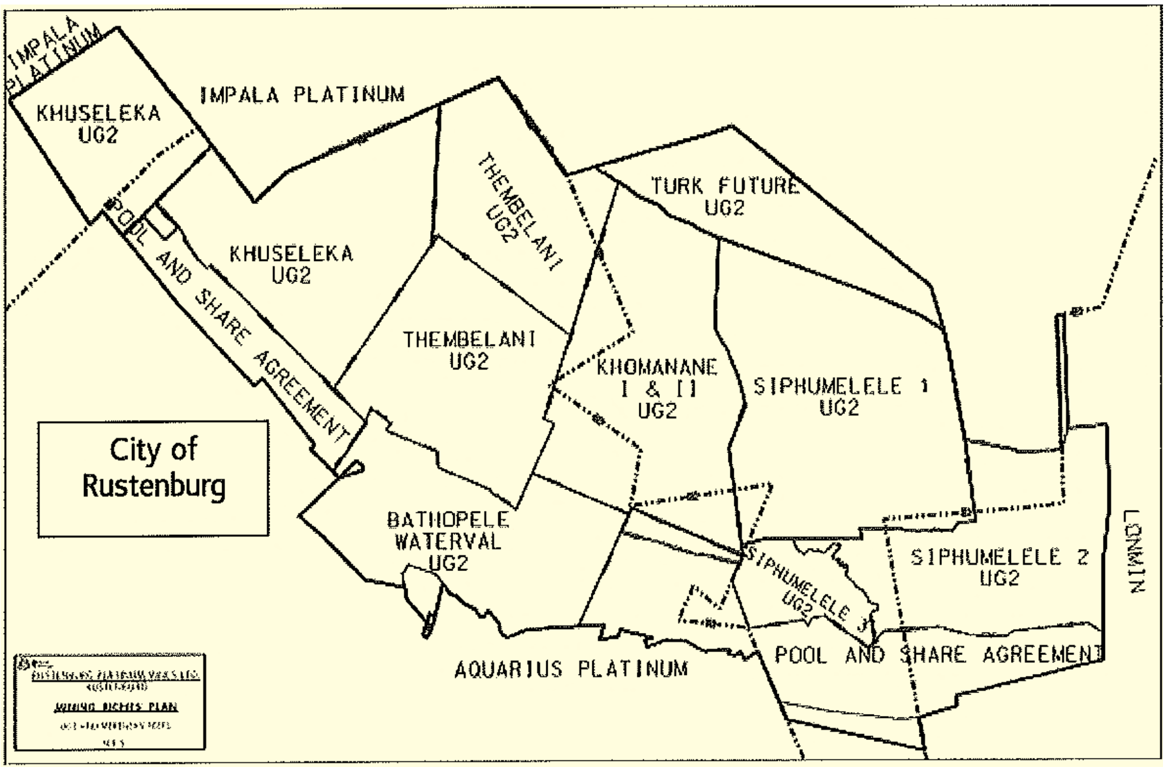

Figure 1.2: Locality map (Langwieder, 2007).

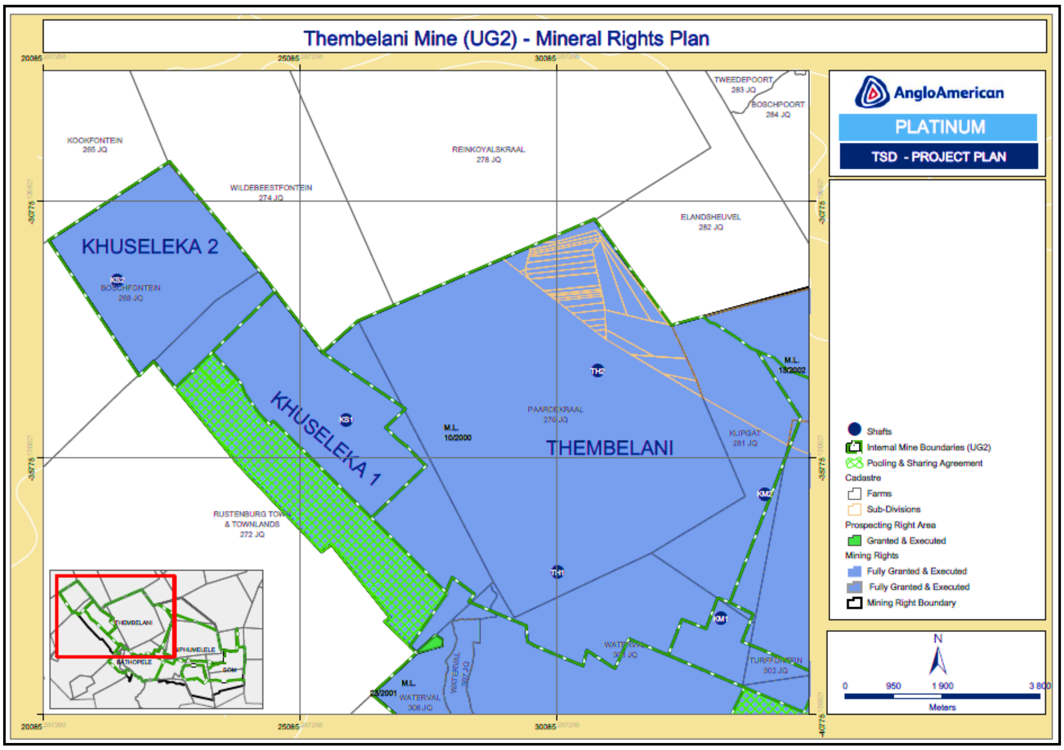

Figure 1.3: Thembelani Mine (Khuseleka and Thembelani Shafts) UG2 Reef Mineral Rights Plan (Langwieder, 2007).

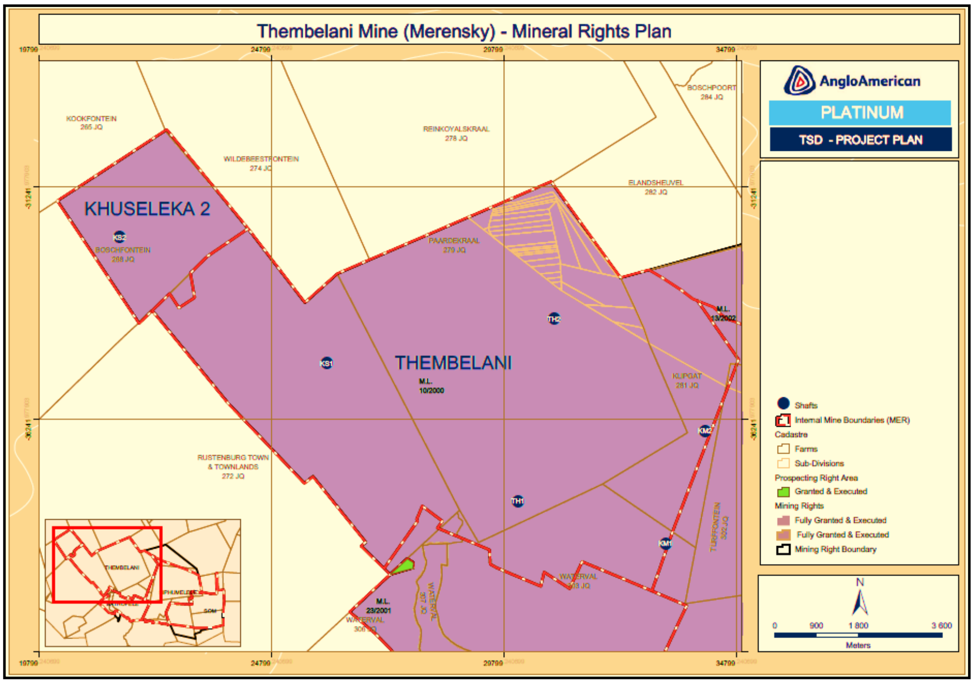

Figure 1.4: Thembelani Mine (Khuseleka and Thembelani Shafts) MR Mineral Rights Plan (Langwieder, 2007).

1.3 Geology

1.3.1 Bushveld Complex

The summary of the geology given in this section is as described by Langwieder, (2007). It gives the reader the background and basis of the pillar design principles and strategies adopted for this project. Langwieder, (2007) states that the Bushveld Complex is the world's largest layered mafic to ultramafic intrusion and is a major source of numerous economic minerals. It is essentially a sheet-like body with east-west and north-south outcrop extremities (approximately 400km and 270km respectively). This does not necessarily imply a continuous body. The complex intruded into older sedimentary and volcanic successions of the Transvaal Sequence and therefore is almost entirely surrounded by these rock types. The Bushveld Complex layered succession generally dips inward towards the centre of the complex, with the exception of the Northern Bushveld, which dips in a westerly direction.

The Rustenburg Layered Sequence of rocks occurs within a basic plutonic phase of the Bushveld Complex, which were intruded into the upper part of the Pretoria Group. It is in these layers that the Upper Group 2 (UG2) Chromitite and Merensky Reef (MR) occur. In the Rustenburg area, the floor-rocks of the Bushveld Complex are predominately Transvaal Sequence quartzites and orthoquartzites. Along the contact of the complex the footwall quartzites have been metamorphosed to hornfels. The lithologies all dip gently to the North, at approximately 10° (Langwieder, 2007).

In the extreme western part of the Rustenburg lease area the lower units of the Bushveld Complex thin substantially, as is reflected in the very small horizontal distance of 1.6km between the floor contact of the complex and the outcrop position of the MR. To the southeast the contact with the floor rock undulates, creating a series of basins and domes resulting in a thicker succession of igneous rock, and the horizontal distance from the floor rock contact to the MR outcrop increases to 4.5km. Over the whole of the central sector of the mine, the floor rocks are well over 7km from the MR and a regional basin exists. The undulations of the floor appear to affect only the thickness of the basal pyroxenite assemblage of the Lower and Critical zones.

Structurally, the region is affected by dunite pipes, large potholes, faults and dykes, all of which have similar orientations (except the dunite pipes) of either northwest-southeast or approximately east-west (Langwieder, 2007).

Figure 1.5 is a map showing the geology of the western part of the Rustenburg Platinum Mines (RPM) lease area under which Khuseleka shaft is located.

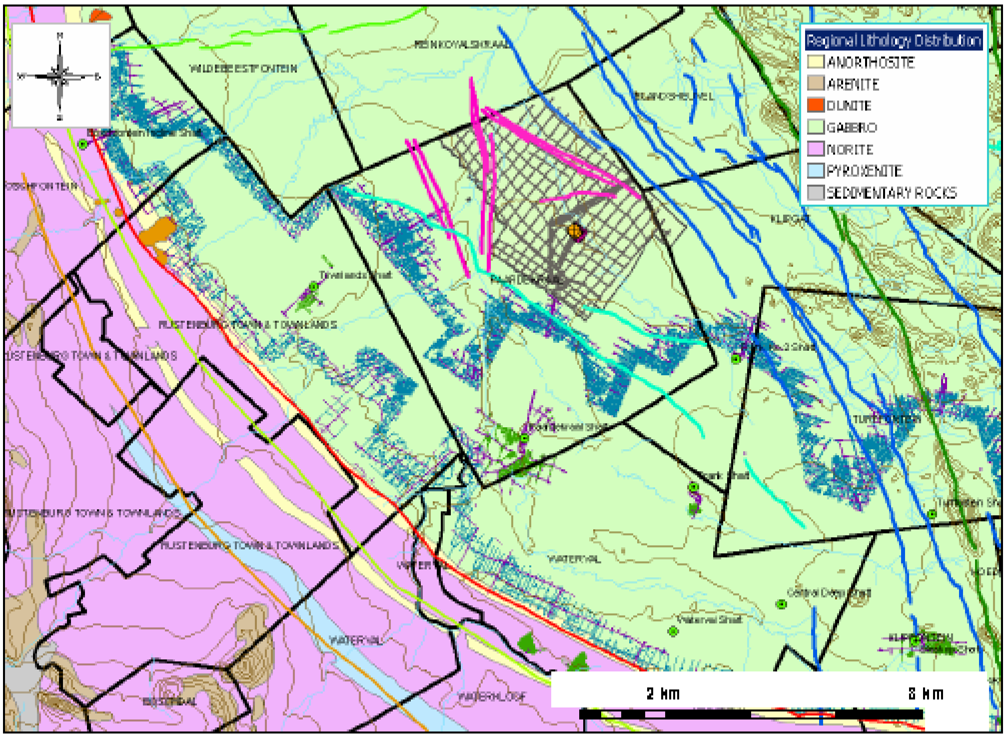

Figure 1.5: General geology map of the western part of the Rustenburg Platinum Mines lease area (underground workings in dark blue for MR and green for UG2), the crosscutting linear features represent dykes (blue and green) and for the project important faults (purple) as well as the suboutcrops of the UG2 (apple green), MR (red) and the LG6 (orange) (Langwieder, 2007).

1.3.2 Stratigraphy

The stratigraphy of the Bushveld Complex has been formalised by the South African Committee for Stratigraphy (SACS, 1980), in which it is fundamentally divided into three suites; the Rustenburg Layered Suite, the Rashoop Granophyre Suite, and the Lebowa Granite Suite. The exposed parts of the complex occur in an area of about 12200km^2 and attain apparent thicknesses of nearly 9000m in the Eastern Bushveld, 7750m in the Western Bushveld, and 7000m in the Northern Bushveld (Langwieder, 2007).

Two platinum group mineral bearing reefs are mined, namely, the MR and UG2, the stratigraphic columns for each are illustrated in Figures 1.6 and 1.7 respectively and the general characteristics summarised in Table 1.2:

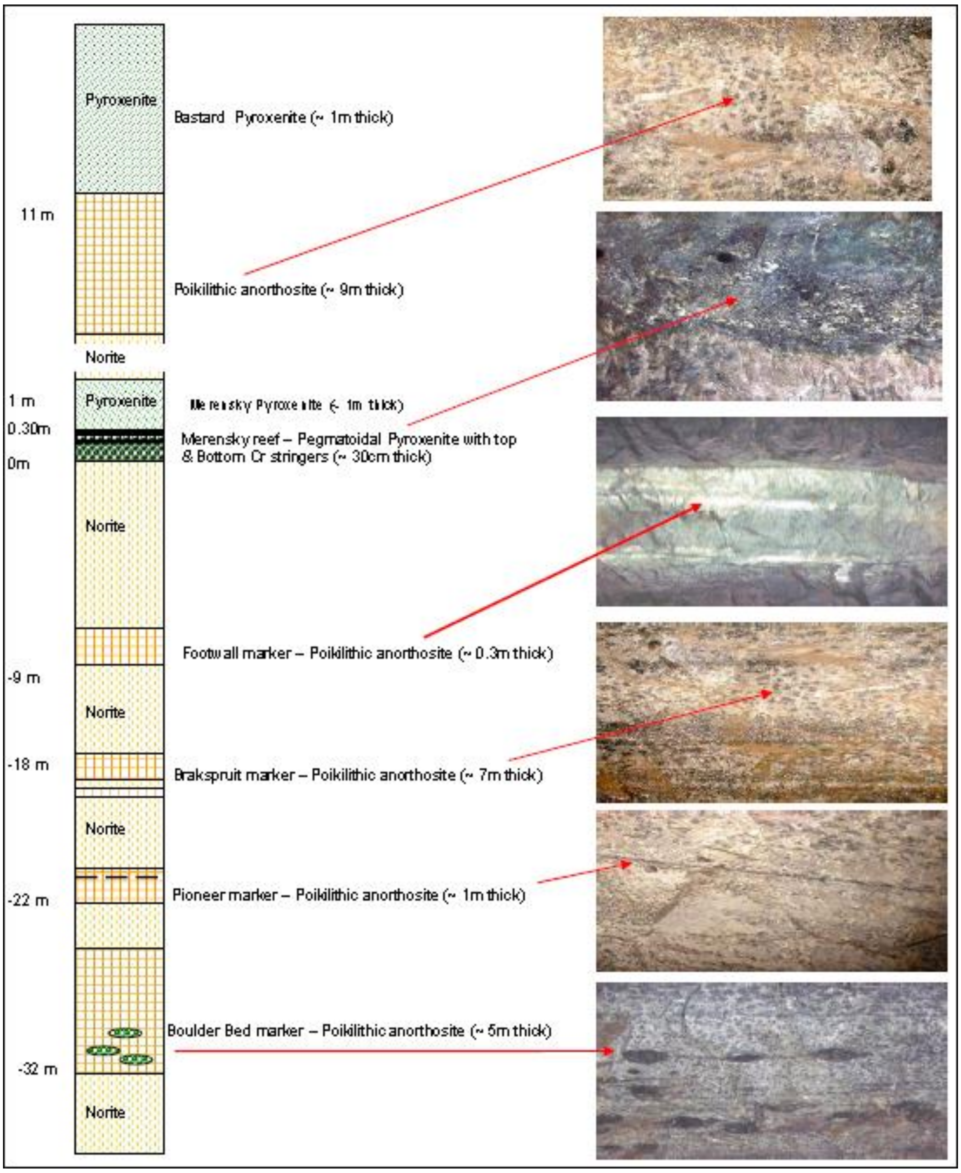

Figure 1.6: Stratigraphic Column for the MR in Rustenburg (Langwieder, 2007).

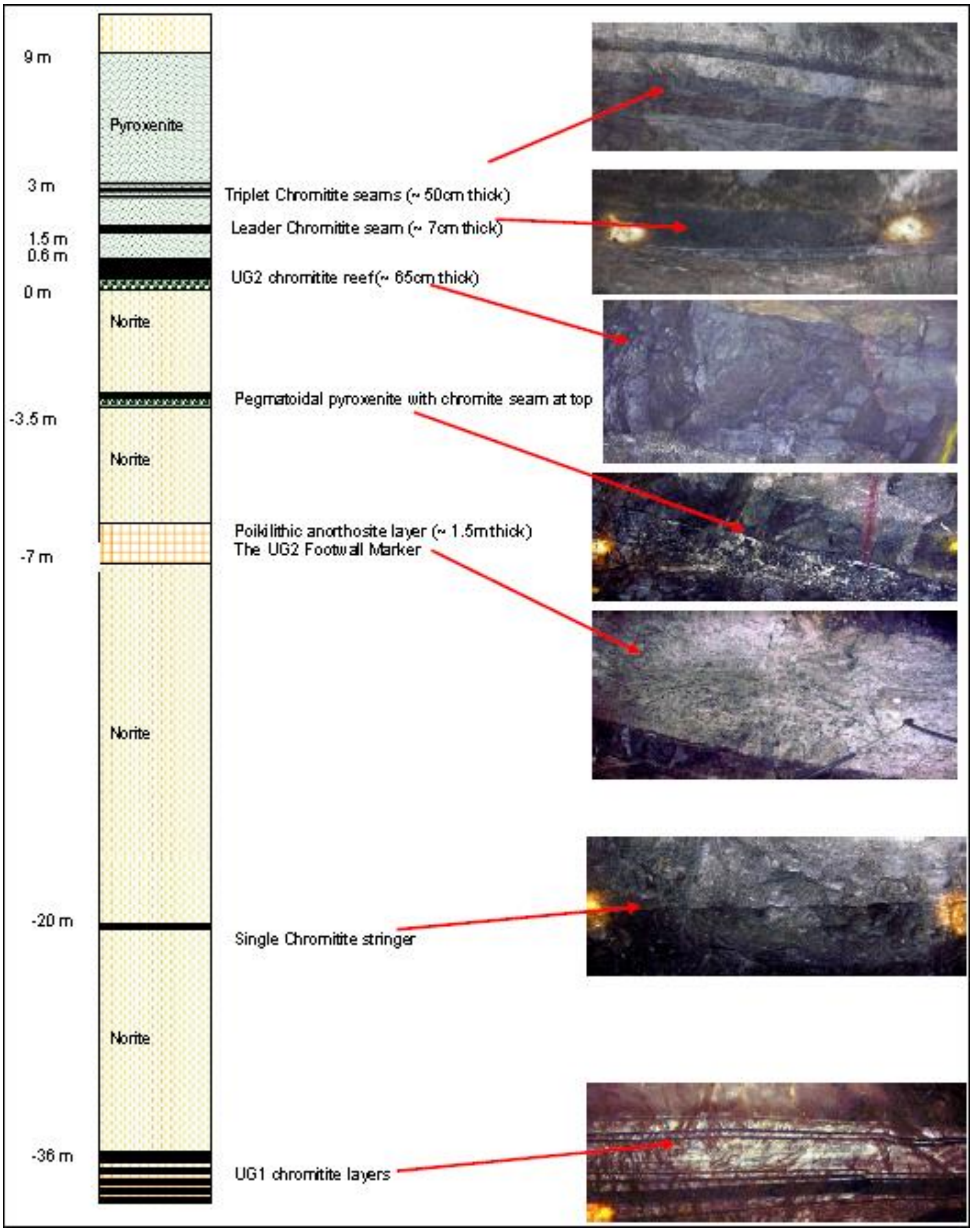

Figure 1.7: Stratigraphic Column for the UG2 Reef at Khuseleka (Langwieder, 2007)

Merensky Stratigraphy

The **Giant Poikilithic Anorthosite** is generally regarded as the start of the Critical Zone.

The stratigraphic column in Figure 1.6, illustrate the stratigraphy from the Bastard Pyroxenite down to below the Boulder Bed for the Rustenburg Section

The **hanging wall of the MR** is a medium grained feldspathic pyroxenite, which grades up into a melanorite and ultimately into a norite and a poikilithic anorthosite, before entering the Bastard pyroxenite unit. The pyroxenite is typically 1 – 3 m thick.

The **footwall of the MR** comprises norite/leuconorite and a thin anorthosite layer (10-20 cm thick), which is underlain by norite. The norite sometimes has a layered texture, where the norite has separated into anorthosite and pyroxenite sub layers.

Several stratigraphic markers exist in the footwall (Footwall Marker, Brakspruit Marker, Pioneer Marker), one of which is the **Boulder Bed**, a poikilithic anorthosite layer, some 20 metres below the reef. Elongated boulders of coarse grained pyroxenite (often pegmatoidal) exist within the layer lending the marker its name (Langwieder, 2007).

UG2 Stratigraphy

The **UG2 succession** (Figure 1.7) occurs within the lower feldspathic pyroxenite package of the UG2 unit and is well known for its undulation over short distances. This is due to the para-conformable relationship with its footwall. It is important to note that the Main Seam demonstrates the sharpest undulation while the Leader Seam and Triplets respond less intensely.

The UG2 reef succession forms at the base of a 120 m thick Unit of the Upper Critical Zone. The UG2 Unit is underlain by the **UG1 Unit**, which has a variable thickness (average 25 m).

The Merensky unit overlies the UG2 unit by approximately 120 m of norites and anorthosites.

The **UG2 reef** itself consists of a chromitite layer with an average thickness of 65 cm. Base metal sulphides are not abundant. Platinum-group minerals are confined to the chromitite layer.

The UG2 reef is commonly underlain by a **pegmatoidal feldspathic pyroxenite layer** of highly variable thickness (few cm to over 2 m) followed by norite**, pyroxenite and another stratigraphic anorthosite marker**. Less commonly, the UG2 reef is directly underlain by an anorthosite layer. In rare cases the UG2 is directly underlain by norite.

The UG2 chromitite is overlain by a 6 m to 7 m thick **medium-grained feldspathic pyroxenite** (the UG2 pyroxenite) which hosts a succession of thinner chromitite layers commonly referred to as the leader seam and triplets. These comprise of:

The "main leader" / "leader seam":

This is a chromitite layer averaging 7cm in thickness. The main leader is separated from the UG2 reef by a layer of feldspathic pyroxenite of between 45cm and 250cm thick at Rustenburg but about 1.5 m on average across the KORP area.

The "triplets":

A 30 cm to 70 cm succession of chromitite stringers/layers interlayered with feldspathic pyroxenite (which often contains disseminated chromitite) occurs. The triplets are typically situated 400cm to 700 cm above the main leader (about 300cm at Khuseleka Section).

Both reefs, namely the MR and UG2 are currently being exploited and developed at the operating Khuseleka Shaft.

All marker horizons also played a significant role with the seismic survey interpretation with regards to middling relationships and positions in the boreholes compared to the seismic reflectors.

The most important factor affecting mining of the UG2 is the variation of the stratigraphic separation between the chromitite layers. The UG2, Leader and Triplets are not constantly spaced or parallel, which results in localized thickening or thinning of the package. The para-conformable relationship of the UG2 chromitite with its footwall adds to the parting variations (Langwieder, 2007).

The UG1 Chromitite Layer:

In the framework of this project the UG1 will have an impact with regards to its middling to the UG2, since current planning indicates the intention to place the footwall development (haulages) about 35 metres below UG2 reef in order to provide the necessary ore pass capacities and production.

The UG1 consists of alternating layers and stringers of chromitite and white anorthosite, which at each change of the respective lithology to the other forms a natural parting plane due to the lack of cohesion between chromite grains and anorthosite competent rock and therefore should be avoided in development for obvious geotechnical reasons. Bifurcations and undulations are common (Langwieder, 2007).

Table 1.2: Information regarding the reefs currently mined at Khuseleka

Reef	Dip (°)	Stoping Width (m)	H/wall	F/wall	Other Geology	Min depth (m)	Max depth (m)	Merensky –UG2 middling (m)
Merensky	7 – 15	1.1 – 1.4	Pyroxenite	Norite	-	400	967	120 – 140
UG2	0 – 15	1.1 – 1.8	Proxenite	Pegmatoid Pyroxenite	Triplets “Leader seam”	370	595	

The MR is underlain by the UG2 reef which lies 120 to 140 m below the MR. Both the UG2 and MRs dip towards the north at 9 to 11 degrees. The planned best-cut stoping width for the UG2 and MR is 105cm, but the actual is currently on 120cm (Mutsvanga, 2017). Studies conducted have indicated that activities on the MR overlying the UG2 do not influence activities below them.

1.4 Pillar Design

The design of pillars requires geotechnical knowledge or information on certain properties of the rocks in which the pillar will be cut. This knowledge or information was used to determine the following:

1.4.1 Pillar Strength

This property is a function of the uniaxial compressive strength of a sample of the rock in which the pillar will be cut as determined from laboratory tests and the rock mass properties as determined through field mapping or core sampling as well as the w/h ratio of the pillar. Once the UCS and rock mass properties have been determined, the pillar strength can be derived using a number of formulas such as Salamon & Munro, (1967), Hedley & Grant, (1972), Watson, et al., (2008), etc.

1.4.2 Pillar Load

In pillar design, pillar load is usually termed the average pillar stress (APS). The basis of determining this stress is knowledge of the virgin stresses acting in the rock mass where the excavation is to be made and where the pillars will be cut. Methods such as the tributary area theory (TAT), Coates method and numerical modelling are then used to calculate the stress or loads acting on the pillars.

1.4.3 Foundation Strength

It is not enough to have knowledge of the strength of the pillars or the stresses acting on those pillars without knowledge of the strength of the material making up the foundation of that pillar. Should the foundations be considerably weaker than the load exerted on the pillar, the possibility exists that the pillar will punch into either the hangingwall or footwall of the excavation, thereby creating instability of the excavation. Jager & Ryder, (1999) stated that a rule of thumb is for the APS to be ≤ 2.5 x the uniaxial compressive strength (UCS) of the foundation rock to prevent foundation failure. Terzaghi, (1943) and Hansen, (1970) also formulated equations to determine the foundation strength.

1.4.4 Pillar Spacing

Pillar span (spacing between pillars) is also very important as it determines the stability of excavations. Ryder & Ozbay, (1990) suggested that a rule of thumb is to keep this span (L) less than one quarter of the depth (H), i.e., $H/L > 4$.

1.4.5 Placement of Footwall Excavations

The position of footwall excavations in relation to pillars on the reef horizon determines the stability of these excavations. This is because the stresses induced on these excavations can make them prone to instability, as they can be several magnitudes higher than the virgin stresses and strength of the rock mass. Methods such as Rockwall Condition Factor (RCF) determination and numerical modelling can be used to determine the effect of stresses acting on the footwall excavations and determine any mitigating measures that can be taken against them. Overstoping is a method that has been used to ensure that the stresses above do not adversely affect footwall excavations. Secondary support is an option that can be considered to stabilise excavations where induced stresses are higher than the rock mass strength or are high enough to induce fracturing and therefore potential for rock failure.

1.5 Research Background/Context

When mining started at Khuseleka Mine in the 1970s, plans of the old workings indicate that there was no structured layout for regional pillar support design. The plans show that regional pillars were left in areas where geological structures such as faults, potholes and reef rolls were encountered during mining (geological losses). As mining deepened adhoc pillars began to get left behind, but again there was no pattern or structure in the way they were being cut.

Currently, starting in the early 2000s there has been a strategy in place on the design of regional pillars (Priest G, 2013). As mining continues to go deeper, seismicity associated with pillar bursts has been experienced at Siphumelele Mine (one of the sister mines using similar regional pillar design strategies) (Van Asegan, et al., 2014). This indicated that there was need to re-evaluate the current pillar design strategy being employed within Rustenburg Platinum Mines (RPM). The KORP section gave the opportunity to design pillars that would help maintain the stability of the mine and also come up with a new pillar design strategy for the RPM operations.

1.6 Definition of the Research Problem

Snyman, (2015) noted that the current mining area is reaching the mine boundaries, with the MR only planned for another 6 – 7 years at current production rates. Khuseleka Ore Replacement Project (KORP) is designed to replace the ore reserves that are being depleted on both the MR and UG2 reef horizons and also to extend the life of mine. The UG2 reef is currently being mined from 10 to 15 level on both the eastern and western parts of the shaft up to the boundary pillars at a depth of up to 600m. The UG2 expansion project ranges from 16 to 28 levels and is currently limited to the 27 raise line with over and under-stoping of the haulage planned. The mining depths planned for UG2 will go down to about 950 m below collar. The

UG2 has not been mined to these depths before and information is limited on the stability of the pillars at these depths.

When the KORP section starts mining, it is important that the section remains both economically viable and stable for the entire life of the mine. The regional pillars should therefore be designed to fulfil these objectives.

1.7 Project Justification

As stated in the research problem section, current resources are being depleted and new areas of the mine have to be opened up to extend the mine life. These areas have to be opened up safely and remain stable for the duration of the mine's life. Since pillars are pieces of ore left behind for stability, their size contributes to the mine's extraction ratio and thus its profitability. Therefore pillars are designed in such a way that they are not too big so as to leave ore behind or too small so as to adversely affect the stability of the mine.

1.8 Project Objectives

The main objectives of the project were:

a) designing the regional pillar layout for the KORP section using current empirical and numerical pillar design methods and comparing the results to come up with the most optimal design.

b) maximisation of extraction ratio, thereby maximising the mines' profitability.

c) ensure the stability of the on and off reef mine infrastructure by determining the Rockwall Condition Factor (RCF) values on the footwall infrastructure due to pillars left above and thus prevent damage to these excavations through stress induced failures. Consideration was given to the standard Khuseleka footwall infrastructure layouts for the design based on the planning department's layout of haulages and crosscuts for the KORP section.

d) numerical modelling analysis of the effects of leaving stabilizing pillars on the 27 raise line where the haulages intersect the reef horizon.

1.9 Contents of the Research Report

In order to meet the objectives of this project logical steps had to be followed in the design of the pillars. These steps involved:

Reviewing of different pillar strength and load theories to determine the factors of safety, as well as assessing the current pillar design strategy for Khuseleka shaft in the literature review chapter. Also discussed in literature review were the different methods of determining the rock mass and foundation strengths and rockwall condition factors for the stability of footwall excavations. In Chapter 3 the methodology of the project was discussed. Chapter 4 was about the determination of the rock mass properties and parameters that were to be used in the project. This involved taking rock samples to the Wits laboratory for elastic property tests, getting results of other laboratory tests done at other operations, as not all tests were conducted, getting stress measurements from other mines in Rustenburg with similar conditions and then using that information for determining the parameters for use in various calculations and numerical modelling. The Chapter 5 focused on the actual design of pillars using empirical methods from the literature review chapter and the parameters determined in Chapter 4. Chapter 6 focused on designing the pillars using three different numerical modelling programs, namely Examine2D, Lamodel and Map3D. These designs were then compared with those obtained from Chapter 5 to determine the optimal design. Using Map3D, the effects of the pillars on footwall excavations and the leaving of stability pillars on the haulage/reef intersections were also analysed. Chapter 7 gave the conclusions and recommendations. Raiseline middling distances, elastic property graphs, stoping widths in the KORP section, rock mass classification input data and KORP log boreholes were given in the appendices section.

CHAPTER 2: LITERATURE REVIEW ON PILLAR DESIGN

2.1 Introduction

Pillars play an important role in the stability of mining operations. Ryder & Ozbay, (1990), defined regional pillars as squat, strong pillars usually rib or rectangular in outline and oriented on dip or strike, which are designed to provide regional support. They further stated that these pillars should remain elastic and not fail over the entire life of the mine, with a width:height ratio of >10 which will ensure they are indestructible. Regional pillars serve to:

a) compartmentalise the mine into distinct regions (to prevent the spread of a collapse).
b) increase strata stiffness substantially so as to reduce the possibility of large-scale instabilities at source.
c) assist in tensile zone, excessive closures and surface subsidence control, thereby limiting convergence to the extent that in-stope support will not be damaged.
d) reduce the shear and compressive stresses on the mine face, which minimises face bursting, thereby reducing the stope seismic risk.
e) reduce shear stresses on major geological features such as dykes and faults (Ryder & Ozbay, 1990).

Important considerations in pillar design are pillar strength, in-situ stresses (depth below surface), stoping width and the span between regional pillars. Figure 2.1 is a flowchart which shows the process and parameters required to designing a pillar layout.

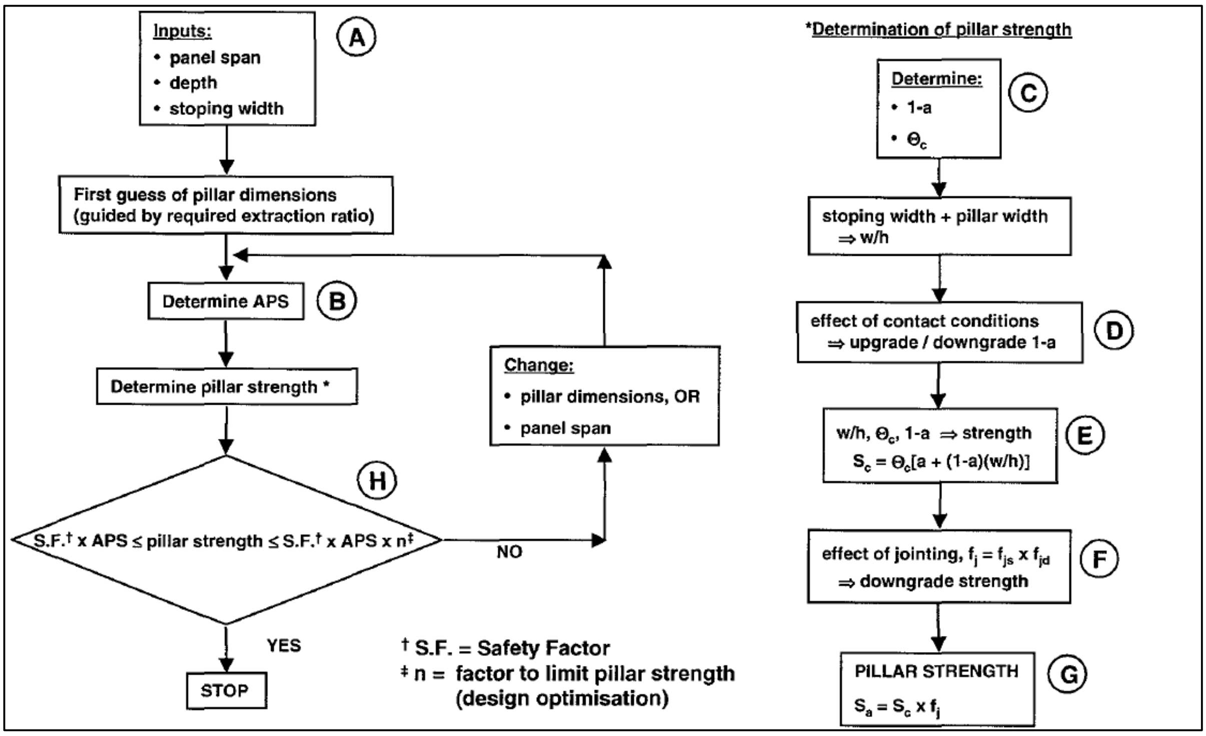

Figure 2.1: Pillar design flowchart (York, et al., 1998).

2.2 Khuseleka Shaft's Current Mining and Stability Strategy

Khuseleka Shaft currently has a regional support design strategy which was looked at, discussed and compared with other pillar design criteria available during the execution of the project.

Priest, (2013) stated that a sound strategy for the stability of the mine is essential to avoid hazards such as surface subsidence, collapse of working areas and major fall of ground incidents. These hazards can be addressed in the design of the mining method and layout. A number of factors influence the local and regional stability of the mining environment. These include, but are not limited to:

- Mining method
- Regional pillars
- Instope pillars
- Instope support
- Barring and examination

The mining method and regional pillars are the two factors which influence regional stability and will be briefly discussed below.

2.2.1 Mining Method

The mining method implemented on a shaft is usually determined by:

- Depth of mining
- Ore body characteristics and geometry
- Surrounding rock mass
- Financial consideration

The mining method most commonly used at Khuseleka shaft is scattered breast using small in-stope pillars and regional pillars to maintain stability of the workings. In all cases the configuration or sequence adopted is that of mining towards solid whenever possible (Figure 2.2).

The middling between the MR and UG2 reef is approximately 140m, therefore it is not expected that the pillars left on the MR horizon will have a significant influence on the underlying UG2 reef.

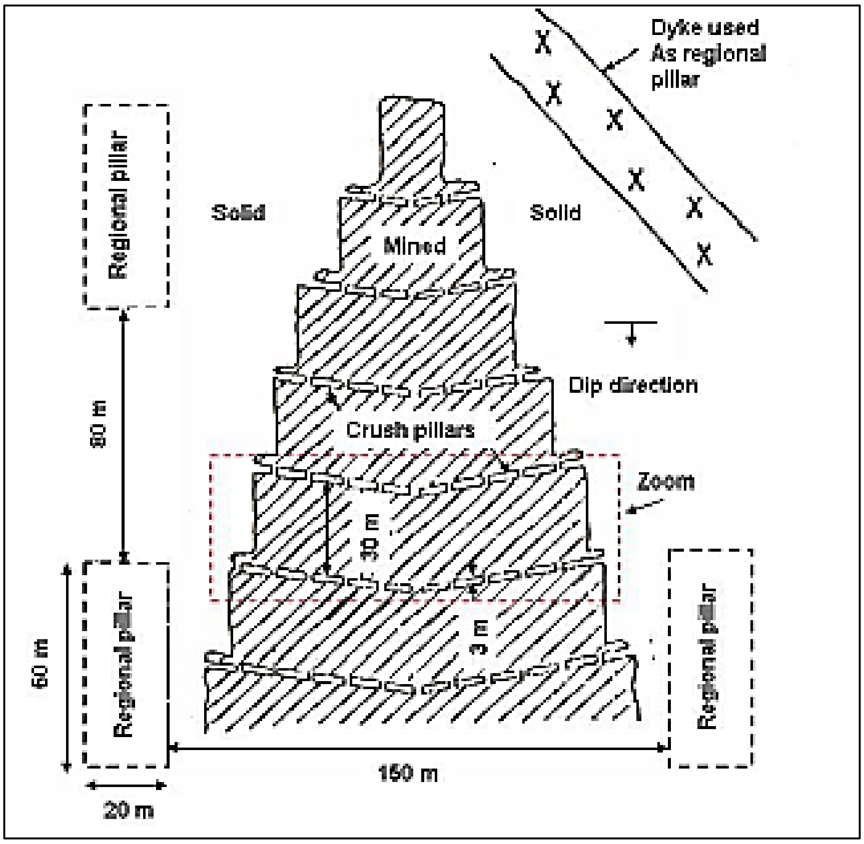

Figure 2.2: Plan view of a typical breast configured stope on the MR (Ozbay & Roberts, 1988).

2.2.2 Regional Pillar Design Strategy

Priest, (2013) stated that the regional pillar design strategy employed by Anglo American Platinum involves the combination of regional pillars, geological losses and mine perimeter boundaries capable of supporting the overburden up to surface. Unless geological losses are known, the regional pillar design assumes "no loss" unless a loss is confirmed.

Size of Regional Pillars

a) Regional pillars shall be of sufficient size and frequency that the average pillar stress (APS) shall be limited to the lesser of:

i) 500 MPa

ii) Strength of the pillar/1.6 as calculated by the squat pillar formula combined with effective pillar width = 4 x area of the pillar / perimeter

Note the effective width shall be limited to 1.33 x the smallest dimension.

b) Average pillar stress shall be calculated by tributary area theory (TAT) or numerical modelling.

c) Consideration and site knowledge should also be given to foundation failure.

d) Regional pillars will have a minimum width: height ratio of 10:1 (Priest, 2013).

Spacing of Regional Pillars

In order to limit the mining span, regional pillars shall be spaced at a maximum span of no more than Depth/2 (Priest, 2013). This design criteria differs considerably from the one proposed by Ryder and Ozbay, (1990) in Section 2.9 of this chapter.

2.2.3 Placement of Regional Pillars

The position to place a regional pillar requires prior knowledge of certain factors which are:

a) Placement of regional pillars should consider practical mining constraints such as effective scraping distances to ensure effective cleaning of working places.

b) The position of regional support relative to off-reef infrastructure where the latter is already in place must be considered. Consideration should be given to potential damage to these excavations from both a static and dynamic perspective. Numerical modelling should be conducted to ensure that these excavations remain stable for the intended life of the excavation.

c) An ideal position for regional pillars is the final remnant between two scattered stopes as illustrated in Figure 2.3 where mining is from crosscut to crosscut towards the pillar (Priest, 2013).

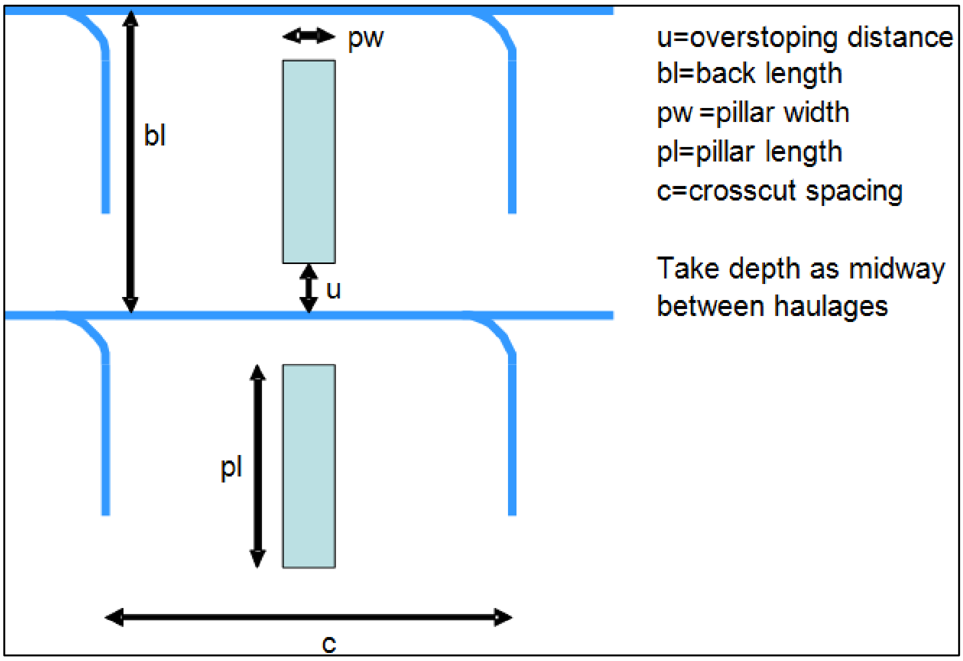

Figure 2.3: Schematic of Khuseleka Pillar Design Layout (Priest, 2013)

2.3 Pillar Loads

The elastic stress distribution in pillars is governed by the pillar shape, size and insitu stress of the rock mass where mining will take place. In order to design pillars, knowledge of the stresses acting on the pillars is very critical. Knowledge of this stress starts by determining the insitu stress in the rock mass to be excavated. The vertical insitu stress magnitude is usually taken as the unit weight of the overlying rock (ɣ) times the depth (z) (Hoek, et al., 1997). The determination of this vertical insitu stress is one of the components used in calculating loads acting on pillars using the tributary area theory (TAT), Coates method and numerical modelling.

2.3.1 Tributary Area Theory

The loads acting on a set of pillars may be estimated by means of a concept known as 'tributary area theory'. The act of mining removes support of the overburden, and for equilibrium to be maintained, this weight has to be transferred to areas of intact rock. The theory is only valid for completely regular layouts where the spans are very large (Ryder & Jager, 2002). This point is illustrated by the diagram in Figure 2.4.

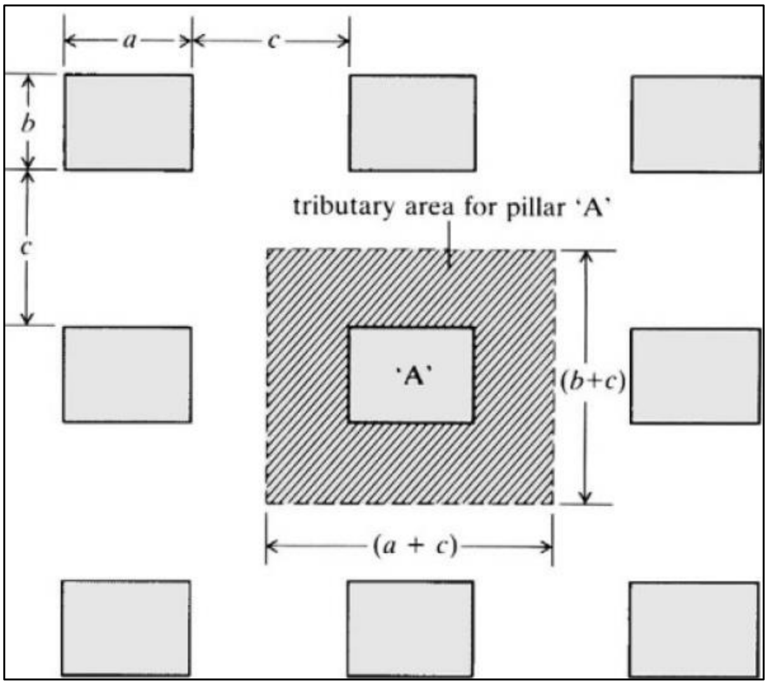

Figure 2.4: Plan showing tributary area theory layout (Brady & Brown, 2005)

The weight or load carried by a particular pillar is what is termed as the average pillar stress. Average pillar stress (APS) according to TAT is given as

$$APS = \frac{\sigma z}{1-e} \tag{1}$$

Where:

σ_z = In situ stress acting normal to the pillar axis given by $\gamma z = \rho g h$

ρ = rock density (kg/m^3)

g= gravitational acceleration (m/s^2)

h = Depth below surface (m)

e =Extraction ratio. Brady & Brown, (2005), gives this extraction ratio for rectangular pillars using Figure 2.4 as

$$e = \frac{[(a+c)(b+c)-ab]}{(a+c)(b+c)} \tag{2}$$

Limitations to the tributary area theory were highlighted by Van der Merwe, (1998) who stated that it is only valid for cases where the panel width is more than the depth to the reef and where the pillars in a panel are the same size. Other factors picked up include the percentage extraction and the stiffness of the overburden. Brady & Brown, (2005) highlight that the average pillar stress is purely a convenient quantity representing the state of loading of a pillar in a direction parallel to the principal direction of confinement. It is not simply or readily related to the state of stress in a pillar that could be determined by a complete analysis of stress. They are also of the view that the tributary area analysis restricts attention to the pre-mining normal stress component directed parallel to the principal axis of the pillar support system. They argue that the implicit assumption that the other components of the pre-mining stress field have no effect on pillar performance is not generally tenable. They further argue the fact that the tributary area theory ignores the effect of the location of the pillar within a mine panel.

Based on these arguments it becomes necessary to find other methods that try to limit or circumvent the arguments highlighted above.

2.3.2 Coates Method

The tributary area theory is unsatisfactory as it does not take geometrical and rock properties into account. Coates, (1981), proposed a formula which would take the properties stated below into consideration:

- The span of the mining zone with respect to depth
- Height of the pillars
- Pillar location within the mining zone
- Horizontal stress, and
- Modulus of deformation of the pillar and wall rock materials

Coates, (1981) came up with a formula applicable to calculating average pillar stress in deep and long mining zones shown below:

$$APS = \sigma z \; x \left[1 + \frac{2e(1+h_s) - kh_s(1-w+nw_p)}{h_s n + 2(1-e)(1+h_s) + \frac{2eb\,(1-w)}{\pi}}\right] \tag{3}$$

$e = \frac{B_o}{B_o+B_p}$, $k = \frac{\sigma_h}{\sigma_v}$, $w = \frac{v}{1-v}$, $w_p = \frac{v_p}{1-v_p}$, $n = \frac{E\,(1-v_p^2)}{E_p(1-v^2)}$, $b = \frac{B_p}{L}$, $h_s = \frac{H}{L}$

Where:

σ_z	is vertical virgin stress, (MPa)
e	is extraction ratio
H	is height of stope, (m)
σ_h	is the horizontal component of the virgin stress, (MPa)
k	is the general expression for k-ratio
w	k-ratio for abutments
w_p	k-ratio for pillars
n	is a simplifying expression relating Poisson ratio and Young Modulus
b	is pillar width to extraction span width ratio
h_s	is height of stope to extraction span width ratio
υ	is Poisson's ratio for abutments
υ_p	is Poisson's ratio for pillars
E	is Young's Modulus for abutments
E_p	is Young's Modulus for pillars
B_o	is room width, (m)
B_p	is pillar width, (m)
L	is width of extraction span, (m)

Just like the TAT, the limitation of the Coates method is that it is only valid in the centre of the mining area with undisturbed long rib pillars, and where the mine span does not exceed half the depth.

2.3.3 Numerical Modelling

Limitations of the empirical methods make it imperative to use numerical modelling in determining the pillar stresses during mining. Starfield & Bleloch, (1986) stated that "a model is a representation or abstraction of a system or process. It is an intellectual abstraction that includes purpose, reference and cost effectiveness."

Diering & Stacey, (1987) highlighted that, "it should not be the aim of a numerical modelling analysis to get absolute answers. The analyses must be regarded only as an aid to design and not a design method in the absolute sense." This statement highlight the fact that when determining loads on pillars (average pillar stresses) using numerical modelling techniques, it is important to note that the idea is not to get absolute values, this is not possible given the complex and numerous variables making up a rock mass that are used as input parameters when modelling. Rather, the idea is to get a trend and feel of the results obtained and making observations underground to validate the assumptions made. It is therefore logical and good practice to compare numerical modelling results with results obtained using empirical methods in order to validate the assumptions made. Back analysis on areas of similar properties is also good practice, so as to calibrate and validate values used. The advantage of numerical modelling versus the traditional empirical methods is that it can cater for different geometries and scenarios that were identified as limitations in tributary area theory and Coates methods.

Three numerical modelling programs were used in this project to give comparisons and also validate the assumptions that were made.

Examine 2D

This is a two dimensional, boundary element stress analysis method that has the advantage of being quick to run and not as complex as other analysis methods. This is because it represents a mining layout in 2D as a cross—section and displacement and strain out of the plane are assumed to be zero (plane strain condition) (Rocscience, 2012).

Map3D

This is a three dimensional, boundary element stress analysis method which uses both displacement discontinuity (DD) and fictitious force (FF), depending on whether the analysis is for stopes or large excavations respectively (Wiles, 2013). The advantage of this program is that the actual layout from the CAD program used on the mine for mine planning purposes can be imported directly into the program and analysed, giving a true representation of the layout.

LaModel

Lamodel is a boundary element numerical modelling program which calculates stresses and displacements in thin bedded deposits.

It consists of three separate programs, Lampre, Lamodel and Lamplt. Lampre is the pre-processor that facilitates creating the input file for Lamodel which then calculates the stresses and displacements at the seam level from the input. Lamplt is the post-processor that allows the user to plot and analyze the output.

The programme simulates the geological overburden stratifications as a stack of layers with frictionless interfaces (NIOSH, 2017).

Other Modelling Work Done by the Institute of Mine Seismology (IMS)

Numerical modelling has been carried out in mined out areas as part of the contract that IMS has with Anglo American Platinum using their IMS programs. This work is detailed and done by professionals with vast experience in numerical modelling. Comparison with this work was carried out.

2.4 Pillar Strength

Stacey & Page, (1986) argued that pillar strength depends on three factors; the rock mass strength of the pillar material, the shape and size of the pillar defined by its width and height, and gross structural features such as clay bands, faults and joints. Since there are no clear cut engineering methods available to determine pillar strength for pillar design, back analysis has been the most popular approach. Back analysis is an empirical method requiring that data on observed failed pillars is collected and best fit strength envelopes are created from this data. This approach was first carried out successfully on coal mines Salamon & Munro, (1967); there has however been limited studies and data collected on hard rock pillars. Most pillar designs on hard rock mines have relied on equations and methods designed for coal pillars with very little or no variation.

The most common strength formulae will be discussed briefly below.

2.4.1 Salamon and Munro (1967) Formula

Following the Coalbrook disaster of 1960 major research in coal mine pillar design was instituted. Salamon & Munro, (1967) postulated that the strength of the pillars can be expressed, in the given range of dimensions, as a power function of the pillar's height and the width. From this they came up with the following equation

$$\text{Strength} = K\frac{w^{0.46}}{h^{0.66}} \qquad (4)$$

Where:

K	is fitted strength of a meter cube of coal (7.2MPa)
h	is height of the pillar (m)
w	is pillar width (m)
0.46, 0.66	are empirical constants

The disadvantage of this formula although used successfully all over the world is that it is based on a limited sample of pillars on one particular mine which is meant to be a representative of what would be expected on all the coal mines throughout the world. Of course this is not possible, with the diversity found in not only the geological setup and mining methods, but also rock structures between even neighbouring mines this equation cannot be used as a blanket equation for all pillars. Worse still, the strength formula and empirical constants are based on coal properties, which are different from hard rock mines' rock mass properties for which it is sometimes being used.

2.4.2 Hedley and Grant (1972) Formula

Hedley & Grant, (1972) developed their formulae for hard rock mines based on uranium pillar strength in Elliot Lake District adopting a similar approach to that of (Salamon and Munro 1967). The data only contained 28 pillars of which 3 were "crashed" and these were mining at a depth ranging from 150m to 1040m. The pillar stresses were calculated using tributary area theory (TAT). They determined the following power law formula

$$\text{Strength} = K\frac{w^a}{h^b} \tag{5}$$

Where:

K	A downgrading value extrapolated from the rock which varies between a third and 100% of UCS (MPa) of the rock
a	was assumed to be 0.5 from previous literature
b	was obtained from the 3 crushed pillars to back calculate and give an average of 0.75
w	width of the pillar (m)
h	height of the pillar (m)

Although this formula is very popular and one of the most used for pillar design in hard rock mines, Hedley and Grant contend that "the information on complete pillar crushing was obtained second-hand because it happened in mines which are closed" (Hedley & Grant, 1972). Therefore this formula cannot be used with full confidence as the basis of the data used is limited.

2.4.3 Watson, et al (2008) Merensky Pillar Strength Formula

Watson, et al., (2008) developed a power formula for MR pillars based on a database with 179 pillars of which 109 were stable. Working on back analysis using similar concepts as Salamon & Munro, (1967) and Hedley & Grant, (1972) they were able to come up with a formula specifically for the Merensky orebody, shown below

$$\text{Strength} = 86\frac{w^{0.76}}{h^{0.36}}\text{MPa} \tag{6}$$

Where:

w	width of the pillar (m)
h	height of the pillar (m)

The advantage of this formula over the others discussed above is that it was developed specific to the conditions observed in the Merensky section of the bushveld complex, making it more relevant to those specific conditions. It is empirical, meaning that it cannot be applied outside the geotechnical range for which it was formulated.

2.4.4 Potvin, Hudyma and Miller (1989) Pillar Strength Formula

Potvin, et al., (1989) formulated an equation based on empirical evidence on rib pillars in open stope mines in Canada. When plotted as pillar stability graph the equation takes the following form:

$$\frac{\sigma_{ps}}{UCS} = 0.4162\,\frac{W}{h} \qquad (7)$$

Where:

σ_{ps}	Pillar strength (MPa)
UCS	uniaxial compressive strength (MPa)
w	width of the pillar (m)
h	height of the pillar (m)

Potvin, et al., (1989) considered their pillar strength curve equation to be less conservative as they incorporated larger pillars in their data base, as compared to Hedley & Grant, (1972) which was developed based on the response of smaller pillars.

2.4.5 Vonn Kimmelmann, Hyde and Madwick (1984) Pillar Strength Formula

Von Kimmelmann, et al., (1984) determined an empirical pillar stability graph based on case studies done at Selebi and Phikwe nickel mines in Botswana. An equation similar to that of Salamon and Munro (1967) was used except that a value of 65MPa was used for K based on their studies and back analysis. The equation formulated is shown below

$$\text{Strength} = 65\,\frac{w^{0.46}}{h^{0.66}}\text{MPa} \qquad (8)$$

Where:

w	width of the pillar (m)
h	height of the pillar (m)

2.4.6 Krauland and Soder (1987) Pillar Strength Formula

Krauland & Soder, (1987) carried out studies of pillars at Black Angel Mine in Greenland. They used the following pillar strength formula proposed by Obert and Duval (1967)

Strength = $\sigma_{ps}\left(0.778 + 0.222\frac{W}{h}\right)$MPa (9)

Where:

w	width of the pillar (m)
h	height of the pillar (m)
σ_{ps}	strength of a pillar (K equivalent) with a w/h ratio of 1 (MPa).

For the rocks they examined with a UCS of 100MPa, they found that the best fit value for $\sigma_{ps}$was 35.4MPa, which was about 35% of UCS.

2.4.7 Sjoberg (1992) Pillar Strength Formula

Sjoberg, (1992) used the equation of Obert and Duval (1967) just like Krauland & Soder, (1987) when they did their study on the pillars at the Zinkgruvan Mine in Sweden. The UCS value of their rocks was 240MPa giving a best fit value of 74MPa for σ_{ps} , which was about 30% of the rock UCS.

2.4.8 Lunder and Pakalnis (1997) Pillar Strength Formula

Lunder & Pakalnis, (1997) compiled a database of pillar case histories from all the authors discussed above. Making use of this database Lunder and Pakalnis formulated the 'Confinement Formula' for determining the strength of hard rock mine pillars shown below

$Strength = (K * UCS)x(C_1 + C_2$*kappa) (10)

Where:

K	is rock mass strength size factor which they averaged at 44%
C_1C_2	empirically derived constants determined to be 0.68 and 0.52 respectively.
kappa	the mine pillar friction term given as

$\tan[Cos^{-1}\left(\frac{1-Cpav}{1+Cpav}\right)]$ (11)

Cpav is the average pillar confinement, defined as the ratio of the average minor to the average major principal stress at the mid-height of the pillar. This can be calculated as follows

$Cpav = 0.46x\left[\log\left(\frac{W}{h} + 0.75\right)\right]^{\frac{1.4}{\frac{W}{h}}}$ (12)

2.4.9 Stacey and Page (1986) Pillar Strength Formula

Stacey & Page, (1986) recognised that at width to height ratios greater than 4.5, strain hardening behaviour can occur. They took this behaviour into account by producing exponential rises in pillar strength at higher width to height ratios

For width: height < 4.5

$$\text{Strength} = K \text{ x } \frac{w^{0.5}}{h^{0.7}} \text{MPa} \qquad (13)$$

For width: height > 4.5

$$\text{Strength} = K \text{ x } \frac{2.5}{V^{0.07}} \text{ x } \{0.13 \text{ x } \{[\frac{\frac{w_{eff}}{h}}{4.5}]^{4.5} - 1\}+1\}\text{MPa} \qquad (14)$$

Where k = σ_m*Design Rock Mass Strength (DRMS)

DRMS is an adjustment factor of the unconfined rock mass strength of rock in a specific underground mining environment.

$V = w^2_{eff} \text{ x } h$

$$w_{eff} = 4 \text{ x } \frac{A_p}{C} \qquad (15)$$

Where: A_p = Plan area of the pillar

C = Perimeter

Wagner, (1980) showed that this ratio of the area, A_p to the circumference, C, of a pillar has a strong influence on the pillar strength for irregularly shaped pillars thus equation (15) was used to calculate the effective widths on all pillar strength calculations for this project.

2.4.10 Summary of Empirical Pillar Strength Equations

Table 2.1 summarises the different pillar strength formulae that were discussed in the preceding section.

Martin & Maybee, (2000) designed a combined pillar stability graph summarising the different empirical formulae shown in Figure 2.5. The graph shows that as the width to height ratio increases ratio of the pillar strength to UCS approaches unity, meaning that pillar strength increases with increase in the pillar to height ratio. This observation agrees with Stacey & Page, (1986) equation which factores in this increase in strength into their formula.

Table 2.1: Summary of empirical pillar strength equations for hard rock pillars

Author	Pillar Strength Equation
Salamon and Munro (1967)	Strength = $\left(K\frac{w^{0.46}}{h^{0.66}}\right)$
Hedley and Grant (1972)	Strength = $\left(K\frac{w^{a}}{h^{b}}\right)$
Watson, et al (2008)	Strength = $\left(86\frac{w^{0.76}}{h^{0.36}}\right)$MPa
Potvin, Hudyma and Miller (1989)	$\frac{\sigma_{ps}}{UCS} = 0.4162\frac{W_p}{h}$
Vonn Kimmelmann, Hyde and Madwick (1984)	Strength = $\left(65\frac{w^{0.46}}{h^{0.66}}\right)$MPa
Kraulan and Soder (1987)	Strength = $\sigma_{ps}\left(0.778 + 0.222\frac{W_p}{h}\right)$MPa
Sjoberg (1992)	Strength = $74\left(0.778 + 0.222\frac{W_p}{h}\right)$MPa
Lunder and Pakalnis (1997)	$Strength = (K * UCS)x(C_1 + C_2$*kappa)
Stacey and Page (1986)	Strength = K x $\frac{2.5}{V^{0.07}}$ x { 0.13 x { $[\frac{\frac{W_{eff}}{h}}{4.5}]^{4.5}$ – 1}+1}MPa

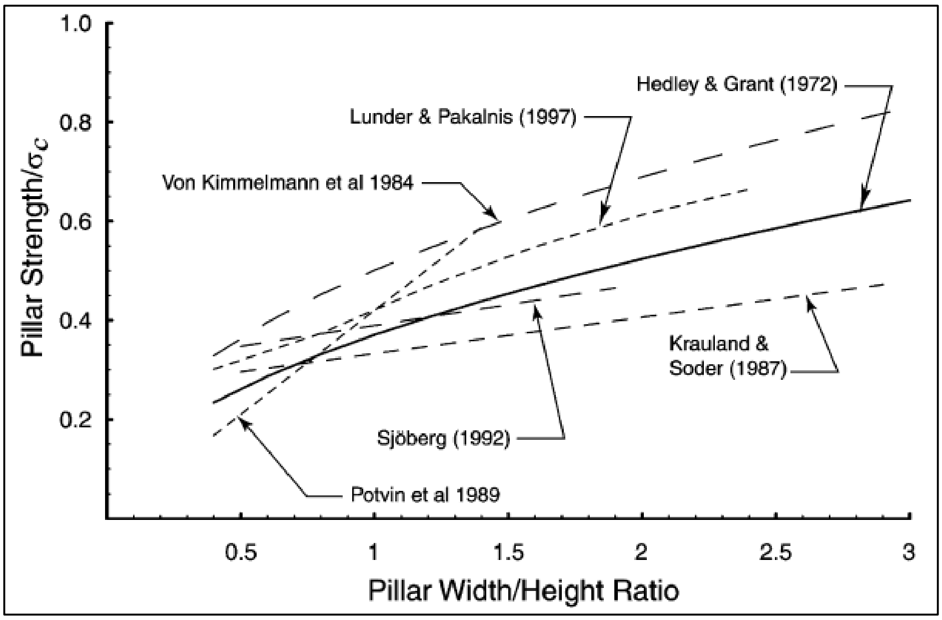

Figure 2.5: Comparison of the empirical pillar strength formulae (Martin & Maybee, 2000).

York, et al., (1998) stated that "Empirical formulae such as these have the limitation that they must be used with caution for design values that fall outside the empirical range. Empirical formulae should also not be used in geotechnical areas different from that which the empirical data was obtained". This statement clearly shows that caution must be exercised when using these formulae and discretion must be exercised by the engineer who uses them. It is very important to first define the conditions under which the design will be made, then choose the most appropriate formula that best suits or is closest to the range of conditions under which the empirical formula was derived.

As Figure 2.5 shows there is a strengthening effect on the pillars associated with an increase in the width to height ratios. Based on this observation the most ideal formulae to use for this project would be the one proposed by Stacey & Page, (1986) which takes this strengthening effect into account.

2.5 Width: Height Ratio

Ryder & Jager, (2002) concluded that the strength of a pillar, assuming normal non-weak foundations, increases significantly as a function of its width: height ratio (w :h ratio), due to essentially friction-induced confinement at the foundation. All the strength formulae above have a w: h ratio as a component, and as the formulae indicates, the larger the ratio the stronger the pillar. It is therefore very important to ensure that the w: h ratio is taken into account when designing the pillars. Ryder & Ozbay, (1990) gave a guide as to the w: h ratio of typical pillars designed for underground excavations. As illustrated in Figure 2.6, regional pillars are non-yielding and are referred to as squat pillars with a w: h ratio equal to 10 or greater.

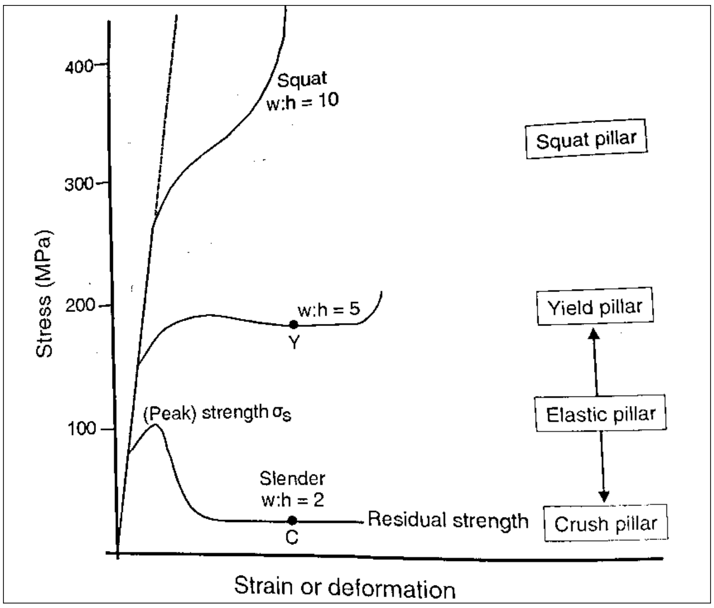

Figure 2.6: Graphical representation of different pillar types with their associated stress-strain curves (Y = yield, C= crush) (Ryder & Jager, 2002)

2.6 Factor of Safety

The factor of safety (FOS) in pillar design is defined as

$$\text{FOS} = \frac{\sigma_s}{APS} \tag{16}$$

Where σ_s = pillar strength (MPa) and APS = average pillar strength (MPa)

Ryder & Jager, (2002) have stated that a FOS of 1.6 for non-yield (elastic) pillars used in coal mines based on back analysis has been adopted for pillar design in hard rock tabular mines. They further stated that higher FOS are sometimes required if damaging subsidence under critical surface structures have to be designed against. Stacey, (2001), stated that for regional pillars an FOS of 2.0 is sufficient.

2.7 Rock mass Strength

Since pillars are cut in the natural rock mass it is critical to know the strength of the rock mass as this is one of the major components that determines the pillar strength. As discussed above, the value of K used in the calculation of pillar strength is derived from the rock mass strength.

The uniaxial compressive strength (UCS) from laboratory tests of core or rock specimens is the starting point when determining the rock mass strength. However, the rock specimen for which the UCS is tested is too small relative to a mining operation and usually does not contain any geological or lithological imperfections. This implies that laboratory test or UCS values are an overestimation of the actual strength of the rock mass and therefore cannot be used on their own as the rock mass strength.

Different criteria have been derived based on empirical evidence to come up with the rock mass strength, these are discussed below and are summarised in Table 2.2.

2.7.1 Mohr-Coulomb Criterion

Goodman, (1989) discussed the Mohr-Coulomb relationship based on two separate theories as follows:

Mohr hypotheses' that the envelope around the Mohr's circles drawn in the σ:τ plane corresponding to the results of a set of triaxial tests expressed a general functional law $\tau = f(\sigma)$. Coulomb's classical analysis took a more direct physical view: that rock failed once the shear stress $\tau - \mu_i\sigma$ across a particular critically-inclined macroscopic plane exceeded a certain inherent cohesion value C_o; where μ_i is an empirical 'coefficient of internal friction and

$\mu_i = \tan\phi_i$, where ϕ_i is the 'angle of internal friction'.

Coulomb's $\tau = C_o + \mu_i\sigma$ analysis represents a linear Mohr-type relation in τ:σ space, hence the designation Mohr-Coulomb criterion – Figure 2.7(b). Moreover, a linear relation in τ: σ space translates in to a linear relation

$$\sigma_1 = \sigma_c + \beta_o\sigma_3 \tag{17}$$

in the $\sigma_1 - \sigma_3$ plane – Figure 2.7(c)

Based on the above, useful inter-relationships apply as follows:

$$\sigma_c = 2C_o\sqrt{\beta_o} \qquad \beta_o = \frac{(1+\sin\phi i)}{(1-\sin\phi i)} \tag{18a}$$

$$\sin\phi i = \frac{(\beta o-1)}{(\beta o+1)} \qquad C_o = \frac{\sigma c}{2\sqrt{\beta o}} \tag{18b}$$

A best-fit straight line can be established in the $\sigma_1 - \sigma_3$ plot Figure 2.7(c), read off the values of σ_1 intercept σ_c and a slope β_o, and calculate the angle of internal friction ϕ_i and cohesion from the final pair of the above relationships (Equation 18b)

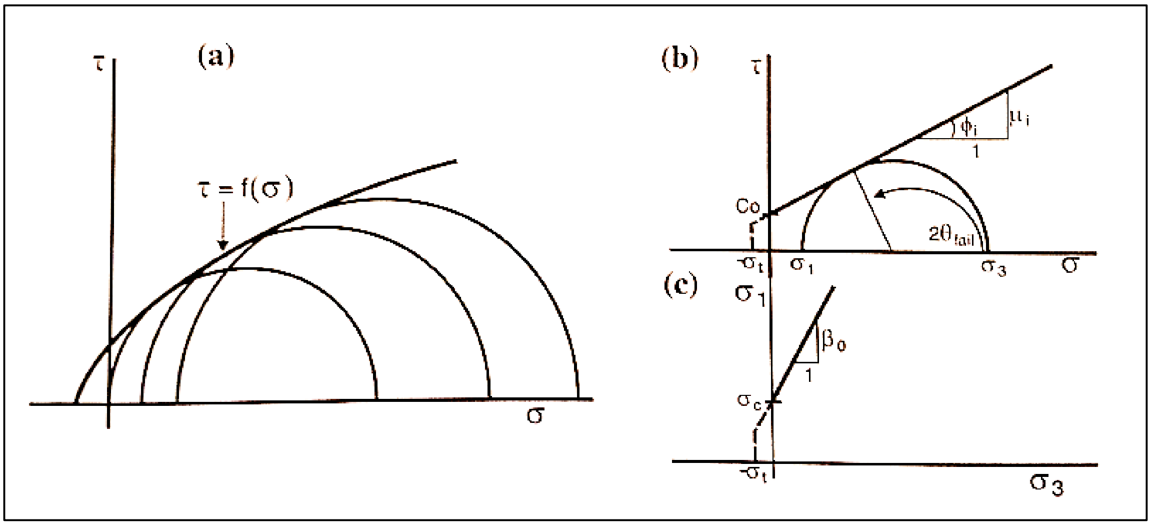

Figure 2.7: (a) Mohr's f(σ) hypothesis (b) Mohr-Coulomb in τ-σ space (c) Mohr-Coulomb in σ1 – σ3 space (Goodman, 1989)

As noted by Goodman, (1989), although the Mohr-Coulomb criterion is widely used, it is not particularly satisfactory for peak strength of rock material. The reasons for this being:

- It is a shear strength criterion which implies a major shear fracture occurs at peak strength.
- It implies a direction of shear failure which does not always agree with experimental observations.
- Experimental peak strength envelopes are generally non-linear.

2.7.2 Hoek-Brown Failure Criterion

Hoek, et al., (2002) developed an empirical criterion for rock mass failure based on tests on intact rock and rock mass models. The generalised form of the Hoek-Brown failure criteria is

$$\sigma_1 = \sigma_3 + \sigma_c\{m_b.\frac{\sigma_3}{\sigma_c} + s\}^a \quad (19)$$

Where:

σ_1, σ_3	major and minor effective principal stresses at failure
σ_c	unconfined compressive strength of the intact rock
m, s, a	parameters which depend on the rock mass characteristics given by

$m_b = m_i e^{\frac{GSI-100}{28}}$

$s = e^{\frac{GSI-100}{9}}$

$a = 0.5$

The strength value obtained through this method can be used in numerical modelling or as the K value when calculating pillar strength. This is because an estimate of the actual strength of the rock mass based on geological and physical conditions and not just the UCS from laboratory tests is derived.

Just like the Mohr-Coulomb failure criterion, this criterion is also shear based. They both do not recognise the influence of the intermediate stress on strength, only the major and minor stress.

2.7.3 Barton's Q criterion

Barton's Q system was originally developed to assist in the empirical design of tunnel and cavern reinforcement and support, but it has been used for several other tasks in rock engineering in recent years (Barton, 2002). One of these tasks is to determine the rock mass strength. The equation below was formulated to determine the rock mass strength based on normalised Q value

$\sigma_1 = 5\gamma Qc^{1/3}$

where $Qc = Q_0 \times \sigma_c/100$, Q_0 is Q calculated with RQD_0 oriented in the loading or measurement direction and Qc is rock mass quality rating (Q_0; normalised by σ_c /100)

γ is rock mass density (kg/m^3)

2.7.4 Design Rock Mass Strength (DRMS)

Laubscher, (1990) came up with a rock mass classification system that calculates rock mass strength (RMS) and design rock mass strength (DRMS) from the intact rock UCS and mining rock mass rating (MRMR) of the rock mass, using the relationship

$$RMS = UCS\ x\ (MRMR - R_{UCS})/100 \qquad (20)$$

Where:

RMS is the rating value corresponding with rock UCS

MRMR is a rock mass classification system that takes into account four parameters namely UCS, RQD, joint spacing, and joint condition and ground water

R_{UCS} The rating value of the UCS

The DRMS is the rock mass strength in a specific mining environment. It is obtained by applying adjustments to the RMS to take into account the effects of weathering, joint orientation and method of excavation.

It is clear from the above that the DRMS value is a value obtained taking into consideration various physical attributes of the rock and mining excavation and attempting to give the actual strength of the rock mass. Thus the value of K for pillar strength design can be assumed to be derived from the DRMS value.

Table 2.2 summaries all the strength criteria that have been discussed in this section.

Table 2.2: Summary of rock mass strength criteria

Author	**Strength Criterion**
Hoek – Brown (2002)	$\sigma_1 = \sigma_3 + \sigma_c\{m_b.\frac{\sigma_3}{\sigma_c} + s\}^a$
Mohr - Coulomb (1979)	$\sigma_c = 2C0\sqrt{\beta_0}$
Laubscher (1990)	$\mathrm{RMS} = \mathrm{UCS\ x\ (MRMR} - \mathrm{R_{UCS}})/100$
Barton, (2002)	$\sigma_1 = 5\gamma Qc^{1/3}$

2.8 Foundation Strength

Jager & Ryder, (1999) suggested that regional pillars are generally squat pillars (w:h ratio ≥ 10) and will not fail by crushing in their own right. An approximate and conservative criterion, that APS < $2.5\sigma_c$, has been proposed to avoid the occurrence of foundations failure, where σ_c is the UCS of the weakest foundation rock material. This criterion does not take into account friction and dilatational properties of the foundation rocks as well as possibly the prevailing k-ratio. Using the UCS values obtained from the tests conducted at the Wits Rock Engineering

Laboratory for pegmatoidal pyroxenite which is the foundation rock, the APS which is ideal for the KORP section using this equation will be calculated.

It is clear that a pillar might be designed not to fail and yet instability of the excavation will occur due to a weaker hangingwall and/or footwall. It is therefore imperative that when designing pillars, the strength of the foundation material is also taken into consideration.

Terzaghi, (1943) and Hansen, (1970) formulated equations to determine the foundation strength.

2.8.1 Terzaghi's Formula

Stacey & Page, (1986) stated that Terzaghi, (1943) formula is the most widely used formula for determining foundation bearing capacity. Referring to Figure 2.8, foundation strength formula is given as:

$$q_u = cN_c + qN_q + \gamma B_p N_\gamma \tag{21}$$

$$N_\gamma = 1.5(N_q - 1)tan\phi \tag{22}$$

$$N_c = (N_q - 1)cot\phi \tag{23}$$

$$N_q = e^{\pi tan\phi} tan^2(\frac{\pi}{4} + \frac{\phi}{2}) \tag{24}$$

Where:

q_u	is foundation strength (MPa)
c	is cohesion of foundation rock (MPa)
B_p	is foundation depth
ϕ	is internal friction angle of foundation rock

Terzaghi, (1943) also stated that q is a parameter which is normally zero unless the failure is likely to take place in a weak bed some distance below or above the floor or roof contact. N_c, N_q and N_γ are bearing capacity factors which depend on the angle of friction of the foundation material. He stated further that if the pillar and the foundation consist of the same material then once a pillar reaches a W: H ratio of approximately 1:7 foundation failure rather than pillar failure can be expected.

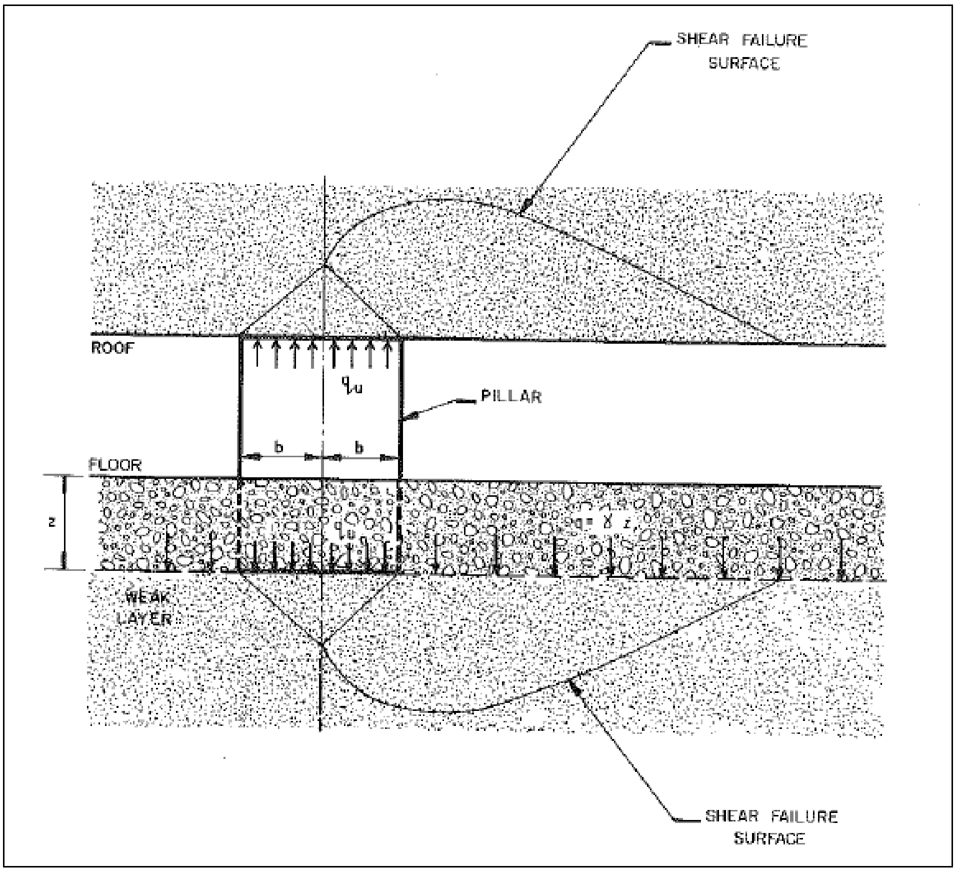

Figure 2.8: Foundation strength for pillar stability (Stacey & Page, 1986)

2.8.2 Hansen's Formula

Hansen, (1970) came up with equations based on Terzaghi, (1943) work with slight changes which are dependent on the shape of the pillar:

Rib Pillar $q_u = cN_c + 0.5\gamma B_p N_\gamma$ (25)

Rectangular Pillar $q_u = cN_q S_q \cot\phi + 0.5\gamma B_p N_\gamma S_\gamma - c\cot\phi$ (26)

Square Pillar $q_u = cN_q(1 + \sin\phi)cot\phi + 0.3\gamma B_p N_\gamma S_\gamma - c\cot\phi$ (27)

$$S_\gamma = 1 - 0.4\frac{B_p}{L_p}$$

$$S_q = 1 + [\sin\phi - \frac{B_p}{L_p}]$$

Where:

B_p	is foundation depth
L_p	is pillar length
γ	is specific weight of rock (MN/m^3), has a positive sign for floor rock and negative sign for roof rock
S_γ, S_q	is a factor of safety depending on the shape of the pillar

2.9 Pillar Spacing

Pillar span (strike spacing between pillars) is one of the most critical considerations in pillar design. Ryder & Ozbay, (1990) suggested that a rule of thumb is to keep this span (L) less than one quarter of the depth (H), i.e., H/L > 4. Numerical modelling and other empirical and analytical methods can also be used to determine the pillar span giving different values to the one proposed by Ryder & Ozbay, (1990) (Swart & Handley, 2005). Although the rule is conservative, there are a number theoretical results that they mentioned which support it:

a) The height of tensile zone is lower at H/L = 4 than it is at H/L = 2, thus reducing the burden placed on the in-stope yield pillars for tensile zone control.
b) The strata regional stiffness falls off fairly rapidly for H/L < about 2; this could prejudice the stability of certain in-stope pillar layouts.
c) In-stope closures and surface subsidences increase in direct proportion to span L, but are often at acceptable levels if H/L ~4.
d) In shallow non-yield pillar layouts, lower H/L ratios, adequate factors may be acceptable since the in-stope pillars themselves provide substantial tensile zone and closure control. For adequate compartmentalisation, however, L should rarely exceed approximately 250m.
e) At low H/L ratios adequate factors of safety against regional instability become difficult if not impossible to achieve, and this places an increased premium on the choice of an adequately high factor of safety for the strength of the in-stope pillars Ryder & Ozbay, (1990).

Ryder & Ozbay, (1990) suggested the use of numerical modelling for the choice of a span for operational regional pillars, but modifications may well be required in practice particularly in the light of local geological conditions that are encountered during mining.

2.10 Placement of Footwall Excavations

The Khuseleka mine layout has a system of footwall excavations in the form of tunnels and haulages. Haulages are developed at a minimum of 35m below reef, whilst crosscuts at the same level are spaced 200m apart (Kuca, 2013). According to Budavari, (1983), service excavations are subjected to stresses and displacement which are induced by the main or productive mining excavations. These effects can be, and often are, severe enough to affect the safety of men and continuity of production. It is clear that the footwall excavations at Khuseleka can be subjected to high field stresses from abutments left in the reef horizon. Thus it is very important to ensure that when designing regional pillars, footwall excavations are taken into consideration. A number of strategies to deal with or determine the effect of pillars on footwall excavations are available.

2.10.1 Rockwall Condition Factor Criterion

A recommended design criterion for expressing and controlling tunnel conditions is the rockwall condition factor (RCF) (Jager & Ryder, 1999). This criterion is given as:

$$RCF = \frac{3\sigma_1 - \sigma_3}{F\sigma_c} \tag{28}$$

Where:

σ_1, σ_3	are the maximum and minimum field stress components in the plane of the excavation cross section
σ_c	is the uniaxial compressive strength of the host rock
F	is a factor representing the downgrading of σ_c depending on rock mass conditions and excavation size

The formulation of the RCF represents a comparison of the maximum induced tangential stress of an assumed circular excavation to the estimated rock mass strength. It has been found that values of RCF < 0.7 represent good conditions requiring minimum support; 0.7 <RCF < 1.4 average conditions with some robust support and RCF > 1.4 represent poor ground conditions with special support requirements.

2.10.2 Overstoping

Overstoping is when haulages are positioned beneath mined-out area. According to COMRO, (1988), based on their guidelines, consideration should be given to the 45^{o} destressing guideline. An overstoping angle of 45^{o} is generally required to distress haulage. At an angle > 45^{o}, the stress concentrations are high. Figure 2.9 is a schematic showing how the overstoping angle is calculated.

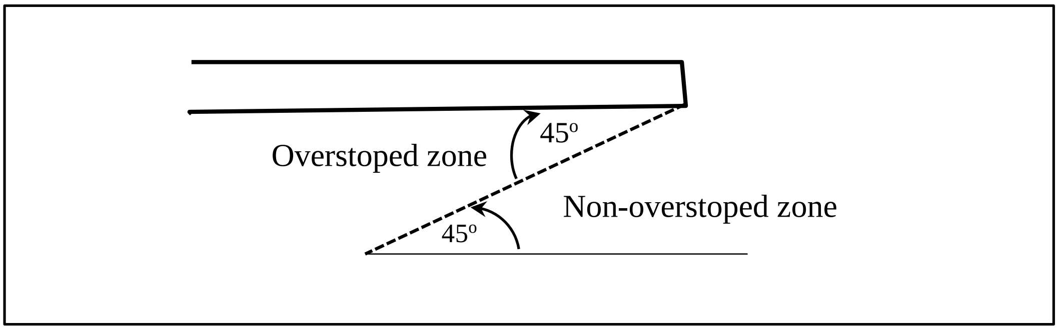

Figure 2.9: Diagram showing concept of overstoping (COMRO, 1988)

2.10.3 Numerical Modelling

"The RCF concept is empirical and thus may not be ideal for certain conditions" (Ryder & Jager, 2002). The overstoping rule "applies only when the section drawn shows a mined out area that is completely horizontal (dip is 0^o). As soon as a reef dip > 0^o is shown on the section used to analyse the position of the tunnel, the angle between the reef and the line that separates the 'highly stressed' and 'de-stressed' zones changes' (COMRO,1988).

Since the reef at Khuseleka dips at about 9^o, the above statements indicate that it would be necessary to apply numerical modelling in determining the best positions to place the footwall excavations to avoid damage from the regional pillars due to elevated stress levels.

2.11 In-situ Stress Determination

From the literature reviewed above it can be noted that no pillar design can take place without knowledge of the virgin stress state of the area to be mined. Numerical modelling, pillar load and RCF calculations all require fairly accurate values of the virgin stress as input parameters. Brady & Brown, (2005) stated that the design of an underground structure in rock differs from other types of structural design in the nature of the loads operating in the system. In conventional surface structures, the geometry of the structure and its operating duty define the loads imposed on the system. For an underground rock structure, the rock medium is subject to initial stress prior to excavation. The final, post-excavation state of stress in the structure is the resultant of the initial state of stress and stresses induced by excavation. Since induced stresses are directly related to the initial stresses, it is clear that specification and determination of the pre-mining state of stress is a necessary precursor to any design analysis (Brady & Brown, 2005).

For this project stress measurements taken at a neighbouring mine by van der Heever & Piper, (2013) were used as input parameters where stress values were required.

To confirm the validity of these stress results for use in this project, blast holes in the KORP section were analysed based on Brady & Brown, (2005) who stated that after a blast initiates in a hole, the longest initial cracks will form in the direction parallel to the major principal field stress, and they will propagate preferentially in that direction under gas pressure. They further stated that, the effect of the minor principal stress is to impede crack development. This is illustrated in Figure 2.10.

Middindi, (2013) also stated, that the in-situ stress field present before the explosion also affects the extension of the blast fractures. Longer blast fractures are in a direction parallel to the major principle stress and shorter blast factures in the direction of the minor principle stress. This interaction of the blast fractures and in-situ stresses is shown in Figure 2.11.

It is therefore possible to estimate the direction of the major principle stress purely from a study of blast fractures around a hole in which explosives had been detonated (socket) (Middindi, 2013).

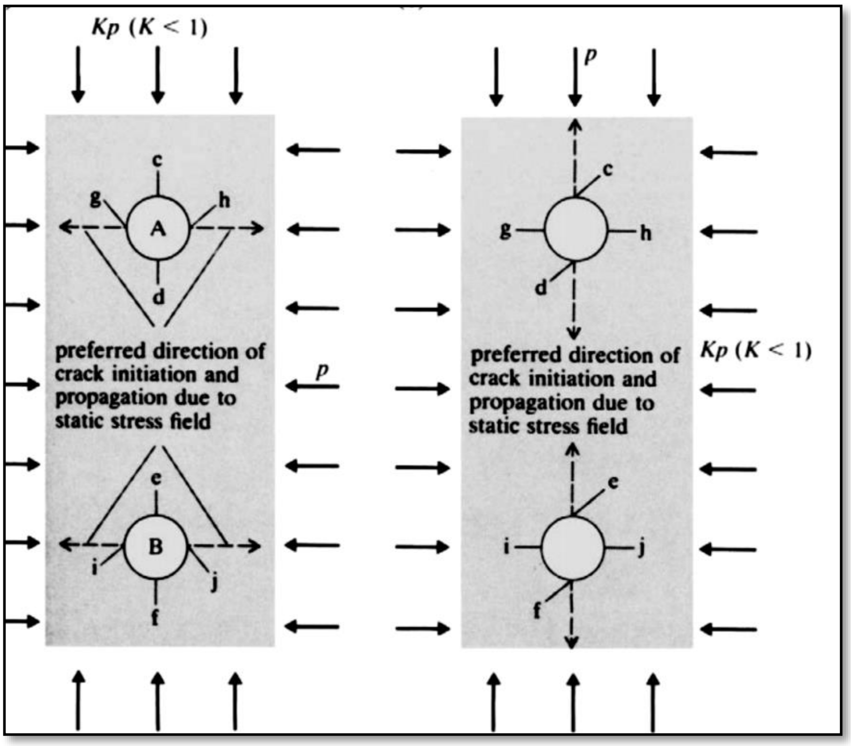

Figure 2.10: Influence of field static stresses on the development of blast fractures (Brady & Brown, 2005)

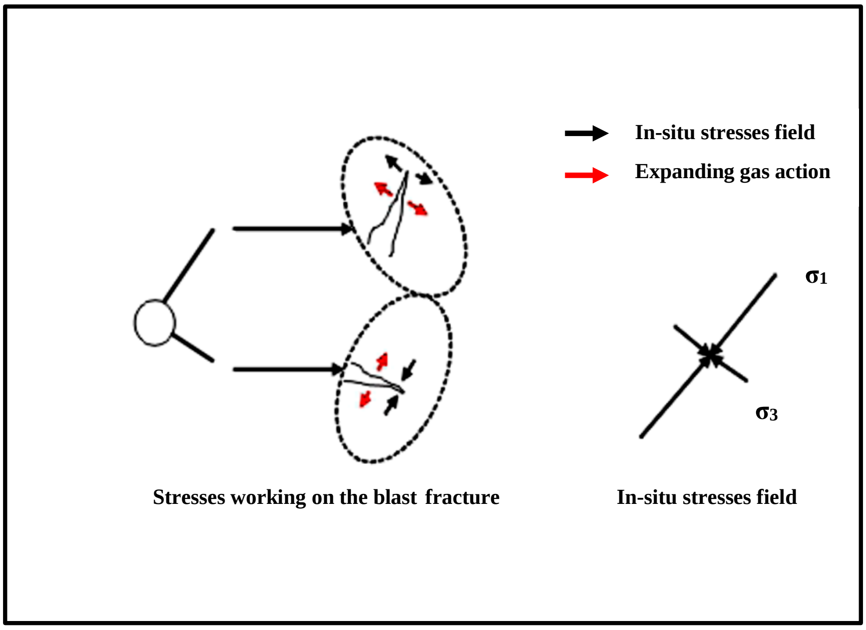

Figure 2.11: Stresses working on the blast fractures (Middindi, 2013)

2.12 Conclusions

The stability of any mining excavation is dependent on its support structures. In the case of underground tabular excavation these support structures are pillars. It is therefore of utmost importance that these pillars are properly designed. In this chapter different literature has been reviewed to find the different ways of designing the pillars. The first step in pillar design is to determine the virgin or in-situ stress in the rock mass and at the depth where the pillars will be cut. This knowledge will then be used to determine the loads acting on the pillars using three main methods which are:

- Tributary area theory (TAT) used in regular mining layouts of large lateral extents, several times greater than the mining depth and assumes that each pillar in the layout is of same size and supports an equal amount of load to the surface. It does not consider the geometrical and rock properties in its formulation and is thus not suited for conditions where the geometry or rock properties are varied.
- Coates method tries to eliminate the shortcomings of the TAT method by taking into account different geometries and rock mass properties. Just like TAT, the limitation to Coates method is that his formula is only valid in the centre of the mining area with undisturbed long rib pillars, and where the mine span does not exceed half the depth.
- Numerical models are used when depth/span becomes too great or when pillar geometry and sizes are different. It tries to eliminate the limitations of the two methods mentioned above.

Pillar strength is another component that is calculated when designing pillars. A lot of formulations have been proposed for determining pillar strength and these are based on two main forms which are the linear form and the power form. The main components of the pillar strength formulae are the width: height ratio of the pillar and the strength of material constituting the pillar (the rock mass strength). It is based on UCS of a sample of the pillar material downgraded to take into account weakening factors such as geological structures found in the rock mass.

Before the loads and strengths of the pillars can be determined, it is important to know the factor of safety (FOS) one is working towards, as pillars are differentiated based on their FOS. For regional or stability pillars this FOS has been determined to be >2.

Also discussed in this chapter is knowledge of the properties making up the foundation of the pillars in the hangingwall and the footwall, as well as the stresses imposed on them in determining the stability of the excavation. Foundation failure can contribute to instability even though the pillars will be deemed stable.

Pillar spacing is also very critical as it affects closure and seismicity on the mine.

Any stability of a mine working is a function of the stresses in that area verses the strength of the rock. It is therefore critical to understand and have knowledge of the virgin stresses acting in the area to be mined.

Table 2.3 shows the criteria that had to be met for the pillars designed for the KORP section to be deemed stable. These design criteria formed the basis of pillar design in the KORP section.

Table 2.3: Design criteria for KORP regional pillars

Design criterion	**Values**
w : h ratio	>10
Spacing between pillars	Depth/Span > 4
APS	$<2.5\sigma_c$
FOS	>2.0
Overstoping distance of footwall excavation	Equal to middling distance for 45^o rule

CHAPTER 3: METHODOLOGY

3.1 Introduction

This chapter looked at the methods and strategies that would be adopted in designing the regional pillars for the Khuseleka Ore Replacement Project (KORP). The methodology utilised to satisfy the objectives of the research expressed in chapter 1 is expressed in this chapter The methodology involved:

- Review of current mine pillar design strategy.
- Literature review of existing design methodologies.
- Analysis of seismic database to identify large seismic events associated with pillar failure in back areas.
- Physical analysis of any failed pillars in the back areas if they were any.
- Conducting elastic numerical modelling analysis for the designed pillar layout.
- Conducting laboratory rock elastic property tests on drilled core from UG2 KORP section underground. These tests were conducted at the Wits University Rock Mechanics Laboratory. The laboratory test results were used in equations for testing different methods of pillar design until an optimum pillar layout was established.
- Laboratory rock test results from other operations with similar conditions were used where tests conducted or where data was not available on the shaft.
- Stress measurement results from Siphumelele shaft (an Anglo American Platinum operation in Rustenburg) were used as an input parameter for calculations requiring measured in-situ stresses, especially in numerical modelling analysis.
- Rock mass classification and strengths were determined using different methods.

3.2 Review of the mine's current pillar design strategy

The current Khuseleka regional support standard was the first area that was looked at in designing the pillars. The Khuseleka standard was analysed and improved upon with other methods available.

3.3 Use of empirical methods for pillar design

An analysis of currently available empirical methods for pillar design was done. Each method was used in turn and the results compared until the most favourable method, using engineering judgement was chosen for the final design of the KORP pillars.

3.4 Analysis of seismic events associated with pillar failure

Data from recorded seismic activities was used to identify any shortcomings that may exist with the current pillar design strategy. Previous seismicity associated with pillars at

Siphumelele shaft were analysed to ensure that the pillars in the KORP section would be designed to prevent seismic damage.

3.5 Physical analysis of any failed pillars in the back areas

Back area visits were conducted to identify the condition of regional pillars that had already been cut. The purpose was to determine if there were any pillars showing signs of failure, so that the information would help to identify any weakness in the current pillar design strategy since failed pillars in the back area can be an indication of pillars designed too small. Pillars not showing any failure although ideal might be an indication of over conservatism in pillar design, indicating that pillars are oversized, and that too much ore is being left (potential loss of revenue). Information from back analysing pillars also helps validate some assumptions made during numerical modelling.

3.6 Conduct numerical modelling to analyse pillar stresses and RCF values on footwall excavations

Three numerical modelling programs, namely Map3D, Examine2D and Lamodel were used to design the regional pillars and the results compared. Validation of the assumptions made for the different parameters used would be through back analysis of pillars in mined out areas. RCF values on the footwall excavations was also analysed using Map3D.

3.7 Rock strength tests on drilled core from UG2 KORP section underground will be undertaken.

These tests were intended to determine stress-strain curves and Young's Modulus and Poisson's Ratio in uniaxial compression of rock specimen collected from diamond drilled core in the KORP section. The tests were conducted at the Wits University Rock Mechanics Laboratory by the author with the assistance of the laboratory personnel. The suggested methods by the ISRM for determination of deformability of rock materials in uniaxial compression were adhered to during the preparation of the specimen, set up of the equipment, testing procedure and determination of the Young's Modulus and Poisson's Ratio (Ulusay & Hudson, (2007)). The information obtained was used as input parameters for the different methods of pillar design.

3.8 Use of laboratory rock test data from other operations

Other operations within the RPM group with similar geotechnical conditions have conducted elastic property tests on their rock samples. An example is Bathopele Mine where various tests were conducted on their UG2 reef samples. The results of their UCM tests were compared with those conducted for Khuseleka, whilst their triaxial compressive test results were used to plot Mohr's circles used for analysis in this project.

3.9 In-situ stresses and k-ratio for project

Stacey & Wesselo, (1998) stated that the safety of mining operations is significantly influenced by the in-situ stress fields in which the mining excavations are created. It is therefore of vital importance that the in-situ stresses of a particular mining environment are known beforehand, to facilitate the accurate design of pillars, support systems and excavations. In 2013 stress measurements were conducted at Siphumelele shaft which is one of the mines owned by Anglo American Platinum and is within the same mining district as Khuseleka shaft. Although orientation and magnitudes of stresses can vary significantly across mining districts and geotechnical areas, the conditions and results of the measurements at Siphumelele were assumed to resemble those of Khuseleka shaft and the results were used to allow the establishment of calibrated, credible and representative input parameters for numerical modelling and for pillar design. The magnitude and orientation of in-situ stresses influences the stability of the designed pillars.

3.10 Rock mass classification and rock mass strength determination

Rock mass classification data for RMR and Q from the KORP trial section was collected during mapping. This data was collated and the average RMR and Q values for the KORP section were calculated. The RMR value was then used to determine the rock mass strength for pillar strength calculations.

3.11 Conclusions

A comprehensive methodology was proposed and executed for this project. It involved researching data already available such as reviewing of the current regional pillar design strategy, use of empirical methods for pillar design, and analysis of seismic data. Laboratory and underground work to gather data that was not available was also undertaken. The gathered data included visiting underground workings to observe cut pillars, rock mass classification in the KORP section, obtaining in-situ stress measurements from Siphumelele Mine and laboratory UCS tests on core drilled from underground at both Khuseleka and Bathopele Mines. This information was then analysed and presented to come up with a design for the regional pillars.

CHAPTER 4: DETERMINATION OF ROCK PROPERTIES AND PARAMETERS TO USE FOR PILLAR DESIGN IN THE KORP SECTION

4.1 Introduction

Data collection formed a very important component of this project, especially for rock mass characterisation. Data used in this project was collected from numerous sources. The Methodology Chapter highlighted the methods and strategies adopted in designing the pillars for the KORP section.

This chapter looks at how the data that was used for this project was collected. This included

i) Elastic properties tests carried out at the Wits University Rock Engineering Laboratory from UG2 rock core samples drilled underground.

ii) Results of rock property laboratory tests carried out on samples from other operations.

iii) Underground observations of pillars already cut and their condition.

iv) Getting stress measurements from Siphumelele mine and using these measurements for stress determination at different mining depths in the KORP section.

v) RMR ratings from the UG2 work places in the KORP section where trial mining is taking place and calculating rock mass strength based on these ratings and elastic rock properties.

4.2 Mining Depths in KORP Section

According to a feasibility study, done by Le Bron, (2006) the KORP section is planned to mine from 16 Level to 28 Level. The mining depths for these levels are given in the Table 4.1, based on data from the survey department. These depths are for the level station landings, but when calculating for pillar stresses, the midlevel depths were used for regional pillar design. The depths used for calculations varied between 500m and 1000m to cover the KORP depth range.

Table 4.1: Mining Depths for KORP Section

Name	**Elevation**	**Depth below surface (m)**
Collar Elevation	**1123.8**	
16 Level	508.2	615.6
19 Level	479.5	644.3
21 Level	422.51	701.3
23 Level	364.7	759.1
25 Level	306.7	817.1
26 Level	277.8	846.0
27 Level	234.5	889.3
28 Level	200.5	923.3

4.3 Reef Elevation-Footwall Excavation Middling

The middling distances between the reef elevation and footwall excavations such as crosscuts and haulages were determined by the survey department based on diamond drilling core drilled for exploration in the KORP section. The range of middling distances for the entire KORP section is given in Table 4.2, with the actual middling distances for each raiseline attached in appendix A.

Table 4.2: Reef elevation-footwall excavation middlings

Station Level	**Middling Depth Range (m)**	**Comment**
16	30.8 – 38.5	Above Reef
19	25.7 – 37.1	Below Reef
21	24.4 – 35.4	Below Reef
23	25.2 – 35.7	Below Reef
25	29.8 – 37.6	Below Reef
26	29.4 – 37.4	Below Reef
27	29.4 – 36.1	Below Reef
28	26.8 – 36.8	Below Reef

4.4 Core

The samples tested for the rock elastic properties at the Wits University Laboratory were obtained from a borehole drilled on 25 level Haulage East (Hole ID: CTM 03). This is a haulage being developed in the KORP section to access ore on 25 level. Figure 4.1 is a generated layout of the position of the hole and the drilling orientation. A BX (32mm) sized bit was used to drill the core, which is the standard core size drilled for underground exploration working at RPM.

The hole was drilled from the hangingwall of the haulage at +90° upwards to intersect reef. As soon as the triplets above reef (see Figure 1.7 for UG2 stratigraphic column of the UG2) were intersected, the hole was stopped at 39.47m. The core was carried to surface in trays where it was kept in a shaded core yard. A day later, the core was logged by the author and portions of the core to be tested (immediate hangingwall, reef, and immediate footwall of the reef were cling wrapped to preserve the moisture and stored in a store room at the core yard. Two days later the core samples were brought to the Wits University for the tests to determine elastic properties of the rocks making up the pillars and the foundation. Table 4.3 is a Sable's (core logging database program) output sheet showing logged information of the hole. Figure 4.2 is the photo of the core taken soon after it was brought to surface from underground.

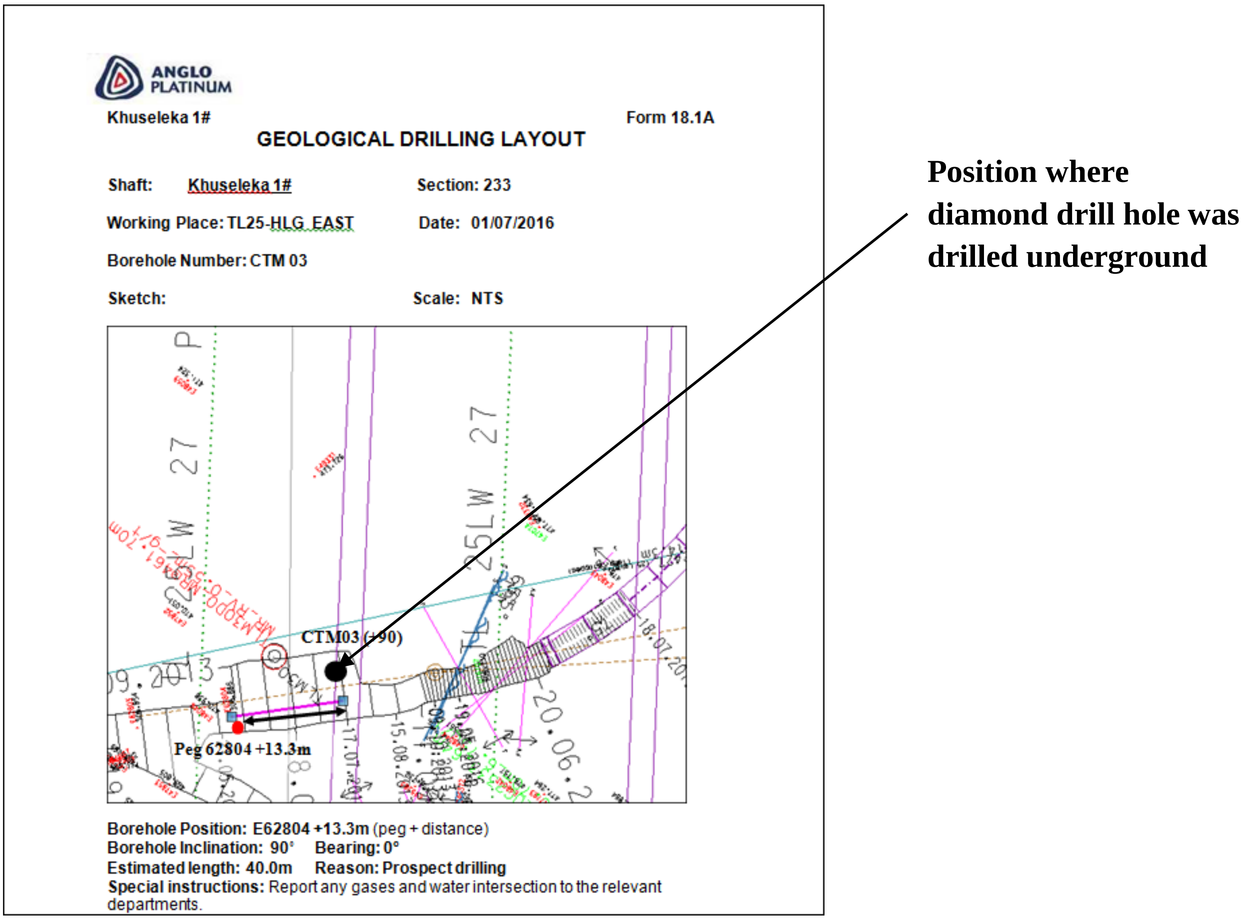

Figure 4.1: Drilling layout for diamond drill hole where testing samples were obtained (Mutsvanga, 2016)

Table 4.3: Logged information of borehole (CTM03) from Sables program

From	To	Entry Type	Lithology Name	Stratigraphy	Stratigraphic Zone	Strat Class	Depth 'From' contact	Depth 'To' contact	Core-Contact Angle	Grain Size	Comments
0.000	0.000	3	COL				COL	COL			
0.000	1.890	1	N	FW13b			COL	GRAD		M	
1.890	12.480	1	LN	FW13b			GRAD	GRAD		M	
12.480	16.200	1	N	FW13b			GRAD	GRAD		M	
16.200	16.830	1	MN	FW13b			GRAD	GRAD		M	
16.830	17.740	1	FPYX	FW13b			GRAD	GRAD		M	
17.740	18.720	1	N	FW13b			GRAD	SHARP	15	M	
18.720	19.160	1	FPD	FW13b			GRAD	SHARP	15	M-F	feldspathic vein
19.160	21.760	1	MN	FW13b			SHARP	GRAD		M	
21.760	26.320	1	N	FW13b			GRAD	SHARP	65	M	
26.320	26.321	1	CR	SC			GRAD	SHARP	65	F	
26.321	26.690	1	POIKAN	FW13a	BL		SHARP	SHARP	60	C-F	
26.690	26.900	1	PEGFPYX	UG2FW	UG2FW		SHARP	SHARP	70	C	
26.900	28.300	1	FPYX	UG2FW	UG2FW		SHARP	GRAD		M	
28.300	29.550	1	PEGFPYX	UG2FW	UG2FW		GRAD	SHARP	65	C	
29.550	30.250	1	CR	UG2	UG2		SHARP	SHARP	85	F	
30.250	36.120	1	FPYX	UG2P	UG2P		SHARP	GRAD		M	
36.120	36.840	1	FPYXCR	UG2P	UG2P		GRAD	SHARP	80	M-F	
36.840	36.935	1	CR	UG2L	UG2L		SHARP	SHARP	80	F	
36.935	36.950	1	FPYXCR	UG2PT	PTR1		SHARP	SHARP	80	M-F	
36.950	36.965	1	CR	UG2T1	UG2T1		SHARP	SHARP	80	F	
36.965	36.970	1	FPYXCR	UG2PT	PTR2		SHARP	SHARP	80	M-F	
36.970	36.975	1	CR	UG2T2	UG2T2		SHARP	SHARP	80	F	
36.975	37.020	1	FPYXCR	UG2PT	PTR3		SHARP	SHARP	80	M-F	
37.020	37.140	1	CR	UG2T3	UG2T3		SHARP	SHARP	80	F	
37.140	37.220	1	FPYXCR	UG2PT	PTR4		SHARP	SHARP	80	M-F	
37.220	37.300	1	CR	UG2T4	UG2T4		SHARP	SHARP	80	F	
37.300	37.820	1	FPYX	UG2PT	UG2PT		SHARP	SHARP	10	M	
37.820	38.120	1	FPD	UG2PT	UG2PT		SHARP	SHARP	10	C-F	feldspathic vein
38.120	39.470	1	FPYX	UG2PT	UG2PT		SHARP	EOH		M	
39.470	39.470	3	EOH				EOH	EOH			

Figure 4.2: Borehole CTM03 soon after being brought to surface

4.5 Determination of Elastic Properties of Rock

The purpose of the laboratory tests was to determine UCS, stress-strain curves and Young's Modulus and Poisson's Ratio in Uniaxial compression of the rock specimens collected from the core drilled at 25 level in the KORP section. The tests were mainly intended for the classification and characterization of intact rock to use as input parameters in pillar design. The ISRM suggested methods were adhered to during the preparation of the specimen, set up of the equipment, testing procedure and determination of the Young's Modulus and Poisson's Ratio (Ulusay & Hudson, 2007).

4.5.1 Apparatus

An Amsler Testing Machine (Soft machine) shown in Figure 4.3 was used for the tests. The samples were fitted with electrical resistance strain gauges in both axial and lateral directions to determine the axial and diametric strain.

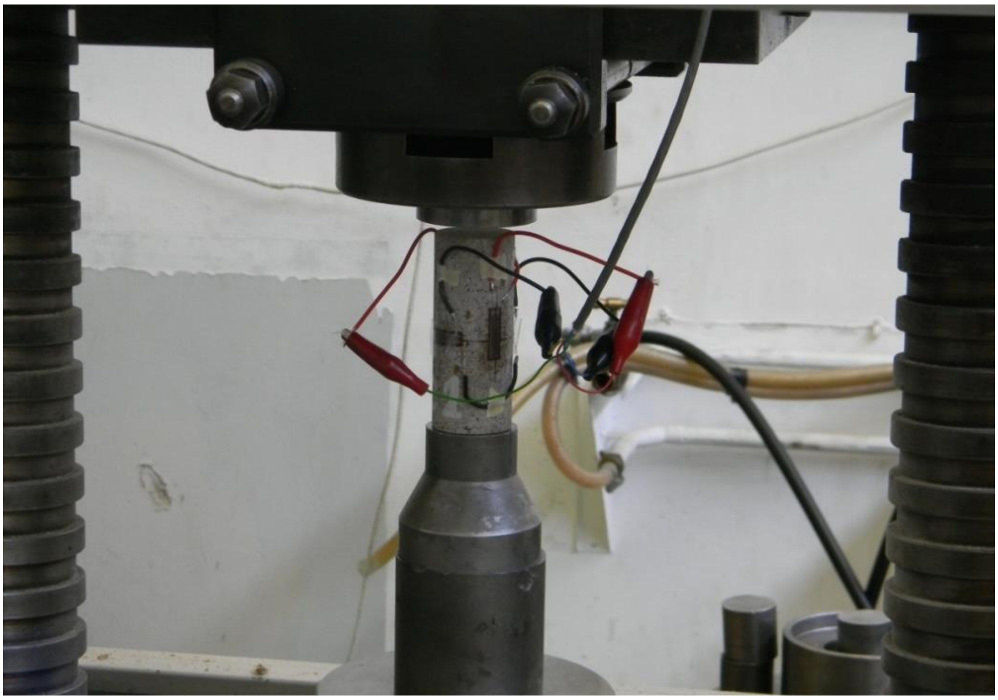

Figure 4.3: Amsler Testing machine with the specimen loaded

4.5.2 Sample Preparation and Test Results

The fifteen specimens (see Table 4.4 for specimen properties) tested were from the 90^{o} inclined diamond hole drilled on 25 level haulage east on the UG2 horizon of the KORP section (plan in Figure 4.1). Preparation of the sample was by the use of a lapping machine to flatten and smoothen the sides as per ISRM suggested methods. Five specimens each were obtained from the hangingwall of the reef (pyroxenite), reef (chromitite) and footwall of the reef (pegmatoidal pyroxenite) of the drilled core to give a total of fifteen samples prepared for testing. Although the moisture content of the samples was unknown, from the time the hole was drilled to the time it was taken to the laboratory for testing (a period of a week after drilling) it was wrapped in plastic and stored in an enclosed room. During testing each specimen had strain gauges connected to it so that axial and diametric strains could be measured. The specimens were loaded onto the Amsler machine and the information recorded. The number of samples (5 for each rock type) used for this test is consistent with the recommendations of ISRM suggested methods that at least 5 specimens for each sample should be tested.

Machine generated data for the individual specimen test is given in graphic form in Appendix B. The specimen dimensions and test results for each of the specimen are given in Table 4.4. Information for each column is explained and how it was calculated.

Column 1 - Specimen ID

Column 2 – The lithology of the specimen tested

Column 3 – Diameter of specimen – The diameter for the specimen used is less than the recommended diameter of at least 54mm. This could have an effect on the UCS of the rock especially the pegmatoidal pyroxenite which is coarse grained.

Column 4 – Height of specimen

Column 5 – Height to diameter ratio – within the recommended 2.5-3.0

Column 6 – Mass of each specimen.

Column 7 – Calculated density of specimen.

Column 8 – Mode of failure of each specimen.

Column 9 – The duration from when loading started to failure of specimen – The durations recorded here were less than the recommended 5 to 10 minutes. This could have an effect on the strengths recorded.

Column 10 – The load applied at which failure occurred.

Column 11 – Calculated UCS of the rock specimen (Maximum applied load/cross sectional area of specimen)

Column 12 – Stress rate/loading rate at which specimen was loaded until failure. The loading rates were generally higher than the recommended rate of 0.5 – 1.0MPa/s.

Column 13 – Axial strain of specimen as recorded by machine.

Column 14 – Radial strain of specimen as recorded by machine.

Column 15 – Young’s Modulus of Elasticity for specimen = Axial stress/axial strain. Average Young's modulus, E, is determined from the average slopes of the more-or-less straight line portion of the axial stress-axial strain curves.

Column 15 – Poisson’s Ratio = Slope of radial strain curve/Slope of axial strain curve. Average Poisson’s Ratio, v, determined from the average slopes of the more-or-less straight line portion of the radial strain-axial strain curves.

Column 16 – Any comments related to the test for each specimen.

The average dimensions and test results and calculations are included in Table 4.4. Specimen FW 05 was discarded as it had a crack which would have rendered the results inaccurate.

Table 4.4: IDs and properties of samples tested

Uniaxial Compressive Strength Tests with Deformability

Date	2016/07/28
Location	25 Level Haulage West (UG2 KORP Section)
Moisture	Moisture content unknown but samples kept in atmospherically stable environment
Test Machine	Amsler Testing Machine - Wits University

Specimen ID	Specimen Lithology	Specimen Dimensions						Specimen Test Results								Comments
		Dia (cm)	Height (cm)	H:D Ratio	Mass (g)	Density (g/cm^3)	Mode of Failure	Test Duration (sec)	Failure Load (kN)	Strength UCS (MPa)	Stress Rate (MPa/s)	Axial Strain (mm/m)	Radial Strain (mm/m)	Average Young's Modulus (GPa) at straight portion of slope	Average Poisson's Ratio at straight portion of slope	
HW 01	Pyroxenite	3.15	7.9	2.5	202.3	3.307	Axial splitting	155	111.1	142.6	0.9	0.9784	-0.82829	170.0	0.26	
HW 02	Pyroxenite	3.16	7.9	2.5	203.7	3.309	Axial splitting	52	107.6	137.1	2.6	0.84178	-0.2359	190.0	0.25	
HW 03	Pyroxenite	3.17	7.9	2.5	202.3	3.261	Axial splitting	42	139.6	176.8	4.2	1.75955	-1.81709	128.0	0.30	
HW 04	Pyroxenite	3.17	7.9	2.5	203.5	3.285	Axial splitting	110	159.2	201.8	1.8	1.19149	-0.93117	170.0	0.23	
HW 05	Pyroxenite	3.17	7.8	2.5	202.5	3.273	Axial splitting	91	134.1	169.9	1.9	1.13875	-0.60107	175.0	0.24	
FW 01	Pegmatoidal Pyroxenite	3.18	7.8	2.5	196.5	3.156	Axial splitting	79	76.6	96.5	1.2	2.59073	-2.91816	52.0	0.30	
FW 02	Pegmatoidal Pyroxenite	3.17	7.9	2.5	198.6	3.201	Axial splitting	34	78.6	99.6	2.9	1.45625	-0.24077	80.0	0.24	
FW 03	Pegmatoidal Pyroxenite	3.17	7.9	2.5	198.6	3.201	Axial splitting	28	58.7	74.4	2.7	1.85513	-0.28017	76.3	0.18	
FW 04	Pegmatoidal Pyroxenite	3.17	7.9	2.5	198.6	3.201	Axial splitting	65	73.4	93.0	1.4	0.77544	-0.96837	83.3	0.22	
FW 05	Pegmatoidal Pyroxenite															There was a crack on the sample so it could not be tested
RF 01	Chromitite	3.20	7.8	2.5	252.0	3.997	Axial splitting	81	55.8	69.4	0.9	1.30668	-1.20338	79.2	0.30	
RF 02	Chromitite	3.17	7.8	2.5	244.4	3.950	Axial splitting	26	55.1	69.8	2.7	0.77494	-0.52026	106.7	0.29	
RF 03	Chromitite	3.17	7.8	2.5	254.3	4.120	Axial splitting	44	50.6	64.1	1.5	1.22791	-2.10743	73.3	0.33	
RF 04	Chromitite	3.18	7.8	2.5	244.4	3.925	Axial splitting	39	46.0	57.9	1.5	1.16772	-3.83072	70.0	0.39	
RF 05	Chromitite	3.17	7.9	2.5	248.3	4.003	Axial splitting	77	43.9	55.6	0.7	1.14161	-3.15507	68.6	0.30	

HW Average	Pyroxenite	3.20	7.85	2.5	202.86	3.286792	Axial splitting	90	130.3	165.7	2.3	1.18199	-0.8827	166.6	0.26
FW Average	Pegmatoidal Pyroxenite	3.20	7.855	2.5	198.075	3.190036	Axial splitting	52	71.8	90.9	2.1	1.66939	-1.10187	72.9	0.23
RF Average	Chromitite	3.20	7.84	2.5	248.68	3.998887	Axial splitting	53	50.3	63.4	1.4	1.12377	-2.16337	79.6	0.32

Figure 4.4 is the photo of one of the specimens at failure. Axial splitting can be noted on the pieces hanging from the strain gauges.

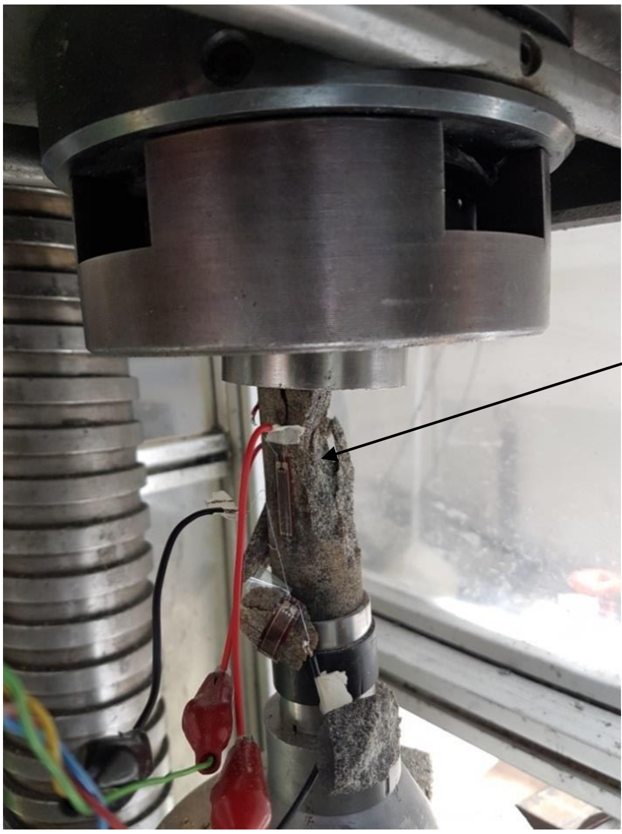

Note axial splitting of rock specimen

Figure 4.4: Specimen at failure after UCM test

4.5.3 Test Notes

During testing the following observations were made that might have an influence on the accuracy of the results obtained:

1) **Moisture content unknown**

It is suggested that when reporting the moisture content must be recorded. This information was unknown although care was taken to minimize exposure of the core to the external environment.

2) **Diameter of sample core less than the suggested diameter:**

It is suggested that the diameter of the tested core should be at least NX core size (54mm). The core diameters for this test were 32mm. This might not have a major influence on the deformability of pyroxenite and chromitite as these rocks grains are fine to medium sized, which makes the diameter to largest grain ratio within the recommended 1:10. The problem might arise on the pegmatoidal pyroxenite which is coarse grained and the diameter to largest grain size is less than 1:10.

3) Test duration less than the recommended time:

It is recommended that the test should be carried out within 5 – 10 minutes. For all the specimens tested the average time was less than 3 minutes. This lead to a stress rate of up to 4.2 MPa/s, which was higher than the recommended ISRM rate of 0.5 – 1.0 MPa/s. Experiments have shown that faster loading rates lead to rather small increases in the measured strength of the rock (Ryder & Jager, 2002). It is therefore possible that the measured specimen strengths are higher than actual values due to the loading rate.

4.6 Rock Property Test Performed on other Operations

Results of other rock property laboratory tests for the UG2 rocks were obtained from Bathopele Mine, which is an RPM mine mining UG2 reef in Rustenburg. The tests included USC tests, triaxial compressive tests, Brazilian tensile strength test, and direct shear tests on open joints. A comparison between the results obtained from the tests done on the Khuseleka rocks and those done on the Bathopele rocks shows a good agreement on the results of the UCS of the different rock types , but not so much on the Poisson's ratio and Young's Modulus where the difference is as high as 60GPa for the chromitite reef.

UCS results obtained from the Khuseleka rock sample tests done at Wits Laboratory were used for all calculations requiring the use of UCS results as input parameters such as in numerical modelling and pillar strength calculations. The results for triaxial compressive strength tests and other tests done for Bathopele mine were used for all other calculations requiring the use of the results of these tests, such as $\sigma_1 - \sigma_3$ plots using triaxial test results. Tables 4.5, 4.6, 4.7 and 4.8 are attached with the results of UCS, triaxial compressive, Brazilian tensile strength, and direct shear tests on open joints tests respectively.

Table 4.5: Bathopele's UCS tests results

RESULTS OF UNIAXIAL COMPRESSIVE STRENGTH TESTS WITH MODULUS & POISSON'S RATIO MEASUREMENTS BY MEANS OF STRAIN GAUGES

Client: Rustenburg Platinum Mines   Sampling Site: Bathopele Mine

12-06-2015

SPECIMEN PARTICULARS			SPECIMEN DIMENSIONS					SPECIMEN TEST RESULTS								
Rocklab Specimen No 6153-	Position	Rock Type	Diameter mm	Height mm	Ratio of Height to Diameter	Mass g	Density g/cm³	Failure Load kN	Strength (UCS) MPa	Tangent Elastic Modulus @ 50% UCS GPa	Secant Elastic Modulus @ 50% UCS GPa	Poisson's Ratio Tangent @ 50% UCS	Poisson's Ratio Secant @ 50% UCS	Linear Axial Strain at Failure mm/mm	Failure Code	Note
UCM-01A			32.35	89.8	2.8	295.97	4.01	90.0	109.5	108.0	118.0	0.29	0.31	0.001029	XA	
UCM-01B	Reef	UG2	32.33	90.2	2.8	314.51	4.25	50.1	61.0	165.0	165.0	0.34	0.33	0.000367	3B	
UCM-01C			32.42	80.3	2.5	260.77	3.93	135.6	164.3	127.0	132.0	0.34	0.32	0.001463	XB	
UCM-02A			32.28	89.1	2.8	240.11	3.29	136.1	166.3	155.0	158.0	0.25	0.25	0.001085	3B	
UCM-02B	HW	Pyroxenite	32.29	93.5	2.9	250.27	3.27	75.4	92.0	158.0	160.0	0.24	0.26	0.000562	5B	
UCM-02C			32.34	94.1	2.9	253.53	3.28	173.2	210.9	164.0	163.0	0.24	0.23	0.001295	3B	
UCM-03A			32.31	90.8	2.8	243.83	3.27	94.4	115.1	154.0	156.0	0.25	0.25	0.000850	3B	
UCM-03B	FW	Peg Pyroxenite	32.27	91.8	2.8	243.92	3.25	112.0	136.9	146.0	145.0	0.27	0.26	0.001065	4B	
UCM-03C			32.23	94.7	2.9	256.67	3.32	92.6	113.5	157.0	158.0	0.28	0.27	0.000731	3B	

Note: All tests were conducted according to the ISRM's specfications.

Table 4.6: Bathopele's TCS tests results

RESULTS OF TRIAXIAL COMPRESSIVE STRENGTH TESTS

Client: Rustenburg Platinum Mines   Sampling Site:

22-06-2015

SPECIMEN PARTICULARS			SPECIMEN DIMENSIONS					SPECIMEN TEST RESULTS				
Rocklab Specimen No 6153-	Position	Rock Type	Diameter mm	Height mm	Ratio of Height to Diameter	Mass g	Density g/cm³	Confining Pressure δ_3 MPa	Failure Load P kN	Strength (TCS) δ_1 MPa	Failure Mode	Note
TCS-01A			28.81	60.7	2.1	168.5	4.25	5.0	51.2	78.5	4B	
TCS-01B			28.78	64.1	2.2	176.5	4.23	10.0	103.1	158.5	XA	
TCS-01C	Reef	UG2	28.88	59.5	2.1	160.9	4.13	15.0	131.4	200.6	XA	
TCS-01D			28.80	62.8	2.2	167.4	4.09	20.0	141.9	217.8	XA	
TCS-01E			28.89	62.0	2.1	167.1	4.11	30.0	175.4	267.6	XA	
TCS-02A			28.76	62.5	2.2	133.9	3.30	5.0	99.0	152.3	3B	
TCS-02B			28.77	63.2	2.2	133.6	3.25	10.0	145.8	224.3	3B	
TCS-02C	HW	Pyroxenite	28.73	60.3	2.1	128.2	3.28	15.0	112.1	172.9	6B	
TCS-02D			28.88	61.7	2.1	131.1	3.25	20.0	176.2	269.0	XA	
TCS-02E			28.77	60.9	2.1	128.0	3.23	30.0	227.0	349.2	XA	
TCS-03A			28.76	61.3	2.1	131.2	3.29	5.0	97.5	150.0	XA	
TCS-03B			28.81	62.4	2.2	134.4	3.30	10.0	126.3	193.8	XA	
TCS-03C	FW	Peg Pyroxenite	28.78	60.2	2.1	130.3	3.33	15.0	111.2	170.9	4B	
TCS-03D			28.80	63.7	2.2	137.7	3.32	20.0	157.8	242.3	XA	
TCS-03E			28.84	59.8	2.1	128.7	3.29	30.0	176.0	269.4	XA	

Note: Alll tests were conducted according to the ISRM suggested method.

Table 4.7: Bathopele's Brazilian Tensile strength tests results

RESULTS OF BRAZILIAN TENSILE STRENGTH TESTS

Client: Rustenburg Platinum Mines Sampling Site: Bathopele Mine

05-06-2015

SPECIMEN PARTICULARS			SPECIMEN DIMENSIONS				SPECIMEN TEST RESULT		
ROCKLAB Specimen No 6153-	Position	Rock Type	Diameter mm	Height mm	Mass gram	Density g/cm³	Failure Load kN	Brazilian Tensile Strength MPa	Note
UTB-01A	Reef	UG2	32.38	18.97	61.9	3.96	6.29	6.5	
UTB-01B			32.36	19.36	63.0	3.96	4.99	5.1	
UTB-01C			32.33	17.86	58.6	3.99	3.84	4.2	
UTB-02A	HW	Pyroxenite	32.26	17.43	45.8	3.22	16.54	18.7	
UTB-02B			32.16	17.74	46.6	3.23	16.00	17.9	
UTB-02C			32.18	18.11	47.9	3.25	18.53	20.2	
UTB-03A	FW	Peg Pyroxenite	32.48	17.57	46.2	3.17	12.06	13.5	
UTB-03B			32.47	17.65	47.2	3.23	14.88	16.5	
UTB-03C			32.48	17.49	47.3	3.26	12.91	14.5	

Note: All tests were conducted according to the ISRM's suggested method.

Table 4.8: Bathopele's Direct Shear tests results

RESULTS OF DIRECT SHEAR TESTS ON OPEN ROCK JOINTS

Client: Rustenburg Platinum Mines Sampling Site: Bathopele Mine

22-06-2015

ROCKLAB Specimen No 6153-	Sample Position	Rock Type	Shear Cycle No	Contact Area mm^2	Shear Force (kN)	Vert. Force (kN)	Dil. Angle (°)	Normal Stress (MPa)	Shear Stress (MPa)	Angle or App Angle (°)	Peak /Residual Friction Angle (°)	Peak /Residual Cohesion (MPa)	Note
SHJO-01	Reef	Reef	P1	726	0.92	1.0	0.6	1.39	1.25	42.0	28.0	0.5	
			P2	636	1.50	2.0	3.5	3.28	2.17	33.4			
			P3	620	2.15	3.0	3.1	5.02	3.20	32.5			
			R 1	669	0.80	1.0	-1.6	1.46	1.24	40.4	30.0	0.3	
			R 2	635	1.44	2.0	2.4	3.25	2.13	33.3			
			R 3	619	2.15	3.0	2.2	4.98	3.29	33.4			
SHJO-02	HW	Pyroxenite	P1	1060	1.50	1.0	14.8	1.27	1.13	41.6	37.0	0.1	
			P2	1074	2.01	2.0	11.2	2.19	1.47	33.9			
			P3	960	2.61	3.0	2.3	3.23	2.59	38.7			
			R 1	872	0.77	1.0	2.4	1.18	0.83	35.0	37.0	0.0	
			R 2	862	1.53	2.0	3.9	2.44	1.61	33.5			
			R 3	943	2.54	3.0	1.1	3.23	2.63	39.1			
SHJO-03	FW	Peg Pyroxenite	P1	936	1.03	1.0	4.8	1.16	1.01	41.2	31.0	0.3	
			P2	952	1.48	2.0	1.6	2.14	1.50	34.9			
			P3	927	2.11	3.0	0.3	3.25	2.26	34.9			
			R 1	854	0.92	1.0	2.2	1.21	1.04	40.5	26.0	0.4	1
			R 2	891	1.39	2.0	2.8	2.32	1.45	32.0			
			R 3	866	1.97	3.0	1.9	3.54	2.16	31.4			

Notes: P1, P2 & P3 : Peak Force; R1, R2 & R3 : Residual Force.
1 - Joint surface was damaged after the 1st stage shearing test, it results lowe 2 - No suitable specimen could be prepared for the test.

4.7 Rock Stresses Measurements and Determination

In order to accurately design pillars, it is important to know the in-situ stresses of the area where excavations are to be made. These in-situ stress values will then be used for both empirical equations as well as in numerical modelling during pillar design. Van der Heever & Piper, (2013) conducted stress measurements at Siphumelele shaft. The site chosen for the measurements was on 34 level approximately 1350m below surface in competent norite rock 30m below the MR horizon. Borehole inclination was 20 degrees above horizontal. The CSIRO thin-walled Hollow Inclusion strain cell was employed and the tests conducted in accordance with ISRM guidelines.

Table 4.9 shows details of the components of the stresses obtained at the measurement site. The major principal stress (Sigma 1) had a magnitude of approximately 40 MPa and acting in a NNW direction, plunging at approximately 30 degrees from the horizontal. The intermediate principal stress (Sigma 2) had a magnitude of approximately 32 MPa, acting in a WSW-direction and plunging at approximately 7 degrees from the horizontal. The minor principal stress (Sigma 3) had a magnitude of approximately 25 MPa, acting in a SSE direction and plunging at approximately 59 degrees from the horizontal.

Table 4.9: Details of the virgin stress tensors (van der Heever & Piper, 2013)

Stress Component	Magnitude (MPa)	Bearing (degrees)	Dip (degrees)
Sigma 1	42.8	357	32
Sigma 2	28.8	252	22
Sigma 3	24.8	134	50
TauXX (south)	38.1±2.8*	See Figure 1	
TauYY (west)	28.0±2.3*		
TauZZ (vertical)	30.4±1.8*		
TauXY	0.2±1.4*		
TauYZ	-1.8±1.1*		
TauZX	7.6±1.4*		
SigHmax	38.1	On bearing 91	
SigHmin	28.0	On bearing 181	
kmax	1.25	On bearing 91	
kmin	0.92	On bearing 181	
* 95% confidence intervals assuming Student's t distribution with 7 degrees of freedom			

The measured maximum horizontal stress SigHmax acts almost due east and the minimum horizontal stress SigHmin acts almost due south (see Table 4.9). The ratio of the measured maximum horizontal to vertical stress (k-ratio) is approximately 1.25, which is within the range for other stress measurements that have been conducted in the in the region (Stacey & Wesselo, 1998).

Using the method of observing blast fracture orientation for estimating the direction of principal stress as suggested by Middindi, (2013) and Brady and Brown (2005) (discussed in Section 2.11), the stress results confirm observations at Khuseleka shaft. The blast socket and shape orientations observed underground in the KORP section indicated that Sigma 1 acts sub-horizontally in a NNW direction. An example is a blast hole shown in Figure 4.5 that was measured in the KORP section in panel 23-27-8E; Figure 4.6 shows the plan of the panel at a depth of approximately 740m below surface (calculated vertical stress 20.7MPa). This panel is mining toward the south easterly direction. The observation is that the longer axis is generally in the direction of higher stresses, which in this case is in an approximately NW – SE direction, this is the orientation of the major horizontal stress. The shorter axis is in the direction of lower stresses which in this case is vertical. Using a crude method of measuring the horizontal axis (12cm) vs vertical axis (9cm) of the blast hole gives a ratio of 1.33 which is in approximate agreement with the measured k-ratio of 1.25. This method although not giving actual k ratios, is a quick check on the general orientation of the major and minor stresses.

Figure 4.5: A blast socket taken in a panel mining towards south-east

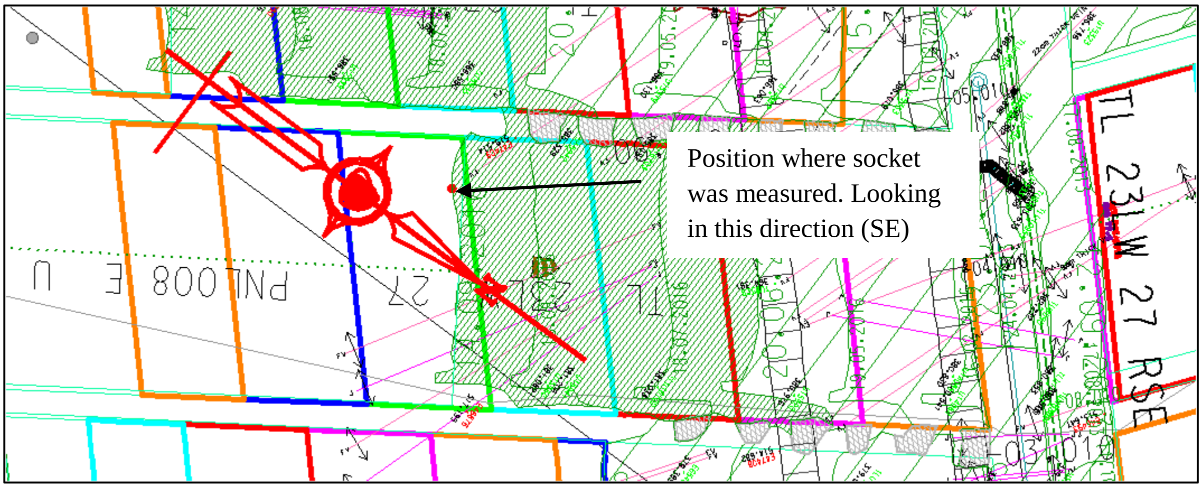

Figure 4.6: Plan of the panel were the socket was observed and measured

Laboratory results of the elastic properties of the norite rock, the rock in which the stress measurements were taken are shown in Table 4.10. The table shows an average density of 2.9g/cm^3 for the norite which coincidently is the major overburden rock on the shaft. This allowed the use of a relative density of 2.9g/cm^3 for the overburden rock when calculating stresses.

Table 4.10: Summary of norite rock properties at the measurement site

POISSON'S RATIO

Client: Groundwork Consulting

Sampling Site: 34 level, Siphumelele Shaft, Rustenburg (Norite/Anorthosite varieties)

9-Nov-13

SPECIMEN PARTICULARS					SPECIMEN DIMENSIONS					SPECIMEN TEST RESULTS								
Rocklab Specimen No 5569-	Location	Sample No	Depth m	Rock Type	Diameter mm	Height mm	Ratio of Height to Diameter	Mass g	Density g/cm³	Failure Load kN	Strength (UCS) MPa	Tangent Elastic Modulus @ 50% UCS GPa	Secant Elastic Modulus @ 50% UCS GPa	Poisson's Ratio Tangent @ 50% UCS	Poisson's Ratio Secant @ 50% UCS	Linear Axial Strain at Failure mm/mm	Failure Code	Note
UCM-01A	Siphumele Mine	Sipo 1		Norite	56.50	137.2	2.4	996.31	2.90	280.9	112.0	62.8	47.0	0.48	0.23	0.002428	XA	
UCM-01B		Sipo 2			56.50	136.8	2.4	989.00	2.88	276.3	110.2	60.2	44.9	0.48	0.25	0.002440	XB	

Note: All tests were conducted according to the ISRM's specfications.

Table 4.11 shows calculations done to compare the measured stresses verses calculated stresses at 1347m below surface. The equations for calculating vertical and horizontal stresses are given below

$$(\sigma_z = \rho g h \quad (29)$$

$$\sigma_h = k\rho g h \quad (30)$$

Where:

σ_z = Virgin stress acting normal to the pillar axis (vertical stress)

σ_h = Virgin stress acting perpendicular to the pillar axis (horizontal stress)

ρ = Rock density (average density for norite in the bushveld complex is 2.9g/m^3)

g= Gravitational acceleration (9.81m/s^2)

h = Depth below surface

k = k ratio = σ_h/σ_z

Table 4.11: Measured vs Calculated virgin stresses for Siphumelele Mine

		Density (g/cm^3)	**Gravity**	**k ratio**	
		2 900	9.81	1.25	
	Depth below Surface (m)	**Measured horizontal stress (MPa)**	**Calculated horizontal stress (MPa)**	**Measured vertical stress (MPa)**	**Calculated vertical stress (MPa)**
Siphumelele Measured Values	1347	38.1	47.9	30.4	38.3

The measured vertical stress component is 20% less than the expected overburden stress of 38MPa at the depth of 1350m. This 20% discrepancy can be attributed to localised gravitational loading and paleo-tectonic forces. Calculated stress values will be used in the design of the pillars at the various depths since no stress measurements were taken at these depths.

4.8 Pillar Height

Based on the Technical Support Document, Snyman, (2015) the best cut for stoping is based on geotechnical and grade considerations. On the UG2 the best cut has been determined as the parting contact between the chromitite main reef and the pyroxenite +105cm towards the footwall (Figure 4.7). The stoping width for the UG2 is therefore planned at 105cm. This stoping width is the one which determines the pillar height which is in turn used when designing pillars. In the KORP section, 27 raise-line is already being trial mined and the average stoping width is currently 1.2m as measured by the survey department. Appendix C shows the monthly stoping widths as measured by the survey department for the different panels that have been mined on the KORP section to date.

Figure 4.7: UG2 reef in a stoping panel

4.9 K value (Rock Mass Strength) Determination

Different methods for determining the rock mass strength (K value) used in pillar strength calculations have been proposed. Most rock engineering practitioners vary this rock mass strength value at between half and a third of the UCS of the rock in which the pillar will be cut.

A more formal approach has been adopted to determine the value of K. This approach is based on using the different rock mass strength criteria which are based on empirical evidence and are summarised in Table 2.2.

The intact rock UCS of 63.4MPa of chromitite rock (UG2) derived from the laboratory tests (Table 4.4) was used to calculate rock mass strength using the different rock mass classification systems as pillars are cut in this rock.

4.9.1 Rock mass Classification at Khuseleka Shaft

The use of rock mass classification as a basis for support and excavation design has been discredited by some critics. Broch, A. & Palmstrom, E., (2006) and Pells & Bertuzzi, (2006), have pointed out that the systems have been extended far beyond their initial purposes, which is, to be simple, preliminary methods of giving a crude estimate of support required at planning and feasibility stages of a project before more data becomes available and advanced techniques are used. They have argued that these systems are now being used as the final determinant of the design process and for a whole range of other applications such as determining the seismic velocities, deformation modulus of rock mass, grouting, etc.

“Although classification systems may be useful tools for estimating the need for tunnel support at the planning stage especially for tunnels in hard and jointed rock mass without overstressing, there are a number of restrictions that should be applied if and when a system is going to be used in other rock masses. When developing classification systems and other tools to evaluate nature, it is of crucial importance to keep in mind the innumerable variations that occur in rock masses and the uncertainties involved in observing and recording the different parameters. It is advisable to use at least two rock mass classification schemes during the design process. Other tools in the rock engineering process must be used as more data is sort and becomes available” (Broch, A. & Palmstrom, E., 2006).

Pells & Bertuzzi, (2006), in discussing the paper by Palmstrom had this to say in support of this criticism, “The design correlations published in the various papers on the Q and RMR systems should be used with great caution in geological environments significantly different from those comprising the original case studies. The use of general classification design approach is contrary to normal engineering design processes. It is not a proper approach Scientific Method. The position of the classification design approach in relation to modern limit state is unknown and unknowable. It covers neither Ultimate nor Serviceability Limit States”.

Regardless of the criticism and reservations against the use of rock mass classification systems, they still remain a valuable, and sometimes only available tool, in determining the rock mass character and giving a number and ‘feel’ for the rock mass of any excavation. Even in situations where modern and advanced techniques such as numerical modelling are used, rock mass classification values are always one of the key input parameters used.

Khuseleka shaft uses Barton, et al., (1974) Q and Bieniawski, (1989) Geomechanics Classification System (RMR) rock mass classification methods for the rock mass characterisation of its working places and in the design of stable excavations and support systems.

Q - System

Barton, et al., (1974), came up with a Tunnelling Quality Index, Q based on case studies done in tunnels all over the world. Q varies from a low of 0.001 to a maximum of 1000; Table 4.12 shows the range of values and their interpretation in relation to the quality of the rock mass. The method is based on six parameters which are as follows; the RQD index, the number of joint sets (J_n), the roughness of the weakest joints (Jr), the degree of alteration of filling along the weakest joints (J_a), and two further parameters which account for the rock load (SRF) and water inflow (J_w). In combination these parameters represent:

1. Block size $\left(\frac{RQD}{Jn}\right)$
2. Inter-block shear strength $\left(\frac{Jr}{Ja}\right)$
3. Active stress $\left(\frac{Jw}{SRF}\right)$

These six parameters are combined in the following way:

$$Q = \left(\frac{RQD}{Jn}\right) \text{ x } \left(\frac{Jr}{Ja}\right) \text{ x } \left(\frac{Jw}{SRF}\right) \quad (31)$$

Table 4.12: Qualitative Classification of rock mass based on Q (Barton, et al., 1974)

Q INDEX VALUE	**ROCK MASS CLASS**
0.0001 – 0.01	**Exceptionally poor**
0.01 – 0.1	**Extremely poor**
0.1 - 1	**Very poor**
1 - 4	**Poor**
4 - 10	**Fair**
10 - 40	**Good**
40 - 100	**Very good**
100 – 400	**Extremely good**
400 - 1000	**Exceptionally good**

Geomechanics Classification System (RMR)

Bieniawski, (1989) formulated the Geomechanics RMR, which is derived by summing up five parameters and adjusting this total by taking the joint orientation in relation to the excavation into account. These five parameters are

- Rock material strength (UCS)
- RQD
- Joint spacing

- Joint Roughness and separation
- Ground water

The qualitative description of the rock mass based on the obtained RMR value is shown in table 4.13

Table 4.13: Qualitative Classification of rock mass based on RMR (Bieniawski, 1989)

CLASS	RMR	DESCRIPTION
I	**81 – 100**	**Very good rock**
II	**61 – 80**	**Good Rock**
III	**41 – 60**	**Fair rock**
IV	**21 – 40**	**Poor rock**
V	**<21**	**Very poor rock**

During underground visits on the mine by rock engineering practitioners, different rock mass classification parameters are collected and Q and RMR values calculated for those excavations.

A total of 53 RMR and Q values have been calculated for the panels being mined in 27 raise line where trial mining is being conducted for the KORP section and the average Q and RMR values are given in Table 4.14. The RMR values calculated have ranged from 52 (Fair) to 84 (Very good) with an average of 70.3, whilst the Q values have ranged between 0.88 (Very poor) to 95 (very good) with an average of 24.7.

Appendix D shows the rock mass classification results for all panels of the KORP section mapped since trial mining started.

Table 4.14: Average Q and RMR values for KORP trial section

RMR	RMR Rating	Q	Q Rating
70.3	Good	24.7	Good

The average RMR value of 70.3 was used to determine the rock mass strength K value, using the rock mass strength criteria given in Table 2.2 and discussed below.

4.9.2 Hoek – Brown

The Hoek – Brown criterion parameters in Table 4.15 were calculated using the rock mass classification rating of 70.3 in Table 4.14. The rock mass strength was determined using equation 19. The m and s constants were derived by using equations developed by (Priest & Brown, 1983) where

$m = m_i e^{\frac{RMR-100}{28}}$

$s = e^{\frac{RMR-100}{9}}$

$$m_i = \frac{1}{\sigma_{ci}}\left[\frac{\Sigma_{xy} - (\Sigma_x \Sigma_y/n)}{\Sigma_x^2 - ((\Sigma_x)^2/n)}\right] \quad (32)$$

Table 4.15: Calculated Hoek-Brown values using the Hoek-Brown Criterion

	sigma 3 (x)	**sigma 1**	**y**	**xy**	**xsq**	**ysq**
	5	78.5	5402.25	27011.25	25	29184305.06
	10	158.5	22052.25	220522.5	100	486301730.1
	15	200.6	34447.36	516710.4	225	1186620611
	20	217.8	39124.84	782496.8	400	1530753105
	30	267.6	56453.76	1693613	900	3187027018
Sum	80	923	157480.5	3240354	1650	6419886769
	Number of tests n		5			
	sigci	18.22				
	mi	106.874				
	r2	0.961509				

a = 0.5 (for intact rock)

The rock mass uniaxial compressive strength is obtained by setting $\sigma_3 = 0$, giving

$$\sigma_1 = \sigma_c \, .s^a \quad (33)$$

Using the average RMR value of 70.3 for the KORP section

$s = e^{\frac{70.3-100}{9}} = 0.04$

Rock mass uniaxial compressive strength = 63MPa x $0.04^{0.5}$ = 12.6MPa

So the rock mass strength using Hoek-Brown criterion = 12.6MPa

With this method the rock mass strength is downgraded to 20% of the intact rock strength.

4.9.3 Mohr – Coulomb

As discussed in the literature review chapter, the Mohr-Coulomb criterion is a linear fit to the Mohr circles.

Using Bathopele's triaxial compressive strength tests results from Table 4.6, Figures 4.8, 4.9 and 4.10 show the Mohr-Coulomb criterion in σ1- σ3 space plots for chromitite (UG2 reef), pyroxenite (HW) and Pegmatoidal pyroxenite (FW) rock respectively to determine the Mohr-Coulomb parameters for those different rocks.

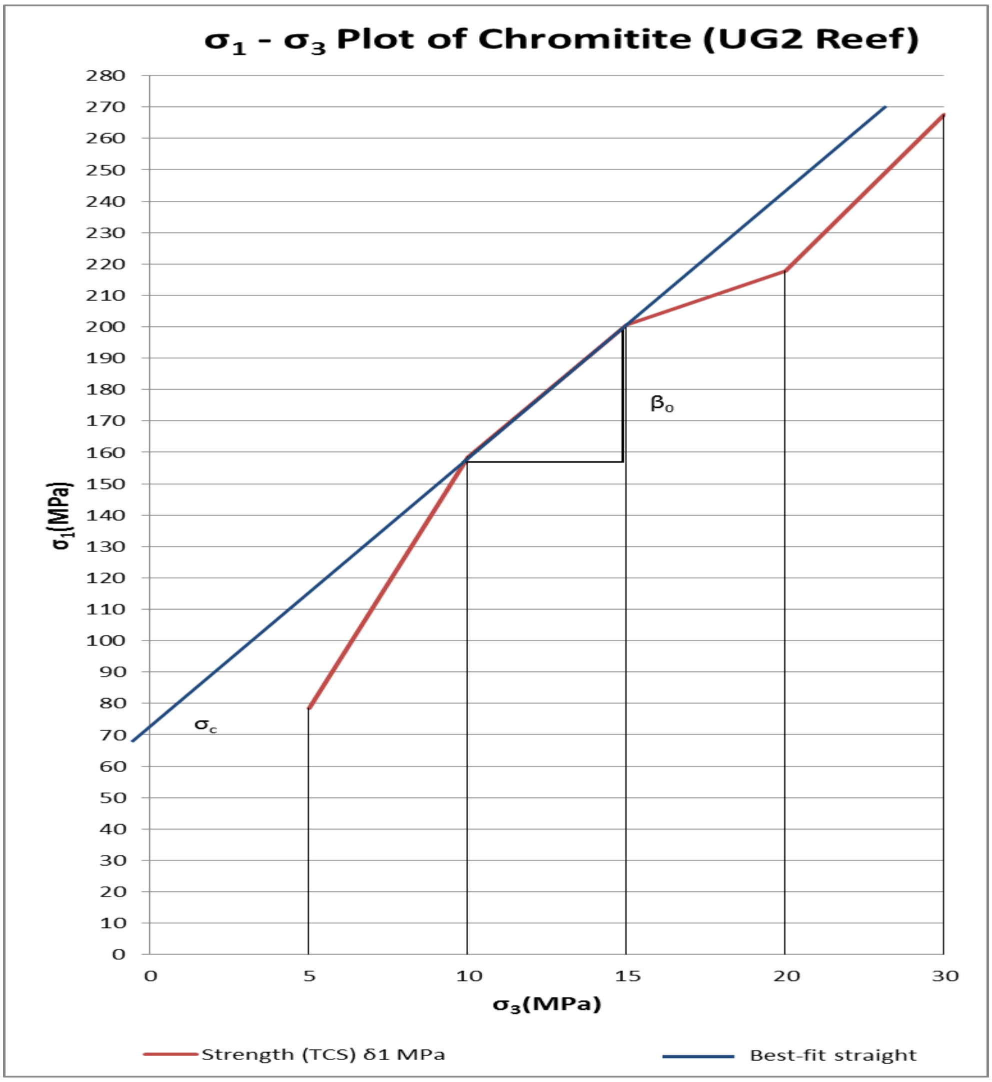

Figure 4.8: Mohr-Coulomb in σ_1- σ_3 space for chromitite (UG2 reef)

The following values were derived from the σ_1- σ_3 space in Figure 4.8.

Uniaxial compressive strength (σ_1) = 73MPa

Slope (β_0) = 7

Using Equations 18b, the following values are calculated

Sin $\phi_i = \frac{7-1}{7+1}$ = 48.6°

Cohesion (c_o) $=\frac{73}{2\sqrt{7}}$ = 13.8MPa

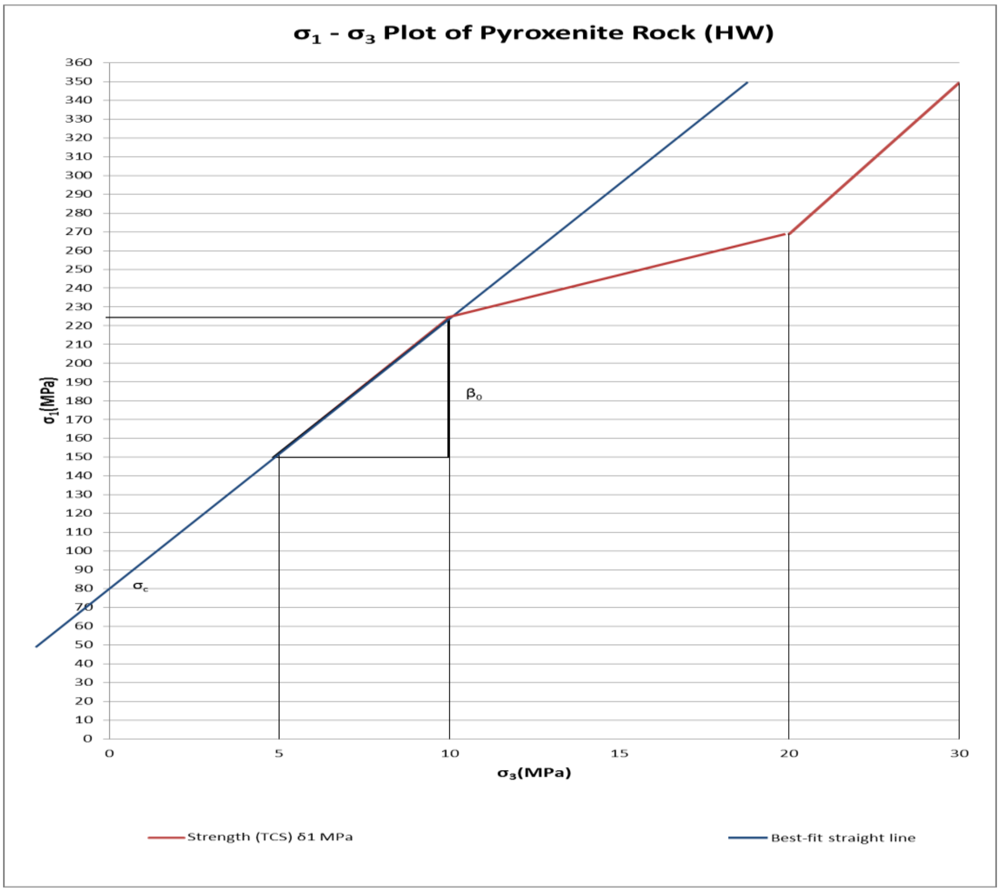

Figure 4.9: Mohr-Coulomb in σ_1- σ_3 space for pyroxenite (HW)

The following values were derived from the σ_1- σ_3 space in Figure 4.9.

Uniaxial compressive strength (σ_1) = 80MPa

Slope (β_0) = 14.4

Using Equations 18b, the following values are calculated

Sin $\phi_i = \frac{14.4-1}{14.4+1}$ = 60.5°

Cohesion (c_o) $=\frac{80}{2\sqrt{14.4}}$ = 10.5MPa

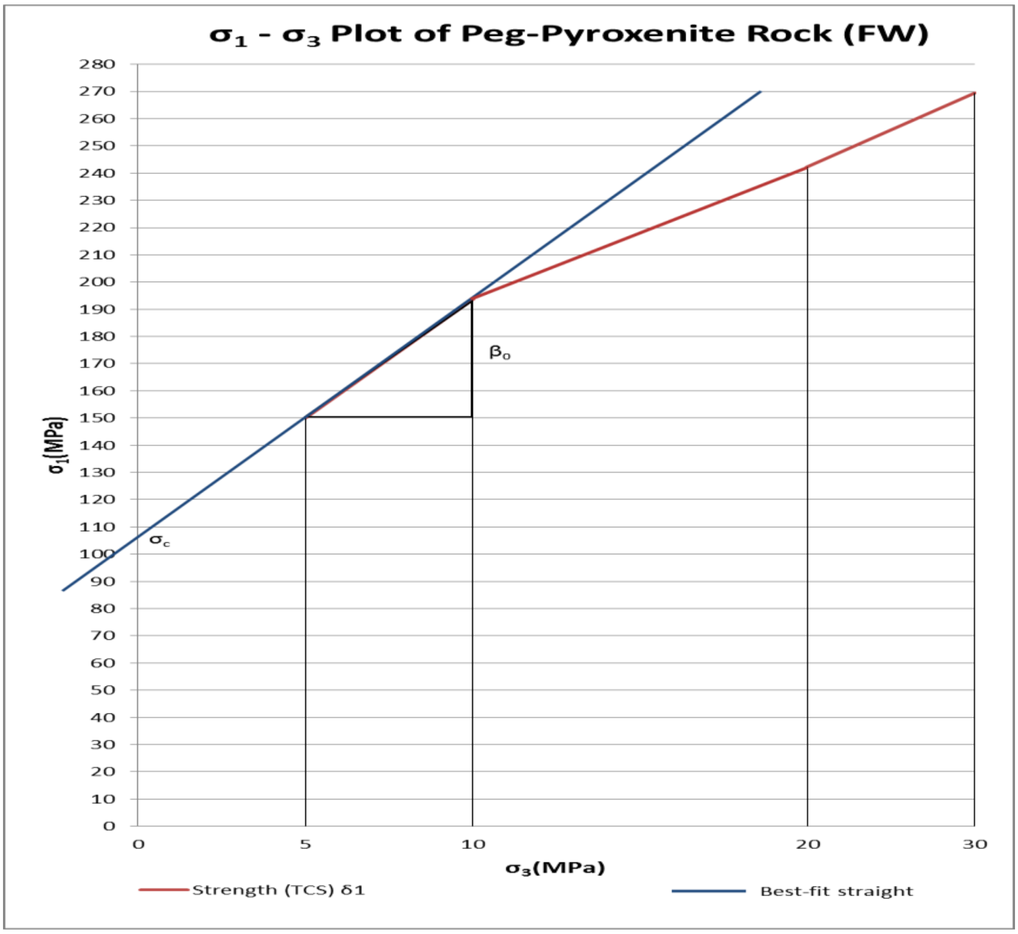

Figure 4.10: Mohr-Coulomb in σ_1- σ_3 space for peg-pyroxenite (FW)

The following values were derived from the σ_1- σ_3 space in Figure 4.10.

Uniaxial compressive strength (σ_1) = 106MPa

Slope (β_0) = 8.6

Using Equations 18b, the following values are calculated

Sin $\phi_i = \frac{8.6-1}{8.6+1} = 52.3^o$

Cohesion (c_o) $= \frac{106}{2\sqrt{8.6}} = 18.1$MPa

4.9.4 Strength Value Using Q system

Barton, (2002) came up with a formula based on a normalised Q which takes into account the direction of excavation and the density of the rock.

$\sigma_1 = 5\gamma Qc^{1/3}$

Where Qc = Q x UCS/100 (normalised Q)

Q = 24.7 (The average Q for the KORP section, Table 4.14)

γ = density of the rock (t/m^3) = 4.0t/m3 for the UG2 rock (Table 4.4)

$= 5 \times 4.0 \times (24.7 \times ((63/100))^{1/3} = 50$MPa

The rock mass strength using Q system = 50MPa

With this method the rock mass strength is downgraded to 79% of the intact rock strength of 63MPa.

4.9.5 Design Rock Mass Strength (DRMS)

The RMR value will be used as the MRMR value as similar parameters are used to derive both classifications. The rock mass strength (RMS) will be calculated from the UCS of the rock and the RMR based on Laubscher, (1990) MRMR,

RMS = UCS x (MRMR – R_{UCS})/100) = 63 x (65 – 6)/100) = 37.2MPa

Adjustments are then made for this RMS value taking into account the effects of weathering, joint orientation, stresses acting around the excavation and adjustment for blasting effect. The values of these were 100%, 85%, 80% and 80% respectively. Multiplying these with the RMS gives,

DRMS = 37.2MPa x 1 x 0.85 x 0.8 x 0.8 = 20.22MPa

With this method the rock mass strength is downgraded to 32% of the intact rock strength.

4.9.6 RocLab Software

RocLab is a software program designed by Rocscience Inc., for determining the Generalized Hoek-Brown strength parameters of a rock mass (m_b, s and a). Rock mass parameters such as tensile strength, compressive strength and deformation modulus are also derived by this program. The parameters derived from this program are used as input for numerical programs, which require material properties in order to perform stability or stress analysis.

The input data that was used was:

• the triaxial test results of UG2 reef rock (chromitite) in Table 4.6, this is because the pillars are cut in this rock.

• unconfined compressive strength of intact rock was calculated by the program based on the triaxial data inputted.

• Young modulus of elasticity obtained from USC tests conducted for UG2 reef rock in Table 4.4

• the intact rock parameter mi was calculated by the program based on the triaxial data inputted.

• the geological strength index GSI (Estimated from The formula RMR = RMR_{89} – 5, which is 70-5 = 65

• the disturbance factor D (0.8 for very poor quality blasting in a hard rock)

Table 4.16 shows the results obtained from the RocLab software, with the top 5 values being the input parameters and the rest being the output.

Table 4.16: Calculated Parameters from RocLab Software

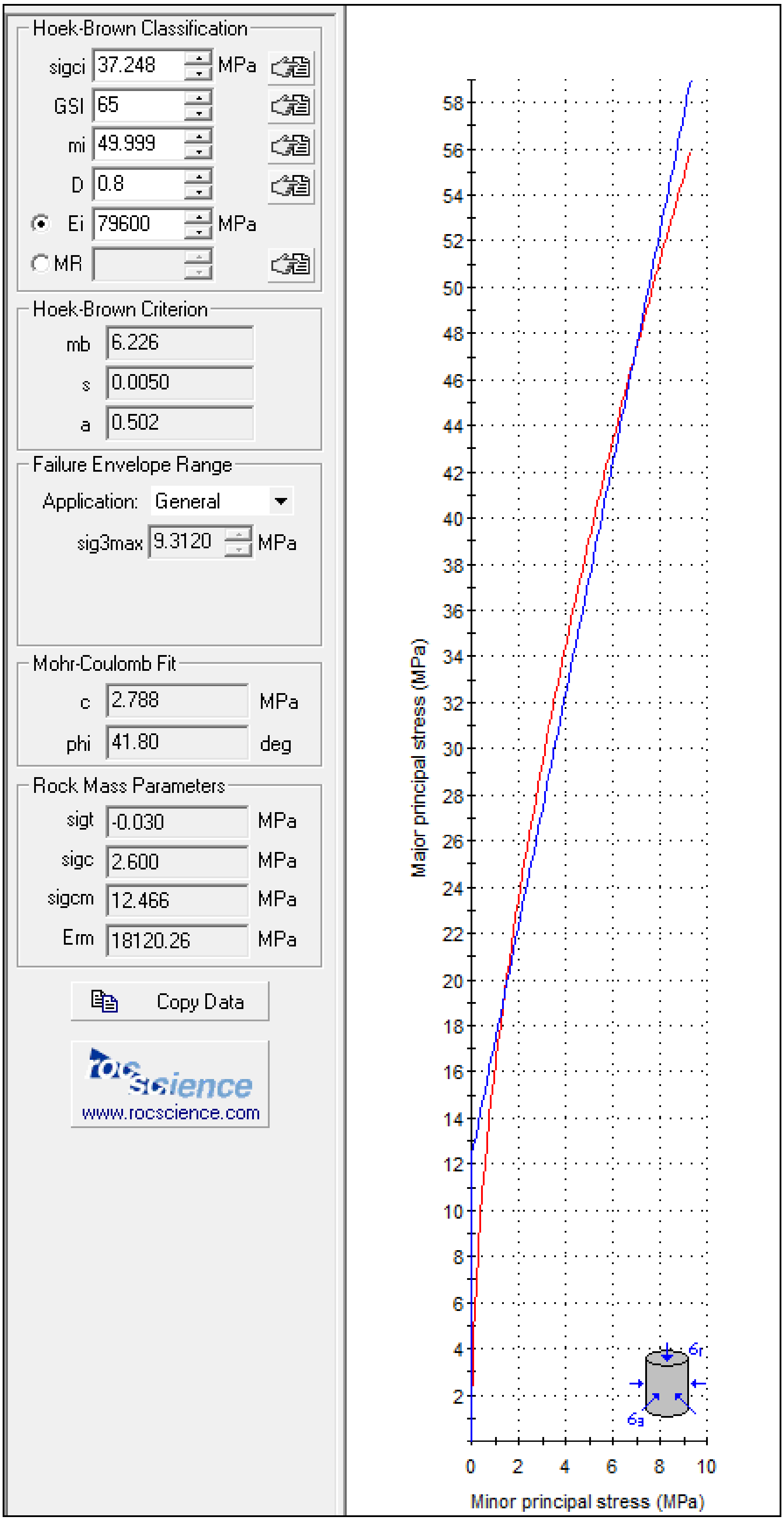

The above results compare favourably with those that were calculated using the Hoek-Brown criterion in Table 4.15. The global rock mass compressive strength (sigcm) of 12.5MPa compares favourably with the rock mass strength of 12.6MPa calculated. The program, does not give mi values greater than 50, any value greater than 50 reverts to 50 by default, and this could explain the 50 obtained verses the 106 calculated. The calculated intact rock UCS value of 18.22MPa in Table 4.15 is about half the 37.2MPa calculated by the program. According to Rocscience, (2016) this could be due to the Marquardt-Levenberg fitting method performed on the data by the program, thereby giving results different to those calculated.

The rock mass strength determined by this method is 12.5MPa.

With this method the rock mass strength is downgraded to 20% of the intact rock strength.

4.10 Choosing the rock mass strength to use in pillar design

Table 4.17 shows the rock mass strength derived using the different criteria available. As can be seen each criterion gives its own value with these values ranging between 20% and 79% of the UCS. This means that the value that will be used for design purposes will either be too conservative or exaggerated. It is therefore very critical that a value that is as close to the actual strength is chosen. The only way this can be done is through back analysing pillars that have been cut and are showing failure. However, no regional pillars have been observed to show failure in the UG2, so as discussed earlier a value of between a third and a half of the UCS of the rock as per the industry standard was chosen. Therefore based on the above results, Laubscher, (1990), value of 20.2MPa which is a third of the UCS of the UG2 reef rock was used as the K rock mass strength value for pillar design purposes.

Table 4.17: Summary of rock mass strengths derived from different strength criteria

Author	**Strength Criterion**	**Calculated Rock mass strength (MPa)**	**% of UCS**
Hoek – Brown (2002)	$\sigma_{1=}\sigma_3 + \sigma_c\{m_b.\frac{\sigma_3}{\sigma_c} + s\}^a$	12.6	20%
Laubscher (1990)	DRMS = RMS x Adjustments	20.2	32%
(Barton, (2002)	$\sigma_1 = 5ɣQc^{1/3}$	50	79%
RocLab Software		12.5	20%

4.11 Foundation Strength

4.11.1 2.5 x rock strength of foundation rock

The foundation strength as stated in Section 2.8 is critical to the stability of the pillars. The accepted rule of thumb to avoid foundation failure is for the APS to be less than 2.5 multiplied by the UCS of the weakest foundation rock (Jager & Ryder, 1999). Based on this equation, the foundation rock of the KORP section is pegmatoidal pyroxenite with a UCS of 91MPa (Table 4.4). Therefore 2.5 x 91MPa = 228MPa. The maximum APS that was calculated for the pillars in the KORP section was 228MP based on this equation.

Two other foundation strength methods were discussed in Section 2.8 which are Terzaghi, (1943) and Hansen, (1970) methods. Both equations were used to calculate the maximum allowed foundation strengths for the KORP section that did not induce failure. The value, B_p, which is the foundation depth, was derived from boreholes drilled in the KORP section as well as the borehole drilled and logged by the author (Hole ID: CTM03). The average foundation depth of the pegmatoidal pyroxenite based on the logged boreholes is 1.5m. Appendix E shows the core logs for holes drilled in the KORP section.

4.11.2 Terzaghi's Formula

Using the results from Bathopele's triaxial compressive strength tests in Table 4.6, a Mohr-Coulomb in $\sigma1$- $\sigma3$ space for pegmatoidal-pyroxenite in Figure 4.10 was plotted in order to determine the cohesion and angle of internal friction of the rock which is the foundation rock of the pillars. Equations 21 to 24 from the Terzaghi, (1943) formula were used to calculate the strength of the foundation rock and the following values were derived.

$N_q = 15.04$

$N_c = 10.85$

$N_\gamma = 27.25$

qu (foundation strength) = 327.2MPa

This value is 14% higher than the $2.5\sigma_c$ APS that was determined for the pillars.

4.11.3 Hansen's Formula

Hansen, (1970), based his formula on Terzaghi, (1943) with changes taking into account the pillar shape. Since these are rib pillars Equation 25 was used, giving foundation strength of 226.7MPa. It is a value almost similar to that obtained by the $2.5\sigma_c$ formula.

4.11 shows the different pillar foundation strengths calculated using the strength formulae discussed.

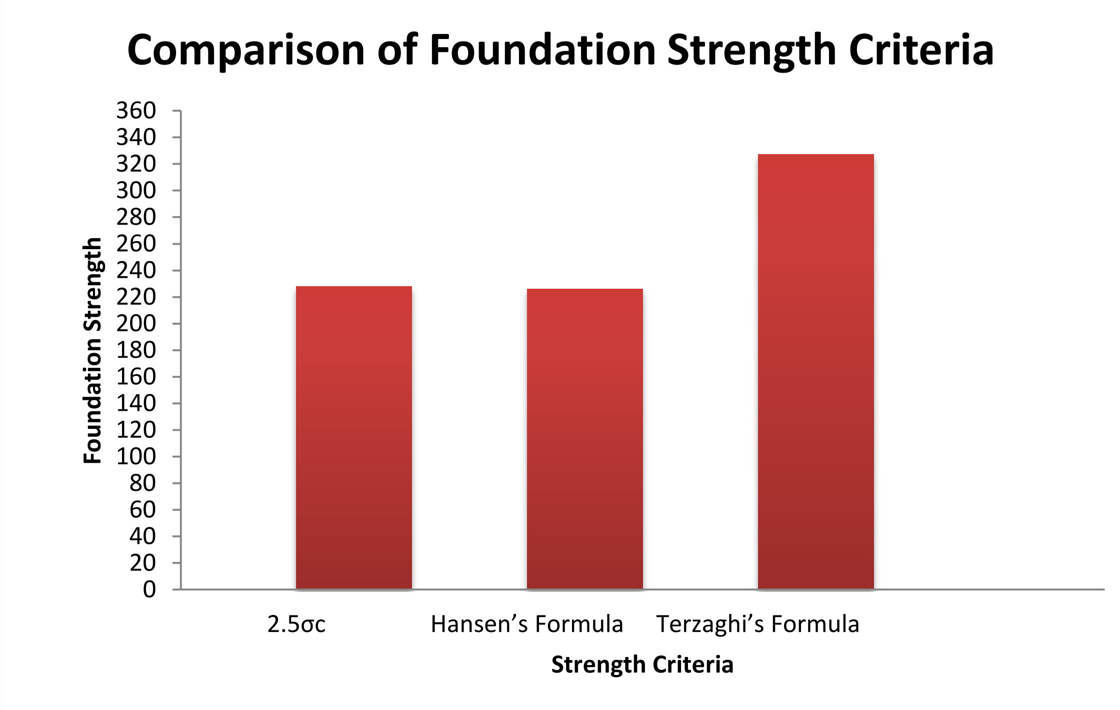

Figure 4.11: Comparison of the different foundation strengths calculated using the different criteria.

It is clear from Figure 4.11 that the calculation of the 2.5 x σ_c as the APS that prevents foundation failure is similar to that derived from Hansen's formula and quite comparable to that derived from Terzaghi's formula although lower. This means the value of 228MPa derived from the 2.5σ_c formula can be used with some confidence and is more conservative compared to the Terzaghi's method. However monitoring and back analysis on cut pillars will be required to validate this value.

4.12 Conclusions

Before pillars can be designed, certain rock properties must be known. Some properties can be visually observed and qualitatively obtained, whilst others require more sophisticated methods to determine them and need to be quantitatively described. With a considerable amount of information on the rock properties gathered, a lot of uncertainty is removed and the results can be confidently used to design the pillars.

Core had to be drilled from underground in the working place where the pillars will be designed and the samples tested at the laboratory to determine the elastic properties of the rock. Since the specimen tested only represents a very small proportion of the entire rock mass, rock characterisation methods, through rock mass classification systems were done. This rock mass classification system together with the elastic properties determined from laboratory work gave the rock mass strength value that was used for designing the pillars.

The other information that is critical in pillar design is the in-situ stress conditions. Stress measurements taken at Siphumelele Mine, with similar conditions to Khuseleka Shaft were adopted and used to determine the stress parameters for this project. Although it is known that stress conditions differ considerably from site to site, it was assumed that the overall stress conditions like the k ratio are almost similar, and based on observation of blast holes, it can be concluded that there is a strong correlation between the stresses measured at other operations and those obtaining at Khuseleka shaft. The in-situ stresses at different depths where the pillars are going to be cut were calculated based on these stress measurements from Siphumelele Mine.

The foundation strength was also determined for the project based on the 2.5 x σ_c equation which also compared favourably with the other equations and could thus be used with some confidence. The value obtained was used as the maximum APS for all the pillars that were designed in the KORP section.

With the information gathered, calculated or observed, the process of designing pillars for the KORP section commenced.

CHAPTER 5: PILLAR DESIGN

5.1 Introduction

Before starting the pillar design process, it was important to discuss and note the pillar design strategy currently being used at Khuseleka mine. This was so that if they were any aspects that could be incorporated to improve the design, they would be considered.

In this chapter, all the empirical methods and equations discussed in the literature review were used to design pillars using the values determined in chapter 4. In the final part of the chapter, justification was given in the choice of the final design.

5.2 Khuseleka Pillar Design Strategy

Khuseleka regional pillars are designed according to a standard that was adopted for all Anglo American Platinum mines. The design strategy mainly focuses on a predetermined APS, FOS and w/h ratio to ensure stability of both on and off reef excavations. Figure 5.1 is a plan of the upper section of the UG2 reef horizon where mining occurred without regional pillars.

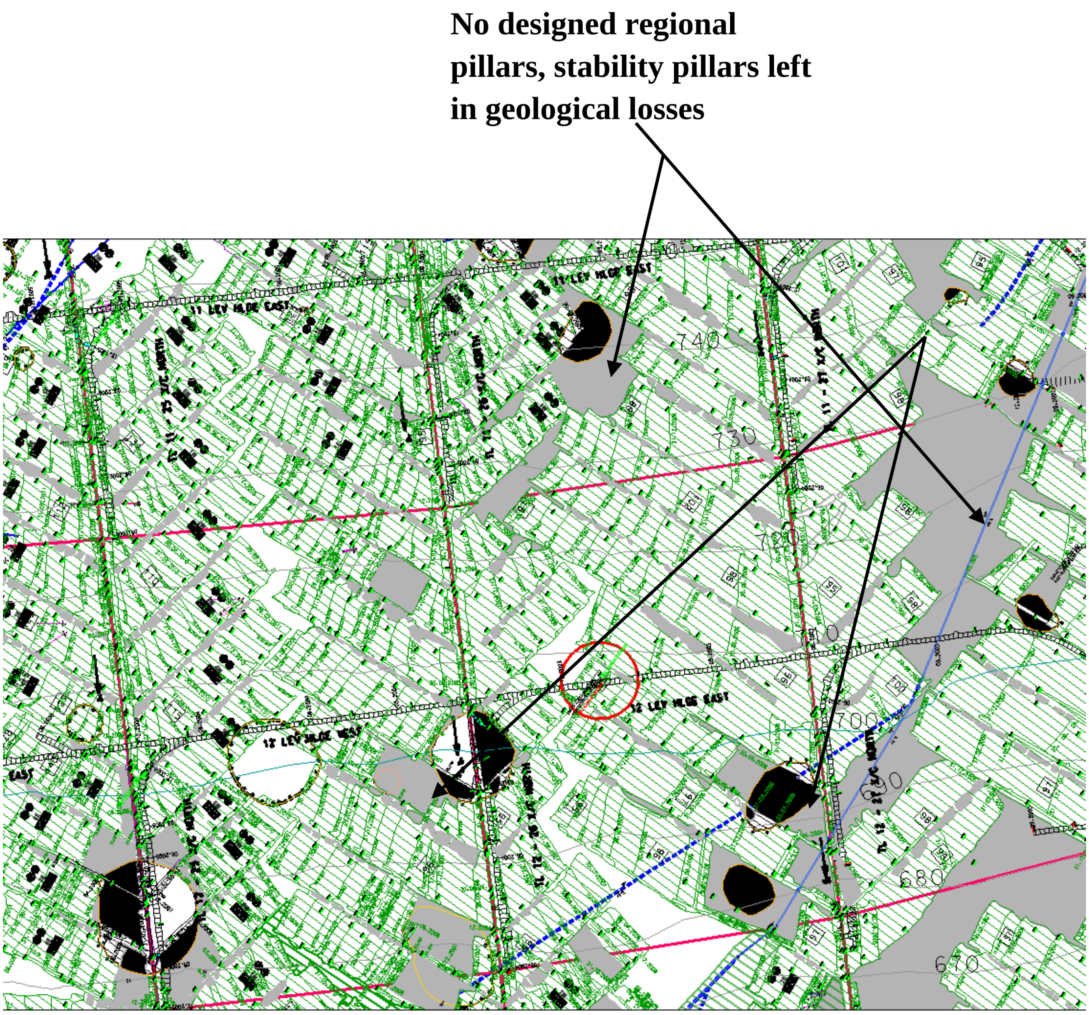

Figure 5.1: Plan showing a typical mining layout in the UG2 reef horizon at Khuseleka prior to the design of regional pillars

The mining method most commonly used at Khuseleka shaft is scattered breast using small in-stope pillars and regional pillars to maintain stability of the workings. In all cases the configuration or sequence adopted is that of mining towards solid whenever possible. As can be observed in the Figure 5.1, prior to 2010 stability pillar design was adhoc, with geological losses (potholes, major faults and dykes, reef rolls) forming regional pillars.

As time went on and mining got deeper it became necessary to have a systematic design of regional pillars. A group standard on regional support was implemented and adopted for the platinum division in 2013 (Priest G, 2013). Section 2.2 discusses the mining and stability strategy for Khuseleka shaft based on this standard.

5.2.1 Pillar Strength

Pillar strength is calculated using, Stacey & Page, (1986) pillar strength equation with the K strength value being a product of the RMR value and rock UCS. The pillar widths designed for the different levels are shown in Table 5.1 (Snyman, 2015).

Table 5.1: The pillar widths at different levels

Level	**Pillar Width (m)**
16	14
19	15
21	18
23	19
25	19
26	19
27	20
28	20

What has been noted from back analysis of all the pillars cut is that surveyors give a stop note (a note indicating were mining should stop) at about 2m from the position of the pillar in a stoping panel. This means that most pillars on average are 4m wider than planned; therefore the pillar strength will be greater than that designed for.

5.2.2 Average Pillar Stress

According to Priest, (2013), the APS of pillars at the Rustenburg Platinum Mines should not be more than 500MPa using the TAT. He based this value on back analysis that was previously done. However, seismic activity has been recorded at Siphumelele mine with pillars having an APS of less than 350MPa (Van Asegan, et al., 2014). This might indicate that the design criterion for an APS of 500MPa is immoderate and exaggerated.

Figures 5.2 to 5.4 are numerical modelling results of the APS for the designed regional pillars in the KORP section using their current design strategy. This analysis was done by the Institute of Mine Seismology (IMS) using their in-house numerical modelling program (Clark, 2016). The results show that the pillars have been designed with a maximum APS of 391MPa. Higher APS can be noted in the central portions of the mine.

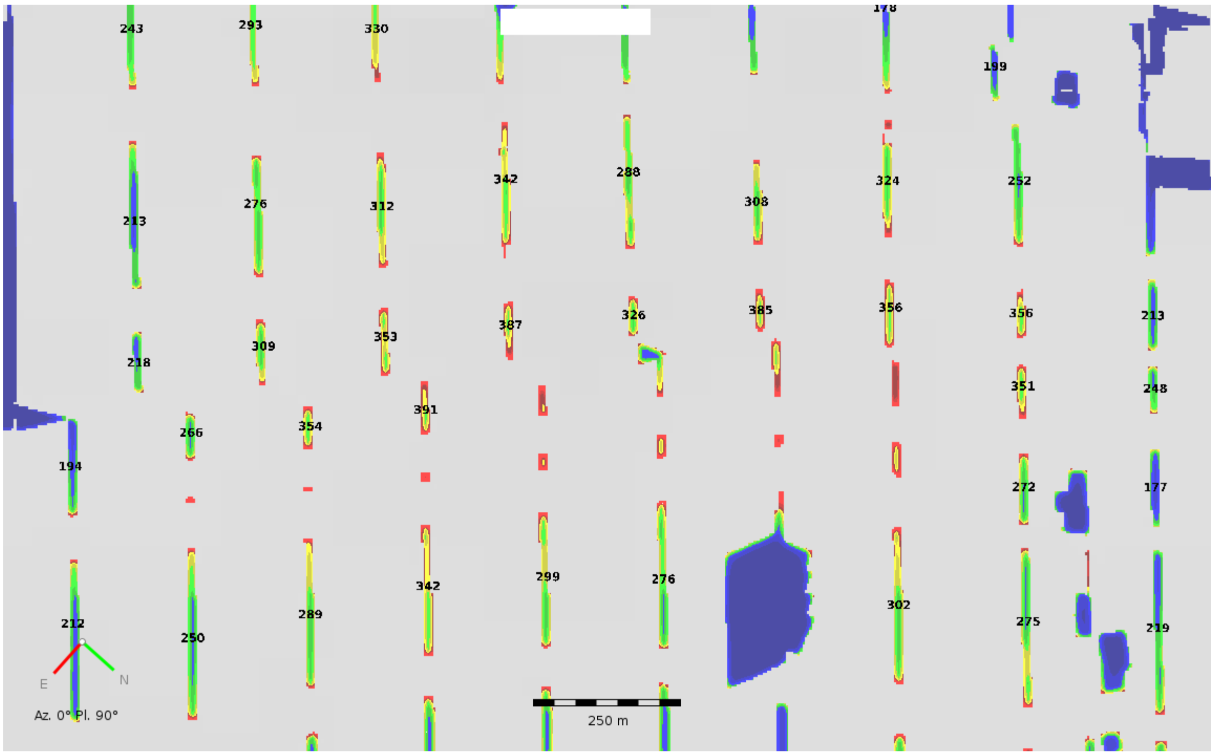

Figure 5.2: APS values for the business plan pillars – Khuseleka UG2, east levels 16 to 23 (Clark, 2016).

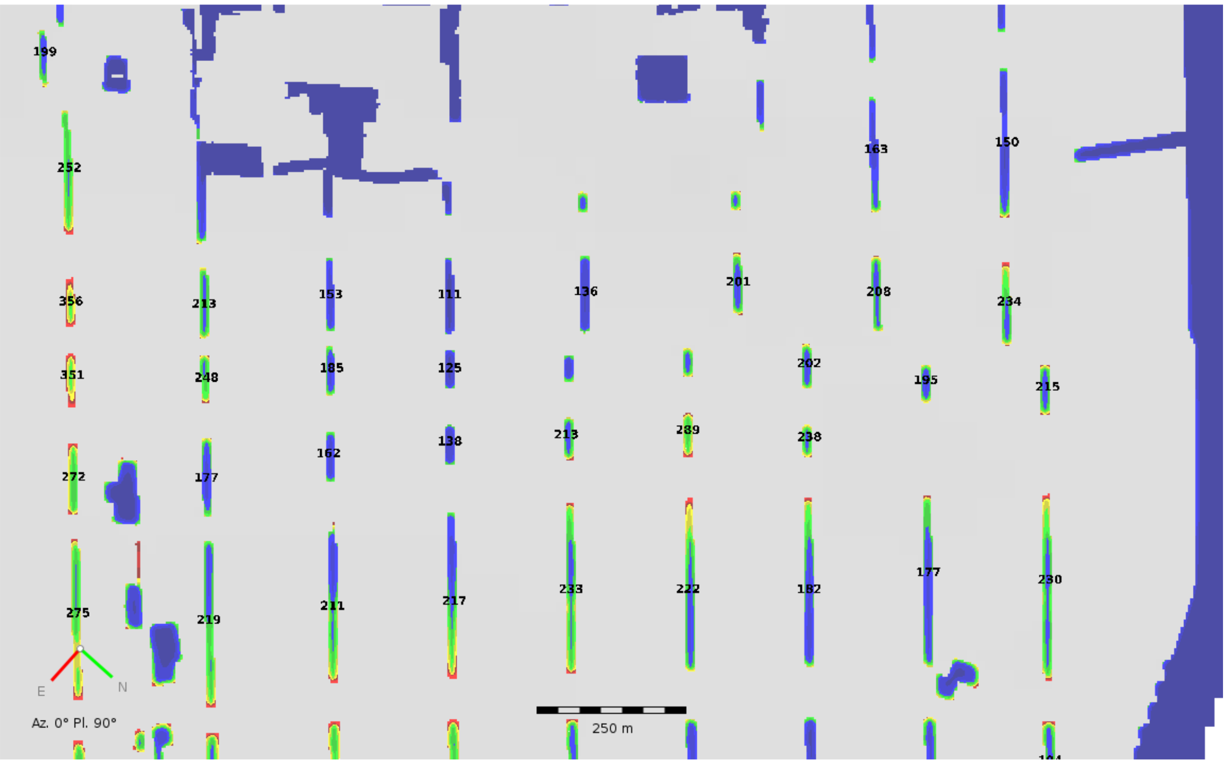

Figure 5.3: APS values for the business plan pillars – Khuseleka UG2, west levels 16 to 23 (Clark, 2016).

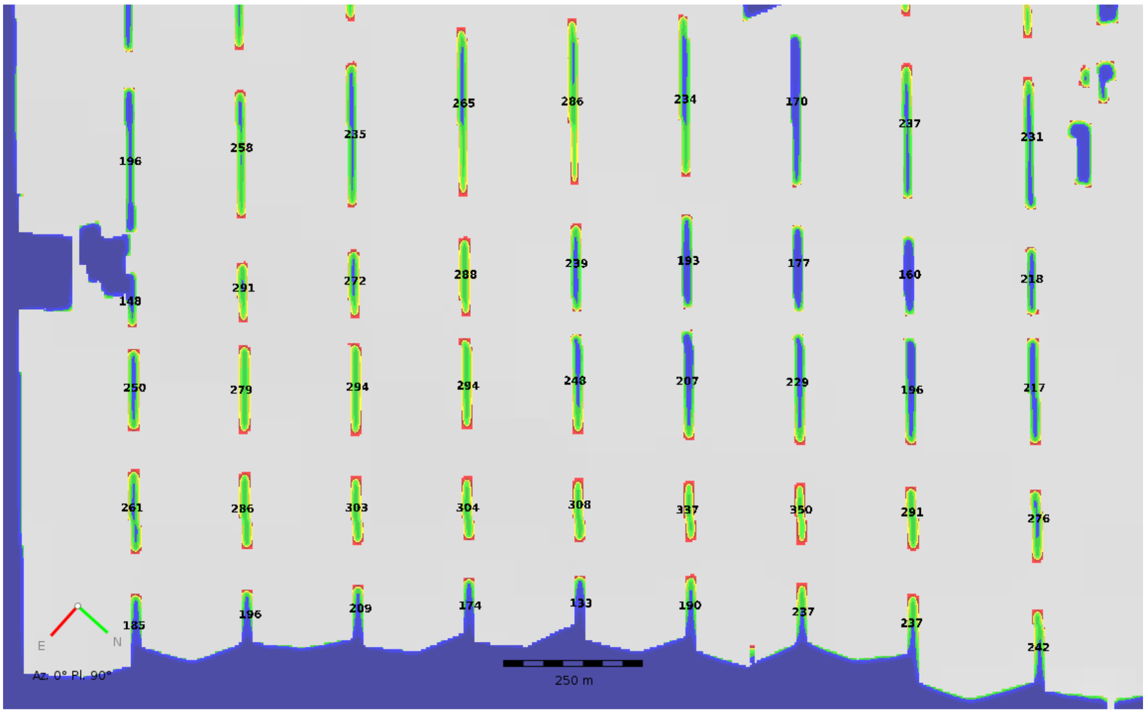

Figure 5.4: APS values for the business plan pillars – Khuseleka UG2, east levels 23 to 27 (Clark, 2016)

5.2.3 Factor of Safety

According to Priest, (2013), the FOS for regional pillars at Khuseleka should not be less than 1.6.

5.2.4 Foundation Strength

Although no foundation strength calculations were done, Priest, (2013), stated that an APS of 500MPa is ideal to ensure foundation stability based on back analysis.

5.2.5 Pillar Spacing

Pillars are spaced at a maximum span of no more than half the depth below surface. This is also a function of the spacing of the cross cuts which is already predetermined at 215m up to 650m below surface and at 200m up to the bottom of the mine and the pillars are placed in the middle of two crosscuts.

5.2.6 Back Analysis of Cut Pillars

During routine underground visits, a number of back areas where regional pillars have been cut were visited to identify if there were any failed pillars. At current mining depths of about 600m, the UG2 is defined as a shallow mine Jager & Ryder, (1999) and no failed regional pillars were identified during those visits. One of the visits was to 15-27 5E and 6E panels, which are currently the deepest stoping areas on the UG2 where a regional pillar has been cut (at a depth of 566m).The pillar was designed at 8m width but was cut at 15m as panels from both ends did not reach the actual pillar positions. Calculating the pillar strength and APS of this pillar using Stacey and Page equation and TAT respectively gives values of 1588MPa, and 307MPa respectively for a FOS of about 5. This APS of 307 is below the 500MPa of the Khuseleka design criteria and within 300MPa of the ideal APS as per Siphumelele Mine experience, (Van Asegan, et al., 2014). The actual APS could be much lower than this calculated value as there is ground not yet mined and other adhoc pillars left around this ground. Numerical modelling is the only way to determine the actual pillar stress. Figure 5.5 is a plan showing the position of this pillar. Photographs showing the pillars as cut are shown in Figures 5.6 and 5.7.

The cut pillar between 15-26 and 15-27 raise lines

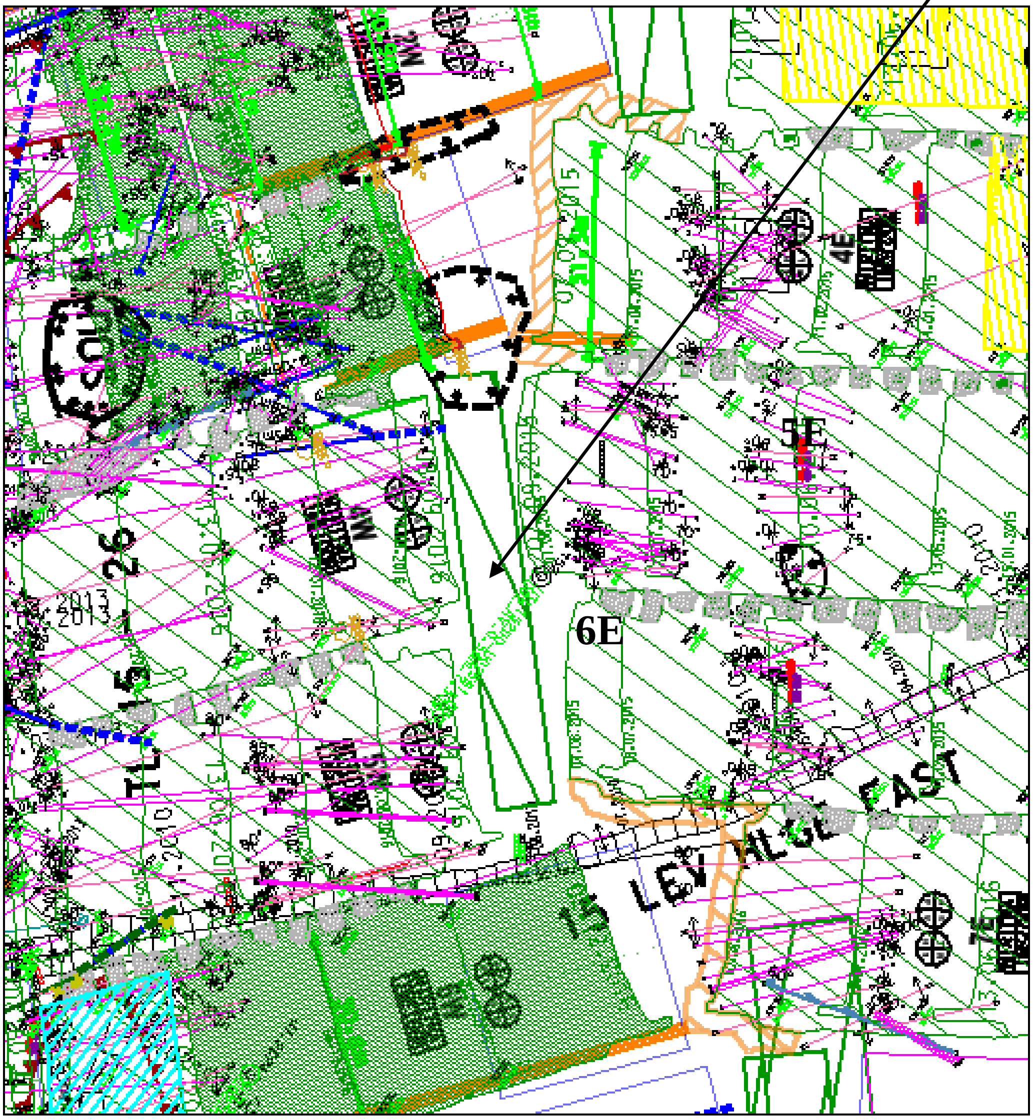

Figure 5.5: Plan showing the regional pillar cut between 27 and 26 cross cuts

Figure 5.6: A photo of the pillar cut in 15-27 5E panel

Figure 5.7: A photo of the pillar cut in 15-27 6E panel

5.3 Pillar Design

The rest of the chapter will look at pillar design using the methods discussed in the literature review as well as the use of parameter values calculated in the preceding chapter. The output obtained for the designs will be presented in tabular forms.

When designing pillars, there are values and properties that are already predetermined and are used as they are; these include;

1) depth below surface,
2) virgin stresses at a given depth,
3) back length,
4) cross cut spacing
5) stoping width,
6) UCS of the rock
7) rock mass characteristics of the rock (for determining the K value),
8) overburden density
9) Required factor of safety (which is 2 for regional pillars)

Other values are calculated using input from those listed above, and these;

1) The pillar length, which is determined by the back length between two different levels and the over-stopping distances to be maintained over the haulages (See Figure 2.3).
2) Extraction ratio, which is a function of the pillar dimensions and area to be mined out.
3) Pillar width, which is the only pillar property that can be adjusted to meet other pillar design criteria.
4) APS, using the criterion suggested by Jager & Ryder, (1999) of approximately $< 2.5\sigma_c$, where σ_c is the UCS of the weakest foundation rock material.

The starting point in calculating extraction ratio, pillar loads (APS), pillar strength and FOS is to determine the pillar widths. This is done by working from the factor of safety first. Since this FOS is already known to be >2 for regional pillars, pillar widths at different depths will be estimated to give this FOS when calculating APS and pillar strength. Also to be remembered is that for regional pillars, the width: height ratio should be ≥ 10. This means that for the KORP section the pillar widths should not be less than 12m since the stoping height on average is 1.2m.

All calculations were done ensuring that the APS did not exceed 228MPa to avoid possible foundation failure, and the FOS would not be below 2.

Each pillar parameter calculated was at a depth below surface range of between 500m and 1000m at 50m intervals, which is within the depth range of the KORP section (see Table 4.1)

In this section the following pillar parameters were calculated using the different methods discussed in the Literature Review chapter and presented in tables form;

- Pillar width based on the tributary area theory (TAT) and Coates methods.
- Effective pillar width based on the tributary area theory and Coates methods.
- Pillar strengths using different pillar strength formulae based on TAT and Coates methods. The effective pillar widths and not actual pillar widths were used on the pillar strength formulae.
- APS based on TAT and Coates methods.
- Extraction ratios based on TAT and Coates methods.
- FOSs based on TAT and Coates methods.
- Pillar width to height ratios based on TAT and Coates method using effective width and not the actual width for the calculations.
- Ratio of depth to span of pillars.

The results obtained were compared against the pillar design criteria given in Table 2.3.

5.3.1 Hedley and Grant Pillar Strength Equation

The Hedley & Grant, (1972) equation was used to calculate the pillar properties in Table 5.2. The factor of safety was maintained at 2.0 throughout. The extraction ratio went down from about 83% at 500m below surface to 73% at 1000m below surface. The APS was below 100MPa from 500m to 1000m below surface. All the criteria in Table 2.3 were met with this equation.

Table 5.2: Design of Pillars using Hedley and Grant Equation

Depth	Back Length	Pillar Width (TAT)	Pillar Width (Coates)	Pillar Length	Weff (TAT)	Weff (Coates)	Crosscut Spacing	Stoping Width	UCS	Modifier	K Value	Overburden Density	Pillar Strength (TAT)	Pillar Strength (Coates)	Vertical virgin stress	APS (TAT)	APS (Coates)	Extraction Ratio (TAT)	Extraction Ratio (Coates)	Factor of safety (TAT)	Factor of safety (Coates)	Ratio of Depth : Span between Pillars	Eff Width: Height Ratio (TAT)	Eff Width: Height Ratio (Coates)
	bl	pw	pw	pl			c																	
[m]	[m]	[m]	[m]	[m]	[m]	[m]	[m]	[m]	[MPa]		[MPa]	[kg/m^3]	[MPa]	[MPa]	MPa	[MPa]	[MPa]							
500	250	52	46	200	69	61	215	1.2	63	0.32	20.16	2900	146	138	14	74	70	0.81	0.83	2.0	2.0	2.3	58	51
550	370	55	50	300	73	67	215	1.2	63	0.32	20.16	2900	151	144	16	75	70	0.79	0.81	2.0	2.0	2.6	61	56
600	370	59	53	300	79	71	215	1.2	63	0.32	20.16	2900	156	148	17	77	73	0.78	0.80	2.0	2.0	2.8	66	59
650	370	62	55	300	83	73	215	1.2	63	0.32	20.16	2900	160	151	18	79	76	0.77	0.79	2.0	2.0	3.0	69	61
700	370	62	55	300	83	73	200	1.2	63	0.32	20.16	2900	160	151	20	79	77	0.75	0.78	2.0	2.0	3.5	69	61
750	370	65	58	300	87	77	200	1.2	63	0.32	20.16	2900	164	155	21	81	79	0.74	0.76	2.0	2.0	3.8	72	64
800	200	80	70	130	99	91	200	1.2	63	0.32	20.16	2900	175	168	23	88	84	0.74	0.77	2.0	2.0	4.0	83	76
850	200	85	75	130	103	95	200	1.2	63	0.32	20.16	2900	178	171	24	88	84	0.72	0.76	2.0	2.0	4.3	86	79
900	180	93	81	110	101	93	200	1.2	63	0.32	20.16	2900	177	170	26	90	87	0.72	0.75	2.0	2.0	4.5	84	78
950	180	97	85	110	103	96	200	1.2	63	0.32	20.16	2900	179	172	27	91	88	0.70	0.74	2.0	2.0	4.8	86	80
1000	180	101	89	110	105	98	200	1.2	63	0.32	20.16	2900	180	174	28	92	89	0.69	0.73	2.0	2.0	5.0	88	82

5.3.2 Watson et al Pillar Strength Equation

Watson, et al., (2008) pillar strength equation was used to calculate the pillar properties in Table 5.3. All the criteria in Table 2.3 were met using this equation. The extraction ratio decreased from 95% at 500m below surface to 90% at 1000m below surface. The only drawback on this equation are its K value of 86MPa and constants a and b which are for conditions only specific to MR. Since the pillars being designed for this project were for UG2 reef, the values obtained could not be used for this project.

Table 5.3: Design of Pillars using Watson et al Equation

Back Length	Pillar Width (TAT)	Pillar Width (Coates)	Pillar Length	Weff (TAT)	Weff (Coates)	Crosscut Spacing	Stoping Width	K Value	Overburden Density	Pillar Strength (TAT)	Pillar Strength (Coates)	Vertical virgin stress	APS (TAT)	APS (Coates)	Extraction Ratio (TAT)	Extraction Ratio (Coates)	Factor of safety (TAT)	Factor of safety (Coates)	Ratio of Depth : Span between Pillars	Eff Width: Height Ratio (TAT)	Eff Width: Height Ratio (Coates)
bl	pw	pw	pl			c															
[m]	[m]	[m]	[m]	[m]	[m]	[m]	[m]	[MPa]	[kg/m^3]	[MPa]	[MPa]	MPa	[MPa]	[MPa]							
250	17	13	200	23	17	215	1.2	86	2900	863	687	14	225	226	0.94	0.95	3.8	3.0	2.3	19	14
370	18	14	300	25	19	215	1.2	86	2900	917	745	16	225	224	0.93	0.95	4.1	3.3	2.6	20	16
370	20	15	300	27	21	215	1.2	86	2900	977	801	17	226	225	0.92	0.94	4.3	3.6	2.8	22	17
370	22	17	300	29	22	215	1.2	86	2900	1050	855	18	223	225	0.92	0.94	4.7	3.8	3.0	24	19
370	22	17	300	29	22	200	1.2	86	2900	1050	855	20	223	226	0.91	0.93	4.7	3.8	3.5	24	19
370	23	18	300	31	24	200	1.2	86	2900	1093	901	21	227	228	0.91	0.93	4.8	4.0	3.8	26	20
200	31	23	130	41	31	200	1.2	86	2900	1363	1093	23	226	227	0.90	0.92	6.0	4.8	4.0	34	26
200	33	25	130	44	33	200	1.2	86	2900	1429	1157	24	225	226	0.89	0.92	6.3	5.1	4.3	37	28
180	37	28	110	49	37	200	1.2	86	2900	1559	1261	26	226	226	0.89	0.91	6.9	5.6	4.5	41	31
180	39	30	110	52	40	200	1.2	86	2900	1622	1329	27	227	224	0.88	0.91	7.2	5.9	4.8	43	33
180	41	32	110	55	43	200	1.2	86	2900	1685	1396	28	227	222	0.87	0.90	7.4	6.3	5.0	46	36

5.3.3 Potvin, et al Pillar Strength Equation

The Potvin, et al., (1989) pillar strength equation was used to design pillars in Table 5.4. The extraction ratios decreased from 94% at 500m below surface to 90% at 1000m below surface. The FOS had to be increased to above 2.0 in order for the APS not to exceed 228MPa. All the criteria in Table 2.3 were met using this formula. The authors stated that their equation was less conservative compared to Hedley & Grant, (1972) and thus the extraction ratios are higher.

Table 5.4: Design of Pillars using Potvin, et al Equation

Depth	Back Length	Pillar Width (TAT)	Pillar Width (Coates)	Pillar Length	Weff (TAT)	Weff (Coates)	Crosscut Spacing	Stoping Width	UCS	Modifier	K Value	Overburden Density	Pillar Strength (TAT)	Pillar Strength (Coates)	Vertical virgin stress	APS (TAT)	APS (Coates)	Extraction Ratio (TAT)	Extraction Ratio (Coates)	Factor of safety (TAT)	Factor of safety (Coates)	Ratio of Depth : Span between Pillars	Eff Width: Height Ratio (TAT)	Eff Width: Height Ratio (Coates)
	bl	pw	pw	pl			c																	
[m]	[m]	[m]	[m]	[m]	[m]	[m]	[m]	[m]	[MPa]		[MPa]	[kg/m^3]	[MPa]	[MPa]	MPa	[MPa]	[MPa]							
500	250	18	17	200	21	34	215	1.2	63	0.4162	26.22	2900	457	734	14	212	178	0.93	0.94	2.2	4.1	2.3	17	28
550	370	19	17	300	25	36	215	1.2	63	0.4162	26.22	2900	538	790	16	218	186	0.93	0.93	2.5	4.3	2.6	21	30
600	370	21	18	300	26	39	215	1.2	63	0.4162	26.22	2900	565	849	17	221	195	0.92	0.93	2.6	4.3	2.8	22	32
650	370	22	19	300	27	42	215	1.2	63	0.4162	26.22	2900	590	907	18	223	202	0.92	0.93	2.6	4.5	3.0	23	35
700	370	22	19	300	27	42	200	1.2	63	0.4162	26.22	2900	590	907	20	223	203	0.91	0.92	2.6	4.5	3.5	23	35
750	370	23	20	300	28	44	200	1.2	63	0.4162	26.22	2900	613	962	21	225	212	0.91	0.92	2.7	4.5	3.8	23	37
800	200	31	23	130	33	54	200	1.2	63	0.4162	26.22	2900	718	1173	23	226	227	0.90	0.92	3.2	5.2	4.0	27	45
850	200	33	25	130	34	57	200	1.2	63	0.4162	26.22	2900	742	1238	24	225	226	0.89	0.92	3.3	5.5	4.3	28	47
900	180	37	28	110	36	61	200	1.2	63	0.4162	26.22	2900	786	1341	26	226	226	0.89	0.91	3.5	5.9	4.5	30	51
950	180	39	30	110	37	64	200	1.2	63	0.4162	26.22	2900	806	1401	27	227	224	0.88	0.91	3.6	6.3	4.8	31	53
1000	180	41	32	110	38	67	200	1.2	63	0.4162	26.22	2900	825	1459	28	227	222	0.87	0.90	3.6	6.6	5.0	31	56

5.3.4 Von Kimmelmann et al Pillar Strength Equation

The Von Kimmelmann, et al., (1984) pillar strength equation was used to design pillars in Table 5.5. The APS were below 200MPa, whilst maintaining a FOS of 2.0 and the extraction ratio decreased from 92% at 500m below surface to 88% at 1000m below surface. All the criteria in Table 2.3 were met using this equation. The only drawback for this equation just like that of Watson, et al., (2008) is that it's K value of 65MPa and the constants a and b are based on case studies done at Selebi and Phikwe nickel mines in Botswana, so it being site and particular rock type specific, could not be used to design the pillars for this project.

Table 5.5: Design of Pillars using Von Kimmelmann et al Equation

Depth	Back Length	Pillar Width (TAT)	Pillar Width (Coates)	Pillar Length	Weff (TAT)	Weff (Coates)	Crosscut Spacing	Stoping Width	K Value	Overburden Density	Pillar Strength (TAT)	Pillar Strength (Coates)	Vertical virgin stress	APS (TAT)	APS (Coates)	Extraction Ratio (TAT)	Extraction Ratio (Coates)	Factor of safety (TAT)	Factor of safety (Coates)	Ratio of Depth : Span between Pillars	Eff Width: Height Ratio (TAT)	Eff Width: Height Ratio (Coates)
	bl	pw	pw	pl			c															
[m]	[m]	[m]	[m]	[m]	[m]	[m]	[m]	[m]	[MPa]	[kg/m^3]	[MPa]	[MPa]	MPa	[MPa]	[MPa]							
500	250	26	22	200	35	30	215	1.2	65	2900	294	275	14	147	135	0.90	0.92	2.0	2.0	2.3	29	25
550	370	28	24	300	37	31	215	1.2	65	2900	302	281	16	151	141	0.90	0.91	2.0	2.0	2.6	31	26
600	370	29	25	300	39	34	215	1.2	65	2900	311	291	17	155	143	0.89	0.90	2.0	2.0	2.8	32	28
650	370	31	27	300	41	36	215	1.2	65	2900	319	300	18	158	146	0.88	0.90	2.0	2.0	3.0	34	30
700	370	31	27	300	41	36	200	1.2	65	2900	319	300	20	158	147	0.87	0.89	2.0	2.0	3.5	34	30
750	370	33	29	300	43	38	200	1.2	65	2900	326	307	21	162	150	0.87	0.88	2.0	2.0	3.8	36	32
800	200	40	33	130	53	45	200	1.2	65	2900	357	330	23	177	164	0.87	0.89	2.0	2.0	4.0	44	37
850	200	42	35	130	55	47	200	1.2	65	2900	365	338	24	179	167	0.87	0.89	2.0	2.0	4.3	46	39
900	180	45	38	110	60	51	200	1.2	65	2900	379	351	26	186	171	0.86	0.88	2.0	2.0	4.5	50	42
950	180	47	39	110	62	53	200	1.2	65	2900	385	356	27	190	175	0.86	0.88	2.0	2.0	4.8	52	44
1000	180	48	40	110	64	54	200	1.2	65	2900	390	361	28	194	180	0.85	0.88	2.0	2.0	5.0	53	45

5.3.5 Krauland and Soder Pillar Strength Equation

The Krauland & Soder, (1987) pillar strength equation was used to design pillars in Table 5.6. The APS was below 200MPa whilst maintaining a FOS of 2.0 up to 1000m and the extraction ratio dropped to 88% from 91% between 500m and 1000m below surface. All the criteria in Table 2.3 were met using this equation. Just like the Von Kimmelmann, et al., (1984) equation, the equation is site specific and works for rocks with a UCS value of 100MPa. Like the other two equations discussed above, it could not be used for this project.

Table 5.6: Design of Pillars using Kraulan and Soder Equation

Depth	Back Length	Pillar Width (TAT)	Pillar Width (Coates)	Pillar Length	Weff (TAT)	Weff (Coates)	Crosscut Spacing	Stoping Width	K Value	Overburden Density	Pillar Strength (TAT)	Pillar Strength (Coates)	Vertical virgin stress	APS (TAT)	APS (Coates)	Extraction Ratio (TAT)	Extraction Ratio (Coates)	Factor of safety (TAT)	Factor of safety (Coates)	Ratio of Depth : Span between Pillars	Eff Pillar Width: Height Ratio (TAT)	Eff Pillar Width: Height Ratio (Coates)
	bl	pw	pw	pl			c															
[m]	[m]	[m]	[m]	[m]	[m]	[m]	[m]	[m]	[MPa]	[kg/m^3]	[MPa]	[MPa]	MPa	[MPa]	[MPa]							
500	250	28	25	200	38	33	215	1.2	35.4	2900	275	246	14	135	122	0.89	0.91	2.0	2.0	2.3	31	28
550	370	29	26	300	39	35	215	1.2	35.4	2900	284	256	16	141	127	0.89	0.90	2.0	2.0	2.6	33	29
600	370	31	28	300	41	37	215	1.2	35.4	2900	298	268	17	146	133	0.88	0.90	2.0	2.0	2.8	34	31
650	370	32	29	300	43	39	215	1.2	35.4	2900	307	281	18	153	137	0.88	0.89	2.0	2.0	3.0	36	32
700	370	32	29	300	43	39	200	1.2	35.4	2900	310	281	20	152	138	0.87	0.88	2.0	2.0	3.5	36	32
750	370	33	30	300	45	40	200	1.2	35.4	2900	319	289	21	158	143	0.86	0.88	2.0	2.0	3.8	37	33
800	200	39	34	130	52	45	200	1.2	35.4	2900	368	324	23	180	161	0.87	0.89	2.0	2.0	4.0	43	38
850	200	40	35	130	53	47	200	1.2	35.4	2900	377	337	24	186	165	0.87	0.88	2.0	2.0	4.3	44	39
900	180	42	37	110	57	50	200	1.2	35.4	2900	398	354	26	198	174	0.87	0.89	2.0	2.0	4.5	47	42
950	180	44	39	110	59	51	200	1.2	35.4	2900	412	364	27	201	179	0.87	0.88	2.0	2.0	4.8	49	43
1000	180	45	40	110	60	53	200	1.2	35.4	2900	420	372	28	207	184	0.86	0.88	2.0	2.0	5.0	50	44

5.3.6 Sjoberg Pillar Strength Equation

The Sjoberg, (1992) pillar strength equation was used to design pillars in Table 5.7. The FOS went above 2.0 to maintain an APS of 228MPa from 750m for TAT and the extraction ratio dropped to 87% from 93% between 500m and 1000m below surface. All the criteria in Table 2.3 were met using this equation. And just like the other three equations discussed above, it is site specific and works for rocks with a UCS value of 240MPa and uses a K value of 74MPa. Like those equations discussed above, it could not be used for this project.

Table 5.7: Design of Pillars using Sjoberg Equation

Depth	Back Length	Pillar Width (TAT)	Pillar Width (Coates)	Pillar Length	Weff (TAT)	Weff (Coates)	Crosscut Spacing	Stoping Width	K Value	Overburden Density	Pillar Strength (TAT)	Pillar Strength (Coates)	Vertical virgin stress	APS (TAT)	APS (Coates)	Extraction Ratio (TAT)	Extraction Ratio (Coates)	Factor of safety (TAT)	Factor of safety (Coates)	Ratio of Depth : Span between Pillars	Eff Pillar Width: Height Ratio (TAT)	Eff Pillar Width: Height Ratio (Coates)
	bl	pw	pw	pl			c															
[m]	[m]	[m]	[m]	[m]	[m]	[m]	[m]	[m]	[MPa]	[kg/m^3]	[MPa]	[MPa]	MPa	[MPa]	[MPa]							
500	250	19	17	200	25	22	215	1.2	74	2900	404	359	14	201	178	0.93	0.94	2.0	2.0	2.3	21	18
550	370	20	17	300	27	23	215	1.2	74	2900	423	375	16	207	185	0.92	0.93	2.0	2.0	2.6	22	19
600	370	21	18	300	28	24	215	1.2	74	2900	441	392	17	216	192	0.92	0.93	2.0	2.0	2.8	23	20
650	370	22	19	300	29	25	215	1.2	74	2900	454	404	18	226	201	0.92	0.93	2.0	2.0	3.0	24	21
700	370	22	19	300	29	25	200	1.2	74	2900	454	406	20	226	201	0.91	0.92	2.0	2.0	3.5	24	21
750	370	23	20	300	31	27	200	1.2	74	2900	483	423	21	226	207	0.91	0.92	2.1	2.0	3.8	26	22
800	200	31	23	130	41	31	200	1.2	74	2900	623	481	23	226	227	0.90	0.92	2.8	2.1	4.0	34	26
850	200	33	25	130	44	33	200	1.2	74	2900	654	516	24	228	225	0.89	0.92	2.9	2.3	4.3	36	28
900	180	37	28	110	49	38	200	1.2	74	2900	733	574	26	226	224	0.89	0.91	3.2	2.6	4.5	41	31
950	180	39	30	110	52	39	200	1.2	74	2900	769	598	27	227	227	0.88	0.91	3.4	2.6	4.8	43	33
1000	180	41	31	110	55	42	200	1.2	74	2900	806	629	28	227	227	0.87	0.90	3.5	2.8	5.0	46	35

5.3.7 Lunder and Pakalnis Pillar Strength Equation

The Lunder & Pakalnis, (1997) pillar strength equation was used to design pillars in Table 5.8. The values obtained especially for the pillar widths and extraction ratio indicate that this equation is not ideal for this project and therefore cannot be used on this project.

Table 5.8: Design of Pillars using Lunder and Pakalnis Equation

Depth	Back Length	Pillar Width (TAT)	Pillar Width (Coates)	Pillar Length	Weff (TAT)	Weff (Coates)	Crosscut Spacing	Stoping Width	UCS	Modifier	K Value	Overburden Density	Pillar Strength (TAT)	Pillar Strength (Coates)	Vertical virgin stress	APS (TAT)	APS (Coates)	Extraction Ratio (TAT)	Extraction Ratio (Coates)	Factor of safety (TAT)	Factor of safety (Coates)	Ratio of Depth : Span between Pillars	Eff Pillar Width: Height Ratio (TAT)	Eff Pillar Width: Height Ratio (Coates)
	bl	pw	pw	pl			c																	
[m]	[m]	[m]	[m]	[m]	[m]	[m]	[m]	[m]	[MPa]		[MPa]	[kg/m^3]	[MPa]	[MPa]	MPa	[MPa]	[MPa]							
500	250	140	130	200	165	158	215	1.2	63	0.44	27.72	2900	55	55	14	27	27	**0.48**	**0.52**	2.0	2.0	2.3	117	108
550	370	150	145	300	200	193	215	1.2	63	0.44	27.72	2900	55	55	16	28	27	**0.43**	**0.45**	2.0	2.0	2.6	125	121
600	370	165	160	300	213	209	215	1.2	63	0.44	27.72	2900	55	55	17	27	27	**0.38**	**0.40**	2.0	2.0	2.8	138	133
650	370	180	175	300	225	221	215	1.2	63	0.44	27.72	2900	55	55	18	27	27	**0.32**	**0.34**	2.0	2.0	3.0	150	146
700	370	180	175	300	225	221	200	1.2	63	0.44	27.72	2900	55	55	20	27	27	**0.27**	**0.29**	2.0	2.0	3.5	150	146
750	370	192	190	300	234	233	200	1.2	63	0.44	27.72	2900	55	55	21	27	27	**0.22**	**0.23**	2.0	2.0	3.8	160	158
800	200	255	250	130	172	171	200	1.2	63	0.44	27.72	2900	55	55	23	27	28	**0.17**	**0.19**	2.0	2.0	4.0	213	208
850	200	275	270	130	177	176	200	1.2	63	0.44	27.72	2900	55	55	24	27	27	**0.11**	**0.12**	2.0	2.0	4.3	229	225
900	180	305	305	110	162	162	200	1.2	63	0.44	27.72	2900	55	55	26	27	27	**0.07**	**0.07**	2.0	2.0	4.5	254	254
950	180	325	325	110	164	164	200	1.2	63	0.44	27.72	2900	55	55	27	27	27	**0.01**	**0.01**	2.0	2.0	4.8	271	271
1000	180	345	340	110	167	166	200	1.2	63	0.44	27.72	2900	55	55	28	28	28	**0.00**	**0.00**	2.0	2.0	5.0	288	283

5.3.8 Stacey and Page Pillar Strength Equation

The Stacey & Page, (1986) pillar strength equation was used to design pillars in Table 5.9. To ensure the APS are maintained below 228MPa, the pillar widths had to be increased causing the FOS to go close to 200 at 1000m. The pillar strength for the equation increased from about 750MPa at 500m depth to about 42 000MPa at 1000m depth. This equation highlights the strengthening effect of the effective width compared to the other equations where the strengthening effect is not applied. The implications of this are high strengths and FOS of the pillars. If it were not for the APS which is required not to exceed a given threshold, the pillar sizes would be very small (very high extraction ratio). The extraction ratio decreased from 95% at 500m below surface to 90% at 1000m below surface. All the criteria in Table 2.3 were met using this equation. The advantage of this equation is that it takes into account the strengthening effect of an increased width: height ratio as well as the effective width due to the length of the pillar.

Table 5.9: Design of Pillars using Stacey and Page Equation

Depth	Middling	Over Stoping (similar to middling for the 45^{o} rule	Back Length	Pillar Width (TAT)	Pillar Width (Coates)	Pillar Length	Crosscut Spacing	Stoping Width	UCS	Modifier	K Value	Overburden Density	w_{eff} (TAT)	V (TAT)	R (TAT)	w_{eff} (Coates)	V (Coates)	R (Coates)	Pillar Strength (TAT)	Pillar Strength (Coates)	Vertical virgin stress	b	h_s	APS (TAT)	APS (Coates)	Extraction Ratio (TAT)	Extraction Ratio (Coates)	Factor of safety (TAT)	Factor of safety (Coates)	Ratio of Depth : Span between Pillars	Eff Pillar Width: Height Ratio (TAT)	Eff Pillar Width: Height Ratio (Coates)
		u	bl	pw	pw	pl	c																									
[m]	[m]	[m]	[m]	[m]	[m]	[m]	[m]	[m]	[MPa]		[MPa]	[kg/m^3]	[m]	[m^3]		[m]	[m^3]		[MPa]	[MPa]	MPa			[MPa]	[MPa]							
500	25	25	250	17	13	200	215	1.2	63	0.32	20.2	2900	22.53	609.3	18.8	16.80	338.7	14.0	2618	749	14	0.0586	0.00558	226	226	0.94	0.95	11.6	3.3	2.3	19	14
550	35	35	370	18	14	300	215	1.2	63	0.32	20.2	2900	24.53	722.2	20.4	18.67	418.1	15.6	3780	1169	16	0.0651	0.00558	225	224	0.93	0.95	16.8	5.2	2.6	20	16
600	35	35	370	20	15	300	215	1.2	63	0.32	20.2	2900	26.67	853.3	22.2	20.53	505.9	17.1	5425	1756	17	0.0716	0.00558	226	225	0.92	0.94	24.0	7.8	2.8	22	17
650	35	35	370	22	17	300	215	1.2	63	0.32	20.2	2900	29.33	1032.5	24.4	22.40	602.1	18.7	8206	2552	18	0.0781	0.00558	223	225	0.92	0.94	36.8	11.3	3.0	24	19
700	35	35	370	22	17	300	200	1.2	63	0.32	20.2	2900	29.33	1032.5	24.4	22.40	602.1	18.7	8206	2552	20	0.0840	0.00600	223	226	0.91	0.93	36.8	11.3	3.5	24	19
750	35	35	370	23	18	300	200	1.2	63	0.32	20.2	2900	31.20	1168.1	26.0	24.00	691.2	20.0	10730	3438	21	0.0900	0.00600	225	228	0.91	0.93	47.7	15.1	3.8	26	20
800	35	35	200	31	23	130	200	1.2	63	0.32	20.2	2900	41.33	2050.0	34.4	30.93	1148.2	25.8	36508	10337	23	0.1160	0.00600	226	227	0.90	0.92	161.6	45.5	4.0	34	26
850	35	35	200	33	25	130	200	1.2	63	0.32	20.2	2900	44.00	2323.1	36.7	33.33	1333.3	27.8	47940	14308	24	0.1250	0.00600	225	226	0.89	0.92	212.6	63.3	4.3	37	28
900	35	35	180	37	28	110	200	1.2	63	0.32	20.2	2900	49.33	2920.4	41.1	37.33	1672.4	31.1	78930	23434	26	0.1400	0.00600	226	226	0.89	0.91	348.5	103.8	4.5	41	31
950	35	35	180	39	30	110	200	1.2	63	0.32	20.2	2900	52.00	3244.6	43.3	40.00	1919.9	33.3	99288	31648	27	0.1500	0.00600	227	224	0.88	0.91	437.8	141.3	4.8	43	33
1000	35	35	180	41	32	110	200	1.2	63	0.32	20.2	2900	54.67	3586.0	45.6	42.67	2184.4	35.6	123472	41924	28	0.1600	0.00600	227	222	0.87	0.90	543.7	188.5	5.0	46	36

5.4 Pillar Loads

Pillar loads, referred to as average pillar stresses (APS) are the loads that a pillar has to carry without failure if a mining operation is to remain stable. This load is a function of the virgin vertical stresses and the extraction ratio for TAT, whilst it includes stoping widths, k-ratio and rock mass properties for the Coates method (Section 2.3). (Ryder & Ozbay, (1990)) stated that pillars of a width to height ratio of ≥10 are indestructible, thus foundation failure becomes the major concern with regards to the stability of an excavation. Thus an APS that ensures foundation failure does not occur has to be established. For the KORP section this APS value is 228MPa. Therefore, whether using the Coates or Tributary Area Theory methods the value should not be more than 228MPa. Tables 5.2 to 5.9 show calculated pillar parameters using both the TAT and Coates methods.

What is clear from these calculations is that the Coates method gives higher extraction ratios as the pillars carrying the same loads have a smaller width than those determined by the TAT method. Although TAT is more conservative and its pillars are assumed to have a lower risk of failure due to their wide widths, Coates takes into account more rock mass parameters which assumes more valid results than those of TAT as the more parameters used for the calculations reduce uncertainty. Based on this, the pillar widths calculated using Coates method were used for this project.

5.5 Factor of Safety

For stability to be guaranteed, it is assumed that a particular minimum ratio of the strength of the pillars to the load exerted on of those pillars has to be achieved. This ratio is referred to as the factor of safety. As discussed in section 2.6, this FOS for regional pillars should not be less than 2.0. Tables 5.2 to 5.9 show that all the pillars designed have an FOS of 2.0 or higher. This value is even higher for the Stacey and Page formula, where values are as high as 213 are calculated at a depth of 1000m below surface (Table 5.9).

5.6 Width: Height Ratio

As discussed in section 2.5 in the Literature Review chapter, the width to height ratio of regional pillars should not be less than 10. All the pillars designed in Tables 5.2 to 5.9 meet this criterion with the value increasing with depth as the pillar widths increased to meet the required loading capacity of the pillars.

5.7 Comparison of the Results Using Different Pillar Strengths Equations

Tables 5.2 to 5.9 show different parameters calculated for pillar design. Pillar strengths, loads, extraction ratios, FOS, width: height ratios and depth to span depth: span ratios are calculated at different depths using the different empirical equations and comparisons between Coates and TAT methods for pillar load calculations are also analysed. The purpose was to determine the best pillar widths that could be designed to achieve the design criteria as set out in Table 2.3. Tables 5.10 to 5.15 show the different pillar parameters calculated using the different pillar strength and stress equations.

Table 5.10: Comparison of Pillar Widths Based on Different Pillar Strength Equations

Depth Below Surface	Hedley and Grant (TAT)	Hedley and Grant (Coates)	Watson et al (TAT)	Watson et al (Coates)	Potvin et al (TAT)	Potvin et al (Coates)	Von Kimmelmann et al (TAT)	Von Kimmelmann et al (Coates	Kraulan & soder (TAT)	Kraulan & soder (Coates)	Sjoberg (TAT)	Sjoberg (Coates)	Lunder & Pakalnis (TAT)	Lunder & Pakalnis (Coates)	Stacey & Page (TAT)	Stacey & Page (Coates)
500	48	43	14	11	16	14	24	21	27	24	18	16	117	108	14	11
550	51	46	15	12	16	14	25	22	28	25	19	17	125	121	15	12
600	54	49	17	13	17	15	27	23	30	26	20	18	138	133	17	13
650	57	52	18	14	18	16	28	25	31	28	21	18	150	146	18	14
700	57	52	18	14	18	16	28	25	31	28	21	18	150	146	18	14
750	59	54	19	15	20	16	30	26	32	29	22	19	158	158	20	15
800	72	65	26	19	26	19	36	31	37	33	26	22	213	208	26	19
850	75	68	28	21	28	21	38	32	38	34	27	23	229	225	28	21
900	82	73	31	23	31	23	41	35	41	36	31	24	254	254	31	23
950	84	76	33	25	33	25	43	36	42	37	33	25	271	271	33	25
1000	87	79	34	27	34	27	44	38	43	38	34	26	288	283	34	27

Table 5.11: Comparison of Pillar Strengths Based on Different Pillar Strength Equations

Depth Below Surface (m)	Hedley and Grant (TAT)	Hedley and Grant (Coates)	Watson et al (TAT)	Watson et al (Coates)	Potvin et al (TAT)	Potvin et al (Coates)	Von Kimmelmann et al (TAT)	Von Kimmelmann et al (Coates)	Kraulan & Soder (TAT)	Kraulan & Soder (Coates)	Sjoberg (TAT)	Sjoberg (Coates)	Lunder & Pakalnis (TAT)	Lunder & Pakalnis (Coates)	Stacey & Page (TAT)	Stacey & Page (Coates)
500	134	127	694	552	413	361	269	251	240	217	355	318	55	56	2618	749
550	137	130	737	598	426	378	278	258	249	225	370	331	55	55	3780	1169
600	142	135	785	643	448	393	284	267	259	234	386	345	55	55	5425	1756
650	145	138	844	687	481	413	292	273	268	244	400	359	55	55	8206	2552
700	145	138	844	687	481	413	292	273	269	246	400	359	55	55	8206	2552
750	148	142	879	724	511	426	300	280	277	253	414	372	55	55	10730	3438
800	163	155	1095	879	677	507	327	303	320	286	482	414	55	55	36508	10337
850	167	158	1148	930	721	546	332	309		295	505	427	55	55	47940	14308
900	174	164	1253	1014	808	612	345	320	348	309	564	448	55	55	78930	23434
950	177	168	1304	1068	852	656	352	325	358	317	591	466	55	55	99288	31648
1000	179	171	1354	1122	896	699	358	332	367	327	619	487	55	55	123472	41924

Table 5.12: Comparison of APS Based on Different Pillar Strength Equations

Depth Below Surface	Hedley and Grant (TAT)	Hedley and Grant (Coates)	Watson et al (TAT)	Watson et al (Coates)	Potvin et al (TAT)	Potvin et al (Coates)	Von Kimmelmann et al (TAT)	Von Kimmelmann et al (Coates)	Kraulan & Soder (TAT)	Kraulan & Soder (Coates)	Sjoberg (TAT)	Sjoberg (Coates)	Lunder & Pakalnis (TAT)	Lunder & Pakalnis (Coates)	Stacey & Page (TAT)	Stacey & Page (Coates)
500	66	62	225	226	202	178	134	124	118	107	176	157	27	27	226	226
550	68	65	225	224	213	186	136	128	123	112	182	163	28	27	225	224
600	70	66	226	225	221	195	141	131	128	117	189	170	27	27	226	225
650	72	68	223	225	223	202	144	135	134	122	196	176	27	27	223	225
700	72	69	223	226	223	203	144	136	133	121	196	177	27	27	223	226
750	74	71	227	228	225	212	146	139	138	126	202	182	28	27	225	228
800	81	76	226	227	226	227	161	149	157	141	226	205	27	28	226	227
850	83	78	225	226	225	226	165	153	162	145	228	211	27	27	225	226
900	86	82	226	226	226	226	171	159	171	153	226	222	27	27	226	226
950	88	83	227	224	227	224	173	162	175	158	227	225	27	27	227	224
1000	90	84	227	222	227	222	176	163	180	161	227	226	27	27	227	222

Table 5.13: Comparison of FOS Based on Different Pillar Strength Equations

Depth Below Surface	Hedley and Grant (TAT)	Hedley and Grant	Watson et al (TAT)	Watson et al (Coates)	Potvin et al (TAT)	Potvin et al (Coate	Von Kimmelmann et al (TAT)	Von Kimmelmann et al (Coates	Kraulan & soder (TAT)	Kraulan & soder (Coates	Sjoberg (TAT)	Sjoberg (Coates)	Lunder & Pakalnis (TAT)	Lunder & Pakalnis (Coates)	Stacey & Page (TAT)	Stacey & Page (Coates)
500	2.0	2.0	3.1	2.4	2.0	2.0	2.0	2.0	2.0	2.0	2.0	2.0	2.0	2.0	11.6	3.3
550	2.0	2.0	3.3	2.7	2.0	2.0	2.0	2.0	2.0	2.0	2.0	2.0	2.0	2.0	16.8	5.2
600	2.0	2.0	3.5	2.9	2.0	2.0	2.0	2.0	2.0	2.0	2.0	2.0	2.0	2.0	24.0	7.8
650	2.0	2.0	3.8	3.1	2.2	2.0	2.0	2.0	2.0	2.0	2.0	2.0	2.0	2.0	36.8	11.3
700	2.0	2.0	3.8	3.0	2.2	2.0	2.0	2.0	2.0	2.0	2.0	2.0	2.0	2.0	36.8	11.3
750	2.0	2.0	3.9	3.2	2.3	2.0	2.0	2.0	2.0	2.0	2.0	2.0	2.0	2.0	47.7	15.1
800	2.0	2.0	4.8	3.9	3.0	2.2	2.0	2.0	2.0	2.0	2.1	2.0	2.0	2.0	161.6	45.5
850	2.0	2.0	5.1	4.1	3.2	2.4	2.0	2.0	2.0	2.0	2.2	2.0	2.0	2.0	212.6	63.3
900	2.0	2.0	5.5	4.5	3.6	2.7	2.0	2.0	2.0	2.0	2.5	2.0	2.0	2.0	348.5	103.8
950	2.0	2.0	5.7	4.8	3.8	2.9	2.0	2.0	2.0	2.0	2.6	2.1	2.0	2.0	437.8	141.3
1000	2.0	2.0	6.0	5.0	3.9	3.1	2.0	2.0	2.0	2.0	2.7	2.2	2.0	2.0	543.7	188.5

Table 5.14: Comparison of W: H Ratio Based on Different Pillar Strength Equations

Depth Below Surface	Hedley and Grant (TAT)	Hedley and Grant (Coates)	Watson et al (TAT)	Watson et al (Coates)	Potvin et al (TAT)	Potvin et al (Coates)	Von Kimmelmann et al (TAT)	Von Kimmelmann et al (Coates	Kraulan & soder (TAT)	Kraulan & soder (Coates)	Sjoberg (TAT)	Sjoberg (Coates)	Lunder & Pakalnis (TAT)	Lunder & Pakalnis (Coates)	Stacey & Page (TAT)	Stacey & Page (Coates)
500	48	43	14	11	16	14	24	21	27	24	18	16	117	108	14	11
550	51	46	15	12	16	14	25	22	28	25	19	17	125	121	15	12
600	54	49	17	13	17	15	27	23	30	26	20	18	138	133	17	13
650	57	52	18	14	18	16	28	25	31	28	21	18	150	146	18	14
700	57	52	18	14	18	16	28	25	31	28	21	18	150	146	18	14
750	59	54	19	15	20	16	30	26	32	29	22	19	158	158	20	15
800	72	65	26	19	26	19	36	31	37	33	26	22	213	208	26	19
850	75	68	28	21	28	21	38	32	38	34	27	23	229	225	28	21
900	82	73	31	23	31	23	41	35	41	36	31	24	254	254	31	23
950	84	76	33	25	33	25	43	36	42	37	33	25	271	271	33	25
1000	87	79	34	27	34	27	44	38	43	38	34	26	288	283	34	27

Table 5.15: Comparison of Extraction Ratio Based on Different Pillar Strength Equations

Depth Below Surface	Hedley and Grant (TAT)	Hedley and Grant (Coates)	Watson et al (TAT)	Watson et al (Coates)	Potvin et al (TAT)	Potvin et al (Coates)	Von Kimmelmann et al (TAT)	Von Kimmelmann et al (Coates)	Kraulan & Soder (TAT)	Kraulan & Soder (Coates)	Sjoberg (TAT)	Sjoberg (Coates)	Lunder & Pakalnis (TAT)	Lunder & Pakalnis (Coates)	Stacey & Page (TAT)	Stacey & Page (Coates)
500	0.78	0.81	0.94	0.95	0.93	0.94	0.89	0.91	0.88	0.89	0.92	0.93	0.48	0.52	0.94	0.95
550	0.77	0.79	0.93	0.95	0.93	0.93	0.88	0.90	0.87	0.89	0.91	0.92	0.43	0.45	0.93	0.95
600	0.75	0.78	0.92	0.94	0.92	0.93	0.88	0.89	0.87	0.88	0.91	0.92	0.38	0.40	0.92	0.94
650	0.74	0.77	0.92	0.94	0.92	0.93	0.87	0.89	0.86	0.88	0.91	0.92	0.32	0.34	0.92	0.94
700	0.72	0.75	0.91	0.93	0.91	0.92	0.86	0.88	0.85	0.86	0.90	0.91	0.27	0.29	0.91	0.93
750	0.71	0.74	0.91	0.93	0.91	0.92	0.85	0.87	0.85	0.86	0.89	0.91	0.23	0.23	0.91	0.93
800	0.72	0.75	0.90	0.92	0.90	0.92	0.86	0.88	0.86	0.87	0.90	0.92	0.17	0.19	0.90	0.92
850	0.71	0.74	0.89	0.92	0.89	0.92	0.85	0.88	0.85	0.87	0.89	0.91	0.11	0.12	0.89	0.92
900	0.70	0.73	0.89	0.91	0.89	0.91	0.85	0.87	0.85	0.87	0.89	0.91	0.07	0.07	0.89	0.91
950	0.69	0.72	0.88	0.91	0.88	0.91	0.84	0.87	0.85	0.86	0.88	0.91	0.01	0.01	0.88	0.91
1000	0.68	0.71	0.87	0.90	0.87	0.90	0.84	0.86	0.84	0.86	0.87	0.90	0.00	0.00	0.87	0.90

5.8 Foundation Strength

Since regional pillars are designed as squat pillars, meaning they will likely not fail on their own, any failure would be assumed to occur on the foundation rock. Therefore, the stability of the foundation rock would be of paramount importance. Based on the criterion that average pillar stress should not exceed 2.5 x compressive strength of the foundation rock, the pillars were designed with an APS value of < 228MPa which is 2.5 x 91MPa (foundation rock UCS). Tables 5.2 to 5.9, show that the pillars were designed with APS values of less than 228MPa.

5.9 Pillar Spacing

Pillar spacing for the KORP section is based on the spacing between the crosscuts. The crosscuts are designed at a spacing of 215m up to a depth of 650m below surface and 200m up to the bottom of the mine at 950m. Pillars are placed between these crosscuts, with the pillar length running parallel to the crosscut, thus being on average 200m apart depending on the pillar width, this layout is schematically illustrated in Figure 2.3. What is critical about this spacing is its ratio to the depth because stoping is done between these pillars, thereby giving the stoping span. Ryder & Ozbay, (1990), suggested, based on valid theoretical considerations that this span should be less than a quarter of the depth. With predetermined crosscut spacing, at depths of less than 800m this ratio is not achieved. However, historical data and back analysis from Khuseleka and other operations within RPM show that a ratio of 1:2 is adequate for stability (Priest G, 2013). The ratio on this project ranges from 2.4 at 500m to 4.9 at 1000m (Tables 5.2 to 5.9).

5.10 Placement of Footwall Excavations

As discussed in Section 2.10, footwall excavations such as haulages, crosscuts and chambers may be placed in positions where their stability is not compromised by either high virgin or induced stresses. It is critical when designing pillars that, they do not generate stresses high enough to cause damage to footwall excavations.

The amount of virgin stresses and/or induced stresses acting on footwall excavations has to be determined, so that a proper support system can be designed for them before instability occurs. The RCF, criterion is an invaluable method of expressing and controlling tunnel conditions.

Overstoping and the RCF criterion are tools that can be used to ensure that induced stresses from hangingwall abutments on tunnels are managed.

5.10.1 Overstoping

Due to high costs and logistical challenges, it is not always feasible to site footwall excavations sufficiently remote from the reef horizon for them not to be affected by induced stresses. In most cases for practical purposes they need to be as close to the reef as possible. A strategy must be developed to deal with the high induced stresses. Overstoping is one way of preventing the footwall excavations from being affected by the pillars. Figure 2.3 shows “u”, (overstoping distance between the edge of the pillar and the haulage). The value of “u” is equivalent to the depth of the excavation below the reef horizon. As discussed in Section 2.10, Figure 2.9 shows that with u equal to the tunnel depth below reef a 45^{o} angle is created in which the footwall excavations will be in a distressed zone where the stresses created by the pillars do not affect them. Tables 5.2 to 5.9 show that all the crosscuts and haulages have been designed with overstoping of haulages incorporated.

5.10.2 Rockwall Condition Factor

Equation 27 is the equation used for calculating the RCF. The stress values for σ_1 and σ_3 at different depths are calculated based on stress measurements discussed in Section 4.6. The footwall excavations occur in pyroxenite rock and the average σ_c value of pyroxenite derived from the UCS tests done for the KORP section given in Table 4.4 is 166MPa. The Condition Factor, F is derived from the average RMR value for the KORP section, which is 70. 0.7 will be used as the F value.

Table 5.16 shows the calculated RCF values from 500m to 1000m below surface, which is the range of depth below surface for the mining levels in the KORP section

Table 5.16: RCF calculations at different depths below surface in the KORP section

Rock Density (kg/m3)	**Gravitational Force**	**K-Ratio**	**Condition Factor**	**UCS (MPa)**
2900	9.81	1.25	0.7	166
Depth Below Surface (m)	**σ_1 (MPa)**	**$3\sigma_1$ (MPa)**	**σ_3 (MPa)**	**RCF**
500	17.8	53.3	14.2	0.3
550	19.6	58.7	15.6	0.4
600	21.3	64.0	17.1	0.4
650	23.1	69.3	18.5	0.4
700	24.9	74.7	19.9	0.5
750	26.7	80.0	21.3	0.5
800	28.4	85.3	22.8	0.5
850	30.2	90.7	24.2	0.6
900	32.0	96.0	25.6	0.6
950	33.8	101.3	27.0	0.6
1000	35.6	106.7	28.4	0.7

Jager & Ryder, (1999) gave an empirical relationship between the RCF value, ground conditions of tunnel and support requirements as shown in Table 5.17:

Table 5.17: An empirical relationship between the RCF value and the support requirements (Jager & Ryder, 1999)

RCF Value Range	Ground conditions	Support Requirements
< 0.7	Good	Minimum
0.7<RCF<1.4	Average	Moderate
>1.4	Poor	Special

Table 5.16 shows that the RCF values calculated for the KORP section are below 0.7 throughout the mining levels indicating good ground conditions and minimal support requirements. This means, no special support to deal with dynamic conditions or stress induced failures will be required. More analysis using numerical modelling in the next chapter will determine what influence mining will have on these haulages as they will be some induced stresses due to pillars left above the excavations, or below in the case of 16 level.

However it must be noted that Anglo American Platinum has minimum support standard for its excavations regardless of the fact that the RCF values dictate that no support has to be installed. This means that even if the RCF values are below 0.7, support will still be installed as per mine standard.

5.11 Pillar Layout Design

Based on previous discussions and pillar parameter calculations in this chapter, it was decided to use parameters obtained using the Stacey and Page equation (Table 5.9) for the pillar design. This was because the equation takes into account the strengthening effect on a pillar of a w: h ratio greater than 5 as well as the pillar length to get an effective width which is greater than the actual width, (Stacey & Page, 1986). All the design criteria are met using this equation. The parameter values obtained using Coates method in Table 5.9 were used for the layout design because this method takes the rock mass properties of the pillar and k ratio into account for the load calculations. Thus the layout shown in Figure 5.8 is a KORP section pillar layout designed using MicroStation CAD program based on the values of Coates method in Table 5.9 (Stacey and Page equation).

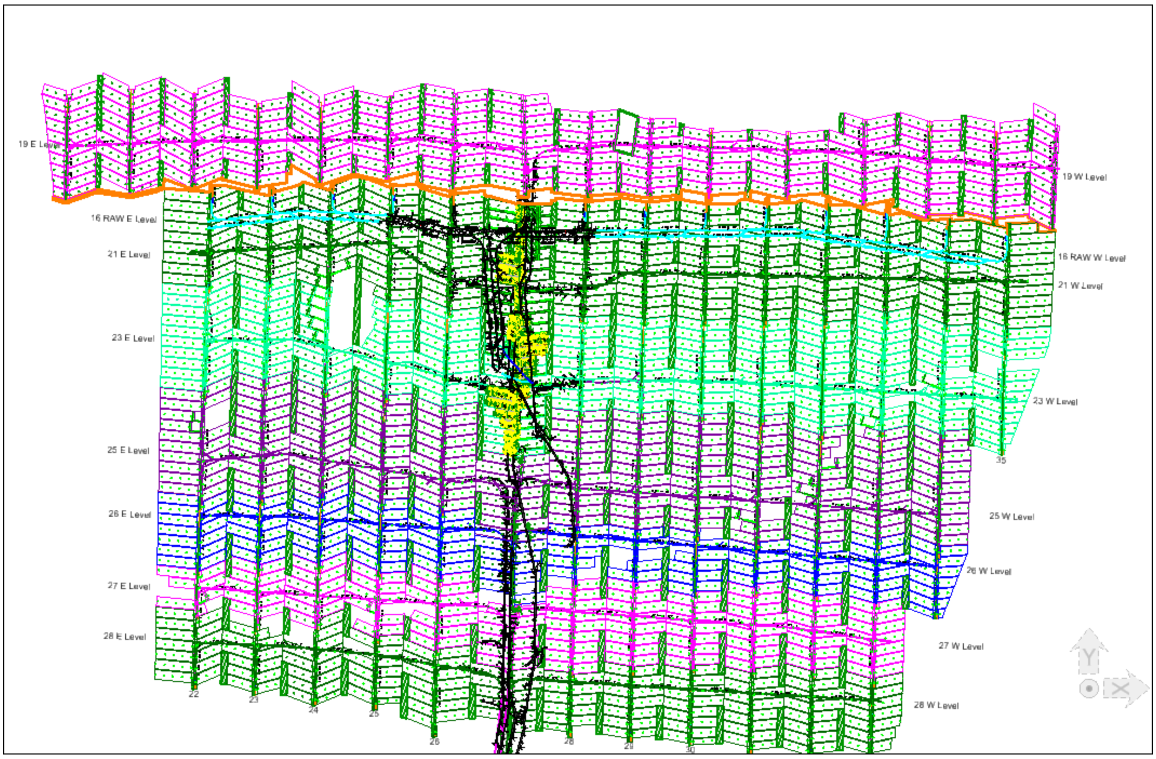

Figure 5.8: MicroStation CAD program pillar layout of the KORP section based on the design criteria

5.12 Conclusions

Each mine and each excavation has its own unique set of geotechnical characteristics. When designing pillars it is important that this variability is taken into consideration. Because rock mass is an inhomogeneous material, it is difficult, if not impossible to ascribe a particular set of properties to it that can be used to calculate its strength. It is even more difficult and unlikely that those same properties can be used to analyse another excavation even though the excavations may appear to be similar. Due to this variability in the rock mass, it very critical that proper rock mass characterisation is done, otherwise the correct equations and techniques will be used based on incorrect input thereby ending up with an incorrect design. Different formula, methods and equations have been formulated to cater for this variability. What is important to note is that these are empirical formulae, and it is important to choose an equation or method that meets the conditions that fall within the range under which that empirical formula was derived in the first place.

In this chapter different pillar strength, loads and foundation strength equations were used giving varied results. The challenge was to choose the formulae most suitable for the conditions on the mine. Certain strength equations such as Watson, et al., (2008), Von Kimmelmann, et al., (1984), Kraulan & Soder, (1987), Sjoberg, (1992), Lunder & Pakalnis, (1997) although discussed, could not be used in designing pillars for this project as the conditions on the mine fell outside the range for which the formulae were derived. With the remaining equations the best approach was to analyse which formulae meets most of the conditions under which it was derived, use it for design and then in the next chapter carry out numerical modelling analyses to further refine the design.

As discussed in Section 5.11, it was concluded that the Stacey and Page equation is the one best suited for Khuseleka as it caters for the strengthening effect of a width to height ratio of >5 as well as the effective width brought on by the length of the pillars.

Other factors such as w\h ratio, FOS, pillar spacing and placement of footwall excavations were also discussed based on best practices and the best parameter values determined. The pillar layout was then designed taking all the factors into consideration.

The final part is to use different numerical modelling programs for analysis then to compare the results with the empirical methods before coming up with the final design for the KORP section.

CHAPTER 6: NUMERICAL MODELLING

6.1 Introduction

Numerical modelling is one of the numerous tools that are available to a designer to help in solving problems. It is not designing in itself as is often incorrectly assumed. When designing it is important to follow the 10 steps presented by Bieniawski, which correspond to the 6 design principles that he also defined. As discussed in the first chapter and shown in Table 1.1, numerical analysis occupies only one step of the overall design methodology. It is only a tool to obtain answers to a problem that has been posed. If the input information is inadequate, and the concept or geotechnical model (including the interpretation of mechanisms of behaviour and choice of appropriate failure or design criteria) is incorrectly formulated, the answers obtained from the analysis may be scientifically correct, but will be wrong with regards to a valid design. That is, the sophisticated analysis has provided results for the wrong problem (Stacey, 2014).

As discussed in the Literature Review and Methodology chapters, three numerical modelling programs were used to assist in the design of the regional pillars for the KORP section. These programs are Examine2D, Lamodel and Map3D. Validation of the numerical modelling results was carried out by comparing them with those from the empirical methods and observations of pillars already cut in underground operations.

In this chapter the Map3D numerical modelling program was used to calculate the RCFs on the haulages below the designed pillars. An analysis on whether to leave pillars or mine out around haulages where the 27 raise line intersects the reef was also done using Map3D.

6.2 Examine2D

Examine2D is a two dimensional, boundary element analysis program. It assumes plane strain conditions. The assumption is that an excavation is 2D, in the sense that their cross sectional geometry in the third dimension is preserved, i.e. one dimension is infinitely long relative to the other two. Thus the strain along that direction is zero, although the stress in that direction is not zero.

To use this program it is assumed that the rock is elastic; thus the following assumptions will be made for the rock mass material;

- The rock mass is homogenous: mechanical properties are the same at all points within the solid body.
- The rock mass is a continuum: material has no structural defects such as discontinuities or fractures.

- The rock mass is isotropic: elastic properties are the same in all directions about any given point (Rocscience, 2012).

6.2.1 Failure Criterion and Material Properties

Failure Criteria are used to determine when failure initiates and what happens after failure has initiated. Although it is an elastic stress analysis program, it has two failure criteria built into it, which are Mohr – Coulomb and Hoek – Brown. For this project the Mohr-Coulomb failure criterion was used although the strength factor was not analysed during the preliminary stages of design. The material properties used in the numerical modelling were those obtained from Chapter 4 (Determination of Rock Properties and Parameters to use for Pillar Design in the KORP Section Parameters) for chromitite rock. These properties are given in Table 6.1.

Table 6.1: Material properties to be used in the analysis

Rock mass Modulus of Elasticity	18.12GPa for chromitite (From Table 4.16)
Depths Below Surface	500m - 1000m
Poisson's Ratio	0.29
Overburden Unit Weight	0.029 MN/m^3
Horizontal Stress Ratio	1.25
Rock mass strength	20.2 MPa downgraded for chromitite
Uniaxial Tensile Strength	0.3 MPa
Cohesion	13.8 MPa (Calculated from Fig 4.8)
Angle of Friction	48.6^o (Calculated from Fig 4.8)
Pillar Widths and Panel Spans	Stacey and Page Table 5.9, Column 6, Coates pillar widths

The "2D" cross sectional pillar widths were used for the numerical models analyses since the model assumes plane strain conditions due to the extensive presence of rock in the third dimension (length of the pillar) which ensures that any induced out-of-plane strains will be zero or negligible along this axis.

6.2.2 Pillar Design

Using input parameters in Table 6.1, APS and strength factors were calculated for the pillars at different depths using Examine2D. Three pillars were constructed, with actual pillar widths and spacing used. The middle pillar was then analysed as it was assumed to give the closest representation of the actual stresses acting on a pillar with mining on both sides. Figure 6.1 is a typical layout of the pillars using Examine2D with stresses calculated from a depth of 500m to 1000m at 50m intervals. The model results were analysed for sigma 1. A query was run across each pillar on all the depths below surface, the results graphed and an excel plot generated from which the average stress for each pillar, at each depth below surface was calculated.

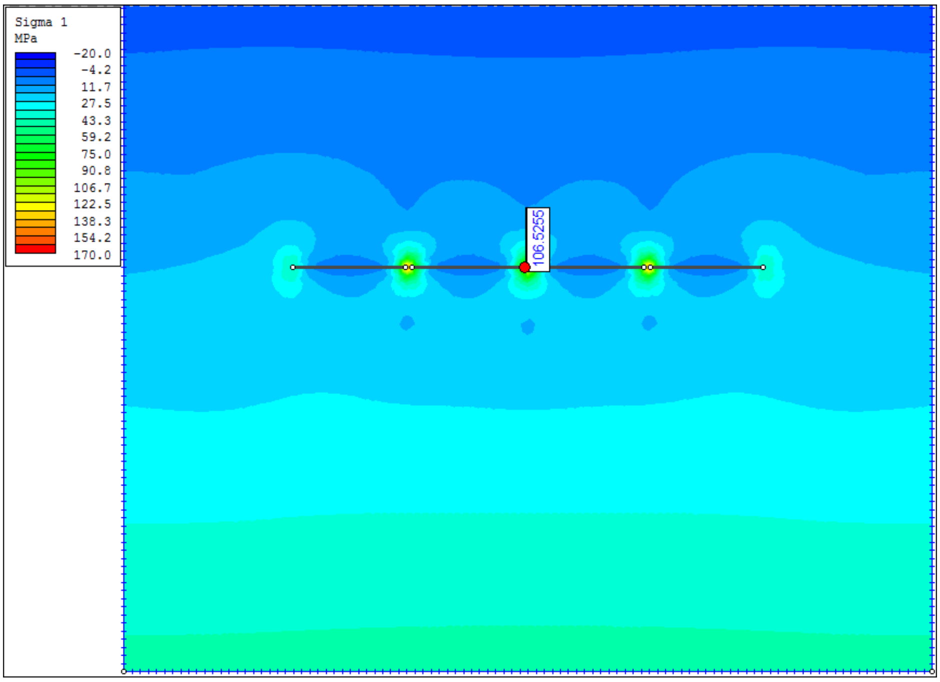

Figure 6.1: A typical layout to calculate APS using Examine2D at different depths

Table 6.2 is a table summarising the APS determined from Examine2D modelling at the different depths using pillar widths from the Coates method in Table 5.1.

Table 6.2: APS results from Examine2D analysis

Pillar Width (m)	Depth (m)	APS (MPa)
13	500	137
15	600	144
17	650	137
17	700	139
18	750	149
23	800	134
25	850	133
28	900	130
30	950	141
32	1000	136

6.2.3 Comparison of Pillar Loads Obtained Using Stacey and Page Pillar Strength Equation Vs Using Examine2D

Figure 6.2 shows the comparison between stresses calculated using Stacey and Page equation and using Examine2D at various depths below surface. The correlation of the actual APS values obtained through empirical calculations and those through Examine2D numerical modelling program is poor with the difference in values at an average of 86MPa. The large discrepancy in APS values can be explained by the fact that Examine2D assumes plane strain conditions meaning that the modelled pillar is of infinite length relative to the plane section of the analysis. This means lower APSs are calculated as the length of the pillar is assumed to be infinite, whereas in the Stacey and Page formula the actual length is used in the calculation giving higher extraction ratios, thus high APS. What is however clear from the graph is that the difference in the APS values is consistent at every depth below surface lying between 33% and 43%.

The results from Examine 2D can be used to validate the results of other analysis since they have shown a consistent difference at different depths (Figure 6.2).

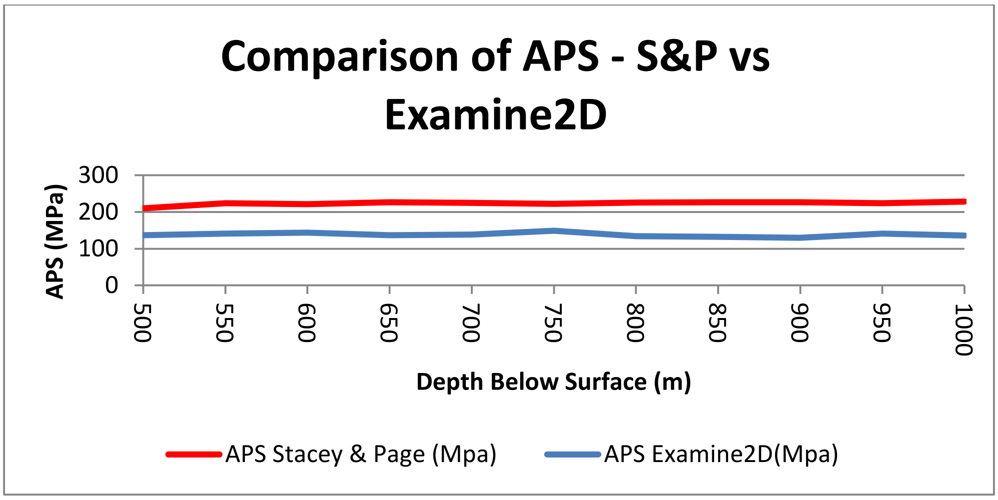

Figure 6.2: Graphical representation of the Comparison of APS calculated using Stacey and Page equation and Examine2D at different depths below surface

6.3 Lamodel

LaModel is a computer based 3D boundary element program for calculating stresses and displacements in coal mines or other thin, tabular seams or veins. It can be used to investigate and optimize pillar sizes and pillar layouts in relation to pillar stress.

The version that was used for this project is LaModel 2.1.

Under the Edit Data Menu, the geometrical parameters for the pillars were specified and are given in Table 6.3:

Table 6.3: Material properties to be used in the analysis

Poisson's Ratio of Overburden	0.24 (For norite from Table 4.9)
Elastic Modulus of Overburden (GPa)	45 (For norite from Table 4.9)
Vertical Stress Gradient (MPa/m)	0.029
Lamination (layer) thickness (m)	15
Number of elements in X axis	1000
Number of elements in Y axis	1000
Overburden depth (m)	500-1000
Seam thickness (m)	1.2
Element width (m)	1
Seam boundary conditions	Rigid
Rock strength (MPa)	63 (From Table 4.3)

At 50m intervals from a depth of 500m to 1000m below surface three pillars were modelled and then the middle pillar was analysed for stresses. The major vertical stresses acting on the pillars were the output results from the analysis, these were then plotted as excel graphs from which the average pillar stresses of the middle pillar were calculated to determine the APS at that particular depth. Table 6.4 shows the APS for the designed pillars at different depths.

Table 6.4: APS results from Lamodel analysis

Pillar Width	Depth (m)	APS (MPa)
13	500	165
14	550	190
15	600	234
17	650	225
17	700	243
18	750	253
23	800	204
25	850	196
28	900	190
30	950	184
32	1000	179

6.3.1 Comparison of Pillar Loads Obtained Using Stacey and Page Pillar Strength Equation Vs Using Lamodel

Figure 6.3 is a graphical representation of the comparison of the stresses calculated using Stacey and Page equation and Lamodel at various depths below surface. The graph shows a good correlation between the empirical Stacey and Page equation stress values and those of Lamodel with an average difference of 18MPa (8%). Unlike Examine2D, Lamodel takes the length of the pillar into consideration (3D) thereby giving values almost similar to the Stacey and Page equation.

This numerical analysis shows pillars at depths between 600m and 750m having an APS greater than 228MPa. If the design of the pillars was based solely on this analysis it would mean some pillars widths would be increased to reduce the APS to less than 228MPa.

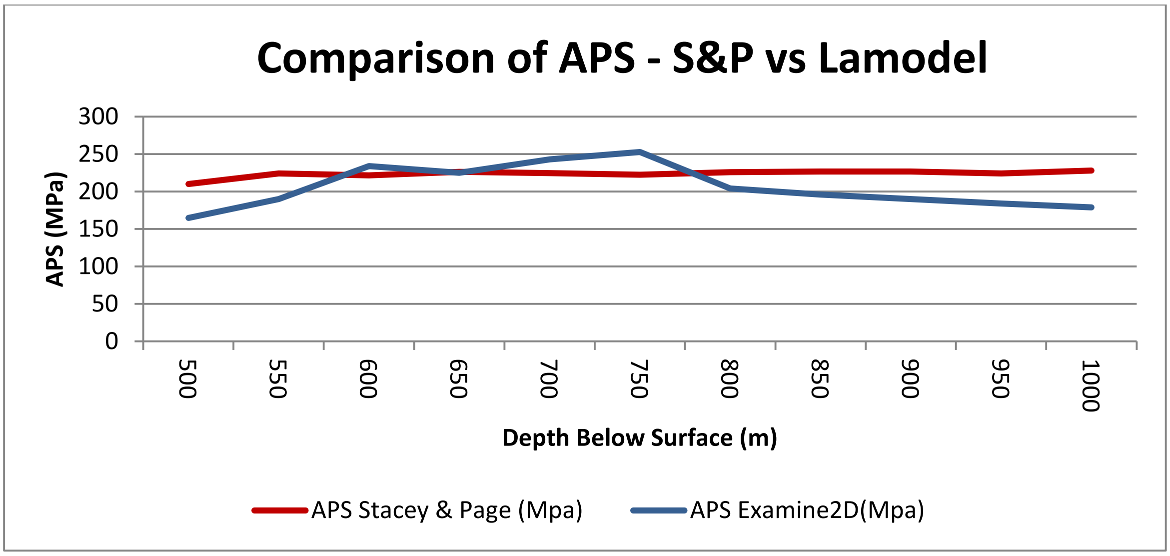

Figure 6.3: Graphical representation of comparison of APS calculated using Stacey and Page formula and those using Lamodel at different depths below surface

6.4 Map3D

Map3D is a fully integrated three-dimensional layout (CAD), visualisation (GIS) and stability analysis package (BEM stress analysis), MineModelling, (2013). Pillar design will be modelled using 'Map3D Fault-Slip'. Both displacement discontinuities and fictitious force formulations of the boundary element technique are available within the package.

This model was built in 3D using displacement discontinuity (DD) elements.

Map3D is limited to elastic or elasto-plastic yield behaviour. Being a boundary element solution, the non-linear behaviour is limited to the surface of the elements.

6.4.1 Methodology of Analysis

Anglo American Platinum underground working plans are created, updated and stored on the 3D CAD program, MicroStation.

The following steps were followed in designing the pillars in MicroStation and transferring them to Map3D,

- Pillars were designed on a predetermined layout of haulages, crosscuts and raises in 3D (Figure 5.8). This layout determined the middling distance between pillars and footwall infrastructure, pillar lengths and pillar spacing. The pillar dimensions, spacing and positioning values used were those calculated in Table 5.9 using the Stacey and Page equation
- On completion of the pillar layout, due to the need to reduce processing run time and limited computational capacity, only five rows of pillars in the middle of the KORP layout were chosen and fenced as representation of the pillar underground and these

would be modelled. Figure 6.4 is a layout on which a model would be built with the pillars highlighted in red.

- The layout file was then saved in dxf format, which is the file format compatible with importing and modelling in Map3D.

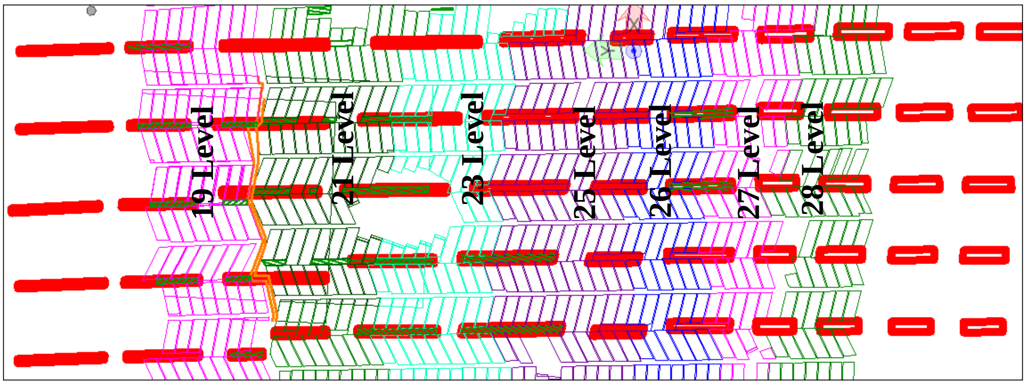

Figure 6.4: The five rows of pillars from 19 to 28 levels fenced in MicroStation for modelling

The dxf file was then opened in Map3D for building the model as a displacement discontinuity (DD) loop.

The pillars in the middle row were chosen for analysis and the mesh spacing, was reduced to a value of 5m for more accurate analysis compared to a mesh spacing of 30m for the rest of the layout outside this zone, the meshing diagram from Map3D is shown in Figure 6.5. These pillars were chosen due to their centrality in relation to the other pillars and excavations and thus would give a representation closer to the reality underground where rock around these pillars is mined out and stress is distributed on these pillars as well as other pillars in the vicinity. This is different from empirical analysis methods where it is assumed that stress is loaded equally on all pillars. Grid planes were then placed on each of these pillars representing the different mining levels to determine the APS on the pillars at different depths as shown in Figure 6.5.

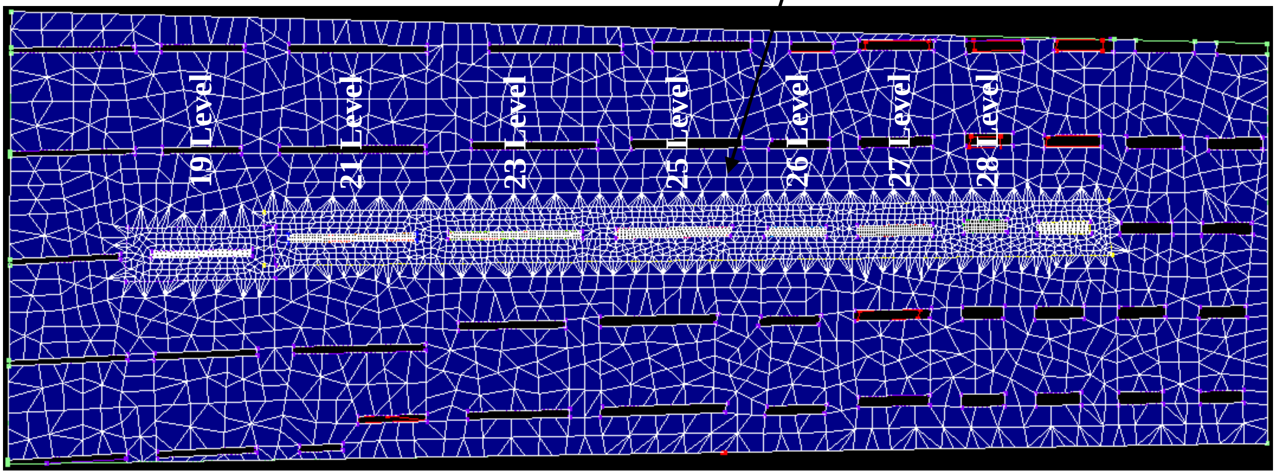

Figure 6.5: The model constructed for the pillars. Note the middle pillars where meshing was reduced for more refined analysis.

The input parameters chosen for the modelling are shown in Figures 6.6, 6.7 and 6.8, based on values obtained in Chapter 4.

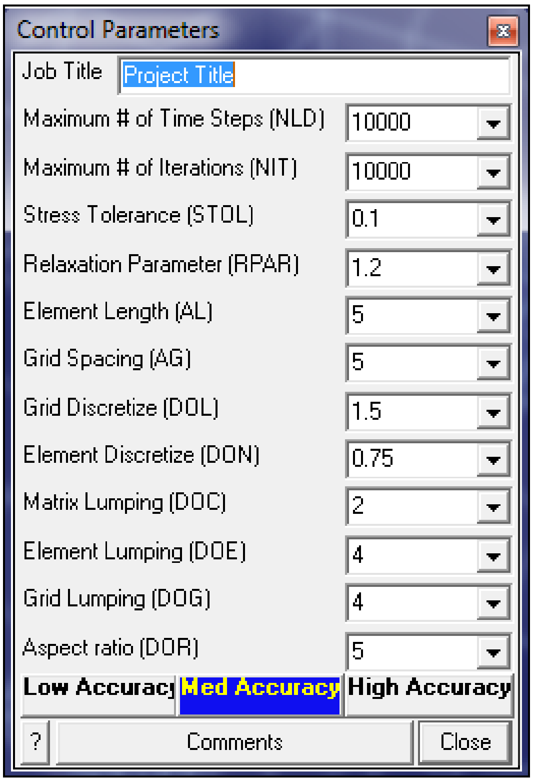

Figure 6.6: Control parameters, these were left as default as per program manual suggestion.

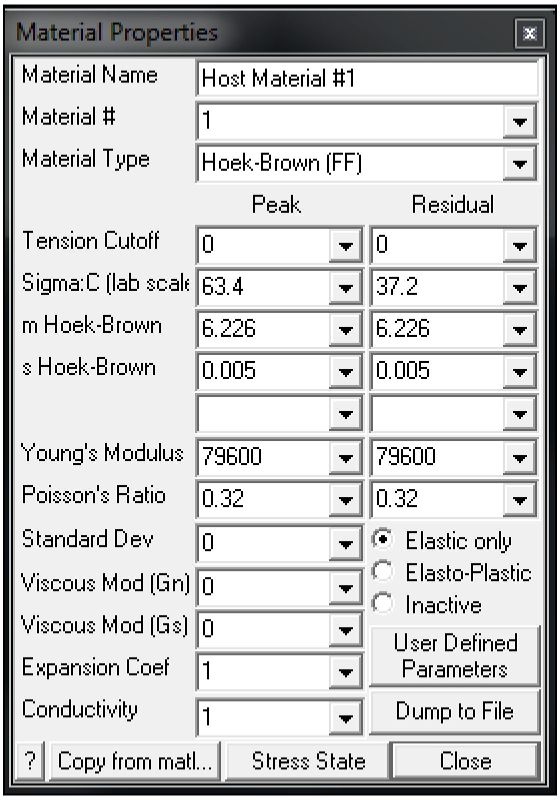

Figure 6.7: Material properties of the UG2 reef rock (chromitite), based on lab values and Rocklab values in Tables 4.4 and 4.16 respectively

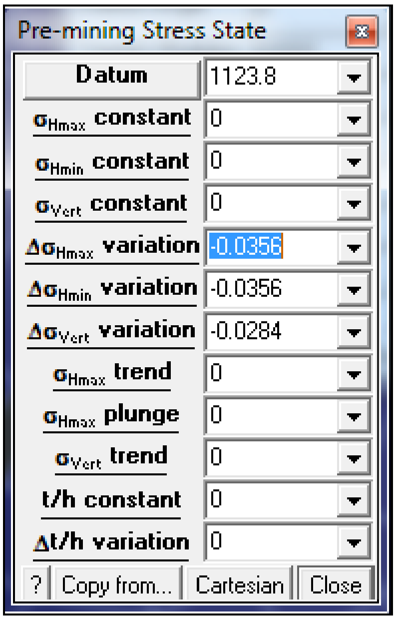

Figure 6.8: Pre-mining stress state based on stress measurement values in Section 4.7 of this report.

6.4.2 Numerical Modelling Results

After running the numerical analysis the model results of σ_1 were queried, and are shown in Figure 6.9 as contour ranges.

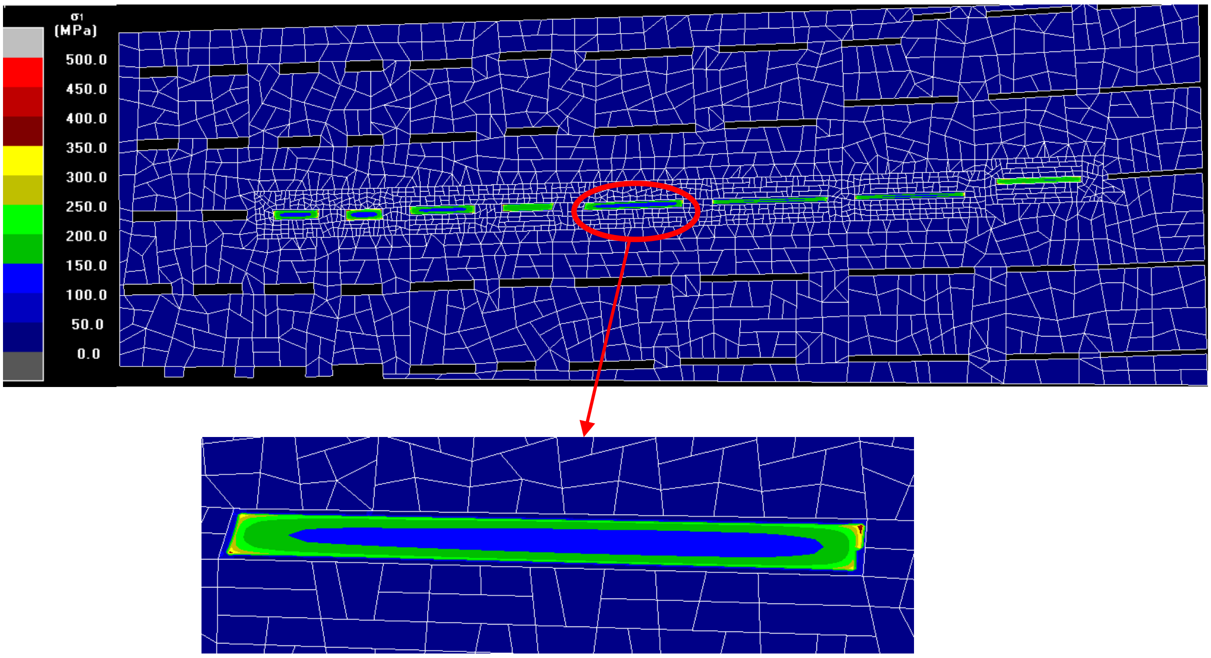

Figure 6.9: Map3D plot of the pillars that were analysed, showing the stress state in the pillars. A single pillar is zoomed in for a clearer plot.

The APSs were analysed by opening the plot tab\Excel plot grid, where the stress calculated for each point on a pillar were generated in an excel spreadsheet, then the APS values were calculated by averaging the total of all the stress at each point on the pillar. Table 6.5 shows the APS for each pillar at the different levels and depths below surface.

Table 6.5: APS results from Map3D analysis

				Depth Below Surface		
Level	**APS (MPa)**	**Pillar length (m)**	**Pillar width (m)**	**From (m)**	**To (m)**	**Comparison Level (m)**
19	156	210	15	557.7	590.2	600
21	102	276	17	603.3	647	650
23	104	299	18	657.8	705	700
25	134	262	23	717.8	759.4	750
26	152	140	23	772.8	794.7	800
27	142	180	25	806.8	835	850
28	146	130	28	866.1	897	900

6.4.3 Comparison of Pillar Loads Obtained Using Stacey and Page Pillar Strength Equation Vs Using Map3D

Figure 6.10 is the comparisons of the APS between Stacey and Page equation and Map3D at various depths below surface. The Stacey and Page APS results are higher than those from the Map3D analysis results. This can be because Map3D takes into account other excavation properties such as the dip of the reef and the influence of other excavations within the mining area during analyses which Stacey and Page does not do.

The numerical analysis shows that the pillars have a maximum APS of 170MPa. There is therefore potential to reduce the pillar widths without compromising on stability as long as the other design criteria of the pillars are met. Reduction in pillar widths will translate to high extraction ratios.

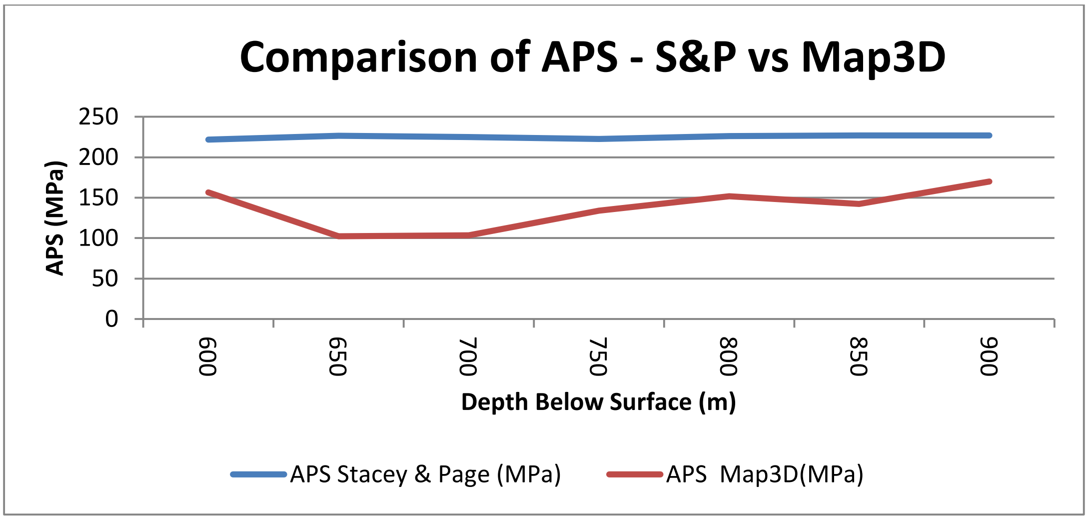

Figure 6.10: Graphical representation of comparison of APS calculated using Stacey and Page formula and those using Map3D at different depths below surface

6.4.4 Comparison of Pillar Loads Using the Different Methods Discussed

A comparison was made between the APS obtained using Stacey and Page equation and the three numerical modelling programs as well as between the numerical modelling programs themselves. This is illustrated in Figure 6.11. All the numerical modelling programs except for Lamodel give values that are lower than those obtained using the Stacey and Page equation. Although the Stacey and Page values are higher than those obtained by Map3D and Examine2D, there is a discrepancy in the actual values where they range in difference between 30% and 50%. Lamodel and Stacey and Page give values that are almost similar with a difference in range of only 10%. This could be because both methods take the length of the pillar into account when calculating the APS. The widest discrepancy in the values is between Examine2D and Map3D where the difference is between -13% at 900m below surface to 25% at 650m below surface giving a total difference of 38% in values. This can be attributed to the fact that Examine2D is a two dimensional program that assumes plane strain conditions whereas Map3D is a three dimensional program.

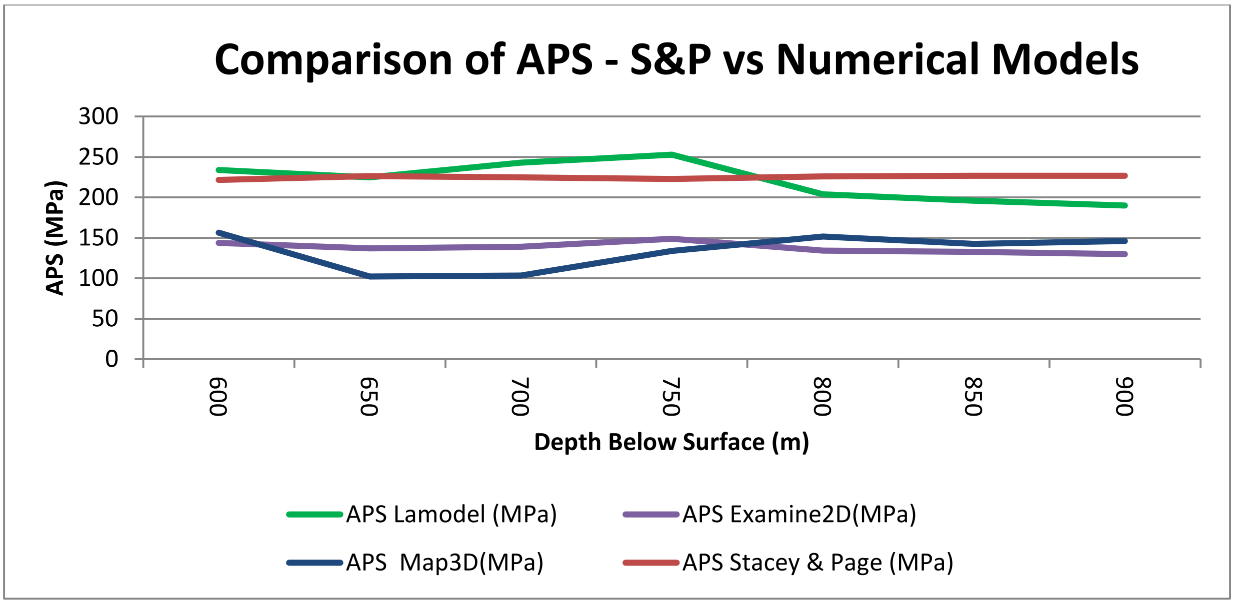

Figure 6.11: Graphical representation of comparison of APS calculated using Stacey and Page formula and the 3 numerical modelling programs

6.5 Redesign of Pillars Using Examine2D and Map3D

Numerical modelling analyses on a new set of pillar widths were required. This was because the previous analysis had indicated low APS on those pillar widths. Therefore there was scope to reduce pillar widths and increase extraction ratio while still meeting the APS design criteria of <228MPa. The pillar widths were reduced then modelled ensuring that the APS did not exceed 228MPa and also ensuring a W: H ratio of ≥ 10. Lamodel indicated APS results that were in most instances greater than 228MPa so there was no scope for reanalysing the pillars using this numerical modelling program as it would mean increasing pillar widths.

6.5.1 Redesign of Pillars Using Examine2D

Examine2D was to be used first for the analysis since it is faster and easier to run than the more complex and time consuming Map3D. The pillar widths derived using Examine2D would then be used to run the first analysis in Map3D.

After numerous model runs to determine the optimal pillar widths that met the design criteria, the final pillar widths and their APS and strength factors are presented in Table 6.6 together with the results that were previously calculated in section 6.2. The pillar widths were reduced by between 8% at 500m below surface to 47% at 1000m below surface, which translates to an improvement in the extraction ratios as highlighted.

Table 6.6: Comparison of Previous and Final results with Examine2D Analysis

DBS (m)	Previous APS (MPa)	Final APS (MPa)	Previous Pillar Width (m)	Final Pillar Width (m)	Previous Extraction Ratios	Final Extraction Ratios	Percentage Difference In Pillar Widths
500	137	160	13	12	0.95	0.96	8%
550	141	176	14	12	0.95	0.95	14%
600	144	192	15	12	0.94	0.95	20%
650	137	208	17	12	0.94	0.95	29%
700	139	213	17	12	0.93	0.95	29%
750	149	221	18	12	0.93	0.95	33%
800	134	219	23	13	0.92	0.96	43%
850	133	217	25	14	0.92	0.95	44%
900	130	222	28	15	0.91	0.95	46%
950	141	221	30	16	0.91	0.95	47%
1000	136	220	32	17	0.90	0.95	47%

6.5.2 Redesign of Pillars Using Map3D

The pillar widths in the layout in Figure 5.8 were reduced in MicroStation then exported as construction lines to Map3D to reanalyse the APS. Several numerical modelling runs were done with pillar widths being adjusted until the APS was as close to 228MPa as possible without going above it so as to maximise the extraction ratio. During the numerical modelling runs all other properties and parameters were left unchanged to those used in the initial analysis, with only the pillar widths being adjusted. The results are compared with analysis results from Table 6.5 and are shown in Table 6.7. The results show that pillar widths were reduced by between 20% at 600m below surface to 44% at 850m below surface, which translates to an improvement in the extraction ratios as highlighted.

Table 6.7: APS results using Map3D on Redesigned Pillars

DBS (m)	Previous Pillar Width(m)	Final Pillar Width(m)	Previous APS (MPa)	Final APS (MPa)	Previous Extraction Ratios	Final Extraction Ratios	Percentage Difference In Pillar Widths
600	15	12	156	121	0.94	0.95	20%
650	17	12	102	131	0.94	0.95	29%
700	17	12	104	140	0.93	0.95	29%
750	18	12	134	155	0.93	0.95	33%
800	23	13	152	197	0.92	0.96	43%
850	25	15	142	210	0.92	0.95	44%
900	28	17	146	213	0.91	0.95	39%

Although the APS values up to 750m below surface are considerably lower than 228MPa, the pillar widths could not be reduced to less than 12m, as the criterion for the regional pillars' w: h ratio should not be ≤10.

Based on this analysis, all the pillars met the proposed design criteria for this project in Table 2.3.

A comparison is also made between the results obtained using the Examine2D and those of Map3D. Lower APS values are calculated for the Map3D analysis for similar pillar widths. Table 6.8 gives the comparison in terms of the pillar widths, APS and extraction ratios.

Table 6.8: Comparison of Examine2D and Map3D values based on final analysis

	Examine2D			Map3D		
Depth (m)	Pillar Width(m)	APS (MPa)	Extraction Ratios	Pillar Width(m)	APS (MPa)	Extraction Ratios
600	12	192	0.95	12	121	0.95
650	12	208	0.95	12	131	0.95
700	12	213	0.95	12	140	0.95
750	12	221	0.95	12	155	0.95
800	13	219	0.96	13	197	0.96
850	14	217	0.95	15	210	0.95
900	15	222	0.95	17	213	0.95

6.5.3 Conclusions

The fact that Map3D is based on the actual 3 dimensional representation of the KORP section, (from a CAD program - MicroStation), with all parameters and conditions incorporated into the analyses, it means the design derived from Map3D is arguably more valid than those from Stacey and Page, Examine2D and Lamodel. Because all the numerical analyses results are lower than those derived using the Stacey and Page equation, there is a good argument to conclude that the Stacey and Page method is too conservative in the sense that it designs oversized pillars than are required. Based on these considerations it was concluded that Map3D was the best method for pillar design.

With the final Map3D analysis with the pillar widths reduced there was a significant increase in the extraction ratios especially at the deeper levels of the mine compared to the initial analysis. Even with the 2 dimensional Examine2D there is significant gain in terms of the extraction ratio.

The difference in values obtained between empirical design and numerical modelling and indeed between the different numerical modelling programs themselves gives a compelling argument that it is prudent not to base the design of any underground layout on only one method. An attempt should be made to use as many different available methods as possible, then from there, use the most optimal one in terms of cost and extraction ratio based on the design criteria.

However, it is important to remember that numerical modelling is not design, but is a part of the process of designing. So as discussed previously, it will be part of good design practice to implement the principles of constructability and optimisation on the pillars once mining commences. This means that a monitoring program should be put in place to ensure that the pillars perform as per the design criteria and that the assumptions and input values used in the modelling are correct. If the pillars or excavations do not perform as predicted, then some aspects of the design may require changes.

The designed pillars must also integrate into the overall strategy and plan of the mine for them to be optimised.

6.6 Determination of RCF values Using Map3D Program

6.6.1 Introduction

Map3D numerical analyses were conducted to determine the effects of mining and the pillars on the reef horizon to the haulages below them. In Section 5.10, RCF values at different depths below surface were calculated using the empirical equation and all the RCF results obtained indicate good ground condition values of < 0.7. These results were based on in-situ stress conditions. To determine the effects of induced stresses on tunnels and haulages requires numerical modelling analysis. Map3D due to its 3D capabilities was the best numerical modelling program to use. A model was constructed in Map3D and grid lines placed along the haulages that have been mined or are planned to be mined in the KORP section and a numerical model analysis ran along those grid lines to determine the RCF values to be expected. The most essential aspect was to analyse the influence of the regional pillars both below in the case of 16 level haulages and above in the case of all the other levels.

The RCF parameters that were used are as follows:

F = 0.7 (based on the RMR value of the KORP section)

σ_c = 166 MPa (the UCS value for pyroxenite rock where the footwall excavations will be situated).

Ideally RCF values of less than 0.7 are desired, but with additional support installed values of up to 1.3 can be managed. RCF values of more than 1.4 should be avoided and values above 2 will indicate to a potential loss of the excavation.

Figures 6.12 to 6.15 are images and graphs of the RCF values obtained along the length of the excavations on each level based on the pillars and mining layout designed in section 6.5. Note the spike in values on each graph; these represent the portion where the excavation passes within a regional pillar.

6.6.2 16 Level RCF

Figure 6.12 is an image of the model of RCF analysis on the Return Airway (RAW) and haulage of 16 level which is mined above the 19 level stoping elevation. The model results are represented graphically in Figures 6.13. The graph shows RCF values spiking in positions where the haulages are directly above the regional pillars. The RCF values of the haulage peak at 1.8, whilst those of the RAW peaks at 2.0. The rest of the excavations indicate values of below 0.5. This indicates that the pillars will have a direct influence on the excavations above and will induce high stresses that have the potential to cause failure in the haulage and RAW. So there is a potential for very poor ground conditions at positions just above the pillars and good conditions on the rest of the excavations. The solution to this is either to install robust support where the excavations are above the pillars or to break up the pillar over the excavations so as to overstope them. However as can be seen in Figure 6.12 if the pillar is broken up a very small pillar will be left on the right side of the image and numerical modelling analyses will be required to determine the effect of this on the RCF values of the haulages, and on the APS of the pillars themselves and ensuring that they continue to meet the design criteria in Table 2.3.

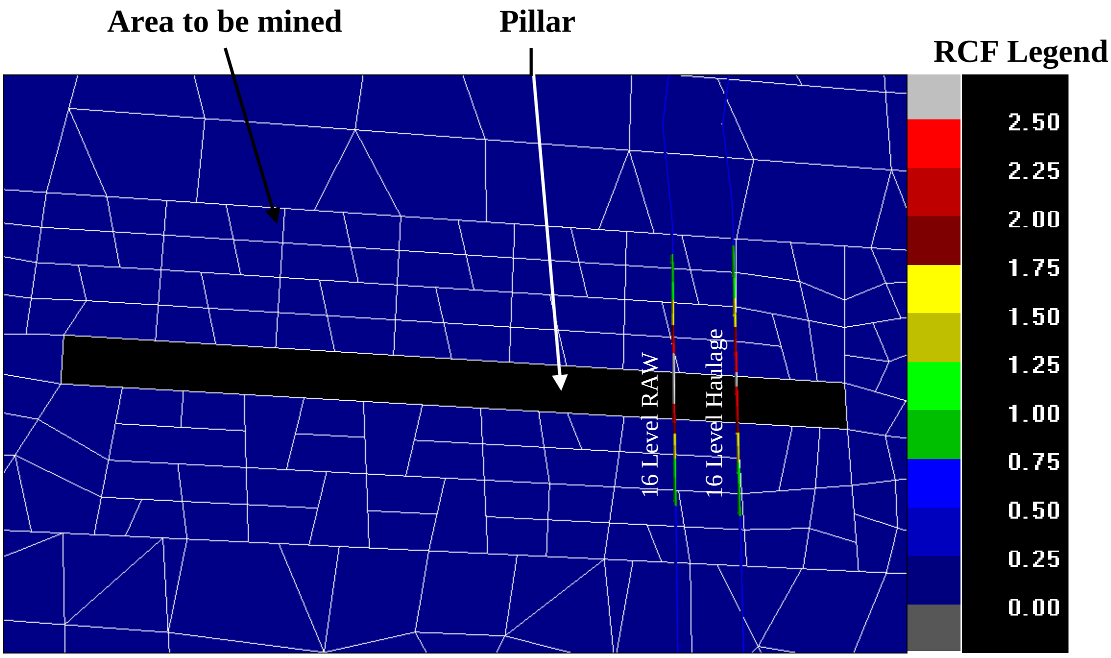

Figure 6.12: A Map3D model of the RAW and haulage at 16 level running above 19 level (note the high RCF values on the pillar position)

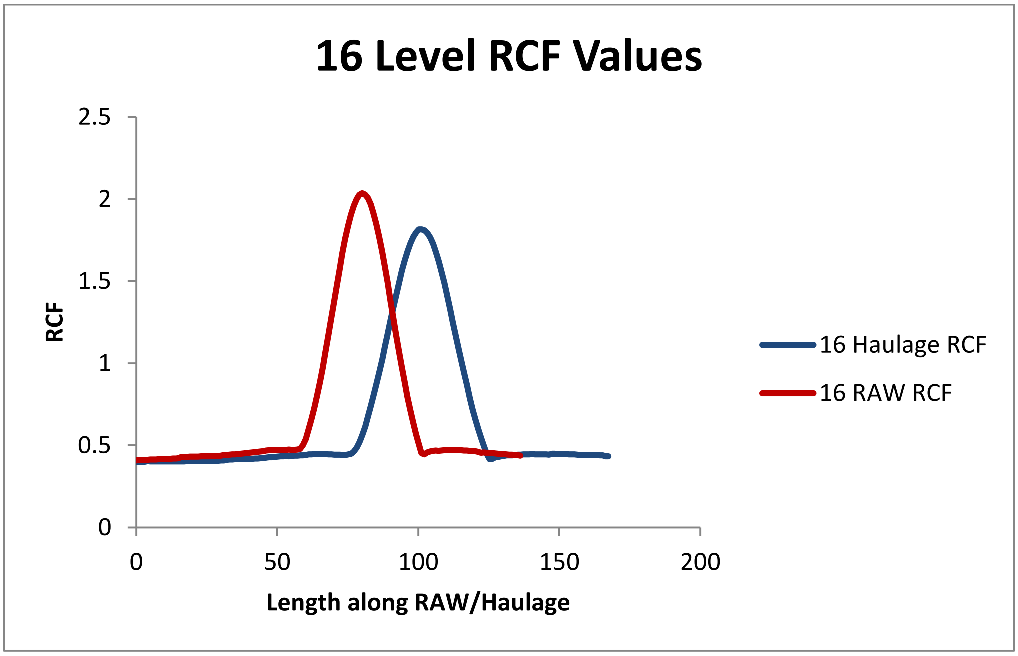

Figure 6.13: Graphical representation of the RCF values modelled along the haulage and RAW on 16 level mined above 19 level stoping

6.6.3 19 - 28 Level RCF

Level 19 to 28 haulages are all situated below their respective stoping levels and are designed to be overstoped, meaning there is no pillar directly above the haulage, i.e., the 45° rule discussed in the Literature Review chapter was applied. As can be seen in Figure 6.14, level 25, has a portion along its length with RCF value >1. Figure 6.15 is a graph showing RCF values along the different haulages at different depths below surface (levels).

All the haulages except on 25 level have RCF values which indicate stability as they are all below 1. At 25 level, some rehabilitation work may be required where the RCF values are >1. An alternative to alleviate this problem would be to reduce pillar lengths so as to increase the overstoping distances, then doing numerical modelling analysis on the shortened pillars to determine the new RCF and APS values.

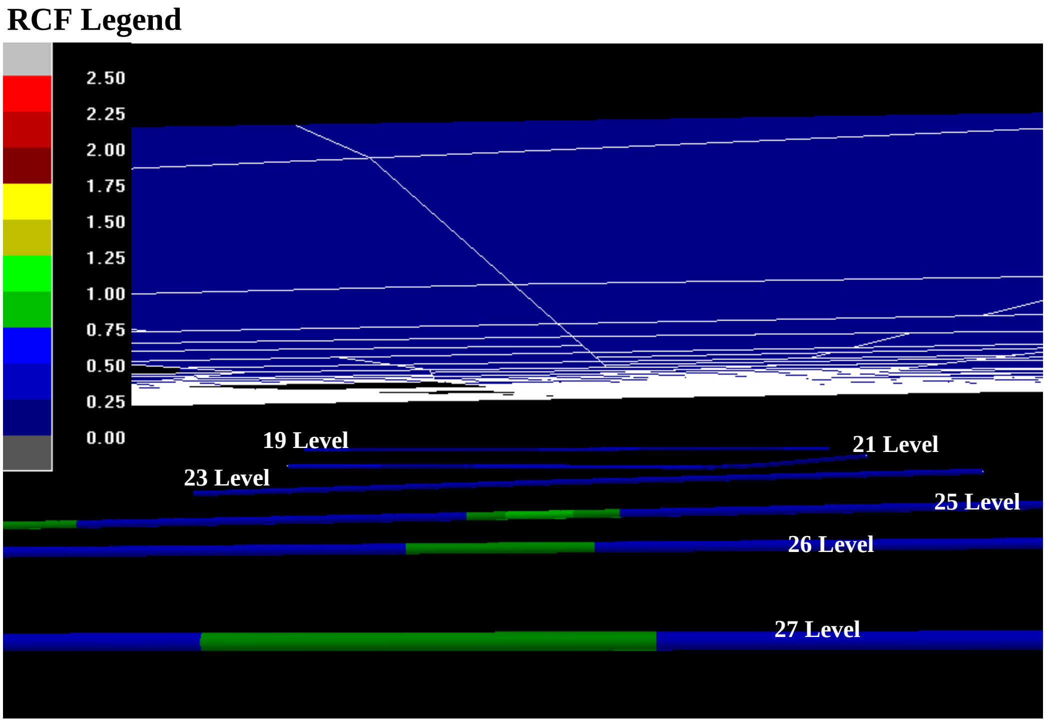

Figure 6.14: A Map3D model of the 19 to 27 level haulages running below their respective levels (No noticeable spike in RCF values)

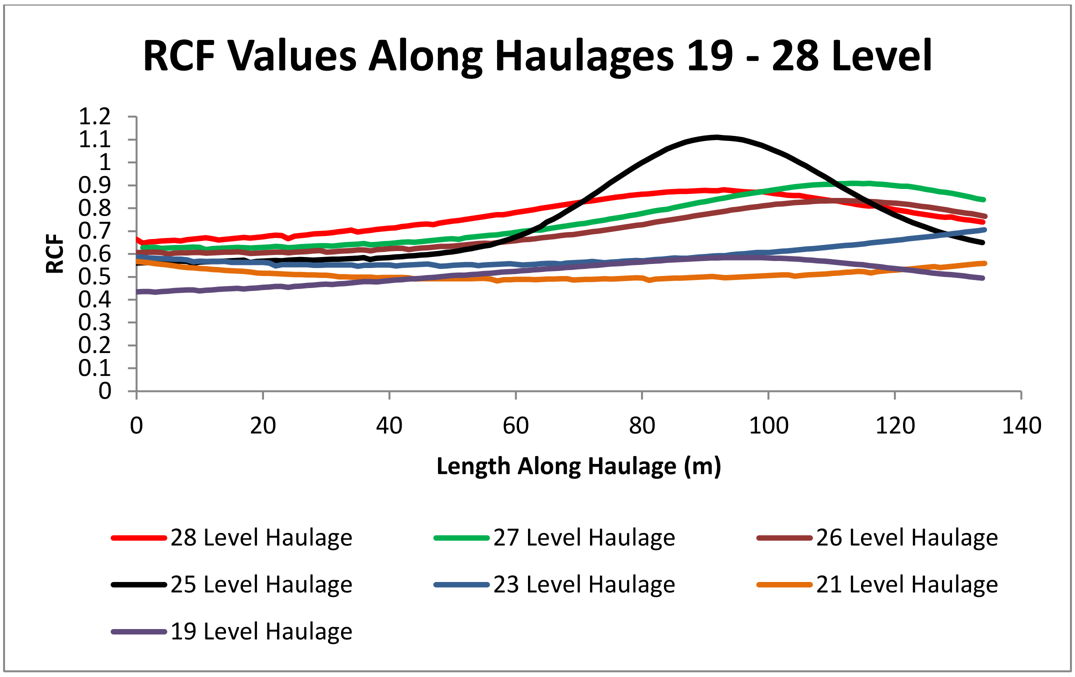

Figure 6.15: Graphical representation of the RCF values modelled along the haulages from 19 to 28 level

6.6.4 Conclusions

Through numerical modelling, 16 level haulages which are mining above 19 level stoping, have indicated RCF values of up to 2. This value represents poor ground conditions requiring robust support. An alternative would be to understope the haulages but this would have consequences on the APS as some of the pillars will be very small due to the layout design.

Due to the overstoping of the haulages from 19 to 28 levels, the RCF values are significantly low to warrant any further action to be taken in terms of support, except monitoring to validate the results. Most of the RCF values are below 0.7 which are good ground conditions values with maximum values slightly above 1 at 25 level. It will be very critical to ensure that no pillars are left above the haulages as this will increase the RCF values which is likely to cause adverse ground conditions in the haulages

Monitoring will be conducted in the haulages when mining commences so as to validate the modelling results and re-evaluate the support strategy where necessary.

6.7 Effect of Leaving Stability Pillars on Haulage-Reef Intersection Using Map3D Program

6.7.1 Introduction

One of the objectives of this project was to determine whether to leave pillars or mine out around haulages where the 27 raise line intersects the reef. The KORP section is designed in such a way that the 16 level haulages are mined above 19 level reef horizon. Due to the dip of the reef there is a position where these haulages intersect the reef at 16 and 19 levels. It is therefore critical to analyse the effects of leaving stability pillars over 16 and 19 haulages. The purpose of these pillars would be to prevent panels mining into 16 and 19 level haulages in areas where the haulages will intersect the reef horizon. Map3D due to its 3 dimensional analytical capabilities and the fact that construction lines can be exported and used from the MicroStation CAD program is the most suitable numerical modelling program for conducting this analysis.

Ledging in 27 raise-line was completed during November 2013; eastern panels at the bottom are currently being mined. The top and bottom west panels will intersect 16 and 19 haulages if mined from the raise line. Figure 6.16 indicate the areas where the panels will intersect the haulages.

The panels were initially planned to be mined from the raise-line up-to to the regional pillar and this was going to result in panels mining through the haulages. This was later deemed not feasible based on history on the mine were ground and support deterioration occurred on 8 level when the reef intersected the haulage and was mined through. Serious creep and support deterioration (both primary and secondary support) occurred at the intersection position and this affected the stability of the excavations with serious financial consequences as the intersection required massive rehabilitation.

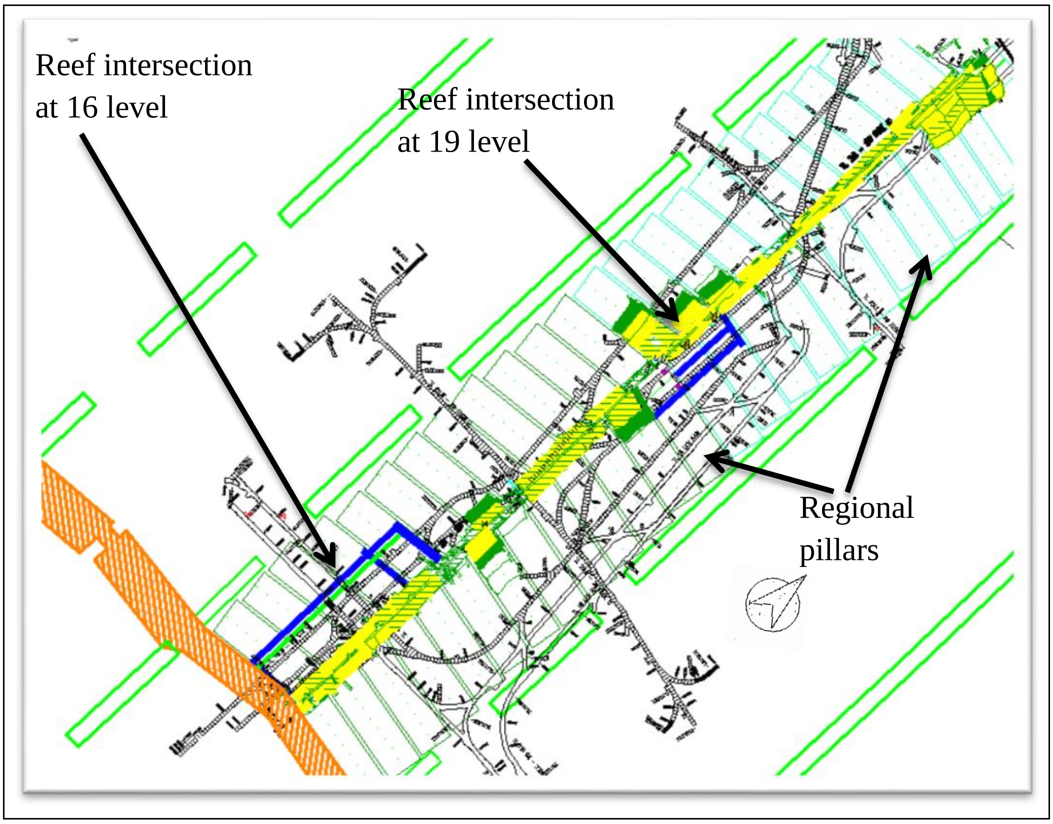

Figure 6.16: Plan showing areas where the reef intersects 16 and 19 haulage

6.7.2 Design Criteria

Similar design criteria values of the stresses and RCF as discussed in Section 6.6 were considered to be ideal in designing the pillars to be left over the haulages on 21 crosscut, that is, the RCF values were not to be greater than 1.4 for stability. It was also important that the maximum field stresses induced on the haulages by the pillars were not to be greater than half of the UCS of the rock to prevent fracturing in the haulages as stated by Hoek & Martin,(2014) who noted that at low confining pressures, tensile fracturing initiates in rock at 40% to 60% of the uniaxial compressive strength.

The rock mass parameter values used for calculating RCF in the preceding section were used for RCF calculations for this numerical model analysis. A pillar with a width of 20m was designed over the 19 level haulage where it intersects reef.

Figure 6.17 is a Map3D plot showing model of pillar to be left over 19 level haulage and the layout of 16 and 19 haulages.

Figure 6.18 shows the Map3D numerical modelling analysis for major principal stress σ_1 along 19 level haulages. The maximum values of Sigma 1 derived from this analysis along the haulages were between 70MPa and 80MPa giving a FOS of about 2 since the haulages mine through pyroxenite rock which has a UCS of 166MPa (Table 4.4). Monitoring will have to be conducted during mining for any possible fracturing and additional support requirements.

Figure 6.19 shows the Map3D numerical modelling analysis for RCF values along 19 level haulages. The picture shows high RCF values of >1.4 closer to the edge of the pillar. These RCF values are illustrated more clearly by the graph generated along these haulages in Figures 6.20. The graph also shows the RCF values before mining takes place. The RCF values are at a maximum of 1.4 on the edge of the pillars. These RCF values indicate average to poor ground conditions, meaning that additional secondary support will be required to ensure that these haulages are stable for the life of the excavation.

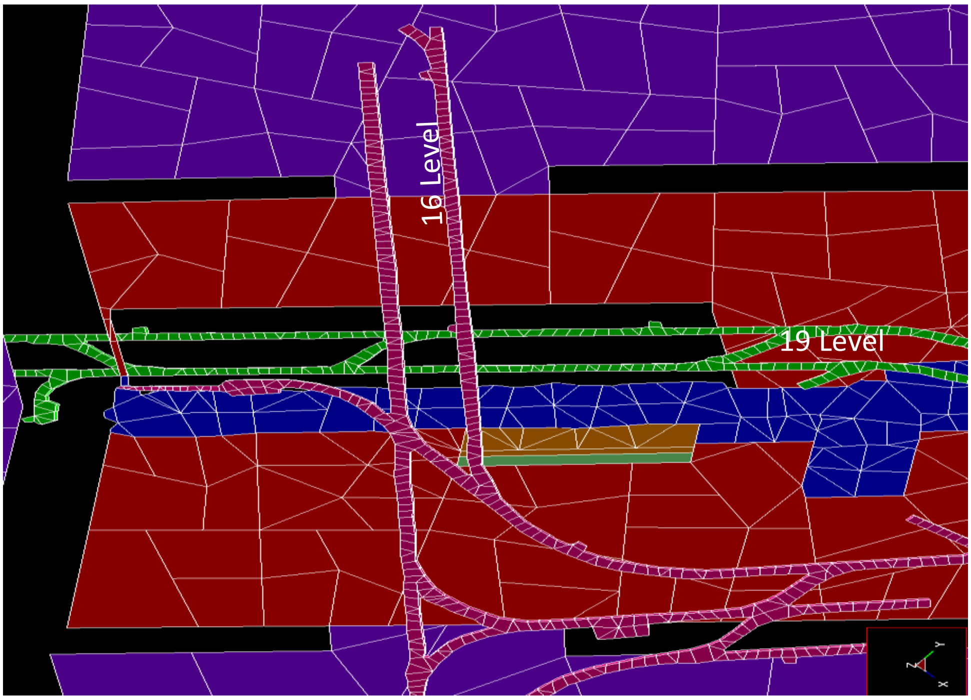

Figure 6.17: Map3D plot showing model of pillar to be left over 19 level haulage (Black portion are the pillars and coloured portion are areas to be mined out)

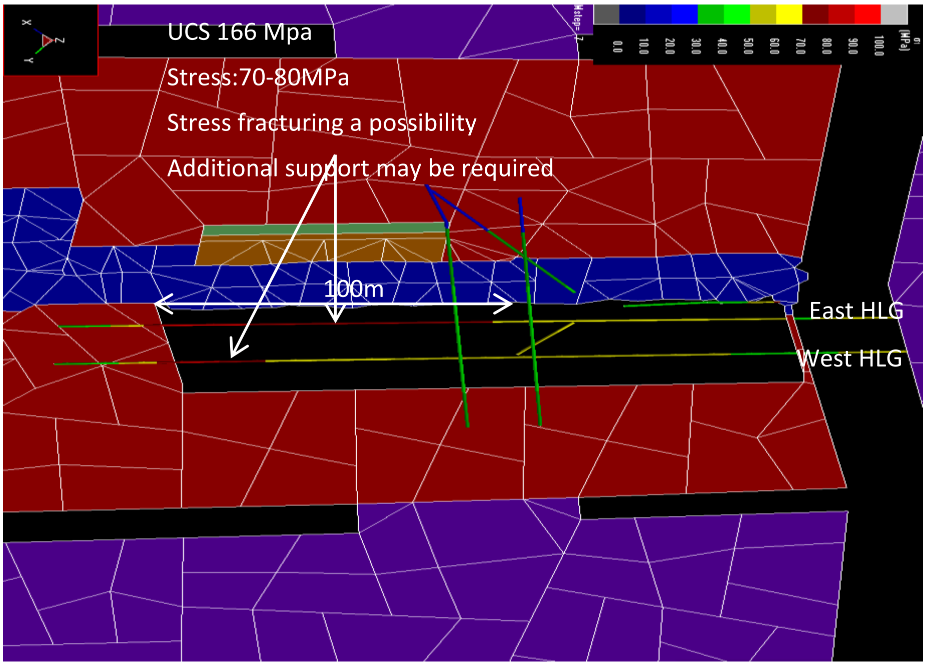

Figure 6.18: Map3D plot showing Sigma 1 along the 19 level haulages.

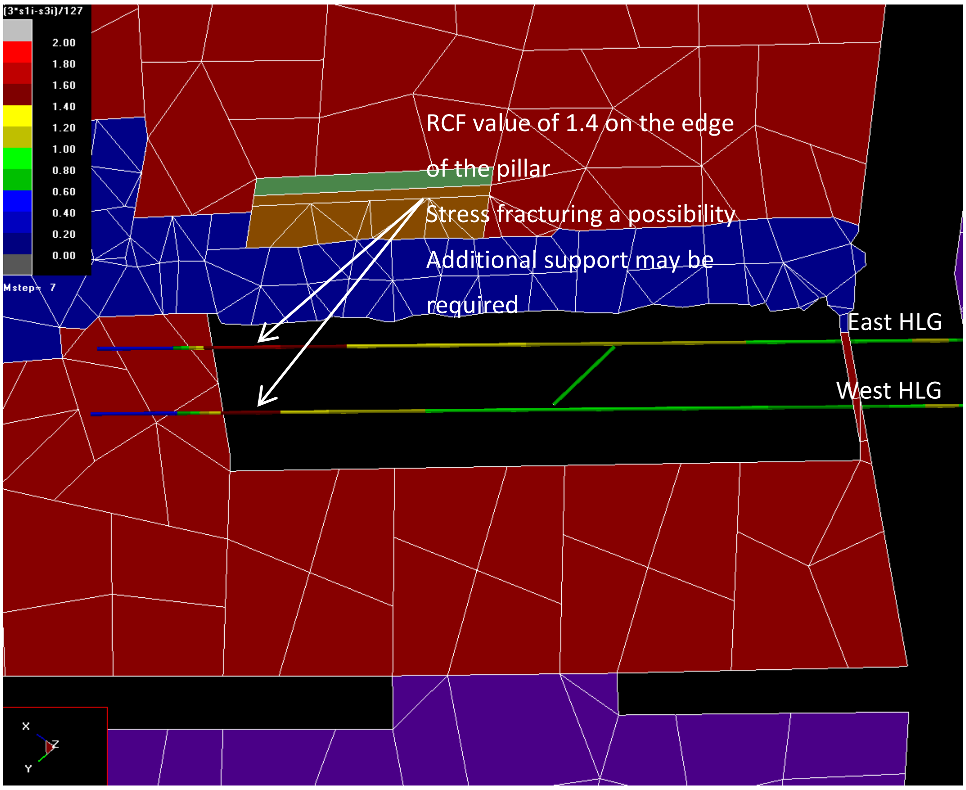

Figure 6.19: Map3D plot showing RCF values along the 19 level haulages.

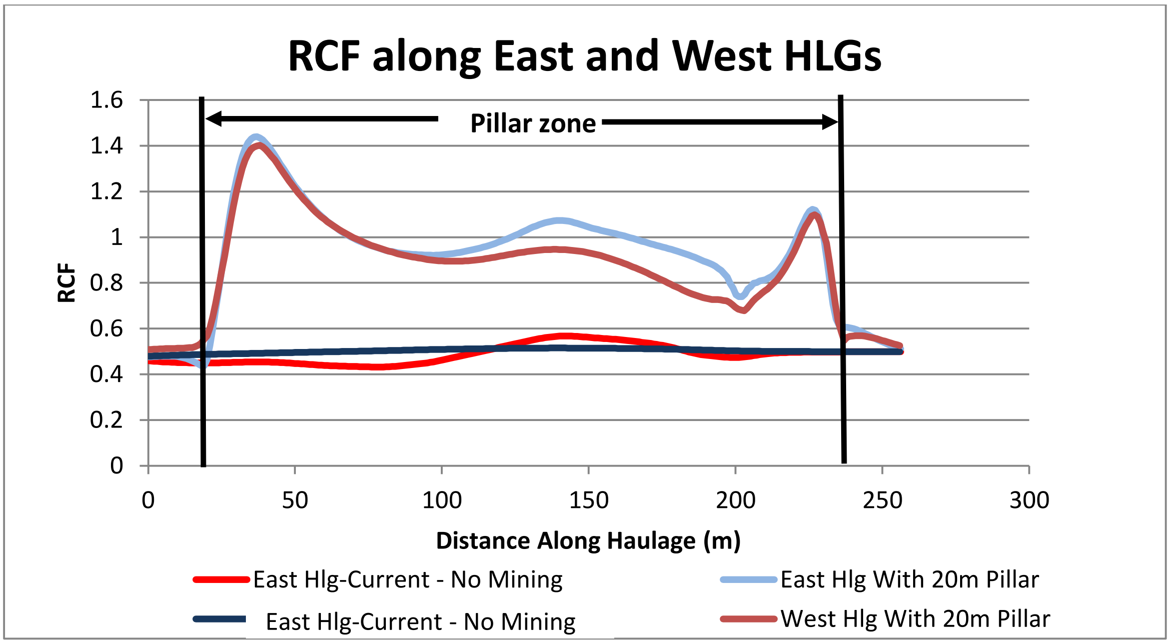

Figure 6.20: RCF values along the 19 level east and west haulages. Current values before mining are also illustrated as well as the position of the pillars

6.7.3 Conclusions

Based on the modelling results it is possible to leave a stability pillar above the haulages at 16 and 19 level to avoid panels from mining into the haulages. Secondary support must be installed along the haulages below the pillar to support them due to fractures that may develop as the result of induced stresses fracturing the edge of the pillar. Monitoring will be conducted in the haulages when mining commences so as to validate the modelling results and re-evaluate the support strategy where necessary.

CHAPTER 7: CONCLUSIONS AND RECOMMENDATIONS

A mine can be profitable while maintaining the stability of its workings. However, this can only be achieved with a well-planned and executed design. The principles and methodologies of design have to be followed and implemented for the pillar design to achieve the degree of stability required for that particular mine. If this is done, the mine can achieve its mining targets without the uncertainty of excavation failure. The major objective of this project was to design a section of the mine that could be profitable whilst maintaining the stability of all the excavations associated with it. Regional pillar design was the major parameter in ensuring that the KORP section is both stable and profitable.

In order to design a stable and profitable mine a number of empirical and numerical equations and tools had to be used and from using these equations and tools, the following conclusions were drawn:

- There are numerous geological and geotechnical variables in the Rustenburg region, even within Khuseleka mine. Khuseleka is mining both the UG2 and the MR and wide variations in the two reef zones can be noted both from a geological and geotechnical perspective. It is therefore very important to identify and quantify these differences so that a different strategy on regional pillar design can be implemented for both Merensky and UG2 reef. The MR has been mining at depths at which the UG2 reef horizon is now being planned to mine but the regional pillar layout of Merensky could not be taken as it is and used on the UG2 as the geological and geotechnical properties of both reefs are different. These differences had to be quantified so that the UG2 regional pillars could be specifically designed.
- Rock mass characterisation plays a very important role in pillar design. All the input parameters whether for empirical or numerical analyses are based on accurate rock mass characterisation. Therefore, before pillars can be designed it is important to have a formal and detailed rock mass characterisation program in place on the mine. Personnel involved in any geotechnical aspects on the mine must be made aware of the importance of capturing or gathering information as accurately as possible. A system must be put in place to ensure that all the required information for any design or decision is captured and human error is eliminated as much as possible.
- Laboratory tests had to be conducted in order to have the elastic properties of the rocks used for pillar design available. Stress measurements were required to determine the in-situ stress states where the excavations had to be made. Since other operations with similar geotechnical conditions to those at Khuseleka shaft had carried out laboratory tests and in-situ stress measurements, the results of these were made available and used on this project.

Because one cannot conduct all the tests required due to various reasons, there is scope to have a database available for specific geographical regions where all the information for all the tests is captured and stored. Most if not all the mining companies can agree on a system where geotechnical results for any test done by any company can be stored and accessed by those requiring the information. What this means is that a system will have to be agreed upon on how to store and present the information. A minimum set of guidelines and standards must be set on how the information is collected, tested and interpreted to make it as accurate as possible. The presence of such a database will make it easier for engineers to have a reliable and accurate source of data which they can get compare and use for design purposes. This will mean that more accurate designs can be made knowing that data is readily available.

- All the empirical equations for pillar design have limitations and an empirical range for which they are best suited. Each equation was formulated based on a set of conditions and particular situation, therefore for it to be used, the conditions must be similar to the ones under which it was formulated. Even then, the variability in geological and geotechnical conditions the equations will never be suitable for all situations. The challenge is to identify which equation best suits the particular circumstances that are present.
- The huge discrepancies in the results using the different pillar strength and pillar load equations indicate that one cannot rely only on empirical equations for design. Other tools must be used to aid in the design. Numerical modelling is an analysis tool that can be used to aid in design.
- Numerical modelling has the advantage over empirical equations in that it takes the whole geometry of the layout and the effects of other excavations into account when making an analysis. It is also easier to analyse pillars with irregular geometries or orientations than it is with empirical equations. The empirical equations only analyse for a regularly shaped pillar and cannot accurately analyse for irregularly shaped or oriented pillars and geometries. This gives more confidence in the values obtained through numerical analysis. The user should however be aware of the limitations available of the numerical modelling program chosen. The difference between a 2D and 3D program needs to be understood and the limitations possessed by each one known. This will help to understand and put into context any results that are obtained through numerical modelling. The results obtained through numerical analysis were found to be more valid and sound.
- Using engineering judgement it was decided to design the pillars using the final values of Map3D analysis in section 6.5.2.

- It should be kept in mind that analysis is just one aspect of the whole design process. Having obtained design values through empirical or numerical analysis, it is easy to think that the design process is complete. A review of the design is also very critical. This is whereby one measures the outcome of the design through observation and measurement. In other words monitoring is as equally important as the analysis process. Monitoring allows one to validate assumptions and input parameters used. If the behaviour of the excavation is not according to the predicted behaviour then the assumptions or input parameters will have to be changed or adjusted. This way there will be an improvement in the overall design and also allow for more accurate designs in the future.
- It can be concluded that with the information and tools available, the objectives set out for the project, that of a stable KORP section, were fulfilled using sound engineering design principles and methods.

The recommendation that can be given is that since all the empirical equations that were used are derived from a narrow empirical range of values, and under conditions not similar to the UG2 conditions, an empirical equation specific to UG2 will have to be formulated. This means an exercise to back analyse and gather as much information as possible on all failed pillars on the UG2 horizon will have to be undertaken. A database will have to be created with information on the pillar dimensions, type of excavations, the mining depths and the geotechnical and geological parameters of all failed pillars. With enough information an empirical formulae specific to UG2 can be developed making it easier for pillar design on the UG2 reef horizon. With the cost of advanced numerical programs prohibitively high, an empirical equation specific to the UG2 will go a long way in helping with the design of pillars for the UG2 reef horizon. Even if an advanced numerical modelling program is available for use, a more UG2 specific equation can be used to validate results obtained through numerical modelling.

REFERENCES

Barton, N., (2002). Some new Q-value correlations to assist in site characterisation and tunnel design. *International Journal of Rock Mechanics & Mining Sciences*, vol. 39, no. 2, pp. 185 - 216.

Barton, N., Lien, R. & Lunde, J., (1974). Engineering Classification of Rock Masses for the Design of Tunnel Support. *Rock Mechanics*, vol. 6, no. 4, pp. 189 - 236.

Bieniawski, Z., (1989). *Engineering Rockmass Classification.* New York: Wiley Interscience.

Bieniawski, Z.T. (1992). Invited paper: Principles of engineering design for rock mechanics, Rock Mechanics, Proc. 33rd U S Symp. on Rock Mech., Tillerson and Wawersik (eds.), Balkema, pp. 1031 – 1040.

BIENIAWSKI, Z.T. (1993). Principles and methodology of design for excavations in geologic media, Research in Engineering Design, vol. 5, pp. 49 – 58.

Brady, B. & Brown, E., 2005. *Rock Mechanics for Underground Mining.* 3rd ed. New York: Kluwer Academic Publishers.

Broch, A. & Palmstrom, E., (2006). Use and misuse of rock mass classification systems with particular reference to the Q system. *Tunneling and Underground Space Technology*, 6 November, pp. 575 - 593.

Budavari, S., (1983). *Rock Mechanics in Mining Practice.* Johannesburg: SAIMM.

Clark, R., (2016). *Assessment of the Business Plan Pillar Layout at Thembelani Platinum Mine, South Africa*, Rustenburg: Institute of Mine Seismology.

Coates, D., (1981). *Rock Mechanics Principles.* 4th ed. Ottawa: CANMET, Department of Energy, Mines and Resources Canada.

COMRO, (1988). *Industry Guide to Methods of Ameliorating the Hazards of Rockfalls and Rockbursts.* Johannesburg: Chamber of Mines.

Goodman, R., (1989). *Introduction to Rock Mechanics.* 2nd Edition ed. New York: John Riley and Sons.

Hansen, J., (1970). A Revised and Extended Formula for Bearing Capacity. *Bulletin of of the Danish Geotechnical Institute*, vol. 28, pp. 5 - 11.

Hedley, D. & Grant, F., (1972). Stope-and-pillar design for Elliot Lake Uranium Mines. *The Bulletin of the Canadian Institute of Mining and Metallurgy*, vol. 65, pp. 37 - 44.

Hoek, E., Carranza-Torres, C. & Corkum, B., (2002). Hoek-Brown failure criterion-2002 edition. *Proceedings of the 5th North American Rock Mechanics Symposium*, pp. 267 - 273.

Hoek, E., Kaiser, P. & Bawden, W., (1997). *Support of Underground excavations In Hard Rock.* 2nd ed. Rotterdam: A.A. Balkema.

Hoek, E. & Martin, C., (2014). Fracture initiation and propagation in intact rock - A review. *Journal of Rock Mechanics and Geotechnical Engineering,* vol. 6, no. 4, pp. 287 - 300.

Jaeger, J. & Cook, N., (1979). *Fundamentals of Rock Mechanics.* 3rd ed. London: Chapman and Hall.

Jager, A. & Ryder, J., (1999). *a handbook on Rock Engineering Practice for tabular hardrock mines.* Johannesburg: SIMRAC.

Krauland, N. & Soder, P., (1987). Determining pillar strength from pillar failure observation. *Engineering & Mining Journal,* vol. 8, pp. 34 - 40.

Kuca, J., (2013). *Group Procedure: Crosscut, raise development and ledging,* Johannesburg: Anglo American Platinum.

Langwieder, G., (2007). *STRUCTURAL GEOLOGY REPORT - Townlands Ore Replacement Project-Feasibility Study (CBE),* Johannesburg: Anglo Platinum.

Laubscher, D., (1990). A geomechanics classification system for the rating of rock mass in mine design. *South African Institute of Mining and Metallurgy,* vol. 90, no. 10, pp. 257 - 273.

Le Bron, K., (2006). *Townlands Ore Replacement Project Feasibility Study Geotechnical,* Rustenburg: Anglo Platinum.

Lunder, P. & Pakalnis, R., (1997). Determination of the strength of hard-rock mine pillars.. *Bulletin of the Canadian Institute of Mining and Metallurgy,* vol. 90, no. 1013, pp. 51 – 55.

Martin, C. & Maybee, W., (2000). The strength of hard rock pillars. *International Journal of Rock Mechanics and Mining Science,* vol. 37, no. 4, pp. 1239 – 1246.

Middindi, C., (2013). *Learning Guide for Part 2: Basic Rock Mechanics Practice.* Johannesburg: South African Institute of Rock Engineering.

MineModelling, P., (2013). *Map3D Users Manual.* Victoria, Australia: Mine Modelling Pty Ltd.

Mutsvanga C, (2016). *Geological Drilling Layout for Borehole CTM03 - Internal Report,* Rustenburg: Anglo Platinum.

Mutsvanga, C., (2017). *2017 - Geothechnical best cut for Khuseleka Shaft -Internal Report,* Rustenburg: Anglo Platinum.

NIOSH, (2017). *NIOSH Mining Software.* [Online]
Available at: http://www.cdc.gov/niosh/mining/products/product54.htm.
[Accessed 7 June 2017].

Ozbay, M. & Roberts, M., (1988). *Yield pillars in stope support.* Swaziland, SANGORM.

Pells, P. & Bertuzzi, R., (2006). Discussion on article titled "Use and misuse of rock mass classification systems with reference to the Q-system" by Palmstrom and Broch. *Tunnelling and Underground Space Technology,* vol. 21, pp. 575 - 593.

Potvin, Y., Hudyma, M. & Miller, H., (1989). Design guidelines for open stope support. *The Bulletin of Canadian Mining and Metallurgy,* vol. 82, pp. 53 - 62.

Priest G, (2013). *Regional Support,* Johannesburg: Anglo American Platinum.

Roberts, D. P., Van der Merwe, J. N., Canbulat, I. & Sellers, E. J. a. C. S., (2002) *Development of a method to estimate coal pillar loading,* Johannesburg: SIMRAC, CSIR Miningtek.

Rocscience, (2012). *Rocscience.* [Online]
Available at:
www.rocscience.com/help/examine2d/webhelp/examine2d/Examine2D_Tutorials.htm
[Accessed 11 November 2016].

Rocscience, (2016). *RocScience.* [Online]
Available at: https://www.rocscience.com/documents/pdfs/uploads/8079.pdf
[Accessed 20 September 2016].

Ryder, J. A. & Jager, A., (2002). *A Text Book on Rock Mechanics for Tabular Hard Rock Mines.* 1st ed. Johannesburg: SIMRAC.

Ryder, J. & Ozbay, M., (1990). *A methodology for designing pillar layouts for shallow mining.* Swaziland, ISRM, pp. 273 - 286.

Salamon, M. & Munro, A., (1967). A study of the strength of Coal Pillars. *Journal of the South African Institute of Mining and Metallurgy,* vol. 68, no. 2, pp. 55 - 67.

Sjoberg, J., (1992). *Failure modes and pillar behaviour in the Zinkgruvan Mine. Rock Mechanics,* Rotterdam: Balkemia.

Snyman, (2015). *Thembelani Mine Rock Engineering Technical Support Document BP2015,* Rustenburg: Anglo American Platinum.

Stacey, T., (2001). *Best practice rock engineering handbook for "other" mines.* First ed. Johannesburg: SIMRAC.

Stacey, T., (2003). Presidential Address: Rock engineering-good design or good judgement?. *The Journal of The South African Insitute of Mining and Metallurgy,* vol. 112, no. 7, pp. 411 - 421.

Stacey, T., (2014). Numerical Modelling Techniques in Rock Engineering. In: Johannesburg: Wits University.

Stacey, T. & Page, C., (1986). Practical Handbook for Underground Rock Mechanics. In: *Series on Rock and Soil Mechanics.*:Transtech Publications, pp. 53 - 63.

Stacey, T. & Wesselo, J., (1998). *Evaluation and Upgrade of Records of Stress Measurement Data in the Mining Industry - GAP 511*, Johannesburg: SIMRAC.

Starfield, A. & Bleloch, A., (1986). *Builiding Models for Conservation and Wildlife Management.* 1st ed. New York: Macmillan.

Swart, A. & Handley, M., (2005). The design of stable stope spans for shallow mining operations. *The Journal of The South African Institute of Mining and Metallurgy,* vol. 105, no. 4, pp. 275 - 286.

Terzaghi, K., (1943). *Theoretical Soil Mechanics.* New York: John Wiley.

Ulusay, R. & Hudson, J., (2007). *The Complete ISRM Suggested Methods for Rock Characterisation, Testing and Monitoring: 1974-2006.* 1st ed. Ankara: ISRM Turkish National Group.

Van Aswegen, G., Clark, R. & Hobson, S., (2014). *A-PLLR: Pillar stability in the RPM mines,* Rustenburg: Institute of Mine Seismology.

van der Heever, P. & Piper, P., (2013). *In-situ Stress Measurements on 34 Level, Siphumelele Shaft, Rustenburg Section,* Johannesburg: Groundwork.

Van der Merwe, N., (1998). *Practical Coal Mining Strata Control.* 2nd ed. Johannesburg: Itasca Africa.

Von Kimmelmann, M., Hyde, B. & Madgwick, R., (1984). *The use of computer applications at BCL in planning pillar extraction and design of mining layouts. Design and performance of underground excavations.* Cambridge, ISRM/BGS, pp. 53 - 63.

Wagner, H., 1980. Pillar design in coal mines. *Journal of South African Institute of Mining and Metallurgy,* vol. 68, no. 81, pp. 37 - 45.

Watson, B.P., Ryder, J.A., Kataka, M.O., Kuijpers, J.S., Leteane, F.P., (2008). Merensky pillar strength formulae based on back-analysis of pillar failures at Impala Platinum. *Journal of South African Institute of Mining and Metallurgy,* vol. 108, no. 8, pp. 449 - 461.

Wiles, T., (2013). *Map3D User's Manual.* Melbourne: Mine Modelling Pty Ltd.

York, G., Canbulat, I., Kabeya, K. & LeBron, K., (1998). *Develop guidelines for the design of pillar systems for shallow and intermediate depth, tabular, hard rock mines and provide a methodology for assessing hangingwall stability and support requirements for the panels between pillars,* Johannesburg: SIMRAC.

APPENDICES

Appendix A: Raiseline Middling Distances in KORP Section

16 LEVEL WEST			
RSE LINE	**HLGE**	**MIDDLING**	**COMMENT**
16 27 RSE	16 Hlge West	38.5	Above Reef
16 28 RSE		33.6	Above Reef
16 29 RSE		31.5	Above Reef
16 30 RSE		32.1	Above Reef
16 31 RSE		32.1	Above Reef
16 32 RSE		32.5	Above Reef
16 33 RSE		31.7	Above Reef
16 34 RSE		35.1	Above Reef
16 35 RSE		35.2	Above Reef
16 LEVEL EAST			
RSE LINE	**HLGE**	**MIDDLING**	**COMMENT**
16 26 RSE	16 Hlge East	35.5	Above Reef
16 25 RSE		31.8	Above Reef
16 24 RSE		34.5	Above Reef
16 23 RSE		30.8	Above Reef
16 22 RSE		35.2	Above Reef
19 LEVEL WEST			
RSE LINE	**HLGE**	**MIDDLING**	**COMMENT**
19 28 RSE	19 Hlge West	30.3	Below Reef
19 29 RSE		31.7	Below Reef
19 30 RSE		32.7	Below Reef
19 32 RSE		32.5	Below Reef
19 33 RSE		32.2	Below Reef
19 34 RSE		35.1	Below Reef
19 35 RSE		34.6	Below Reef
19 36 RSE		32.2	Below Reef

19 LEVEL EAST			
RSE LINE	**HLGE**	**MIDDLING**	**COMMENT**
19 27 Rse	19 Hlge East	25.7	Below Reef
19 26 Rse		29.8	Below Reef
19 25 Rse		30.2	Below Reef
19 24 Rse		37.1	Below Reef
19 23 Rse		33.5	Below Reef
19 22 Rse		30.5	Below Reef
19 21 Rse		30.6	Below Reef
19 20 Rse		32.8	Below Reef
21 LEVEL WEST			
RSE LINE	**HLGE**	**MIDDLING**	**COMMENT**
21 27 RSE	21 Hlge West	24.4	Below Reef
21 28 RSE		19.1	Below Reef
21 29 RSE		30.9	Below Reef
21 30 RSE		29.8	Below Reef
21 31 RSE		28.2	Below Reef
21 32 RSE		30.2	Below Reef
21 33 RSE		31.6	Below Reef
21 34 RSE		32.6	Below Reef
21 35 RSE		35.4	Below Reef
21 LEVEL EAST			
RSE LINE	HLGE	MIDDLING	COMMENT
21 26 RSE	21 Hlge East	25.0	Below Reef
21 25 RSE		35.4	Below Reef
21 24 RSE		31.5	Below Reef
21 23 RSE		31.1	Below Reef
21 22 RSE		29.8	Below Reef
23 LEVEL WEST			
RSE LINE	**HLGE**	**MIDDLING**	**COMMENT**
23 27 RSE	23 Hlge West	30.2	Below Reef
23 28 RSE		25.2	Below Reef
23 29 RSE		31.9	Below Reef
23 30 RSE		34.7	Below Reef
23 31 RSE		35.7	Below Reef

23 32 RSE		33.2	Below Reef
23 33 RSE		25.3	Below Reef
23 34 RSE		27.9	Below Reef
23 35 RSE		35.3	Below Reef
23 LEVEL EAST			
RSE LINE	HLGE	MIDDLING	COMMENT
23 26 RSE	23 Hlge East	29.4	Below Reef
23 25 RSE		32.6	Below Reef
23 24 RSE		33.2	Below Reef
23 23 RSE		31.7	Below Reef
23 22 RSE		26.7	Below Reef
25 LEVEL WEST			
RSE LINE	**HLGE**	**MIDDLING**	**COMMENT**
25 27 RSE	25 Hlge West	30.5	Below Reef
25 28 RSE		33.9	Below Reef
25 29 RSE		34.4	Below Reef
25 30 RSE		34.5	Below Reef
25 31 RSE		37.6	Below Reef
25 32 RSE		35.0	Below Reef
25 33 RSE		34.3	Below Reef
25 34 RSE		32.6	Below Reef
25 LEVEL EAST			
RSE LINE	HLGE	MIDDLING	COMMENT
25 26 RSE	25 Hlge East	30.6	Below Reef
25 25 RSE		30.8	Below Reef
25 24 RSE		31.2	Below Reef
25 23 RSE		29.8	Below Reef
25 22 RSE		32.9	Below Reef
26 LEVEL WEST			
RSE LINE	**HLGE**	**MIDDLING**	**COMMENT**
26 27 RSE	26 Hlge West	30.9	Below Reef
26 28 RSE		37.4	Below Reef
26 29 RSE		34.6	Below Reef
26 30 RSE		33.2	Below Reef
26 31 RSE		34.4	Below Reef

26 32 RSE		32.1	Below Reef
26 33 RSE		29.4	Below Reef
26 34 RSE		31.8	Below Reef
26 LEVEL EAST			
RSE LINE	HLGE	MIDDLING	COMMENT
26 26 RSE	26 Hlge East	30.6	Below Reef
26 25 RSE		30.3	Below Reef
26 24 RSE		31.3	Below Reef
26 23 RSE		31.6	Below Reef
26 22 RSE		33.6	Below Reef
27 LEVEL WEST			
RSE LINE	**HLGE**	**MIDDLING**	**COMMENT**
27 27 RSE	27 Hlge West	33.5	Below Reef
27 28 RSE		35.4	Below Reef
27 29 RSE		33.6	Below Reef
27 30 RSE		31.8	Below Reef
27 31 RSE		33.3	Below Reef
27 32 RSE		29.4	Below Reef
27 33 RSE		30.6	Below Reef
27 LEVEL EAST			
RSE LINE	HLGE	MIDDLING	COMMENT
27 26 RSE	27 Hlge East	35.8	Below Reef
27 25 RSE		32.4	Below Reef
27 24 RSE		30.9	Below Reef
27 23 RSE		36.1	Below Reef
27 22 RSE		35.9	Below Reef
28 LEVEL WEST			
RSE LINE	**HLGE**	**MIDDLING**	**COMMENT**
28 27 RSE	28 Hlge West	30.2	Below Reef
28 28 RSE		36.8	Below Reef
28 29 RSE		34.7	Below Reef
28 30 RSE		33.3	Below Reef
28 31 RSE		33.2	Below Reef
28 32 RSE		32.6	Below Reef
28 33 RSE		34.4	Below Reef

28 LEVEL EAST			
RSE LINE	HLGE	MIDDLING	COMMENT
28 26 RSE	28 Hlge East	36.6	Below Reef
28 25 RSE		35.9	Below Reef
28 24 RSE		33.5	Below Reef
28 23 RSE		31.4	Below Reef
28 22 RSE		26.8	Below Reef

Appendix B: Elastic Property Graphs for KORP Rock Samples

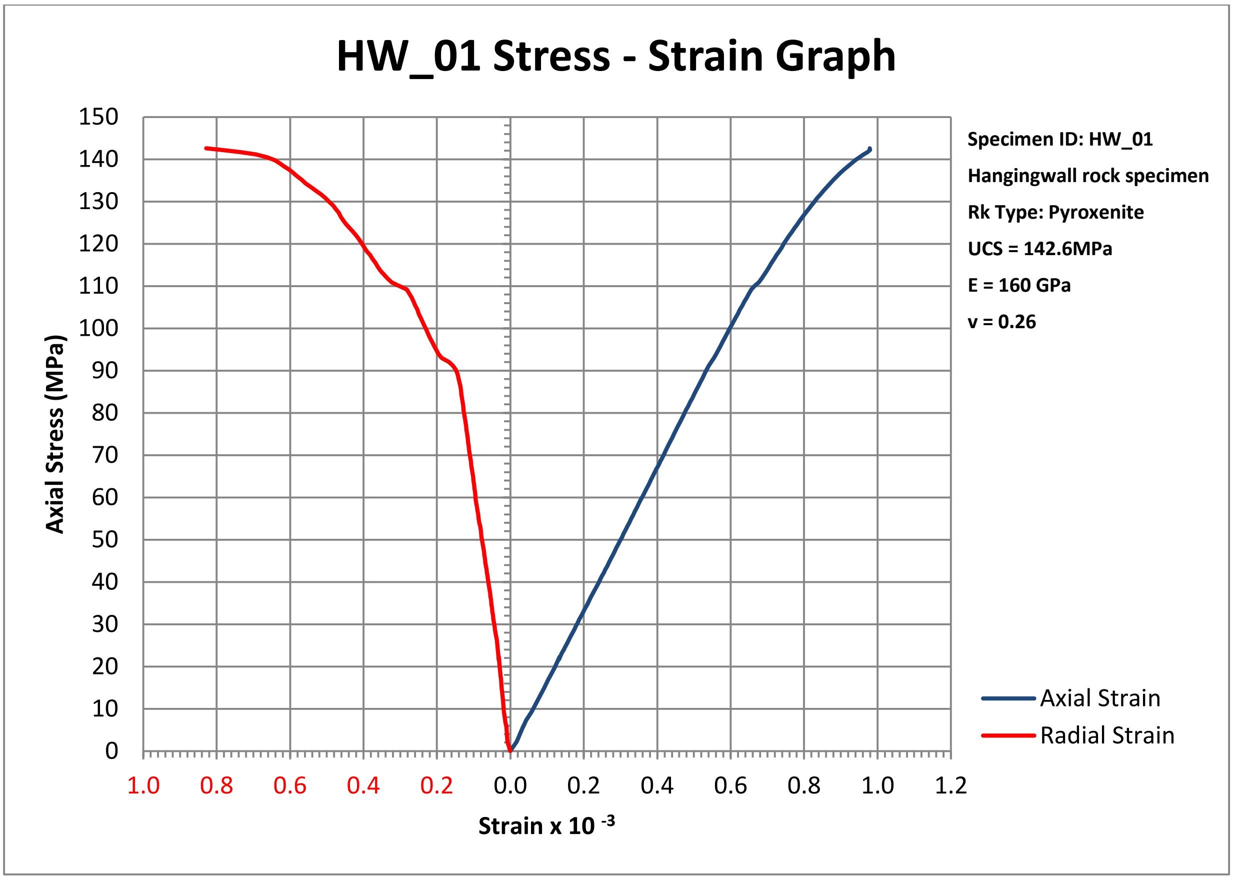

Figure B1: Stress-Strain Graph for Sample HW-01 (Pyroxenite, hangingwall specimen)

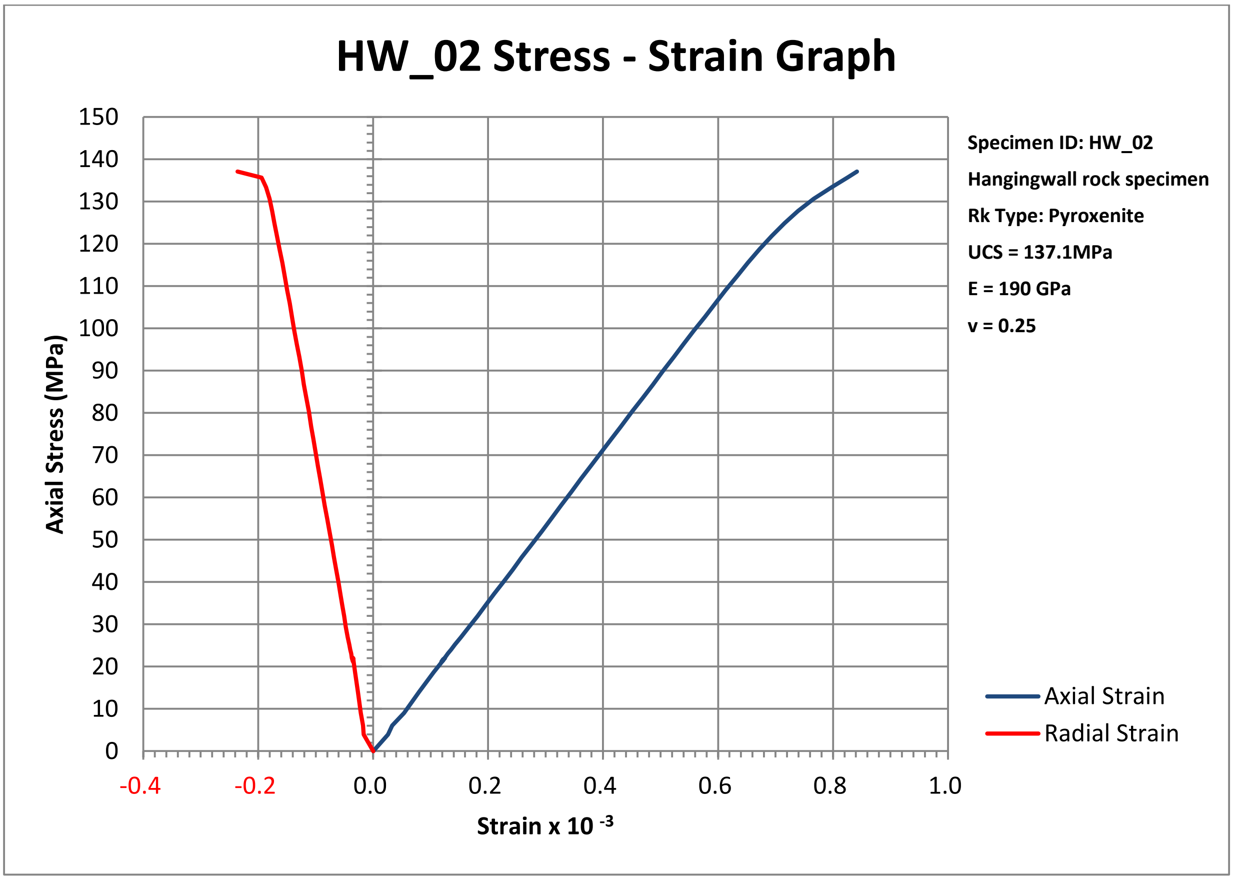

Figure B2: Stress-Strain Graph for Sample HW-02 (Pyroxenite, hangingwall specimen)

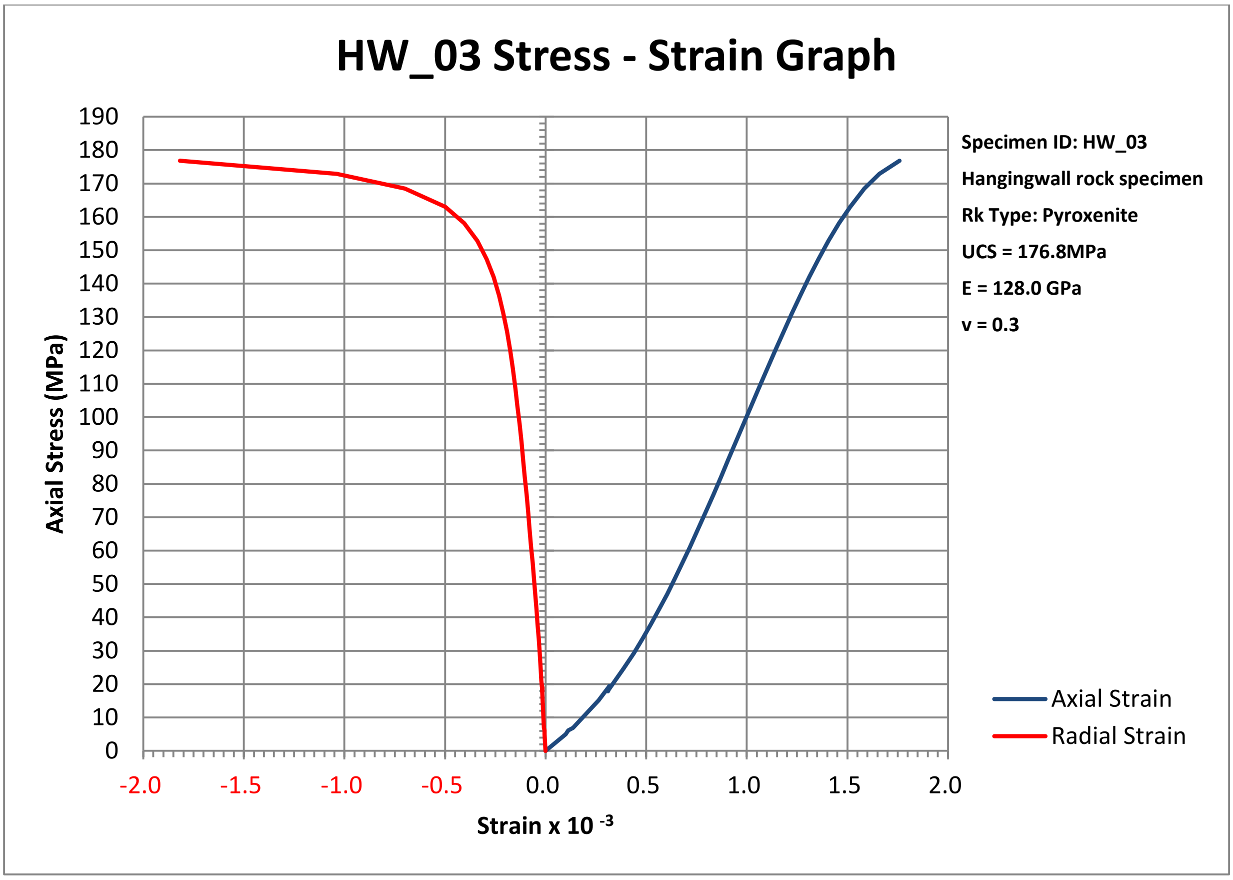

Figure B3: Stress-Strain Graph for Sample HW-03 (Pyroxenite, hangingwall specimen)

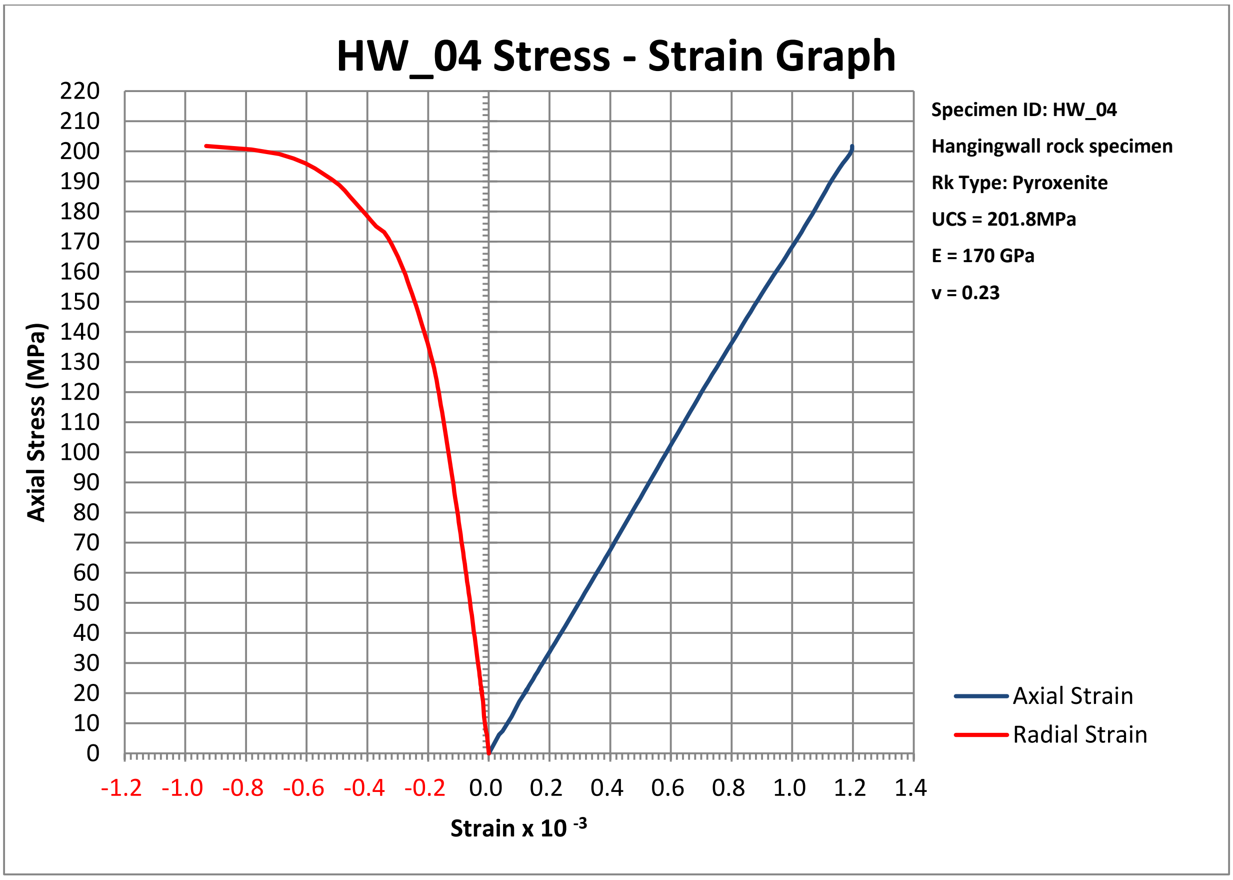

Figure B4: Stress-Strain Graph for Sample HW-04 (Pyroxenite, hangingwall specimen)

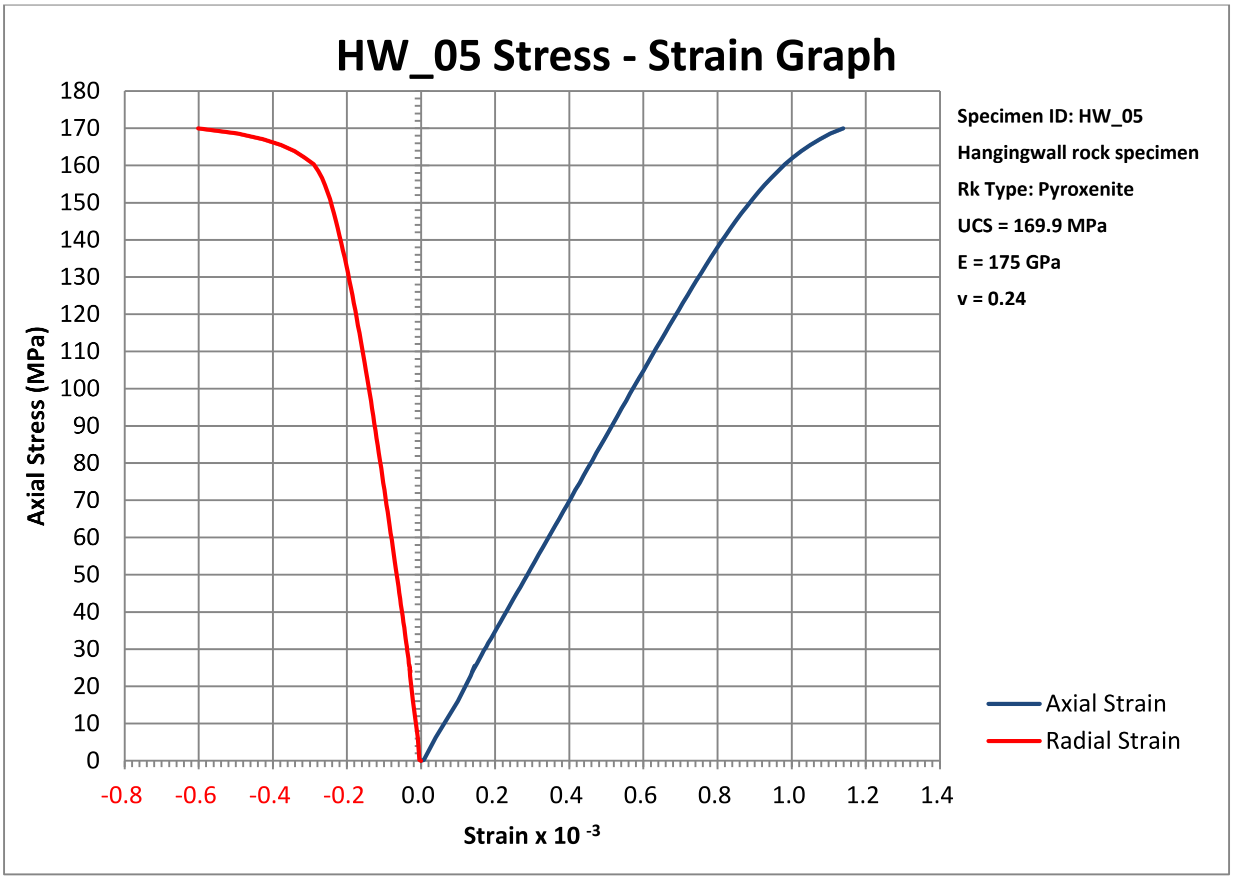

Figure B5: Stress-Strain Graph for Sample HW-05 (Pyroxenite, hangingwall specimen)

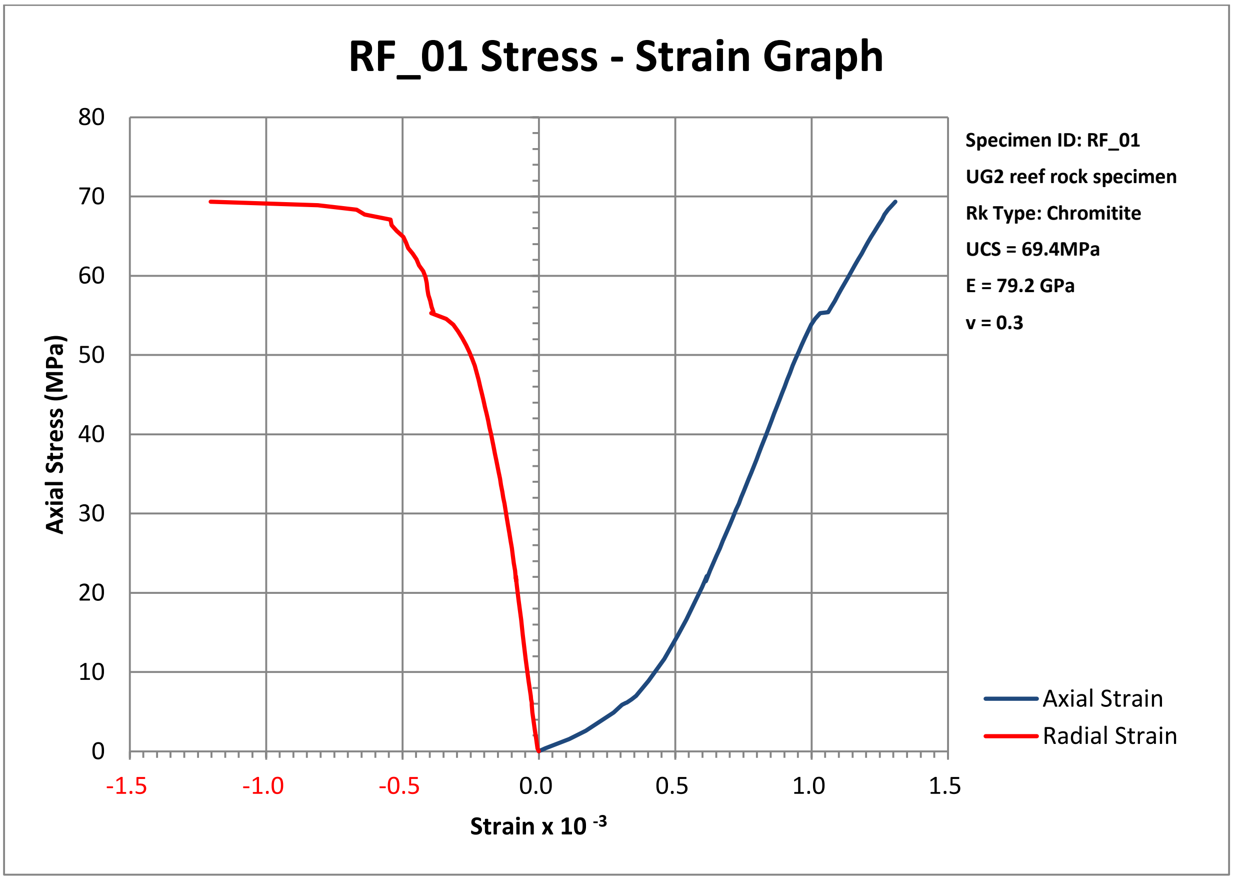

Figure B6: Stress-Strain Graph for Sample RF-01 (Chromitite, UG2 reef specimen)

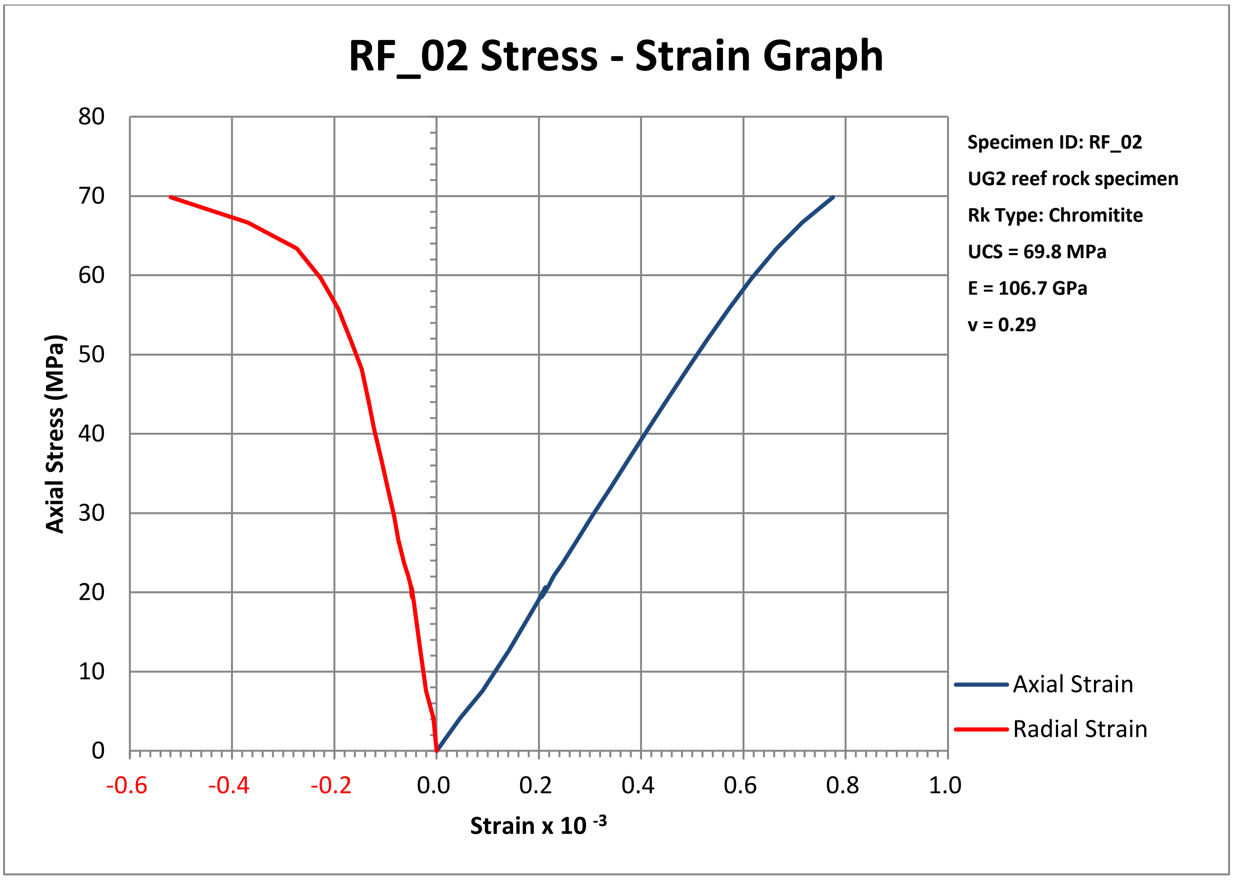

Figure B7: Stress-Strain Graph for Sample RF-02 (Chromitite, UG2 reef specimen)

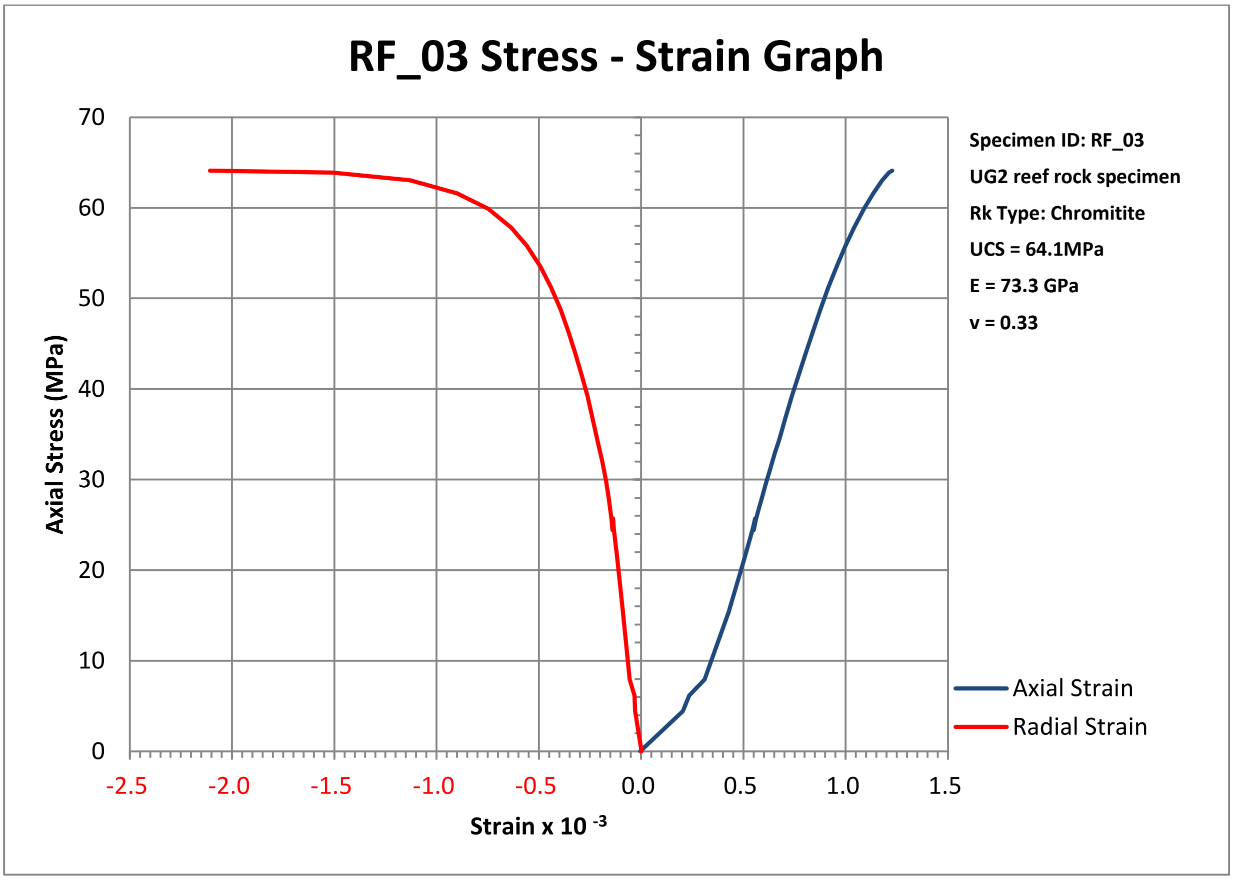

Figure B8: Stress-Strain Graph for Sample RF-03 (Chromitite, UG2 reef specimen)

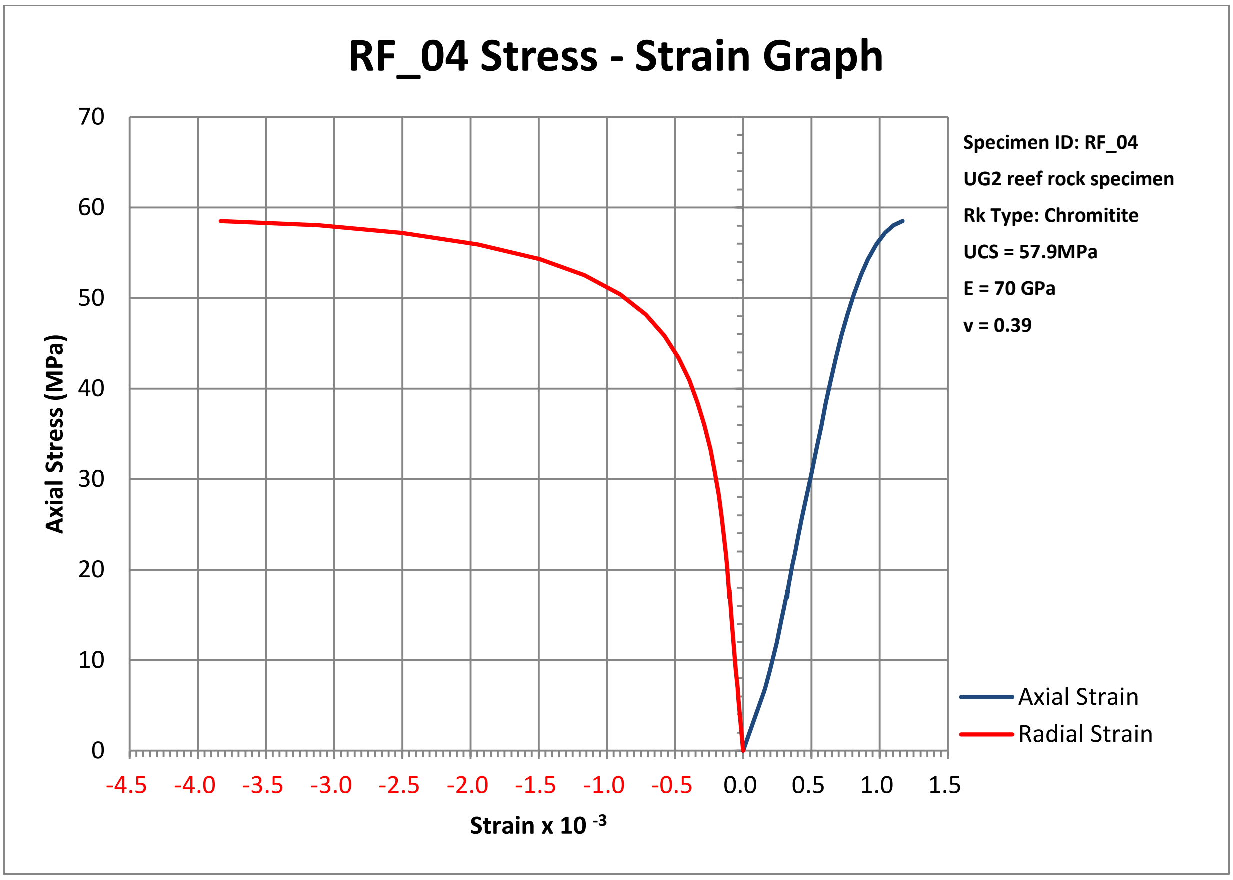

Figure B9: Stress-Strain Graph for Sample RF-04 (Chromitite, UG2 reef specimen)

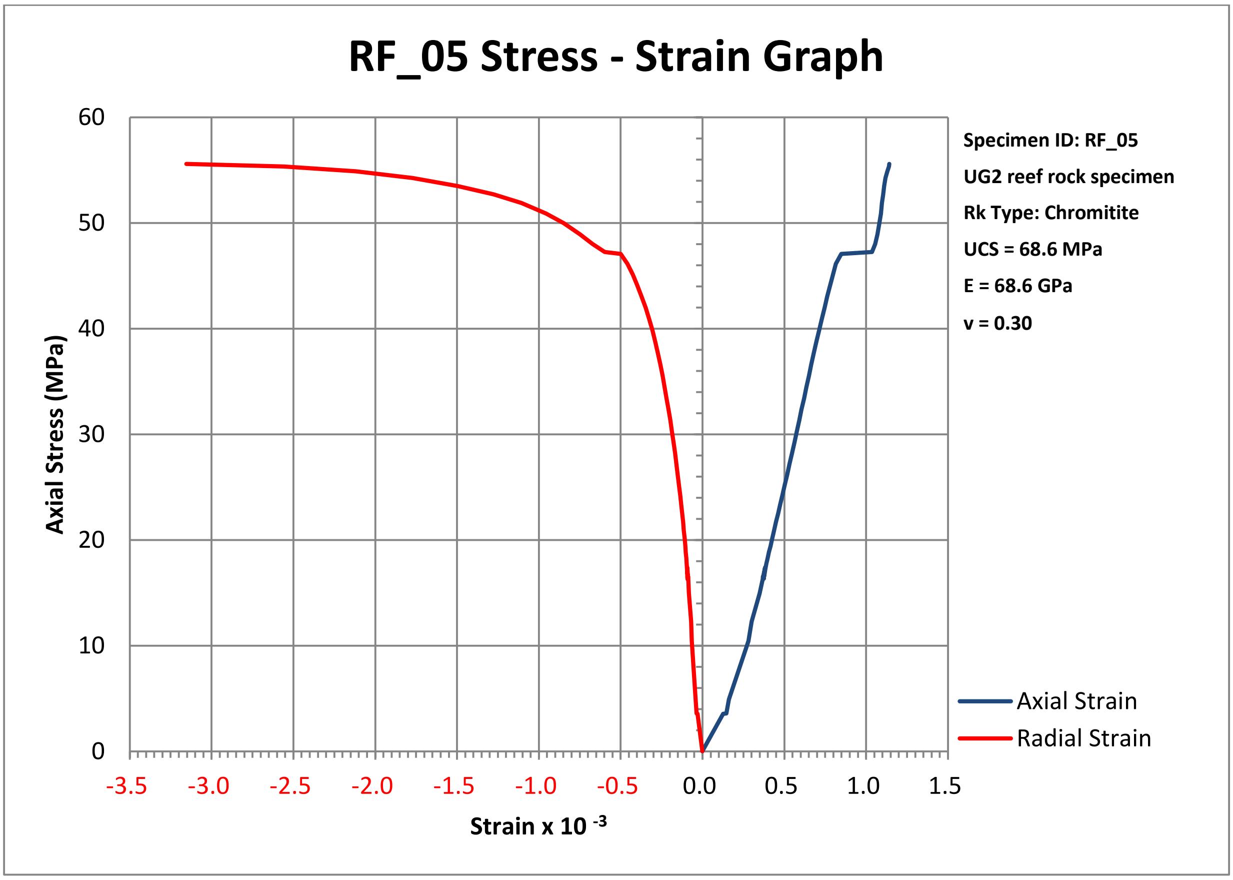

Figure B10: Stress-Strain Graph for Sample RF-05 (Chromitite, UG2 reef specimen)

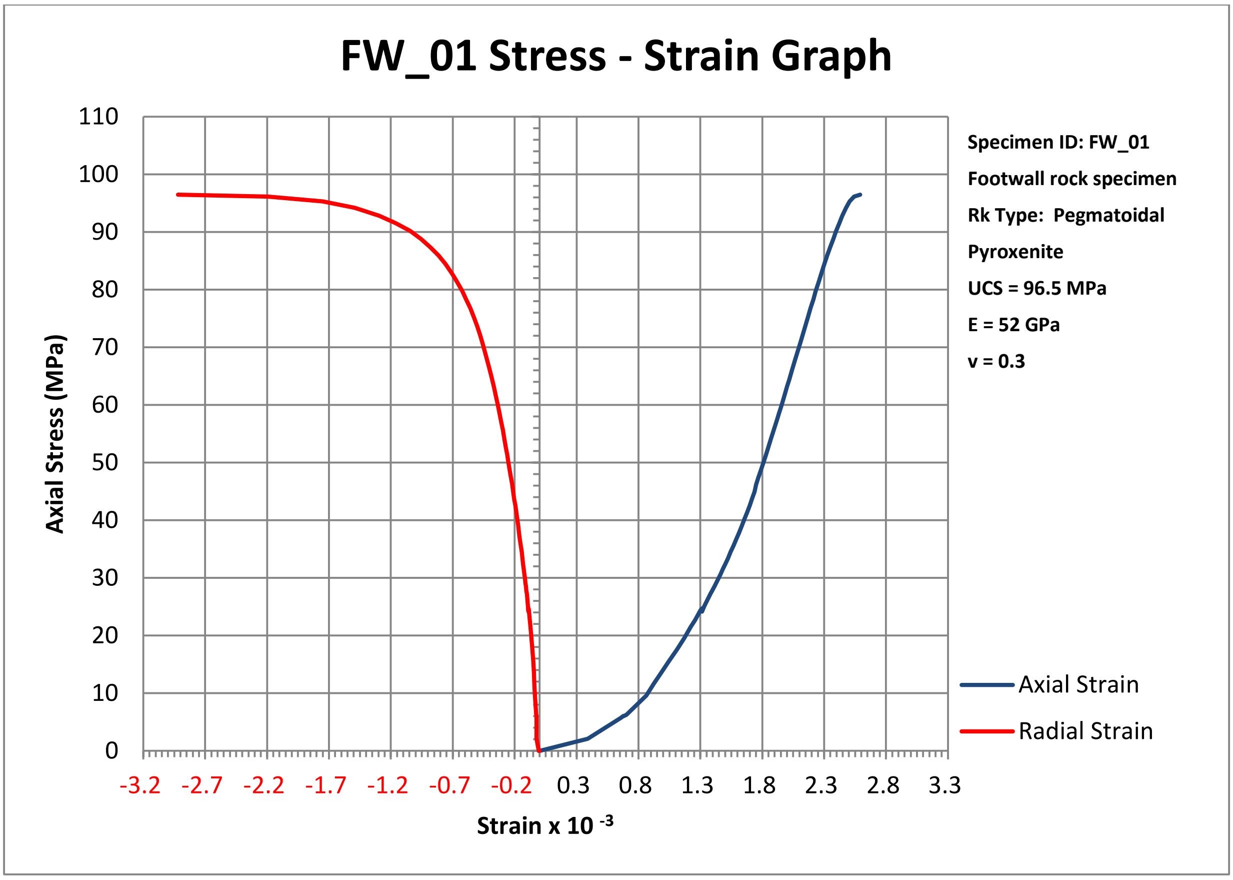

Figure B11: Stress-Strain Graph for Sample FW-01 (Pegmatoidal pyroxenite, footwall specimen)

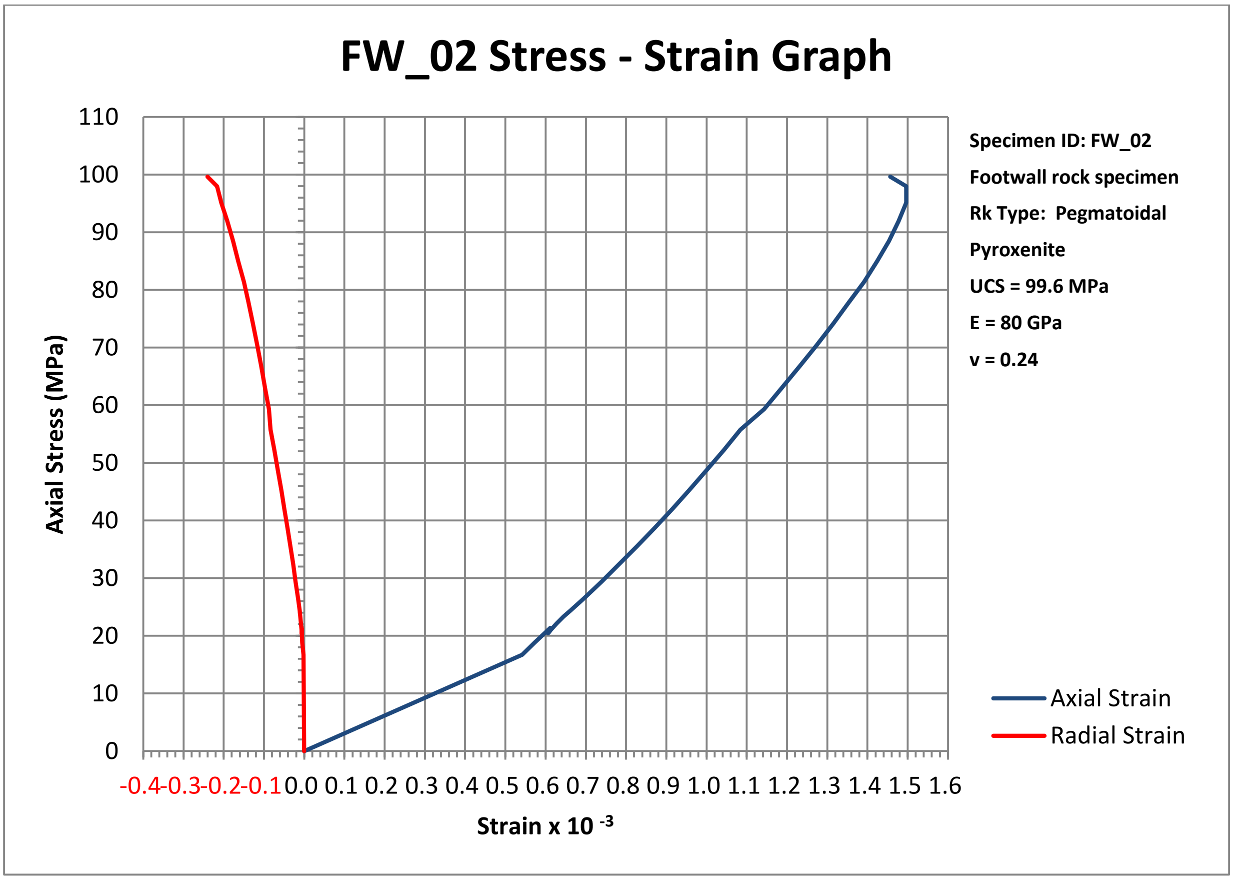

Figure B12: Stress-Strain Graph for Sample FW-02 (Pegmatoidal pyroxenite, footwall specimen)

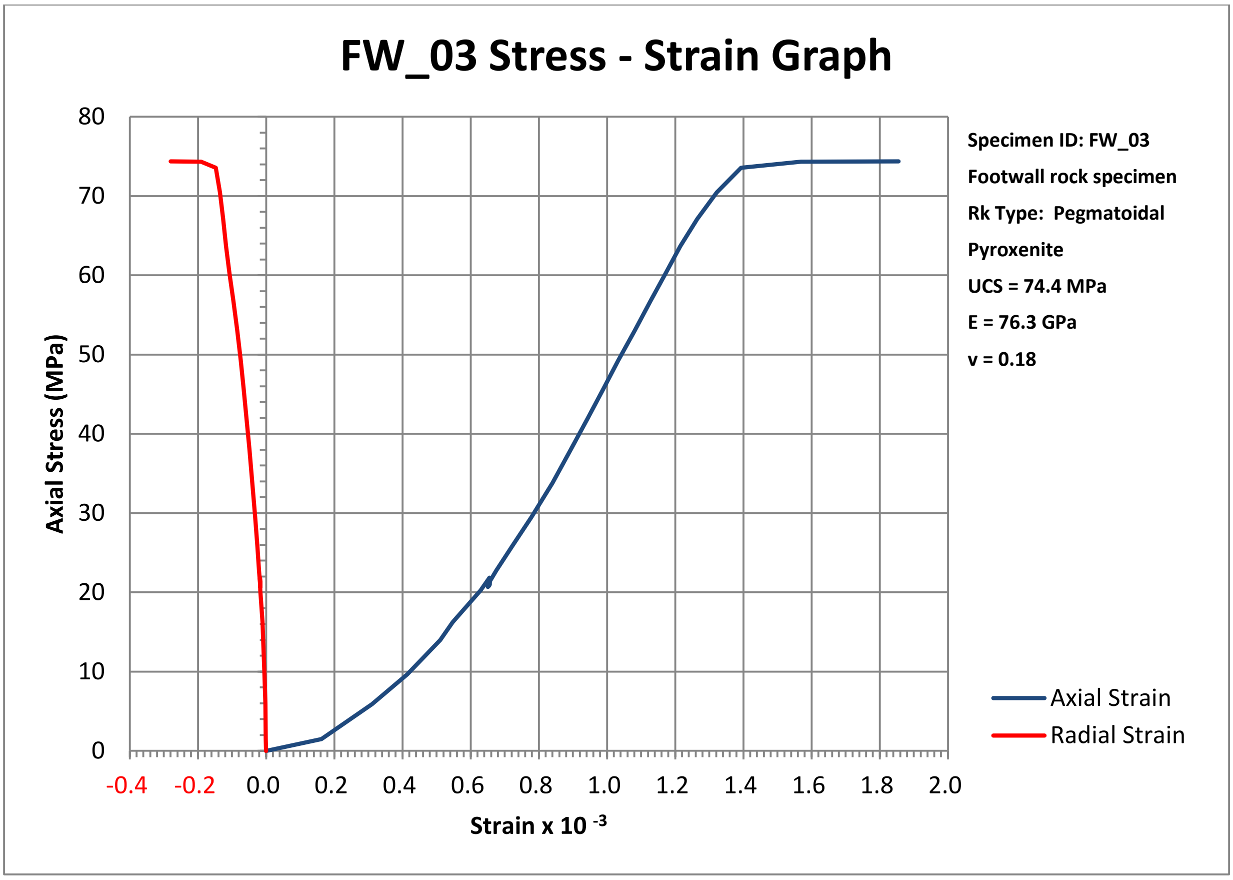

Figure B13: Stress-Strain Graph for Sample FW-03 (Pegmatoidal pyroxenite, footwall specimen)

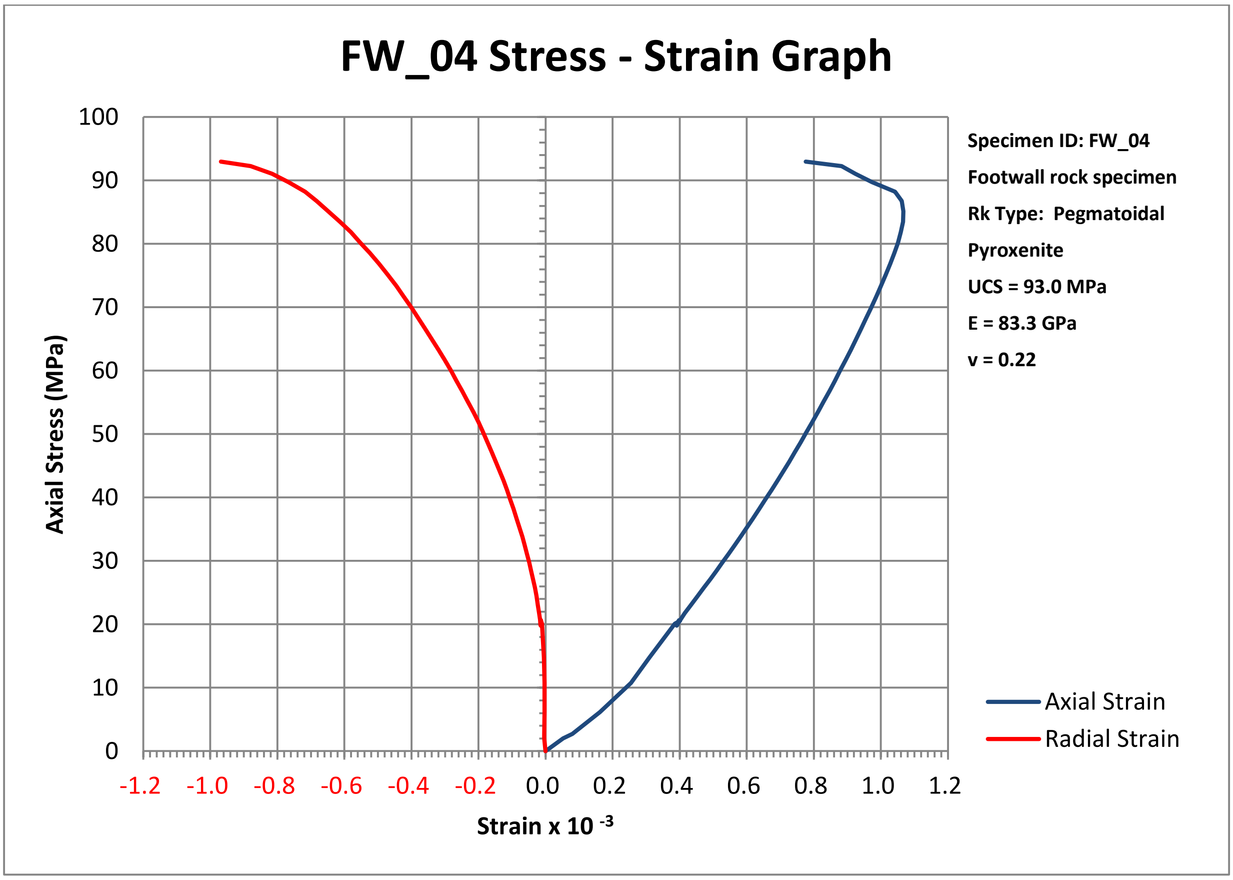

Figure B14: Stress-Strain Graph for Sample FW-04 (Pegmatoidal pyroxenite, footwall specimen)

Appendix C: KORP Stoping Widths from Survey

Workplace	Period	Type	Planned SW (cm)	Actual SW (cm)
TL 21LE 27 PNL001 W U	201206	Ledge	110	115
TL 21LE 27 PNL002 E U	201206	Ledge	110	115
TL 23LE 27 LED013 W U	201206	Ledge	110	115
TL 21LE 27 LED001 E U	201207	Ledge	110	115
TL 21LE 27 LED002 E U	201207	Ledge	110	115
TL 21LE 27 LED002 W U	201207	Ledge	110	115
TL 23LE 27 LED010 W U	201207	Ledge	110	115
TL 23LE 27 LED012 W U	201207	Ledge	110	115
TL 21LE 27 LED002 W U	201208	Ledge	110	122
TL 21LE 27 LED003 W U	201208	Ledge	110	121
TL 23LE 27 LED010 W U	201208	Ledge	110	127
TL 23LE 27 LED003 E U	201209	Ledge	110	115
TL 23LE 27 LED004 E U	201209	Ledge	110	115
TL 23LE 27 LED010 E U	201209	Ledge	110	115
TL 23LE 27 LED010 W U	201209	Ledge	110	115
TL 23LE 27 LED004 W U	201212	Ledge	110	118
TL 23LE 27 LED004 W U	201301	Ledge	110	115
TL 23LE 27 LED005 W U	201301	Ledge	110	115
TL 23LE 27 LED010 E U	201301	Stope	110	115
TL 21LE 27 LED001 E U	201302	Ledge	110	115
TL 21LE 27 LED001 W U	201302	Ledge	110	201
TL 23LE 27 LED005 E U	201302	Ledge	110	112
TL 23LE 27 LED006 E U	201302	Ledge	110	112
TL 23LE 27 LED005 E U	201303	Ledge	110	115
TL 23LE 27 LED006 W U	201303	Ledge	110	116
TL 21LE 27 LED001 E U	201304	Ledge	110	202
TL 21LE 27 LED001 W U	201304	Ledge	110	115
TL 23LE 27 LED007 W U	201304	Ledge	110	105
TL 23LE 27 LED008 E U	201304	Ledge	110	115
TL 21LE 27 LED001 E U	201305	Stope	110	205
TL 21LE 27 LED001 W U	201305	Stope	110	214
TL 23LE 27 LED007 E U	201305	Ledge	110	118

Workplace	Period	Type	Planned SW (cm)	Actual SW (cm)
TL 23LE 27 LED008 E U	201305	Stope	110	218
TL 21LE 27 LED001 E U	201306	Stope	110	215
TL 21LE 27 LED001 W U	201306	Stope	110	214
TL 21LE 27 LED001 E U	201307	Ledge	110	117
TL 21LE 27 LED001 W U	201307	Ledge	110	113
TL 21LE 27 LED001 E U	201308	Ledge	110	124
TL 21LE 27 LED001 W U	201308	Ledge	110	112
TL 23LE 27 LED008 W U	201308	Ledge	110	118
TL 23LE 27 LED009 W U	201308	Ledge	110	117
TL 21LE 27 LED001 E U	201309	Ledge	110	115
TL 21LE 27 LED001 W U	201309	Ledge	110	113
TL 23LE 27 LED009 E U	201309	Ledge	110	115
TL 23LE 27 LED009 W U	201309	Ledge	110	111
TL 23LE 27 LED011 E U	201309	Ledge	110	114
TL 21LW 27 LED001 E U	201310	Ledge	118	118
TL 21LW 27 LED001 W U	201310	Ledge	110	120
TL 21LW 27 LED002 E U	201310	Ledge	110	108
TL 23LW 27 LED009 W U	201310	Ledge	110	111
TL 23LW 27 LED011 E U	201310	Ledge	110	112
TL 23LW 27 LED011 W U	201310	Ledge	110	116
TL 21LW 27 LED001 E U	201311	Ledge	110	113
TL 21LW 27 LED001 W U	201311	Ledge	110	110
TL 21LW 27 LED003 E U	201311	Stope	110	224
TL 21LW 27 LED003 W U	201311	Ledge	110	118
TL 23LW 27 LED010 E U	201311	Stope	110	110
TL 23LW 27 LED011 E U	201311	Stope	110	107
TL 23LW 27 LED011 W U	201311	Ledge	110	110
TL 21LW 27 LED001 E U	201312	Ledge	110	117
TL 21LW 27 LED001 W U	201312	Ledge	110	119
TL 21LW 27 LED003 E U	201312	Ledge	110	128
TL 21LW 27 LED003 W U	201312	Ledge	110	119
TL 23LW 27 LED010 E U	201312	Stope	110	118
TL 23LW 27 LED011 E U	201312	Stope	110	203

Workplace	Period	Type	Planned SW (cm)	Actual SW (cm)
TL 21LW 27 LED001 E U	201401	Ledge	110	124
TL 21LW 27 LED001 W U	201401	Ledge	110	120
TL 21LW 27 LED003 E U	201401	Ledge	110	116
TL 21LW 27 LED003 W U	201401	Ledge	110	112
TL 21LW 27 LED001 E U	201408	Ledge	105	109
TL 21LW 27 LED001 W U	201408	Ledge	105	109
TL 21LW 27 LED003 E U	201408	Ledge	105	109
TL 21LW 27 LED003 W U	201408	Stope	105	208
TL 23LW 27 LED010 E U	201408	Stope	105	104
TL 23LW 27 LED011 E U	201408	Stope	105	108
TL 21LW 27 LED001 E U	201409	Ledge	105	120
TL 21LW 27 LED001 W U	201409	Ledge	105	113
TL 21LW 27 LED003 E U	201409	Ledge	105	112
TL 21LW 27 LED003 W U	201409	Ledge	105	113
TL 21LW 27 LED001 E U	201410	Ledge	105	183
TL 21LW 27 LED001 W U	201410	Ledge	105	111
TL 21LW 27 LED003 E U	201410	Ledge	105	99
TL 21LW 27 LED003 W U	201410	Ledge	105	102
TL 23LW 27 PNL001 W U	201410	Stope	105	109
TL 21LW 27 LED001 E U	201411	Ledge	105	109
TL 21LW 27 LED001 W U	201411	Ledge	105	113
TL 21LW 27 LED003 E U	201411	Ledge	105	103
TL 21LW 27 LED003 W U	201411	Ledge	105	111
TL 21LW 27 LED006 W U	201411	Ledge	105	108
TL 21LW 27 LED011 W U	201411	Ledge	105	108
TL 23LW 27 PNL001 W U	201411	Stope	105	101
TL 21LW 27 LED005 E U	201412	Ledge	105	113
TL 21LW 27 LED006 W U	201412	Ledge	105	112
TL 21LW 27 LED007 E U	201412	Ledge	105	124
TL 21LW 27 LED011 W U	201412	Ledge	105	112
TL 21LW 27 LED012 W U	201412	Ledge	105	113
TL 23LW 27 PNL001 W U	201412	Stope	105	111
TL 23LW 27 PNL002 W U	201412	Stope	105	114

Workplace	Period	Type	Planned SW (cm)	Actual SW (cm)
TL 21LW 27 LED006 E U	201501	Ledge	105	116
TL 21LW 27 LED007 W U	201501	Ledge	105	111
TL 21LW 27 LED011 E U	201501	Ledge	105	110
TL 23LW 27 LED012 E U	201501	Ledge	105	111
TL 21LW 27 LED008 E U	201502	Ledge	105	111
TL 21LW 27 LED008 W U	201502	Ledge	105	113
TL 21LW 27 LED011 E U	201502	Stope	105	122
TL 21LW 27 PNL007 W U	201502	Stope	105	112
TL 23LW 27 LED012 E U	201502	Ledge	105	116
TL 21LW 27 LED011 E U	201503	Stope	105	115
TL 21LW 27 PNL007 W U	201503	Stope	105	116
TL 23LW 27 LED012 E U	201503	Ledge	105	116
TL 21LW 27 LED013 E U	201504	Ledge	105	109
TL 21LW 27 PNL007 E U	201504	Stope	105	110
TL 21LW 27 PNL007 W U	201504	Stope	105	106
TL 23LW 27 PNL001 W U	201504	Stope	105	109
TL 23LW 27 PNL002 W U	201504	Stope	105	104
TL 23LW 27 PNL003 W U	201504	Stope	105	113
TL 21LW 27 PNL007 E U	201505	Stope	105	119
TL 23LW 27 PNL001 W U	201505	Stope	105	111
TL 23LW 27 PNL002 W U	201505	Stope	105	116
TL 23LW 27 PNL003 W U	201505	Stope	105	116
TL 21LW 27 PNL007 E U	201506	Stope	105	109
TL 23LW 27 PNL001 W U	201506	Stope	105	110
TL 23LW 27 PNL003 W U	201506	Stope	105	110
TL 21LW 27 PNL006 E U	201507	Stope	105	109
TL 21LW 27 PNL007 E U	201507	Stope	105	114
TL 21LW 27 PNL008 E U	201507	Stope	105	123
TL 23LW 27 PNL002 W U	201507	Stope	105	125
TL 21LW 27 PNL006 E U	201508	Stope	105	112
TL 21LW 27 PNL007 E U	201508	Stope	105	122
TL 21LW 27 PNL008 E U	201508	Stope	105	112
TL 23LW 27 PNL002 W U	201508	Stope	105	117

Workplace	Period	Type	Planned SW (cm)	Actual SW (cm)
TL 21LW 27 PNL006 E U	201509	Stope	105	117
TL 21LW 27 PNL008 E U	201509	Stope	105	121
TL 23LW 27 PNL003 W U	201509	Stope	105	116
TL 21LW 27 PNL006 E U	201510	Stope	105	112
TL 21LW 27 PNL008 E U	201510	Stope	105	112
TL 23LW 27 PNL003 W U	201510	Stope	105	114
TL 23LW 27 PNL006 W U	201510	Stope	105	116
TL 21LW 27 PNL008 E U	201511	Stope	105	110
TL 23LW 27 PNL006 W U	201511	Stope	105	110
TL 21LW 27 LED013 E U	201512	Stope	105	103
TL 23LW 27 PNL006 W U	201512	Stope	105	110
TL 23LW 27 PNL007 W U	201512	Stope	105	113
TL 23LW 27 PNL009 E U	201512	Stope	105	118
TL 21LW 27 LED013 E U	201601	Stope	105	115
TL 23LW 27 PNL006 E U	201601	Stope	105	111
TL 23LW 27 PNL007 W U	201601	Stope	105	117
TL 23LW 27 PNL009 E U	201601	Stope	105	116
TL 21LW 27 LED013 E U	201602	Ledge	105	113
TL 23LW 27 PNL006 E U	201602	Stope	105	111
TL 23LW 27 PNL007 E U	201602	Stope	105	113
TL 23LW 27 PNL007 W U	201602	Stope	105	111
TL 23LW 27 PNL009 E U	201602	Stope	105	114
TL 21LW 27 LED013 E U	201603	Ledge	105	216
TL 23LW 27 PNL001 W U	201603	Stope	105	114
TL 23LW 27 PNL002 W U	201603	Stope	105	107
TL 23LW 27 PNL006 E U	201603	Stope	105	116
TL 23LW 27 PNL007 E U	201603	Stope	105	112
TL 21LW 27 LED013 E U	201604	Ledge	105	114
TL 23LW 27 PNL001 W U	201604	Stope	105	107
TL 23LW 27 PNL002 W U	201604	Stope	105	114
TL 23LW 27 PNL006 E U	201604	Stope	105	114
TL 23LW 27 PNL007 E U	201604	Stope	105	114
TL 23LW 27 PNL008 E U	201604	Stope	105	110

Workplace	Period	Type	Planned SW (cm)	Actual SW (cm)
TL 21LW 27 LED013 E U	201605	Ledge	105	115
TL 23LW 27 PNL001 W U	201605	Stope	105	126
TL 23LW 27 PNL002 W U	201605	Stope	105	119
TL 23LW 27 PNL006 E U	201605	Stope	105	121
TL 23LW 27 PNL007 E U	201605	Stope	105	118
TL 23LW 27 PNL008 E U	201605	Stope	105	118
TL 23LW 27 PNL001 W U	201606	Stope	105	119
TL 23LW 27 PNL002 W U	201606	Stope	105	122
TL 23LW 27 PNL006 E U	201606	Stope	105	121
TL 23LW 27 PNL007 E U	201606	Stope	105	118
TL 23LW 27 PNL008 E U	201606	Stope	105	116
TL 21LW 27 PNL006 E U	201607	Stope	105	115
TL 23LW 27 PNL004 W U	201607	Stope	105	128
TL 23LW 27 PNL006 E U	201607	Stope	105	115
TL 23LW 27 PNL007 E U	201607	Stope	105	127
TL 23LW 27 PNL008 E U	201607	Stope	105	121
TL 21LW 27 PNL006 E U	201608	Stope	105	126
TL 21LW 27 PNL008 E U	201608	Stope	105	121
TL 21LW 27 PNL011 W U	201608	Stope	105	121
TL 21LW 27 PNL012 W U	201608	Stope	105	119
TL 23LW 27 PNL003 W U	201608	Stope	105	119
TL 23LW 27 PNL004 W U	201608	Stope	105	123
TL 23LW 27 PNL005 W U	201608	Stope	105	113
TL 23LW 27 PNL007 E U	201608	Stope	105	118
TL 23LW 27 PNL008 E U	201608	Stope	105	116
Average Stoping Width				**120**

Appendix D: Rock Mass Classification Input Data for KORP Section

Date of Mapping	Level	Crosscut	Panel	Strength of intact Rock Material (UCS)	RQD	Joint Spacing	Joint Sets	Joint Condition	Joint Roughness	Joint Alteration	Groundwater	Joint Orientation	Stress Reduction Factor	RMR	RMR Rating	Q	Q Rating
2013/11/12	21	27	1W&1E	c) 50-100MPa	a) 90-100	c) 0.2 - 0.6m	c) 2 Sets	a) Very rough surfaces, discontinuous, no separation, unweathered	e) Rough/ Irregular, planar	d) Serpentine, mica, calcite < 5mm	a) Completely dry	b) Favourable	b) Medium stress	**80.0**	Good	**5.94**	Fair
2013/11/12	21	27	3E& W	c) 50-100MPa	b) 75-90	c) 0.2 - 0.6m	d) 2 Sets + Random	a) Very rough surfaces, discontinuous, no separation, unweathered	e) Rough/ Irregular, planar	e) Swelling clay, disintegrated rock, gouge > 5mm.	a) Completely dry	d) Unfavourable	b) Medium stress	**69.0**	Good	**2.58**	Poor
2013/11/12	23	27	10E	c) 50-100MPa	a) 90-100	c) 0.2 - 0.6m	d) 2 Sets + Random	a) Very rough surfaces, discontinuous, no separation, unweathered	e) Rough/Irregular, planar	e) Swelling clay, disintegrated rock, gouge > 5mm.	a) Completely dry	c) Fair	b) Medium stress	**77.0**	Good	**2.97**	Poor
2013/11/12	23	27	11E	b) 100-250MPa	b) 75-90	c) 0.2 - 0.6m	c) 2 Sets	a) Very rough surfaces, discontinuous, no separation, unweathered	b) Rough or irregular	d) Serpentine, mica, calcite < 5mm	a) Completely dry	c) Fair	b) Medium stress	**79.0**	Good	**10.31**	Good
2014/01/17	21	27	1W & 1E	c) 50-100MPa	a) 90-100	b) 0.6 - 2.0m	d) 2 Sets + Random	b) Slightly rough surfaces, separation <1mm, slightly weathered walls	b) Rough or irregular	d) Serpentine, mica, calcite < 5mm	a) Completely dry	b) Favourable	b) Medium stress	**80.0**	Good	**7.92**	Fair
2014/01/17	21	27	3E & 3W	c) 50-100MPa	a) 90-100	c) 0.2 - 0.6m	e) 3 Sets	d) Slickensided surfaces or gouge < 5mm thick or Separation 1-5mm Continuous	g) Slickensided, planar	d) Serpentine, mica, calcite < 5mm	a) Completely dry	d) Unfavourable	b) Medium stress	**52.0**	Fair	**0.88**	V/ poor
2014/07/09	21	27	1W & 1E	c) 50-100MPa	a) 90-100	b) 0.6 - 2.0m	d) 2 Sets + Random	b) Slightly rough surfaces, separation <1mm, slightly weathered walls	b) Rough or irregular	d) Serpentine, mica, calcite < 5mm	a) Completely dry	b) Favourable	b) Medium stress	**80.0**	Good	**7.92**	Fair
2014/07/09	21	27	3E & 3W	c) 50-100MPa	a) 90-100	c) 0.2 - 0.6m	e) 3 Sets	d) Slickensided surfaces or gouge < 5mm thick or Separation 1-5mm Continuous	g) Slickensided, planar	d) Serpentine, mica, calcite < 5mm	a) Completely dry	d) Unfavourable	b) Medium stress	**52.0**	Fair	**0.88**	V/Poor
2014/09/09	23	27	1W	c) 50-100MPa	b) 75-90	c) 0.2 - 0.6m	d) 2 Sets + Random	b) Slightly rough surfaces, separation <1mm, slightly weathered walls	e) Rough/Irregular, planar	d) Serpentine, mica, calcite < 5mm	a) Completely dry	c) Fair	b) Medium stress	**69.0**	Good	**3.44**	Poor
2014/10/01	21	27	1E & 1W DD	c) 50-100MPa	b) 75-90	c) 0.2 - 0.6m	c) 2 Sets	b) Slightly rough surfaces, separation <1mm, slightly weathered walls	b) Rough or irregular	a) Surface staining only	a) Completely dry	b) Favourable	b) Medium stress	**72.0**	Good	**61.88**	Very good

Date of Mapping	Level	Crosscut	Panel	Strength of intact Rock Material (UCS)	RQD	Joint Spacing	Joint Sets	Joint Condition	Joint Roughness	Joint Alteration	Groundwater	Joint Orientation	Stress Reduction Factor	RMR	RMR Rating	Q	Q Rating
2014/10/01	21	27	3E & 3W DD	c) 50-100MPa	b) 75-90	c) 0.2 - 0.6m	c) 2 Sets	b) Slightly rough surfaces, separation <1mm, slightly weathered walls	b) Rough or irregular	a) Surface staining only	a) Completely dry	c) Fair	b) Medium stress	**69.0**	Good	**61.88**	Very good
2014/10/01	23	27	1W	c) 50-100MPa	b) 75-90	c) 0.2 - 0.6m	c) 2 Sets	a) Very rough surfaces, discontinuous, no separation, unweathered	b) Rough or irregular	a) Surface staining only	a) Completely dry	c) Fair	b) Medium stress	**74.0**	Good	**61.88**	Very good
2014/11/12	23	27	2W	c) 50-100MPa	b) 75-90	c) 0.2 - 0.6m	d) 2 Sets + Random	a) Very rough surfaces, discontinuous, no separation, unweathered	e) Rough/Irregular, planar	a) Surface staining only	a) Completely dry	d) Unfavourable	b) Medium stress	**69.0**	Good	**20.63**	Good
2014/12/09	23	27	12E	c) 50-100MPa	b) 75-90	b) 0.6 - 2.0m	d) 2 Sets + Random	b) Slightly rough surfaces, separation <1mm, slightly weathered walls	b) Rough or irregular	d) Serpentine, mica, calcite < 5mm	a) Completely dry	b) Favourable	b) Medium stress	**77.0**	Good	**6.88**	Fair
2015/03/10	23	27	1W	c) 50-100MPa	a) 90-100	b) 0.6 - 2.0m	b) 1 Set + random	b) Slightly rough surfaces, separation <1mm, slightly weathered walls	b) Rough or irregular	a) Surface staining only	Completely dry	e) Very unfavourable	b) Medium stress	**70.0**	Good	**95.00**	Very good
2015/03/10	23	27	2W	c) 50-100MPa	b) 75-90	c) 0.2 - 0.6m	d) 2 Sets + Random	d) Slickensided surfaces or gouge < 5mm thick or Separation 1-5mm Continuous	d) Slickensided, undulating	d) Serpentine, mica, calcite < 5mm	a) Completely dry	b) Favourable	b) Medium stress	**57.0**	Fair	**3.44**	Poor
2015/03/10	23	27	3W	c) 50-100MPa	b) 75-90	b) 0.6 - 2.0m	d) 2 Sets + Random	d) Slickensided surfaces or gouge < 5mm thick or Separation 1-5mm Continuous	d) Slickensided, undulating	d) Serpentine, mica, calcite < 5mm	a) Completely dry	b) Favourable	b) Medium stress	**62.0**	Good	**3.44**	Poor
2015/04/20	21	27	7E	c) 50-100MPa	b) 75-90	b) 0.6 - 2.0m	c) 2 Sets	a) Very rough surfaces, discontinuous, no separation, unweathered	b) Rough or irregular	a) Surface staining only	a) Completely dry	b) Favourable	b) Medium stress	**82.0**	Very	**61.88**	Very good
2015/06/03	23	27	3W	c) 50-100MPa	b) 75-90	c) 0.2 - 0.6m	c) 2 Sets	a) Very rough surfaces, discontinuous, no separation, unweathered	e) Rough/Irregular, planar	a) Surface staining only	a) Completely dry	b) Favourable	b) Medium stress	**77.0**	Good	**30.94**	Good
2015/06/03	21	27	7E	c) 50-100MPa	b) 75-90	c) 0.2 - 0.6m	d) 2 Sets + Random	a) Very rough surfaces, discontinuous, no separation, unweathered	e) Rough/Irregular, planar	a) Surface staining only	a) Completely dry	c) Fair	b) Medium stress	**74.0**	Good	**20.63**	Good
2015/07/23	21	27	7E	c) 50-100MPa	b) 75-90	c) 0.2 - 0.6m	d) 2 Sets + Random	b) Slightly rough surfaces, separation <1mm, slightly weathered walls	c) Smooth, undulating	b) Slightly altered, sandy particles	a) Completely dry	d) Unfavourable	b) Medium stress	**64.0**	Good	**13.75**	Good

Date of Mapping	Level	Crosscut	Panel	Strength of intact Rock Material (UCS)	RQD	Joint Spacing	Joint Sets	Joint Condition	Joint Roughness	Joint Alteration	Groundwater	Joint Orientation	Stress Reduction Factor	RMR	RMR Rating	Q	Q Rating
2015/08/13	23	27	2W	c) 50-100MPa	b) 75-90	c) 0.2 - 0.6m	d) 2 Sets + Random	a) Very rough surfaces, discontinuous, no separation, unweathered	b) Rough or irregular	a) Surface staining only	a) Completely dry	d) Unfavourable	b) Medium stress	**69.0**	Good	**41.25**	Very good
2015/08/13	21	27	6E	c) 50-100MPa	b) 75-90	c) 0.2 - 0.6m	c) 2 Sets	a) Very rough surfaces, discontinuous, no separation, unweathered	b) Rough or irregular	a) Surface staining only	a) Completely dry	c) Fair	b) Medium stress	**74.0**	Good	**61.88**	Very good
2015/08/13	21	27	7E	c) 50-100MPa	b) 75-90	c) 0.2 - 0.6m	d) 2 Sets + Random	a) Very rough surfaces, discontinuous, no separation, unweathered	b) Rough or irregular	a) Surface staining only	a) Completely dry	d) Unfavourable	b) Medium stress	**69.0**	Good	**41.25**	Very good
2015/08/13	21	27	8E	c) 50-100MPa	b) 75-90	c) 0.2 - 0.6m	c) 2 Sets	a) Very rough surfaces, discontinuous, no separation, unweathered	b) Rough or irregular	a) Surface staining only	a) Completely dry	c) Fair	b) Medium stress	**74.0**	Good	**61.88**	Very good
2015/08/12	23	27	6W	c) 50-100MPa	b) 75-90	c) 0.2 - 0.6m	d) 2 Sets + Random	a) Very rough surfaces, discontinuous, no separation, unweathered	e) Rough/Irregular, planar	a) Surface staining only	a) Completely dry	b) Favourable	b) Medium stress	**77.0**	Good	**20.63**	Good
2015/08/12	23	27	7W	c) 50-100MPa	b) 75-90	c) 0.2 - 0.6m	d) 2 Sets + Random	a) Very rough surfaces, discontinuous, no separation, unweathered	e) Rough/Irregular, planar	a) Surface staining only	a) Completely dry	b) Favourable	b) Medium stress	**77.0**	Good	**20.63**	Good
2015/08/12	23	27	8W	c) 50-100MPa	b) 75-90	c) 0.2 - 0.6m	d) 2 Sets + Random	a) Very rough surfaces, discontinuous, no separation, unweathered	e) Rough/Irregular, planar	a) Surface staining only	a) Completely dry	b) Favourable	b) Medium stress	**77.0**	Good	**20.63**	Good
2015/09/29	21	27	13E	c) 50-100MPa	b) 75-90	b) 0.6 - 2.0m	c) 2 Sets	b) Slightly rough surfaces, separation <1mm, slightly weathered walls	b) Rough or irregular	d) Serpentine, mica, calcite < 5mm	a) Completely dry	e) Very unfavourable	b) Medium stress	**67.0**	Good	**10.31**	Good
2015/09/29	23	27	9E	c) 50-100MPa	b) 75-90	b) 0.6 - 2.0m	c) 2 Sets	d) Slickensided surfaces or gouge < 5mm thick or Separation 1-5mm Continuous	d) Slickensided, undulating	d) Serpentine, mica, calcite < 5mm	a) Completely dry	b) Favourable	b) Medium stress	**62.0**	Good	**5.16**	Fair
2015/10/14	21	27	8E	c) 50-100MPa	b) 75-90	c) 0.2 - 0.6m	d) 2 Sets + Random	d) Slickensided surfaces or gouge < 5mm thick or Separation 1-5mm Continuous	e) Rough/Irregular, planar	d) Serpentine, mica, calcite < 5mm	a) Completely dry	b) Favourable	b) Medium stress	**57.0**	Fair	**3.44**	Poor
2015/10/14	23	27	6W	c) 50-100MPa	b) 75-90	c) 0.2 - 0.6m	d) 2 Sets + Random	b) Slightly rough surfaces, separation <1mm, slightly weathered walls	e) Rough/Irregular, planar	d) Serpentine, mica, calcite < 5mm	a) Completely dry	c) Fair	b) Medium stress	**69.0**	Good	**3.44**	Poor

Date of Mapping	Level	Crosscut	Panel	Strength of intact Rock Material (UCS)	RQD	Joint Spacing	Joint Sets	Joint Condition	Joint Roughness	Joint Alteration	Groundwater	Joint Orientation	Stress Reduction Factor	RMR	RMR Rating	Q	Q Rating
2015/12/04	23	27	6E	c) 50-100MPa	b) 75-90	b) 0.6 - 2.0m	c) 2 Sets	a) Very rough surfaces, discontinuous, no separation, unweathered	b) Rough or irregular	d) Serpentine, mica, calcite < 5mm	a) Completely dry	a) Very favourable	b) Medium stress	**84.0**	Very	**10.31**	Good
2015/12/04	23	27	7E	c) 50-100MPa	b) 75-90	b) 0.6 - 2.0m	c) 2 Sets	a) Very rough surfaces, discontinuous, no separation, unweathered	b) Rough or irregular	d) Serpentine, mica, calcite < 5mm	a) Completely dry	a) Very favourable	b) Medium stress	**84.0**	Very	**10.31**	Good
2016/02/17	23	27	1W	c) 50-100MPa	b) 75-90	c) 0.2 - 0.6m	d) 2 Sets + Random	b) Slightly rough surfaces, separation <1mm, slightly weathered walls	c) Smooth, undulating	d) Serpentine, mica, calcite < 5mm	a) Completely dry	d) Unfavourable	b) Medium stress	**64.0**	Good	**4.58**	Fair
2016/02/17	23	27	2W	c) 50-100MPa	b) 75-90	c) 0.2 - 0.6m	d) 2 Sets + Random	d) Slickensided surfaces or gouge < 5mm thick or Separation 1-5mm Continuous	c) Smooth, undulating	d) Serpentine, mica, calcite < 5mm	a) Completely dry	d) Unfavourable	b) Medium stress	**49.0**	Fair	**4.58**	Fair
2016/03/17	23	27	8E	c) 50-100MPa	b) 75-90	c) 0.2 - 0.6m	d) 2 Sets + Random	a) Very rough surfaces, discontinuous, no separation, unweathered	b) Rough or irregular	a) Surface staining only	a) Completely dry	c) Fair	b) Medium stress	**74.0**	Good	**41.25**	Very good
2016/04/12	23	27	1W	c) 50-100MPa	b) 75-90	c) 0.2 - 0.6m	d) 2 Sets + Random	b) Slightly rough surfaces, separation <1mm, slightly weathered walls	c) Smooth, undulating	a) Surface staining only	a) Completely dry	d) Unfavourable	b) Medium stress	**64.0**	Good	**27.50**	Good
2016/04/12	23	27	2W	c) 50-100MPa	b) 75-90	c) 0.2 - 0.6m	d) 2 Sets + Random	b) Slightly rough surfaces, separation <1mm, slightly weathered walls	c) Smooth, undulating	a) Surface staining only	a) Completely dry	d) Unfavourable	b) Medium stress	**64.0**	Good	**27.50**	Good
2016/04/12	23	27	6E	c) 50-100MPa	b) 75-90	c) 0.2 - 0.6m	c) 2 Sets	a) Very rough surfaces, discontinuous, no separation, unweathered	b) Rough or irregular	a) Surface staining only	a) Completely dry	b) Favourable	b) Medium stress	**77.0**	Good	**61.88**	Very good
2016/04/12	23	27	7E	c) 50-100MPa	b) 75-90	c) 0.2 - 0.6m	c) 2 Sets	a) Very rough surfaces, discontinuous, no separation, unweathered	b) Rough or irregular	a) Surface staining only	a) Completely dry	b) Favourable	b) Medium stress	**77.0**	Good	**61.88**	Very good
2016/04/12	21	27	13E	c) 50-100MPa	b) 75-90	c) 0.2 - 0.6m	d) 2 Sets + Random	b) Slightly rough surfaces, separation <1mm, slightly weathered walls	b) Rough or irregular	a) Surface staining only	a) Completely dry	c) Fair	b) Medium stress	**69.0**	Good	**41.25**	Very good

Date of Mapping	Level	Crosscut	Panel	Strength of intact Rock Material (UCS)	RQD	Joint Spacing	Joint Sets	Joint Condition	Joint Roughness	Joint Alteration	Groundwater	Joint Orientation	Stress Reduction Factor	RMR	RMR Rating	Q	Q Rating
2016/04/25	23	27	4W	c) 50-100MPa	b) 75-90	c) 0.2 - 0.6m	d) 2 Sets + Random	b) Slightly rough surfaces, separation <1mm, slightly weathered walls	b) Rough or irregular	a) Surface staining only	a) Completely dry	b) Favourable	b) Medium stress	**72.0**	Good	**41.25**	Very good
2016/04/25	23	27	5W	c) 50-100MPa	b) 75-90	b) 0.6 - 2.0m	d) 2 Sets + Random	b) Slightly rough surfaces, separation <1mm, slightly weathered walls	b) Rough or irregular	a) Surface staining only	a) Completely dry	b) Favourable	b) Medium stress	**77.0**	Good	**41.25**	Very good
2016/05/27	23	27	8E	c) 50-100MPa	b) 75-90	c) 0.2 - 0.6m	d) 2 Sets + Random	a) Very rough surfaces, discontinuous, no separation, unweathered	b) Rough or irregular	a) Surface staining only	a) Completely dry	b) Favourable	b) Medium stress	**77.0**	Good	**41.25**	Very good
2016/05/30	21	27	6E	c) 50-100MPa	b) 75-90	b) 0.6 - 2.0m	d) 2 Sets + Random	d) Slickensided surfaces or gouge < 5mm thick or Separation 1-5mm Continuous	b) Rough or irregular	d) Serpentine, mica, calcite < 5mm	a) Completely dry	e) Very unfavourable	b) Medium stress	**52.0**	Fair	**6.88**	Fair
2016/05/30	21	27	8E	c) 50-100MPa	b) 75-90	c) 0.2 - 0.6m	c) 2 Sets	b) Slightly rough surfaces, separation <1mm, slightly weathered walls	b) Rough or irregular	d) Serpentine, mica, calcite < 5mm	a) Completely dry	b) Favourable	b) Medium stress	**72.0**	Good	**10.31**	Good
2016/06/22	23	27	3W	c) 50-100MPa	c) 50-75	d) 0.06 - 0.2m	d) 2 Sets + Random	d) Slickensided surfaces or gouge < 5mm thick or Separation 1-5mm Continuous	d) Slickensided, undulating	d) Serpentine, mica, calcite < 5mm	a) Completely dry	b) Favourable	b) Medium stress	**51.0**	Fair	**2.60**	Poor
2016/06/24	23	27	6E	c) 50-100MPa	b) 75-90	b) 0.6 - 2.0m	d) 2 Sets + Random	a) Very rough surfaces, discontinuous, no separation, unweathered	c) Smooth, undulating	d) Serpentine, mica, calcite < 5mm	a) Completely dry	a) Very favourable	b) Medium stress	**84.0**	Very	**4.58**	Fair
2016/06/24	23	27	7E	c) 50-100MPa	b) 75-90	b) 0.6 - 2.0m	d) 2 Sets + Random	a) Very rough surfaces, discontinuous, no separation, unweathered	b) Rough or irregular	d) Serpentine, mica, calcite < 5mm	a) Completely dry	a) Very favourable	b) Medium stress	**84.0**	Very	**6.88**	Fair
2016/08/31	21	27	12W	c) 50-100MPa	c) 50-75	c) 0.2 - 0.6m	d) 2 Sets + Random	b) Slightly rough surfaces, separation <1mm, slightly weathered walls	b) Rough or irregular	d) Serpentine, mica, calcite < 5mm	a) Completely dry	d) Unfavourable	b) Medium stress	**60.0**	Fair	**5.21**	Fair
2016/08/31	23	27	4W	c) 50-100MPa	b) 75-90	c) 0.2 - 0.6m	d) 2 Sets + Random	b) Slightly rough surfaces, separation <1mm, slightly weathered walls	b) Rough or irregular	a) Surface staining only	a) Completely dry	c) Fair	b) Medium stress	**69.0**	Good	**41.25**	Very good
2016/08/31	23	27	5W	c) 50-100MPa	b) 75-90	c) 0.2 - 0.6m	d) 2 Sets + Random	b) Slightly rough surfaces, separation <1mm, slightly weathered walls	b) Rough or irregular	a) Surface staining only	a) Completely dry	d) Unfavourable	b) Medium stress	**64.0**	Good	**41.25**	Very good

Appendix E: KORP Geoassay Log Boreholes

ANGLO PLATINUM GEOASSAY LOG

BH: UTL4001	X _COORD :2833693.90	Bearing D0: 0	
DEFL: D0	Y_COORD : -28203.00	Inclination D0: -90	
Farm: Khuseleka Shaft	ELEV : 275.82	Date Surveyed: 2011/05/23	
Geologist: GThobejane	End Depth : 31.40 m		

Geological Description

Lithology	From	To
COL	0.00	0.00
POIKAN	0.00	6.44
FPYX	6.44	10.35
CR	10.35	10.46
FPYX	10.46	10.47
CR	10.47	10.58
FPYX	10.58	10.85
FV	10.85	12.23
FPYX	12.23	14.98
CR	14.98	15.04
FPYX	15.04	16.78
CR	16.78	17.40
PEGFPYX	17.40	18.81
FPYX	18.81	19.46
PEGFPYX	19.46	19.58
CR	19.58	19.59
VTAN	19.59	20.19
N	20.19	21.60
FV	21.60	23.33

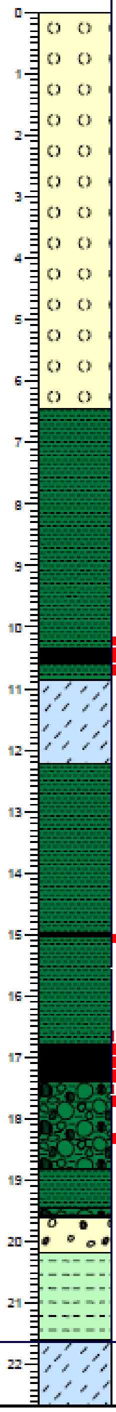

Sampling / Assay Results

From	To	Sample	3PGE + Au (g/t)	Cu (%)	Ni (%)
10.13	10.33	UTL4001/001	2.13	0.00	0.10
10.33	10.60	UTL4001/002	2.03	0.00	0.11
10.60	10.80	UTL4001/003	1.24	0.01	0.08
14.96	15.16	UTL4001/004	0.88	0.00	0.07
15.16	15.36	UTL4001/005	0.10	0.00	0.04
15.36	15.56	UTL4001/006	0.07	0.00	0.05
15.56	15.56	UTL4001/007	2.06	0.00	0.11
15.56	15.76	UTL4001/008	0.09	0.00	0.06
15.76	15.96	UTL4001/009	0.06	0.00	0.06
15.96	16.16	UTL4001/010	0.06	0.00	0.07
16.16	16.36	UTL4001/011	0.08	0.00	0.07
16.36	16.56	UTL4001/012	0.03	0.11	0.23
16.56	16.76	UTL4001/013	0.17	0.00	0.07
16.76	16.98	UTL4001/014	8.75	0.00	0.14
16.98	17.20	UTL4001/015	4.80	0.00	0.16
17.20	17.42	UTL4001/016	7.11	0.01	0.16
17.42	17.62	UTL4001/017	0.17	0.00	0.09
17.62	17.62	UTL4001/018	2.17	0.00	0.12
17.62	17.82	UTL4001/019	0.28	0.00	0.10
17.82	18.02	UTL4001/020	0.10	0.00	0.12
18.02	18.22	UTL4001/021	0.10	0.00	0.07
18.22	18.42	UTL4001/022	0.78	0.00	0.11

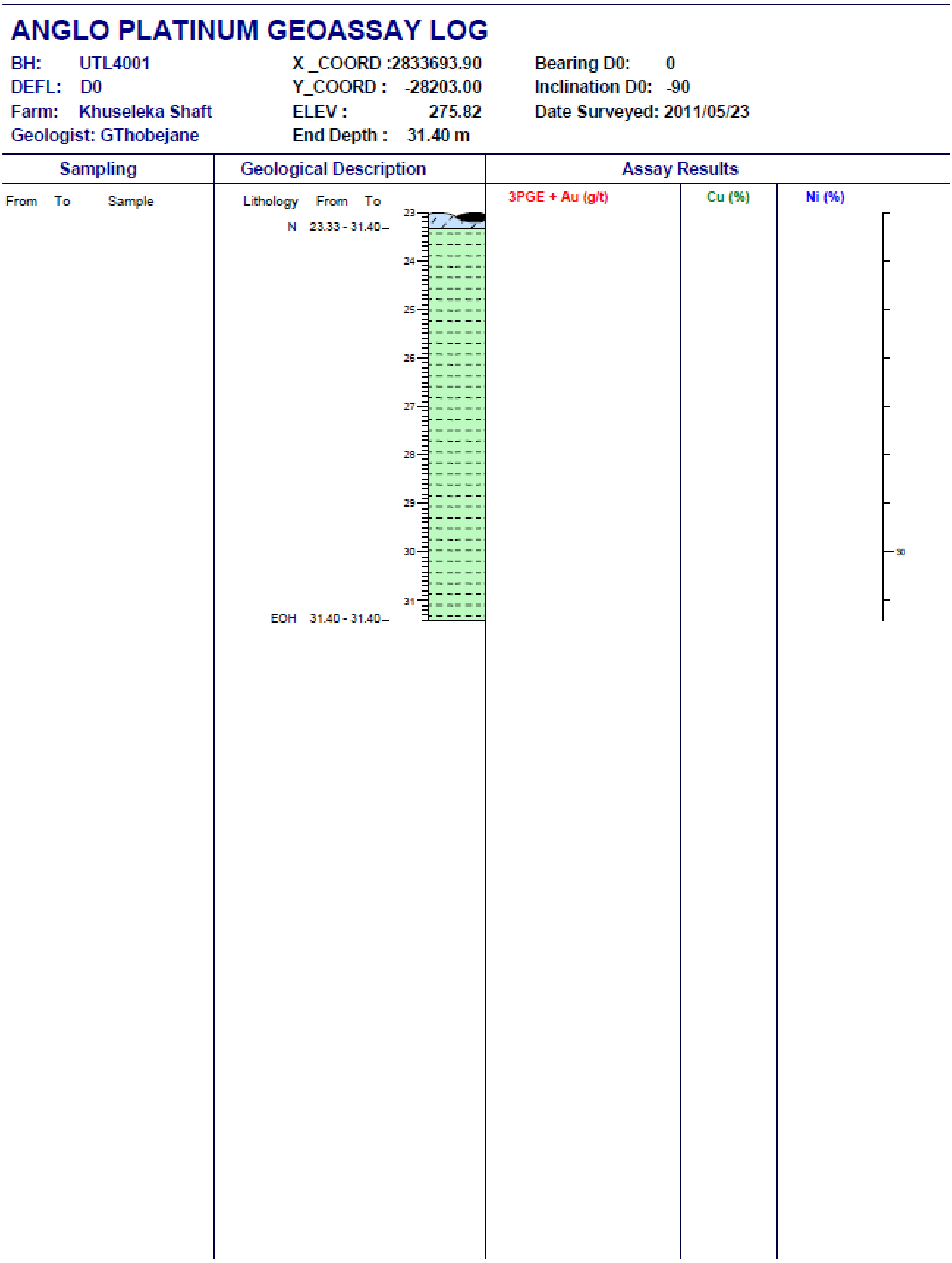

Figure E1: Geoassay Log for -90º Borehole UTL4001 Drilled in KORP Section 27/27 x/cut

ANGLO PLATINUM GEOASSAY LOG

BH:	UTL4002	X _COORD :	2834635.59	Bearing D0:	0
DEFL:	D0	Y_COORD :	-27262.94	Inclination D0:	-90
Farm:	Khuseleka Shaft	ELEV :	506.37	Date Surveyed:	2011/11/25
Geologist:	TMakamu	End Depth :	68.81 m		

Sampling	Geological Description	Assay Results

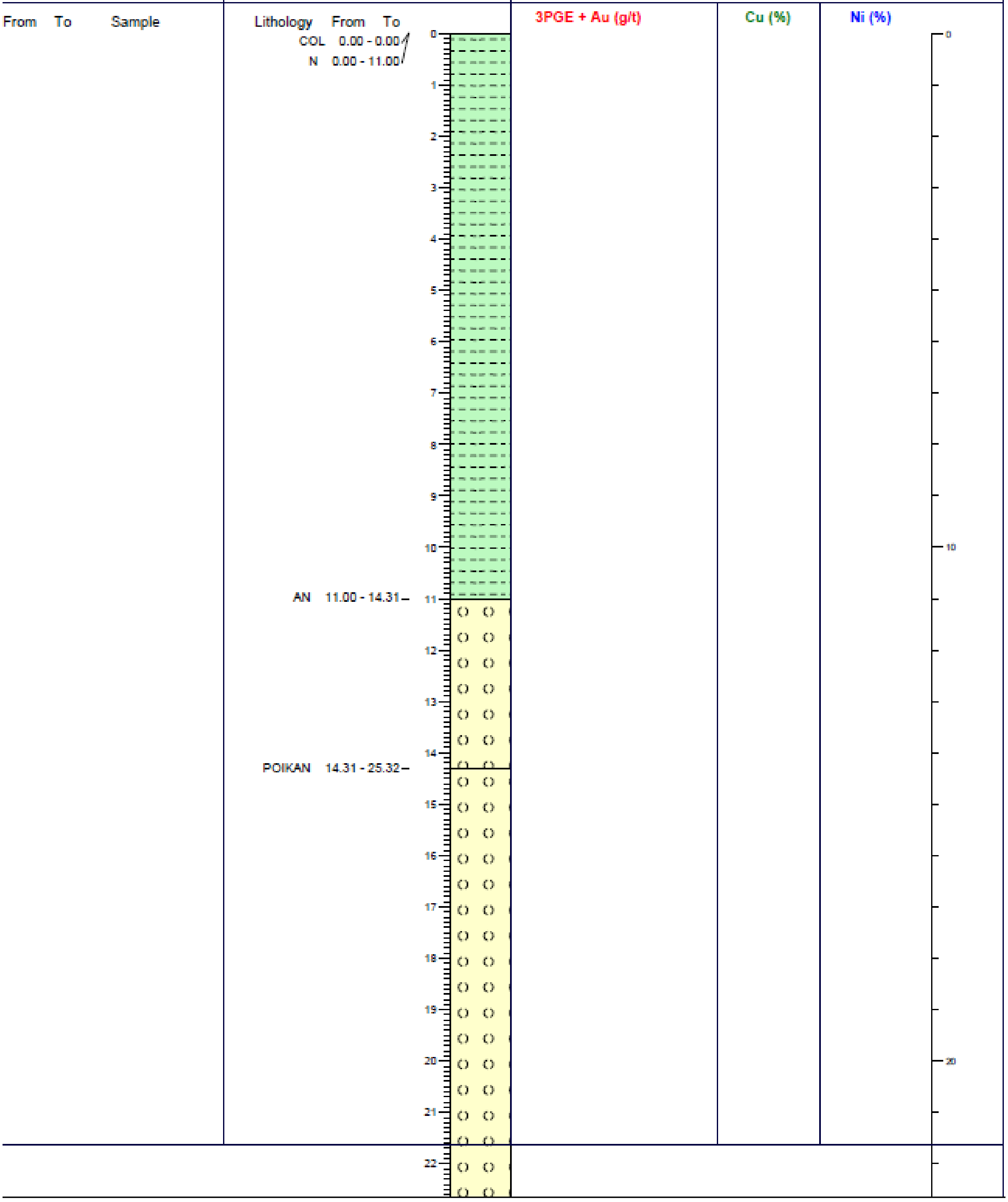

ANGLO PLATINUM GEOASSAY LOG

BH: UTL4002	X _COORD :2834635.59	Bearing D0: 0
DEFL: D0	Y_COORD : -27262.94	Inclination D0: -90
Farm: Khuseleka Shaft	ELEV : 506.37	Date Surveyed: 2011/11/25
Geologist: TMakamu	End Depth : 68.81 m	

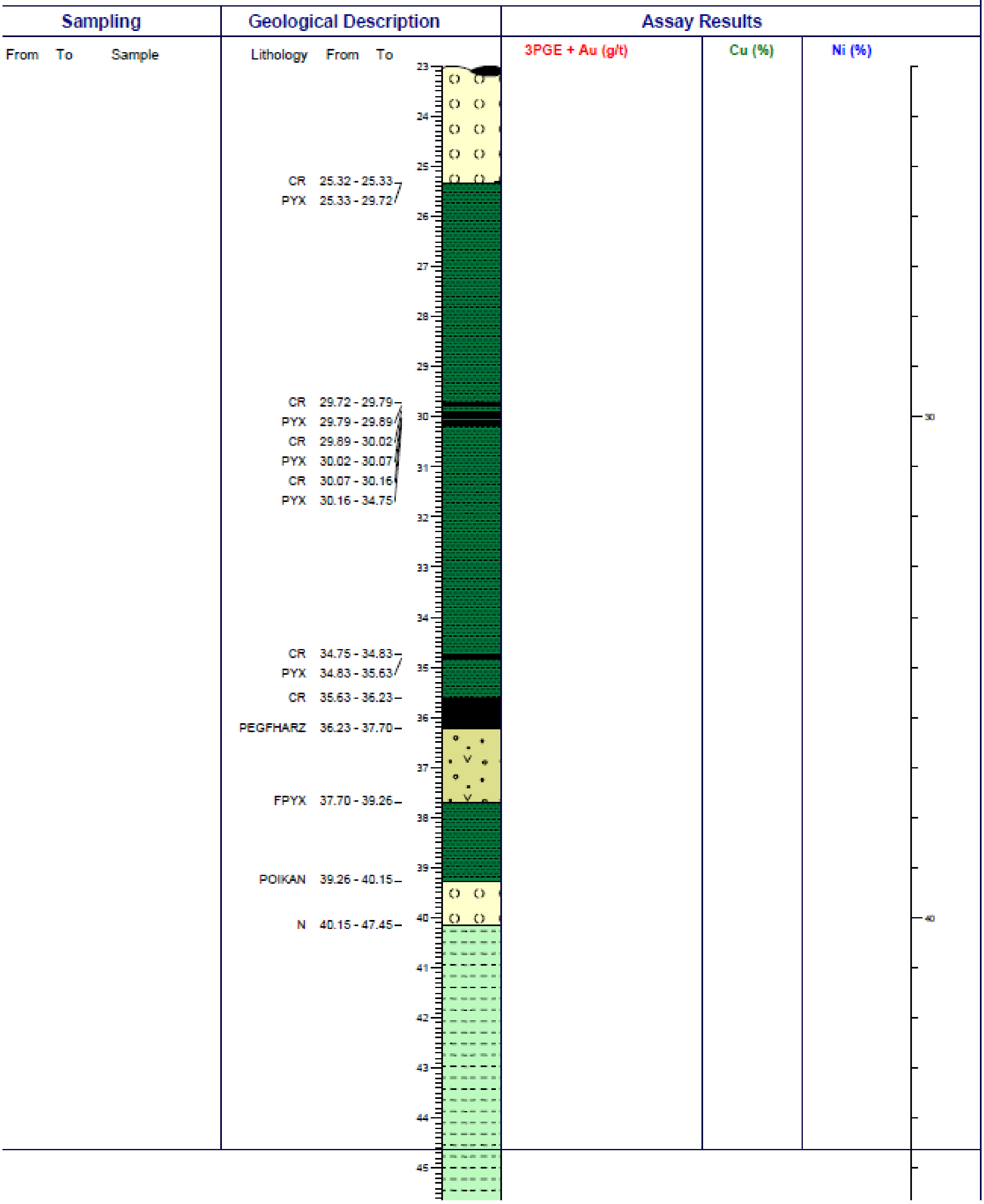

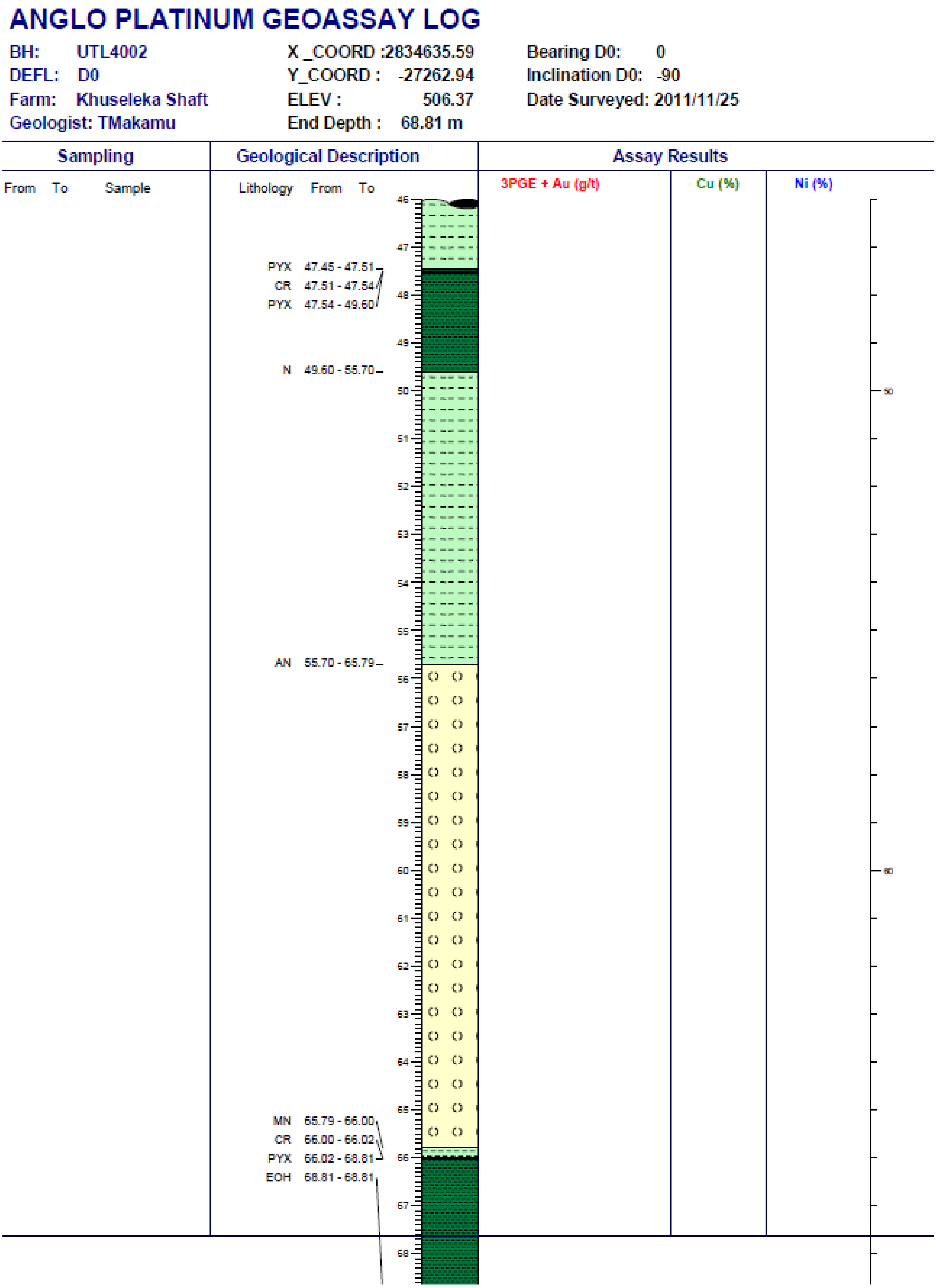

Figure E2: Geoassay Log for -90º Borehole UTL4002 Drilled in KORP Section 16/27 haulage

ANGLO PLATINUM GEOASSAY LOG

BH:	UTL4003	X _COORD :	2833802.50	Bearing D0:	0
DEFL:	D0	Y_COORD :	-28053.50	Inclination D0:	90
Farm:	Khuseleka Shaft	ELEV :	276.60	Date Surveyed:	2012/01/27
Geologist:	TMakamu	End Depth :	26.50 m		

Sampling			Geological Description			Assay Results		
From	To	Sample	Lithology	From	To	3PGE + Au (g/t)	Cu (%)	Ni (%)
			COL	0.00	0.00			
			MN	0.00	2.60			
			PEGFPYX	2.60	3.53			
			CR	3.53	3.76			
			FPYX	3.76	5.50			
			MN	5.50	6.69			
			CR	6.69	6.73			
			FPYX	6.73	7.57			
			FV	7.57	7.81			
			FPYX	7.81	11.20			
			PYXCR	11.20	11.73			
			CR	11.73	11.81			
			FPYX	11.81	11.81			
			CR	11.81	11.86			
			FPYX	11.86	11.88			
			CR	11.88	11.93			
			FPYX	11.93	16.98			
			POIKAN	16.98	25.42			

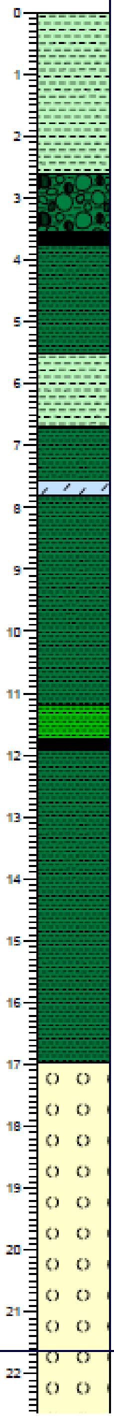

ANGLO PLATINUM GEOASSAY LOG

BH: UTL4003 X _COORD :2833802.50 Bearing D0: 0
DEFL: D0 Y_COORD : -28053.50 Inclination D0: 90
Farm: Khuseleka Shaft ELEV : 276.60 Date Surveyed: 2012/01/27
Geologist: TMakamu End Depth : 26.50 m

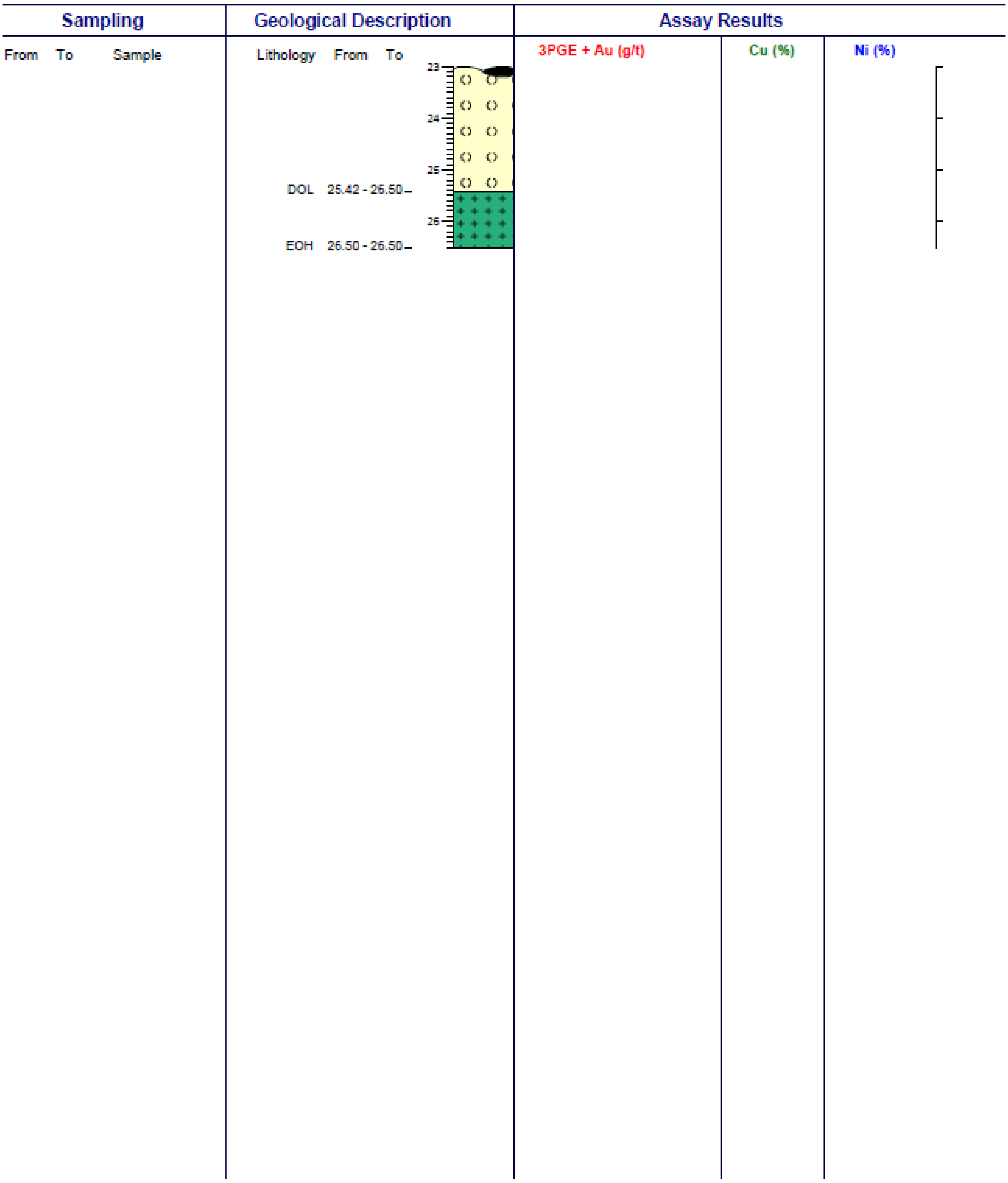

Figure E3: Geoassay Log for -90º Borehole UTL4003 Drilled in KORP Section 26/27 STX

ANGLO PLATINUM GEOASSAY LOG

BH:	UTL4004	X _COORD :	2833828.90	Bearing D0:	0
DEFL:	D0	Y_COORD :	-28026.80	Inclination D0:	90
Farm:	Khuseleka Shaft	ELEV :	277.00	Date Surveyed:	2012/02/08
Geologist:	TMakamu	End Depth :	26.48 m		

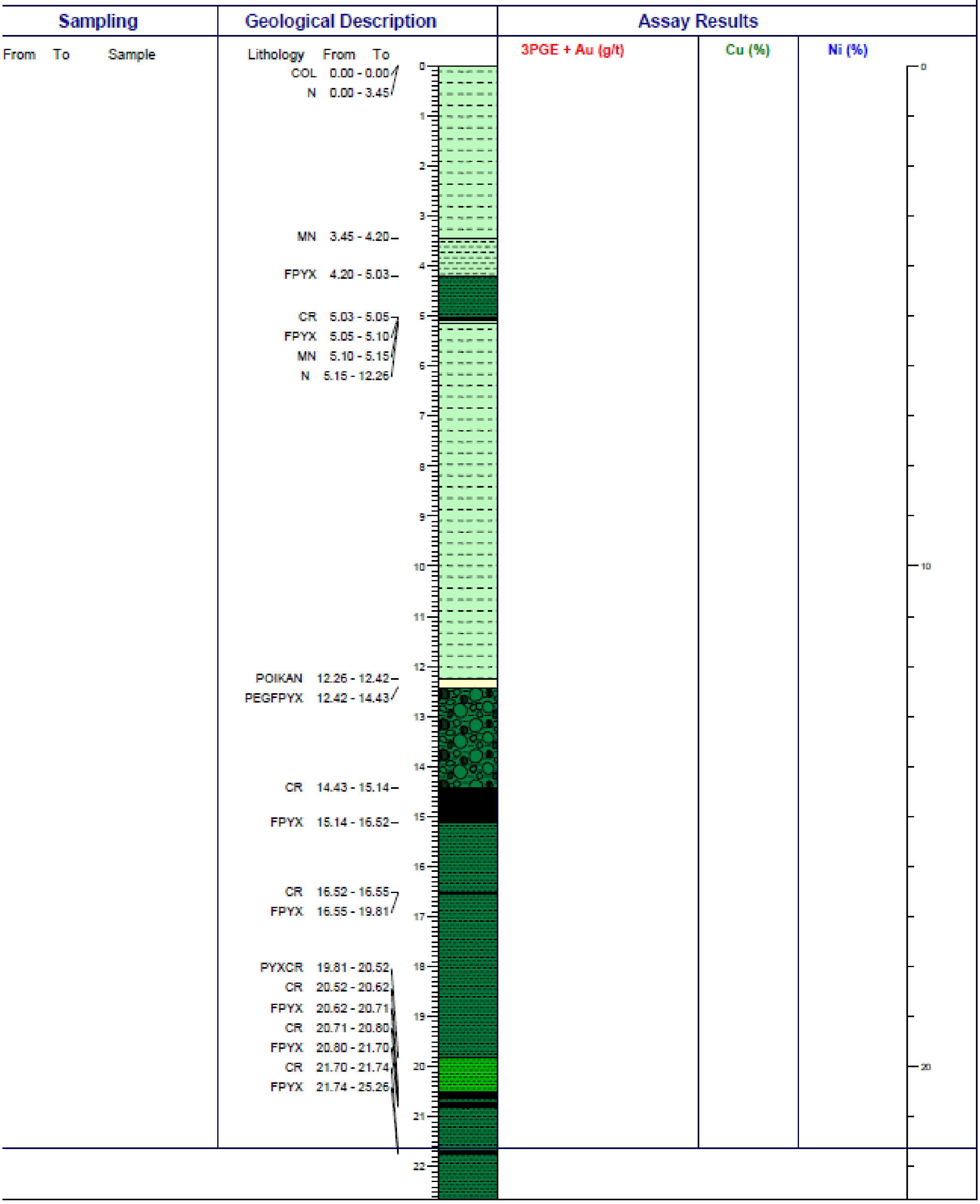

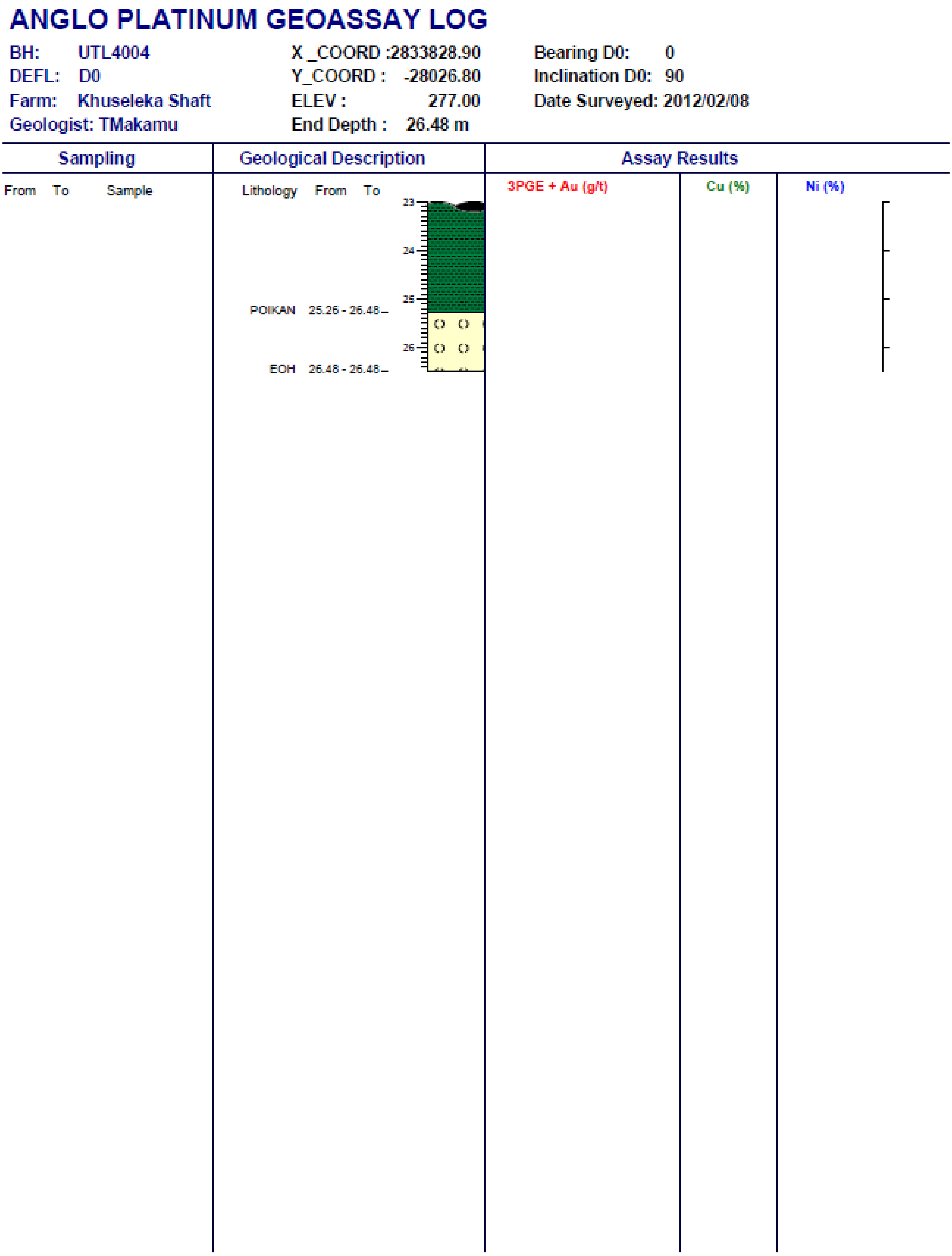

Figure E4: Geoassay Log for -90º Borehole UTL4004 Drilled in KORP Section 26/27 STX

ANGLO PLATINUM GEOASSAY LOG

BH: UTL4007A	X _COORD :2834378.43	Bearing D0: 0
DEFL: D0	Y_COORD : -27230.24	Inclination D0: 90
Farm: Khuseleka Shaft	ELEV : 423.33	Date Surveyed: 2013/05/10
Geologist: TMakamu	End Depth : 39.29 m	

Sampling	Geological Description	Assay Results
From To Sample	Lithology From To	3PGE + Au (g/t) Cu (%) Ni (%)

Lithology	From - To
COL	0.00 - 0.00
LN	0.00 - 0.68
MN	0.68 - 0.83
CR	0.83 - 0.85
MN	0.85 - 3.55
FPYX	3.55 - 9.90
CR	9.90 - 10.27
LN	10.27 - 11.97
MN	11.97 - 20.74
AN	20.74 - 21.36
PEGFPYX	21.36 - 22.88
HARZ	22.88 - 23.66

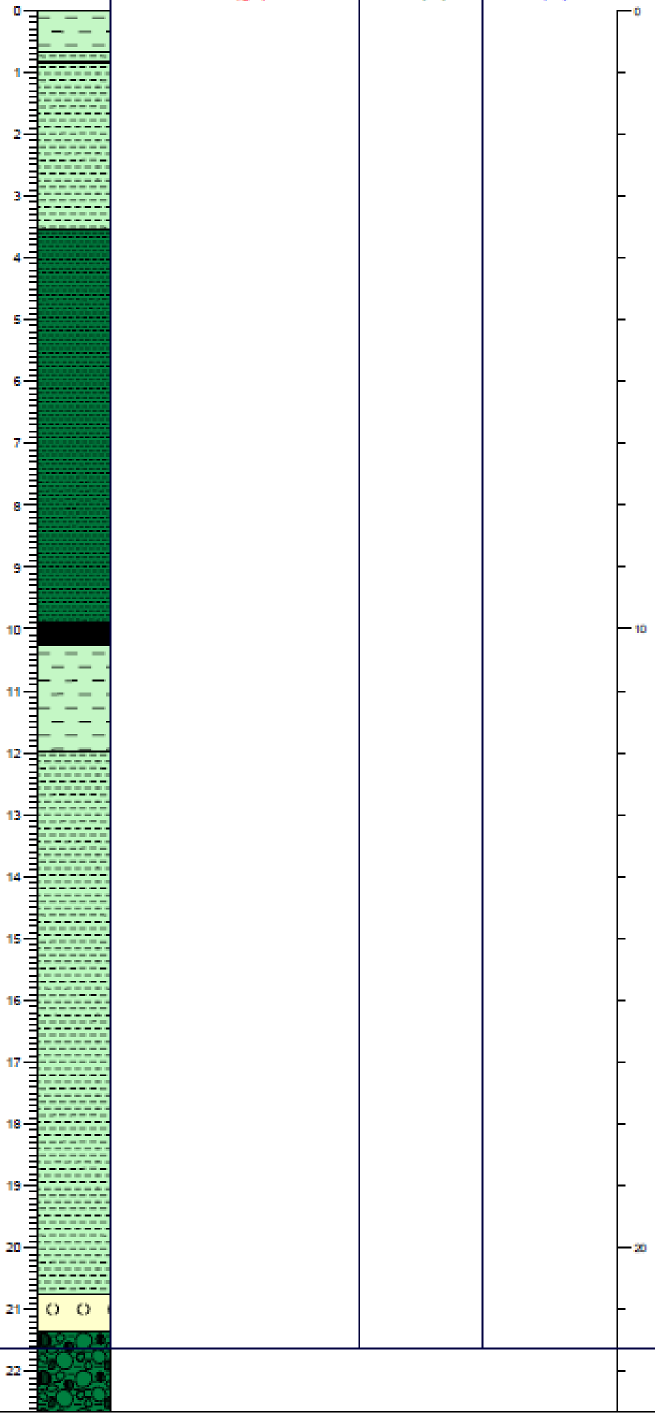

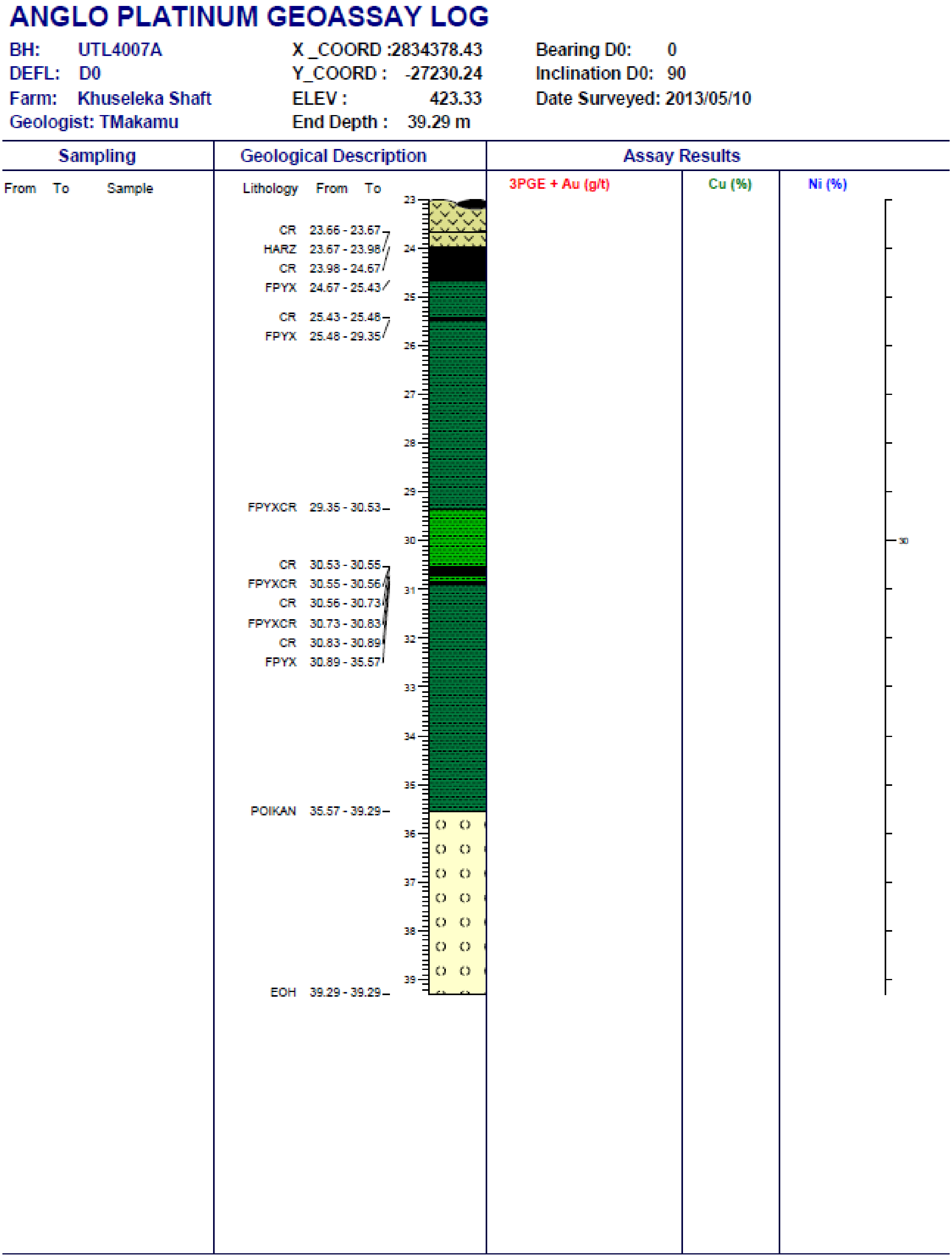

Figure E 5: Geoassay Log for -90º Borehole UTL4004 Drilled in KORP Section 21/28 haulage